UNIVERSITY OF Southampton

University of Southampton Research Repository
ePrints Soton

Copyright © and Moral Rights for this thesis are retained by the author and/or other copyright owners. A copy can be downloaded for personal non-commercial research or study, without prior permission or charge. This thesis cannot be reproduced or quoted extensively from without first obtaining permission in writing from the copyright holder/s. The content must not be changed in any way or sold commercially in any format or medium without the formal permission of the copyright holders.

When referring to this work, full bibliographic details including the author, title, awarding institution and date of the thesis must be given e.g.

AUTHOR (year of submission) "Full thesis title", University of Southampton, name of the University School or Department, PhD Thesis, pagination

http://eprints.soton.ac.uk

UNIVERSITY OF SOUTHAMPTON

FACULTY OF ENGINEERING AND THE ENVIRONMENT

Civil. Maritime and Environmental Engineering and Science

Raceway system requirements for low-cost energy-efficient algal biomass cultivation

by

Jose Luis Mendoza Martín

Thesis for the degree of Doctor of Philosophy

September 2016

UNIVERSITY OF SOUTHAMPTON

ABSTRACT

FACULTY OF ENGINEERING AND THE ENVIRONMENT

Thesis for the degree of Doctor of Philosophy

RACEWAY SYSTEM REQUIREMENTS FOR LOW-COST ENERGY-EFFICIENT ALGAL BIOMASS CULTIVATION

Jose Luis Mendoza Martín

The overall aim of the research was to investigate the hydraulic mixing characteristics and energy efficiency of raceway systems for the large-scale cultivation of micro-algae. For this purpose, two pilot-scale raceway reactors (100 m length x 1 m wide channel), each with a paddlewheel for liquid circulation and a sump for gas exchange, were built and tested under different conditions. The optimal depth to run the raceway was 0.20 m. At this depth, a typical velocity for liquid circulation in raceways of 0.20 m s^{-1} was obtained with a power consumption of 2.10 W m^{-3}, which was reduced to 1.6 W m^{-3} by using one baffle in the bend. At this velocity, addition of two and three baffles did not influence the power consumption significantly. The study of mixing as indicated by the Bodenstein number showed that mixing took place mainly in the paddlewheel, sump and bends although the overall behaviour of the system was plug flow since most of the liquid was contained in the channels.

A study with and without a sump baffle showed that the maximum velocity achieved when it was in place was 37 % lower than without the baffle, while at the same time the power consumption increased by 79 %. In addition, its presence reduced mixing, while the improvement in mass transfer was very low. For all these reasons, a sump baffle with the studied configuration was not recommended unless its hydrodynamic performance can be significantly improved. The selection of a membrane plate diffuser giving a small bubble size and low pressure drop enhanced mass transfer efficiency. Oxygen was desorbed mainly in the sump and paddlewheel due to high turbulence which increased the mass transfer coefficient. Peaks in dissolved oxygen at midday, however, were identified as a major problem causing growth inhibition. Accumulation of oxygen in the culture can be reduced by gas bubbling in the sump, although in cultures with a high concentration of bicarbonates CO_2 stripping may occur. CO_2 mass transfers above 96 % were achieved in the raceway, highlighting the efficiency of the sump as a device for gas exchange. The use of flue gas was effective to control pH, provide carbon to the culture and reduce dissolved oxygen peaks. A carbon balance showed that outgassing in the raceway was almost negligible and main carbon loss was through the liquid phase in the harvesting process.

Use of a hydrostatic pressure wheel for lifting water increased the hydraulic efficiency of the raceway between 15-20 %. The paddlewheel equipped with shoe used around 40-50 % of the energy required by flat configuration. This corresponds to an improvement of 2-5 times existing efficiencies, with higher values occurring at longer simulated channel lengths where the hydrostatic head losses are greater. This efficiency, however, is still well below theoretical values, and there is scope for further optimization the improved paddlewheel design for specific raceways.

Contents

List of tables

List of figures

DECLARATION OF AUTHORSHIP

I, Jose Luis Mendoza Martín, declare that the thesis entitled;

Raceway system requirements for low-cost energy-efficient algal biomass cultivation

and the work presented in the thesis are both my own, and has been generated by me as the result of my own original research. I confirm that:

- this work was done wholly or mainly while in candidature for a research degree at this University;
- where any part of this thesis has previously been submitted for a degree or any other qualification at this University or any other institution, this has been clearly stated;
- where I have consulted the published work of others, this is always clearly attributed;
- where I have quoted from the work of others, the source is always given. With the exception of such quotations, this thesis is entirely my own work;
- I have acknowledged all main sources of help;
- where the thesis is based on work done by myself jointly with others, I have made clear exactly what was done by others and what I have contributed myself;
- parts of this work have been published (Appendix III);

Signed: Jose Luis Mendoza Martín

Date: 31 January 2016

Acknowledgements

This work was funded by a University of Southampton post-graduate scholarship, with additional support from the company Aqualia SA as part of the EU FP7 ALL-GAS project "Industrial-scale demonstration of microalgae biofuels" (ENERGY.2010.3.4-1, Nº268208). I was also able to benefit from an exchange visit under the ECOFUEL project (FP7-PEOPLE-2009-IRSES Grant 246772).

First, I would like to thank my supervisors Professor Charles Banks and Dr Sonia Heaven for believing in me. I will never forget the day we met and how the opportunity you gave me changed my life. Thanks for letting me be part of your great academic family.

Thanks also to Professor Francisco Gabriel Acién Fernández for his assistance and supervision during the experimental work in Almeria. Without your enthusiasm and optimism none of this would have been possible.

Thanks to all the colleagues with whom I have worked in Almeria and Southampton. Your support has helped me to improve myself every day.

Specially, I would like to thank the support of my family during this long and exciting period. You have always been there to celebrate my successes and, especially, to help in bad times.

Thanks Pilar for appearing in my life. Your continuous encouragement and the warmth of your hugs are the energy I need to keep going.

.

List of abbreviations

Abs	Absorbance
Bo	Bodenstein Number
CFD	Computational Fluid Dynamics
DO	Dissolved Oxygen
FTU	Formazine Turbidity Units
GHG	Greenhouse Gases
GWP	Global Warming Potential
HPW	Hydrostatic Pressure Wheel
L/G	Liquid to Gas ratio
NTU	Nephelometric Turbidity Units
PBR	Photobioreactor
PSII	Photosystem II
TC	Total Carbon
TIC	Total Inorganic Carbon
TOC	Total Organic Carbon
TSS	Total Suspended Solids
% Sat	% Saturation

List of variables

Variable	Meaning	Units
$[CO_2^*]$	Equilibrium CO_2 concentration	g L^{-1}
$[CO_2]$	CO_2 concentration	g L^{-1}
$[CO_2]$- $[CO_2^*]$	Driving force	g L^{-1}
$[O_2^*]$	Equilibrium DO concentration	mg L^{-1}
$[O_2^*]$-$[O_2]$	Driving force	mg L^{-1}
$[O_2]$	DO concentration	mg L^{-1}
[TIC]	Total inorganic carbon concentration	g C L^{-1}
μ	Viscosity	Pa s
A	Pond area	m^2
A_b	Area of the blade	m^2
Bo	Bodenstein number	
C	Discharge coefficient	
$C_{absorbed}$	Mass flow of inorganic carbon absorbed	g C min^{-1}
$C_{accumulated}$	Mass of inorganic carbon accumulated	g C min^{-1}
C_b	Biomass concentration	g TSS L^{-1}
$C_{desorbed}$	Mass of inorganic carbon desorbed	g C min^{-1}
C_m	Cycles for mixing	Cycles
$CO_{2absorbed}$	CO_2 transferred to the liquid phase	g CO_2 min^{-1}
d	Depth of liquid	m
D	Equivalent diameter	m
d_1	Shallowest section before the wheel	m

d_2	Deepest section after the wheel	m
d_3	Height of water upstream of the weir	m
D_z	Dispersion coefficient	$m^2\ s^{-1}$
e	Mixing system efficiency	%
E	Fractional approach to equilibrium	
F	Force	N
f_F	Fanning friction factor	
Fv/Fm	Chlorophyll fluorescence	
g	Gravitational acceleration	$m\ s^2$
H	Head difference	m
I	Electrical current	A
I_0	Solar radiation	$\mu E\ m^{-2}\ s^{-1}$
I_{av}	Average irradiance	$\mu E\ m^{-2}\ s^{-1}$
K_a	Biomass extinction coefficient	$m^2\ g^{-1}$ biomass
$K_{feature}$	Loss coefficient feature	
K_la_l	Mass transfer coefficient	s^{-1}
L	Reactor length	m
$L_{section}$	Length of section	m
m	Mass	Kg
$M_{C/CO2}$	Mass C to mol CO_2 ratio	g C mol^{-1} CO_2
$mO_{2,zone}$	Mass flow of O_2 into the zone	mg O_2 s^{-1}
n	Manning´s roughness	$s\ m^{-0.3}$
N	Gas molar flow	$mol\ s^{-1}$
N_{Re}	Reynolds number	
P	Power consumption	W
p	Hydrostatic pressure	$N\ m^{-2}$
p_1	Atmospheric pressure	atm

p_2	Diffuser overpressure	atm
P_{elec}	Electric power	W
P_{hyd}	Hydraulic power	W
P_{in}	Input power	W
P_{mech}	Mechanical power	W
Q	Liquid flow	$m^3\ s^{-1}$
Q_{gas}	Gas flow	L gas min^{-1}
R	Ideal gas constant	J K^{-1} mol^{-1}
r	Radius of the wheel	m
R_h	Hydraulic radio	m
RO_{2max}	Specific maximum photosynthesis rate	mg O_2 L^{-1} h^{-1}
RO_{2phot}	Oxygen production by photosynthesis	mg O_2 L^{-1} h^{-1}
t	time	s
T	Temperature	K
T	Torque	N m
t_c	Cycling time	s
t_m	Mixing time	s
t_{pH}	Time of pH peaks	s
t_r	Residence time	s
TSS	Total Suspended Solids	g L^{-1}
t_{wheel}	Period of the wheel	s
v	Liquid velocity	m s^{-1}
V	Volume	m^3
V’	Voltage	V
v_1	Velocity of the blade	m s^{-1}
V_{mol}	Molar volume	L gas mol^{-1} gas
W	Weight	g

w	Channel width	m
W	Weight	N
W_b	Width of the blade	m
y_{CO2}	CO_2 molar fraction	%
y_{O2}	O_2 molar fraction	%
z	Height of the weir	m
ε	Absolute roughness	
η_{Exp}	Experimental efficiency of the paddlewheel	%
$\eta_{theoretical}$	Theoretical efficiency	%
ρ	Liquid density	kg m^{-3}
ΣF	Head loss	J kg^{-1}
ω	Angular velocity	rad s^{-1}

Chapter I

1. INTRODUCTION

1.1 Greenhouse effect and global warming

Energy and development are two concepts linked throughout history. Without energy, there would be no human society as we know it and the world would be completely different. Energy is used in the form of heat and light, and allows daily tasks such as travel, cultivation of food or manufacture of machines that work for us. The use of traditional energy sources, however, is associated with two inherent characteristics that human beings have not been fully aware of until recently:

- Shortage of energy resources: reserves of petroleum, natural gas or coal are limited, and the lack of energy sources could cause conflicts worldwide.
- Harmful impacts on the environment, from the extraction/generation through to the utilization of the energy.

Alternative renewable energies try to solve these two problems in order to end the progressive worsening of pollution, depletion of the ozone layer, and increase in greenhouse gas production; and thus, to prevent or reduce stop climate change.

According to some major international organizations, climate change is the greatest environmental threat facing the planet (Moomaw et al., 2011). The importance of the development of sustainable ways to produce energy has been identified, and it is essential to support a global revolution determined to change this situation and reduce harmful emissions. This calls for a change in the way we produce and use energy that is the largest source of CO_2 emissions.

1.2 Consequences of climate change

Predicting the consequences of global warming is a difficult task for the world's climate researchers. The natural processes that cause precipitation, storms, increases in sea level and other effects are dependent on many different factors. In addition, it is difficult to predict the volume of the emissions of greenhouse gases (GHG) in the next few decades, as this is

determined to a great extent by economic factors, political decisions and technological breakthroughs. Many of the effects of global warming have been well documented, however, and observations from real life are very much consistent with earlier predictions. It is the precise extent that is difficult to predict. Among the effects that can be predicted are: more droughts and flooding, less ice due to glaciers shrinking, more extreme weather incidents, and rising sea levels (IPCC).

1.3 The role of CO_2 in climate change

The Earth's climate is affected by multiple factors such as atmospheric aerosols and greenhouse gases, the radiation received from the Sun, the Earth's surface and atmospheric properties. When the balance between these elements is broken, either though natural or human processes, it modifies the energy balance of the Earth causing heating or cooling. It is widely accepted that climate change has occurred throughout the history of the planet (Pearson & Palmer, 2000). Until recently, however, it has always originated from natural causes, without the human influence which, in this case, is accelerating the process of global climate change. The anthropogenic origin of the current process goes back to the industrial revolution, when the use of fossil fuels was increased in most production processes. Since the nineteenth century, the atmospheric concentration of CO_2 has increased by around 25 % (Etheridge et al., 1996). Motors, industry, heating, millions of cars, planes… media broadcasts each hour, minute, second… These have all led to greenhouse gases in the atmosphere retaining radiation and, consequently, causing an increase in temperatures on the planet. Although there is more than one greenhouse gas with anthropogenic origins, the most abundant and the one mainly responsible for climate change is carbon dioxide which accounts for 80 % of the contribution to global warming of current GHG emissions (Lashof & Ahuja, 1999). The European Environment Agency (EEA, 2012) has noted the increase in the use of other substances like fluorinated gases that, although they are emitted in relatively small quantities, have a harmful impact on the environment several thousand times more powerful than carbon dioxide. The Global Warming Potential (GWP) is a relative measurement of the heat retention by a GHG in comparison to a reference gas, which is usually carbon dioxide. It can be calculated for periods of 20, 100 and 500 years. For example, methane

has a GWP 21 at 100 years (UN, 1995), which means that if the same masses of methane and carbon dioxide are emitted to the atmosphere, the methane retains 21 times more heat than the CO_2 during the next 100 years. For N_2O, the GWP is 310, so it is important to highlight that these GHG that are emitted in lower quantities than CO_2 may still have an important contribution to greenhouse effect. It was estimated that trace gases are responsible for around 43 % of the total heat retention (Lashof & Ahuja, 1999).

The Kyoto Protocol is an agreement achieved in 1997 by the most of the industrialized to promote sustainable development. This protocol obliges to signatory nations to reduce their GHG emissions to the atmosphere by 5 % taking the emissions in 1990 as base, and considering carbon dioxide (CO_2), methane (CH_4), nitrous oxide (N_2O), sulphur hexafluoride (SF_6) and two groups of gases, hydrofluorocarbons (HFCs) and perfluorocarbons (PFCs). All these gases are translated into CO_2 equivalents in determining reductions in emissions, which must be eliminated particularly from the combustion of fossil fuels. This reduction in emissions should have been achieved in the period between 2005 and 2012. To meet the requirements specified in the Protocol, two mechanisms were adopted:

- The European Union Emissions Trading Scheme was created in which between 90-95 % of Emission Allowances were freely assigned to the industries regulated by means of the National Allocation Plan which covered the mineral, energy, metal, glass, paper and cement sectors. The rest of the assigned allowances were entered in the Carbon Market and could be purchased through auction.
- The Clean Development Mechanism, based on projects which help towards the objective of reduction of emissions or the development of systems able to capture greenhouse gases from anthropogenic sources.

A number of follow-up meetings have occurred since 1997. The 2012 United Nations Climate Change Conference (Doha, Qatar) was the 18th yearly session of the Conference of the Parties to the 1992 United Nations Framework Convention on Climate Change and the 8th session of the Meeting of the Parties to the 1997 Kyoto Protocol (COP, 2012). The objective of this meeting was to

set the basis for a global climate agreement to continue the Kyoto Protocol. The 194 participant countries achieved a minimum agreement which extend the commitment of the Kyoto Protocol until 2020, with the opposition of developed countries such as Russia, Japan and Canada. Furthermore, an optimistic goal was established for 2015, when it was decided that a global pact must be achieved including United States (which never ratified the Protocol), Russia and emergent countries like India and China (UN, 2012). At present, this agreement has not been reached yet despite the growing concern about the harmful effect of global warming in the environment and, subsequently, in the population.

1.4 Renewable energies and sustainable development

In the current global situation, the use of conventional energy is not discussed since our economy is highly dependent on petroleum. A commitment, however, to renewable energies as a complement of conventional energy sources is a challenge that should be faced globally and soon to palliate global warming effects. Moreover, alternative energies, although renewable, are finite and have a maximum limit of exploitation. Therefore, a soft transition from traditional to new energy sources will not be possible if we continue with lifestyles based on perpetual growth. For this reason, the concept of sustainable development has arisen: “Sustainable development is development that meets the needs of the present without compromising the ability of future generations to meet their own needs” (UN).

Renewable energy is energy that can be obtained from natural sources which are virtually inexhaustible, some due to the vast amount of energy they contain, others because they are able to be regenerated by natural means. According to the Intergovernmental Panel on Climate Change, only the 12.9 % of the total primary energy supply in 2008 corresponded to renewable energies (Figure 1).

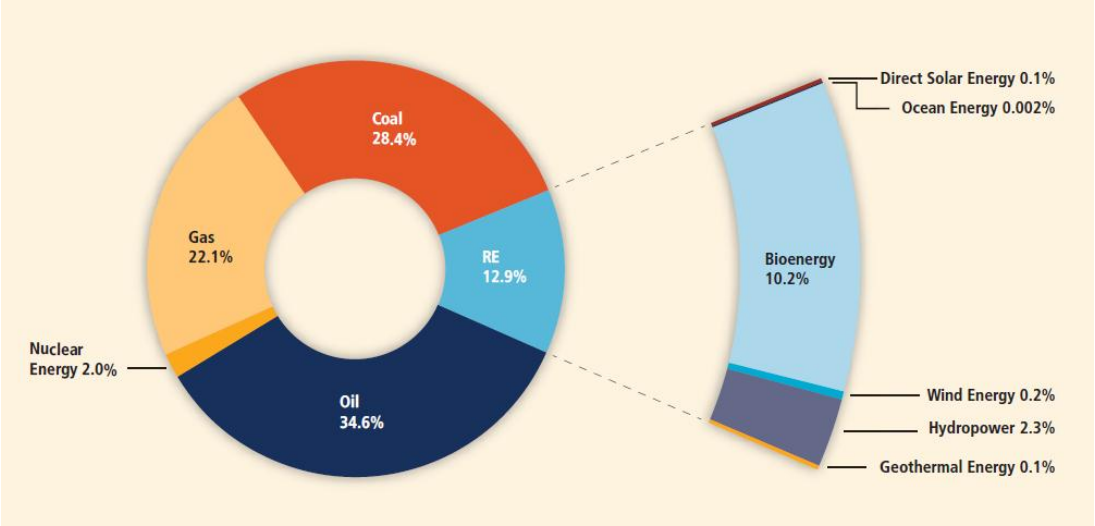

Figure 1.- Shares of energy sources in total global primary energy supply in 2008 (Moomaw et al., 2011)

The largest contributor in the group of renewable energies was biomass-based technologies, which accounted for 10.2 %. On the other hand, around 87 % of the energy used worldwide is derived from fossil fuels and it is estimated that CO_2 emissions produced by this source are increasing by 2.1 % per year (International Energy Outlook 2008). The solution to this problem is not easy and, currently, there is no single strategy for tackling the situation.

The substitution of fossil derived fuels by other less polluting carbon technologies (for example biogas could help to achieve the goal of emissions reduction. On the other hand, many governments in the developed world are investing in the construction of new nuclear energy plants to reduce atmospheric emissions and assure their energy independence (UCC, 2010), although previous and recent history has demonstrated that the security of those facilities must be improved to reduce the risk of major humanitarian catastrophes, and address the low public confidence in nuclear energy and the problems associated with the storage of nuclear waste. In any case, since renewable and nuclear energy are not enough to satisfy the current energy demand, they need to be complemented with fossil fuels and the transition to cleaner technologies must be made gradually.

It seems reasonable that reductions in energy consumption, advances in combustion processes and improvements in the efficiency of energy use can help in reducing CO_2 emissions (Acien Fernandez et al., 2012). Other strategies

are focused on the active capture of CO_2 from flue gases before it is released to the atmosphere, and its subsequent sequestration in the subsoil. Alternatively, this sequestration can be made by natural or biological processes carried out by plants and photosynthetic microorganisms like microalgae.

1.5 The potential of microalgae

The contribution of terrestrial plants to biofuel production is lower than needed to meet the gap between future energy supply and demand. For this reason, alternatives like microalgae have received increasing attention over the last few years (Benemann, 2013; Borowitzka, 2010; Chisti, 2007; Chisti, 2008; Demirbas, 2011). Microalgae are able to capture CO_2 from flue gases, where its concentration is high in comparison with that in the atmosphere, and also have the potential to help in the replacement of traditional fossil fuels by sustainable biofuels. These biofuels do not produce an increase in the atmospheric CO_2 concentration, since the CO_2 released in the combustion of biofuels has been previously fixed in the photosynthetic process: this is sometimes referred to as short-term cycling of carbon (Mathez, 2009). Thus, major efforts have been focused on the production of biodiesel, biogas or bioethanol derived from microalgal biomass. Moreover, the production of biofuels linked to the capture and sequestration of the produced flue gas could potentially produce a net reduction in the atmospheric CO_2 concentration (Azar, 2003).

The potential of microalgae for CO_2 capture is determined by their high adaptability to extreme conditions of pH, temperature, medium composition, etc. Microalgae do not require fertile land or useful water to grow, sometimes with higher growth rates than terrestrial plants, and they can use solar energy at efficiencies up to 5 % (Acien et al., 2012). Despite this, microalgal biomass production is not generally considered as a CO_2 storage technology since the storage is for a short period only. Thus, the main way in which microalgae can contribute to the reduction of emissions is through the production of biofuels as substitutes for traditional fossil fuels and, on the other hand, the production of other co-products using flue gas as a carbon source to obtain credits in the Carbon Market. The production of microalgae has an added value associated with the possibility of producing useful chemical or commodities. Moreover, it could contribute effectively to the sustainability of waste treatment processes,

reducing the energy consumed in the process and improving the recycling of nutrients contained within the microalgal biomass (Acien Fernandez et al., 2012).

1.6 Justification for the research

The growing social and political awareness of the existence of global warning and its effects in nature point to the necessity of developing new strategies to reduce its progress by means of investments in new R&D based projects. In that context, the policies focused on changing the productive system in the developed world and emerging countries with the objective of reducing emissions, seem to be insufficient to control the accumulation of greenhouse gases in the atmosphere. It is essential to design active programs not only to palliate the emissions of industrialized countries, but also to propose reliable alternatives as substitutes of traditional energy sources. Microalgae are one of the bio-technology based potential substitutes that meet the requirements for achieving this goal, since their growth is based on natural processes; they have the potential to capture CO_2 in places where it is emitted to the atmosphere; it is possible to obtain energy from the microalgal biomass; and they can participate in other environmentally friendly processes such as in bioremediation or waste water treatment processes.

The greatest drawback which prevents the introduction of microalgal production worldwide as an energy source is the high cost of microalgal growth systems in comparison to fossil fuel production. That means that microalgae biofuels are clearly at a competitive disadvantage in energy market in the current global context. This is, therefore, the bottleneck in the general establishment of microalgae technologies worldwide for biofuel production, and research in this field must be focused in overcome this unfavourable situation to make the production of microalgae for biofuels feasible.

In general, it has been concluded that the only realistic alternative for microalgal growth at a large scale for the purposes of energy production is by means of raceway reactors (Chisti, 2007; Ketheesan & Nirmalakhandan, 2011). Capital and operating costs of raceways for micro-algal production are considerably lower than enclosed reactor configurations such as tubular or flat panel photobioreactors. Raceways tend to have a low biomass productivity,

however, which is less than the maximum yields based on theoretical conversion efficiencies and those that can be achieved in enclosed photobioreactors (Benemann et al., 1987; Brennan & Owende, 2010; Chisti, 2007). Many factors contribute towards this, including greater risk of contamination and predation; nutrient limitations; sub-optimal light and temperature conditions; and inappropriate dilution and harvesting rates. In any microalgal cultivation system where the biomass is grown as an energy source, the energy potential of the product must be greater than the energy input into the cultivation: if this is not the case, then the system is unsustainable from an energetic point of view. Thus, improvements to microalgal production systems have two purposes: to increase the biomass productivity and to reduce the energy input. In practice these goals are often conflicting and a compromise has to be reached in the raceway design that must also take into account any impact this optimisation process may have on the overall capital and operation costs.

To achieve these improvements a staged approach is necessary as, in the current state of knowledge, it is not feasible to optimise the entire system in a single stage. In reality the different components need first to be assessed in relation to their performance, taking into account both the energetic and cost elements. Only when each component is understood in engineering terms can its inter-relationship and interaction with other components be fully understood and a whole system assessment made. The net result of the optimisation process should be a final positive energy balance, a reduction in costs, both of which are reflected in improved biomass productivity.

The work described in the thesis is therefore primarily concerned with the assessment of the performance of the raceway system in relation to the mass transfer of gases into and out of the culture medium and the use of energy in the system. Factors considered in this are the degree of mixing, the carbon demand, mechanism of gas supply and the nature of the gas and head difference for liquid circulation. In the assessments the raceway is considered as a number of components based on their function or hydraulic properties in the case of channel sections.

1.7 Aims, objectives and experiments

The overall aim of the research is to improve raceway channel design and its mass transfer characteristics through an enhanced knowledge of the function and performance of the component parts, as means of enhancing productivity in microalgal biomass cultivation.

To achieve this overall aim, the following major objectives were identified and experimental work undertaken to achieve them:

1. To carry out an initial assessment of mixing in the raceway channel.
    a. Experiments to determine the optimal depth of the system relative to the power consumption per unit volume of culture.
    b. Fluid-dynamic characterization of the raceway using basic tracers with continuous monitoring of dispersion using pH electrodes.
    c. Assessment of the mixing capacity of each section of the raceway and the potential for energy loss in the channel and gas transfer sump.

2. To develop a system to improve the mechanism of carbon supply to the raceway.
    a. Experiments to determine the efficiency of carbon transfer using pure CO_2 and flue gases from a diesel-powered combustion engine with around 10 % CO_2.
    b. In vitro assessment of different sump configurations and their efficiency as gas exchange devices.
    c. In vivo assessment of the gas exchange capacity of an unbaffled sump under different culture conditions as influenced by flow, velocity and depth of media in the channel.
    d. Determination of carbon limitations in microalgal culture under different conditions and the establishment of empirical coefficients for the design of full-scale raceway culture systems.

3. To assess the capacity of the system to produce microalgal biomass at a high productivity and consistently.
    a. Establishment of microalgal growth through staged inoculation with a selected strain, and maintenance of the culture under

different growth conditions and seasons, accompanied by extensive monitoring to establish factors influencing productivity.

b. Harvesting and preparation of microalgal samples for accompanying experiments (by others) on the energy conversion potential of the biomass. Feedback of information allowing more general assessment of the energy productivity of the culture system.
c. Assessment of the energy efficiency of the system for liquid circulation in the raceway and the possibility of testing new systems.

The results of this work will provide a sound basis for aspects of the design and engineering of cost-effective mass culture systems for microalgal biofuel production.

Chapter II

2. LITERATURE REVIEW

2.1 Background to microalgal culture

2.1.1 Introduction

Growing global awareness of the environmental consequences of massive use of traditional energy sources, linked to the fact of the limited reserves of fossil fuels, has produced an increasing interest in renewable energies. People demand a change in the energetic model based on the 'green' habits that they are progressively acquiring. In addition, the energy independence of countries is a crucial strategy that all the governments would like to achieve around the world. Most nations are not able to produce the energy that they consume and have to import it, causing disequilibrium in the commercial balance and dependence on other territories, some of them politically unstable. This situation makes nations vulnerable to a global energy crisis, converting their economies to hostages of external factors which may not coincide with local interests. In this context, there is an increasing interest around the world in microalgal biofuels, motivated by several aspects such as (Brennan & Owende, 2010; Pienkos & Darzins, 2009):

- Capability of all year round production with rapid growth potential and oil productivity much higher than oilseed crops.
- High productivity per square metre of land and possibility of using non-productive and non-arable land.
- Microalgal feedstock based on non-food resource.
- Microalgae grow in aqueous media, but need less water than terrestrial crops. In addition, they can use a wide variety of water sources: fresh, brackish, saline and wastewater. In case of wastewater, it is a source of nutrients (mainly nitrogen and phosphorus) and the cultivation process could be used for treatment of organic effluent from agri-food industry.
- Mitigation of release of GHG into the atmosphere. Capable of fixing CO_2 to produce biomass more efficiently and rapidly than terrestrial plants (1 kg of dry microalgal biomass utilizes about 1.83 kg of CO_2).
- Production of biofuels and valuable co-products such as proteins and residual biomass after oil extraction with feed or fertilizer applications,

or can even be subjected to fermentation processes to produce methanol or ethanol.

The following sections in the literature review consider aspects of algal biomass and mass cultivation that are relevant to the current research.

2.1.2 What are microalgae?

The phycological definition of algae includes any organisms with chlorophyll *a* and a thallus not differentiated into roots, stem and leaves. Microalgae are generally unicellular microorganisms: they can be individual cells or can form chains but unlike the macroalgae do not form differentiated multicellular organisms (Bahadar & Bilal Khan, 2013). In the context of mass cultivation of algal biomass for renewable energy production, cyanobacteria are traditionally considered together with microalgae, since they synthesize the essential substances for metabolism from inorganic constituents like carbon dioxide as the only carbon source, nitrogen, phosphorus, potassium, magnesium and other micronutrients, using the light as the only energy source, and thus grow under similar conditions. In scientific terms, however, it must be remembered that cyanobacteria are prokaryotes and belong to a different kingdom from microalgae. This process called photosynthesis is similar to the process carried out by vascular plants, whereby CO_2 fixation reaction is catalysed producing organic matter as a result. Thus, microalgae refers to the microscopic algae and the oxygen photosynthetic cyanobacteria or blue-green algae, formerly known as Cyanophycae (Tomaselli, 2004).

Algae can either be autotrophic, requiring only inorganic compounds such as CO_2, salts and a light energy source for growth; or heterotrophic, requiring an external source of organic compounds as well as nutrients as an energy source. In autotrophic algae, CO_2 is converted to organic matter in the photosynthesis reaction. In the light phase of photosynthesis, the transport of electrons between the different reactions involved (electron chain) produces the energy which is stored in form of ATP (adenosine triphosphate) and reducing power which is stored in form of NADPH (nicotinamide adenine dinucleotide phosphate), which is then used to reduce the CO_2 into organic matter. Other algae are called mixotrophic because they have the capacity to perform photosynthesis and acquire exogenous organic nutrients at the same time. Since algae do not have functionally distinct structures analogous to the

leaves, stems and roots of higher plants, in unicellular algae all the functions of a plant are carried out in a single microscopic cell and, therefore, material manufactured in one part of an alga does not readily move to another part (Burlew, 1976).

Around 35,000 different species of microalgae have been described to date, although it is believed that the total number of species is much higher (Borowitzka, 2013). Interest in algae started in the late 1800s, when several authors described microalgal culture techniques, although the concept of mass production of algae was first introduced in Germany during the Second World War with the aim of producing lipids for use as an energy source using flue gases, as well as anti-microbial substances and various bio-chemicals, and of providing sewage treatment (Grobbelaar, 2012). At the same time, the use of microalgae for animal and human feeding was studied, with the aim of develop an efficient protein source to replace plant and animal conventional proteins (Andersen, 2005), although the first plant for the production of microalgae at a large scale was only built in the 1960s in Trebon, Czech Republic (Setlik et al., 1970).

2.1.3 Why are microalgae important?

Interest in the potential for large-scale microalgal cultivation has grown significantly in the past few decades, but micro-algae and especially cyanobacteria are considered to be one of the earliest forms of life on Earth. Over millions of years, microalgae have had the capacity adaptation to the most extreme habitats on Earth including deep-sea vents, hot springs and Antarctica's ice. This means they can survive in almost the entire range of known habitats, although most species live in aquatic environments, in both fresh and sea water. In the oceans, they belong mainly to the phytoplankton, although there are species of microalgae not included in this group such as benthic organisms living near the seabed, diatoms living on rocks, etc. Microalgae, therefore, form the base of the marine food chain and contribute approximately 50 % of the molecular oxygen in the atmosphere. Thus, they support most of the life in the seas and on land (Van den Hoek et al., 1995).

Microalgae have natural pigments and a high protein, vitamin and carbohydrate content. In addition they are rich in oil and fatty acids, including

essential polyunsaturated fatty acids. The combination of all those factors makes microalgal biomass suitable for different purposes, and there is commercial interest in this technology around the world. In addition, effective designs for microalgal production systems could bring not only an economic benefit, but also social and environmental advantages in terms of the reduction of CO_2 emissions and development of new renewable energy sources. One of the main problems humans must face this century is the development and implementation of technologies able to replace petroleum dependence in a world where fuel demand is continuously increasing. The maintenance of our life-style in the future is incompatible with the finite character of fossil fuels and the harmful impact on the environment associated with their use. In this context, different biomass feedstocks have been proposed to produce renewable alternatives to replace fossil fuels and mitigate carbon dioxide emissions (Williams & Laurens, 2010); but, while other micro-organisms such as bacteria have been suggested as a source of biomass for biogas production, only micro-algae have the potential for rapid growth with high biomass yields while still being relatively easy to harvest. If the practical engineering problems can be overcome, it thus has excellent commercial potential as a sustainable environmentally-friendly carbon-neutral fuel source (Bahadar & Bilal Khan, 2013), in comparison with terrestrial crops whose productivities per unit area are usually much lower (Kheshgi et al., 2000).

The special interest in microalgae is not only because of its capacity to grow exponentially under optimal conditions, but also due to the content of the biomass produced. For example, some strains of microalgae are able to contain more than 70% on a dry weight basis of lipids (mainly triacylglycerols), which are the basis of the transesterification reaction in the production of biodiesel (Spolaore et al., 2006). Besides its lipids content, microalgal biomass contains a range of sugars as storage compounds that can potentially be used in the production of bioethanol or biobutanol; or by mean of a pyrolysis this biomass can be transformed to crude oils, methane or hydrogen (Benemann, 2000; Borowitzka, 2010; Chisti, 2007; Demirbas, 2006; Lee, 2008; Torzillo et al., 2009). In addition, the high photosynthetic rates and efficiency (e.g. 6.9 x 10^4 cells mL^{-1} h^{-1}) (Suali & Sarbatly, 2012) of microalgae exceed the grow capacity of terrestrial plants (Schenk et al., 2008). Moreover, the nutrient requirements for microalgal growth can be satisfied by the use of residues

from cities or industries like flue gas or wastewater, helping to make the process economically and environmentally sustainable.

2.2 Commercial uses of microalgae

In all the stages of evolution human beings have lived in contact with microalgae, and for thousands of years have known their properties as food, in species such as *Nostoc*, *Arthrospira* (*Spirulina*) and *Aphanizomenon* (Jensen et al., 2001). These authors also remark that the nutritional characteristics of microalgae depend on the harvest procedures, quality control for contaminating species, adherence to proper processing to preserve nutrients from degradation, and storage conditions. The conditions used for microalgal growth also determine the nutrient composition, with differences for example in the lipid and pigment composition depending on variables as temperature, nutrient availability and sun exposure (Van den Hoek et al., 1995). Microalgae grown in a natural environment will differ from those grown in canals or tanks due to differences in aeration, nutrient circulation and degree of competition with other microalgal species.

The commercial uses of microalgae are diverse. For example, microalgae offer the potential for production of high-value compounds (Pulz & Gross, 2004), wastewater treatment (Muñoz et al., 2009), CO_2 mitigation (Brune et al., 2009) and bioenergy production (Chisti, 2007). The selection of adequate strains and species depending on the final use of the biomass and the production system is essential for the successful commercialization of microalgae, since high productivities must be guaranteed at a large scale in order to assure the availability of feedstock in the later downstream process (Griffiths & Harrison, 2009).

2.2.1 Human and animal nutrition

The production of microalgae for health food, food additives and feed supplements is a growing global market. Species like *Spirulina* (*Arthrospira*), *Chlorella* and *Dunaliella salina* have been investigated for their therapeutic properties (Yamaguchi, 1997), being added into pastas, snack foods, candy bars, gums and beverages. Some of the world's largest microalgae producers are: Hainan Simai Enterprising located in the Hainan province of China with an

annual production of 200 t of *Arthrospira* powder (10 % of world production); Taiwan Chlorella Manufacturing and Co. located in Taipei and with a production of 400 t of dried *Chlorella* per year; and Cognis Nutrition and Health for production of *Dunaliella salina* (Spolaore et al., 2006). Although the nutritional composition of microalgae varies from strain to strain and from batch to batch and depends on multiple factors (Becker, 2004), a general overview of microalgae composition is given in Table 1, compared to some food sources.

Table 1.- General composition of human food sources and different algae strains (% of dry matter)

Species	**Protein**	**Carbohydrates**	**Lipids**
Spirulina platensis	61.32-64.43	15.09-15.81	7.09-8.03
Arthrospira maxima	60-71	13-16	6-7
Chlorella vulgaris	51-58	12-17	14-22
Chlorella pyrenoidosa	57	26	2
Dunaliella salina	57	32	6
Porphyridium cruentum	28-39	40-57	9-14
Scenedesmus obliquus	50-56	10-17	12-14
Aphanizomenon flos-aquae	62	23	3
Chlamydomonas rheinhardtii	48	17	21
Anabaena cylindrical	43-56	25-30	4-7
Euglena gracilis	39-61	14-18	14-20
Spirogyra sp.	6-20	33-64	11-21
Synechococcus sp.	46-63	8-14	4-9
Nannochloropsis spp.	28.8	35.9	18.36
Haematococcus pluvialis	48	27	15
Isochrysis galbana	26.99	16.98	17.16
Conventional foods			
Baker's yeast	39	38	1
Meat	43	1	34
Egg	47	4	41
Milk	26	38	28
Rice	8	77	2
Soya	37	30	20

Source: (Chacón-Lee & González-Mariño, 2010)

Most of the microalgae strains of commercial importance have a rigid indigestible cell wall, making it necessary for the cell to be ruptured by physical or chemical methods, with the drawback in some cases of the need to recover solvents to avoid making the product toxic (Becker, 2004). The studies carried out in some specific microalgae strains revealed, however, that the entire biomass including the cell wall is nutritious, in comparison with terrestrial plants which have to use the available nutrients not only to produce the edible parts such as fruits, seeds or roots, but also the non-edible parts in the plant structure which only have mechanical purposes. Then, there is an optimization of the available nutrients that are used for the production of edible structures in the microalgae, with more protein content than any other higher plant, amino acids considered essential and with low molecular weight which means that it can be digested readily (Burlew, 1976). This is the case for the cyanobacteria *Spirulina* sp. and *Aphanizomenon flos-aquae*, where analyses of the cell walls revealed the absence of cellulosic material that could present a potential barrier to proteolytic enzymes. These microalgae can therefore be digested by monogastric vertebrates like humans without previous physical or chemical rupture of the cell wall (Becker, 2004). This creates the potential to contribute to improving human nutrition worldwide, since large number of people do not have access to animal protein due to the large area of land required to grow grass and other crops to support animal husbandry and, on the other hand, do not have easy access to fish or sea food, leading to malnutrition in the population.

Animal nutrition is another important commercial use of microalgae biomass. For instance, it is calculated that about 30 % of the world production of 2000 t of *Spirulina* is sold for animal feed supplements due to the positive effect on animal growth and survival (Belay et al., 1996). Among the applications of microalgae in animal feed, aquaculture is of strategic interest since its contribution to human nutrition is constantly increasing and microalgae are the basis of the aquatic food chain. Microalgae are a potential diet for some important food products, most of which are carnivorous as adult organisms but herbivorous in the larval stage. The production of microalgae for world aquaculture, which was around 1000 t in 1999, is shared unequally between the consuming species, at 62 % for molluscs, 21 % shrimps and 16 % fish (Sialve et al., 2009).

2.2.2 Cosmetics

Substances extracted from microalgae can be found in a wide variety of cosmetics products. Benefits have been reported from the use of species such as *Arthrospira*, *Chlorella* or *Nannochloropsis* in face and skin care products, making the use of microalgae suitable in the manufacturing of anti-ageing cream, refreshing or regenerant care products, in emollients and as an anti-irritant in peelers (Spolaore et al., 2006).

2.2.3 High-value molecules

While the direct use of microalgae has benefits in fields like human nutrition or cosmetics, there also are some compounds with special characteristics that can be extracted from the microalgae. Depending of the strain or growth conditions, microalgae trend to accumulate exceptional substances with high application in different areas.

Fatty acids and, specially, polyunsaturated fatty acids (PUFA) have attracted attention by their importance in health and dietary requirements. The commercial production of fatty acids from microalgae has to compete with plant oils and animal fats, taking into account that the price of microbial oils is higher than similar traditional lipid sources. However, the possibility of obtaining highly specific oils that are expensive to obtain from agricultural and animal sources, or not commonly synthesized by these sources, suggests a promising future for the mass production of microalgal oils (Certik & Shimizu, 1999).

Regarding pigments, carotenoids and phycobiliproteins are the main groups. Although there are over 400 known carotenoids, only a very few are used commercially at present. These include β-carotene, astaxanthin and, of lesser importance, lutein, zeaxanthin, lycopene and bixin. Their most important applications are in natural food colorants, additive for animal feed, cosmetics and nutritional and therapeutic uses (Spolaore et al., 2006). Phycobiliproteins (i.e. phycoerythrin and phycocyanin) have a high potential in the field of natural dyes, although their health-promoting properties also make them suitable for pharmaceutical used(Spolaore et al., 2006).

2.2.4 Bioremediation

Microalgae have the potential to remove excess nitrogen and phosphorus from wastewater from different sources such as industry, urban areas or farms (Narasimhan, 2010), although some constituents of wastewater can, in high concentrations, inhibit microalgae growth. These constituents are mainly urea, ammonium, organic acids, phenolic compounds and pesticides (Hodaifa et al., 2008). Furthermore, taking into account that microalgae capture CO_2 for the photosynthesis reaction which could be provided from flue gases produced in highly polluting factories, they could also be considered as decontaminating air (Lundquist & Benemann, 2007). It has been calculated that microalgae can use up to 9% of incoming solar energy to produce 280 tons of dry biomass per ha^{-1} $year^{-1}$ while absorbing roughly 513 tons of CO_2 (Bilanovic et al., 2009).

Microalgae are able to sequester heavy metal ions by the same adsorption and absorption mechanisms as other microbial biomass, as well as by the formation of phytochelatins which they synthesize in response to toxic heavy metal stress (Wilde & Benemann, 1993). This allows the development of novel microalgal-based bioremoval processes for the abatement of heavy metal pollution based on the requirement of microalgae of different metals for biological functions in aquatic systems. Several researchers have established that metals such as Ti, Pb, Mg, Zn, Cd, Sr, Co, Hg, Ni, Cu are sequestered in polyphosphate bodies in green algae (Narasimhan, 2010).

2.3 Microalgae as biofuel feedstock

Microalgae derived fuels seem to have a promising future in the field of renewable energies. They have the potential to make a contribution to sustainable development in the field of biofuels, which are intended to reduce the world's dependence on fossil fuels. The increase in global population and, therefore, in fuel demand has caused a growing interest in energy sources based on biomass transformation (Collet et al., 2011; Stephens et al., 2010). The use of traditional agricultural sources to produce biofuels generally induces a lower climate change potential, but is associated with other environmental problems such as eutrophication, resource depletion and reduced biodiversity due to current farming practices, besides generating competition with food crops for the use of arable land (Zah et al., 2007).

The idea of using microalgae as a source of fuel appeared several decades ago (Chisti, 1980), but has recently emerged more strongly due to uncertainties over the long-term availability, price and political stability of petroleum supplies and the negative consequences in the environment and in the global warming phenomenon associated with burning fossil fuels (Gavrilescu & Chisti, 2005). The advantages of using microalgal biomass in comparison to traditional agricultural crops are based on its higher production yield and hence lower land use footprint. Furthermore, land not suitable for crops could be used in algae farms, reducing the competition with food production, while introducing the potential for production of a carbon neutral biofuel by using CO_2 emissions (Ward et al., 2014).

The use of liquid biofuels has grown considerably in recent years, mainly in the transport sector due to the necessity of implementing policies to assure economic independence and to palliate environmental damage by GHG emissions (Brennan & Owende, 2010). The extension of the use of first generation of biofuels, obtained from edible raw materials such as sunflower seeds, sugarcane or maize, is limited due to the competition with food and fibre production for the use of arable land, the high water and fertilizer requirements and the need for conservation of bio-diversity, among other drawbacks (IEA, 2007). Furthermore, it has a potential impact on global food markets, increasing the price of basic foods mainly in poor regions and creating food supply insecurities worldwide. This problem can be solved in part by the use of second generation biofuels from non-edible raw materials such as agricultural or forest harvesting residues. Unfortunately, the need for huge areas to supply the biomass in second generation biofuels is still a problem since these could compete for arable land with food crops. As an example of the extent of the problem, currently around 1 % of the world's available arable land is used for the production of 1 % of global transport requirements in form of biofuels; so to supply 100 % of transport requirements vast areas of arable land would have to be used (IEA, 2006). Therefore, several conditions has been stablished for technically and economically viable biofuel resource (Brennan & Owende, 2010):

- The price of the biofuel production has to be competitive with petroleum derived fuels.
- It must be non-competitive in land with crops.

- Its use must be linked to an improvement in air quality, as indicated by the prefix bio-.
- The water requirement must be at a minimum and its use should be optimized.

Microalgae could potentially put together all these conditions, helping to meet the primary energy demand while contributing to environmental benefits.

Several start-up companies are attempting to commercialize microalgal fuels as diesel, gasoline or jet fuels (Table 2); there is, however, a long way to go to achieve the huge production required to cover the worldwide demand for fuel. The competition with traditional energy sources based on fossil fuels is enormous and research must focus on the reduction of production costs to make microalgae based fuel competitive. It has been reported that, although microalgae has the potential to replace petroleum as source of hydrocarbon feedstock for the petrochemical industry, the cost of microalgal derived oil has to meet the condition expressed in Eq(1), where $C_{algal\ oil}$ (\$ L^{-1}) is the price of microalgal oil and $C_{petroleum}$ (\$ $barrel^{-1}$) is the price of crude oil, assuming that algal oil has roughly 80 % of the energy content of crude petroleum (Chisti, 2007).

$$C_{algal\ oil} = 6.9 \cdot 10^{-3} C_{petroleum} \quad (1)$$

Table 2.- Examples of start-up companies attempting to commercialize microalgal fuels

Company	Location	Web site
Algenol Biofuels	Bonita Spring, FL, USA	www.algenolbiofuels.com
Aquaflow	Nelson, New Zealand	www.aquaflowgroup.com
Aurora Algae, Inc.	Haywar, CA, USA	www.aurorainc.com
Bioalgene	Seattle, WA, USA	www.bioalgene.com
Bionavitas, Inc.	Redmond, WA, USA	www.bionavitas.com
Bodega Algae, LLC	Boston, MA, USA	www.bodegaalgae.com
LiveFuels, Inc.	San Carlos, CA, USA	www.livefuels.com
PetroAlgae, Inc.	Melbourne, FL, USA	www.petroalgae.com
Phyco Biosciences	Chandler, AZ, USA	www.phyco.net
Sapphire Energy, Inc.	San Diego, CA, USA	www.sapphireenergy.com
Seambiotic Ltd.	Tel Aviv, Israel	www.seambiotic.com
Solazyme, Inc.	San Francisco, CA, USA	www.solazyme.com
Solix Biofuels, Inc.	Fort Collins, CO, USA	www.solixbiofuels.com
Synthetic Genomic, Inc.	La Jolla, CA, USA	www.syntheticgenomic.com

Source: (Chisti & Yan, 2011)

To meet this equation several conditions have to be taken into account: on the one hand the petroleum cost that is influenced by factors such as the availability of oil reserves to be exploited or the international political and economic context; on the other hand the cost microalgae based fuels depends on parameters such as the available land for microalgae cultivation and its price, availability of resources as water or nutrients or the technological advances in the production process and the downstream treatment of the biomass.

Figure 2 shows the different stages and routes for transformation of microalgae to produce biofuels. The process is divided in 3 main steps: first the cultivation of the microalgae where they grow and multiply their population; second the harvesting process where the water of the culture is removed to obtain a concentrated or dried biomass; and finally the processes carried out to prepare the biomass and convert it into the final biofuel product which can be used as a source of energy.

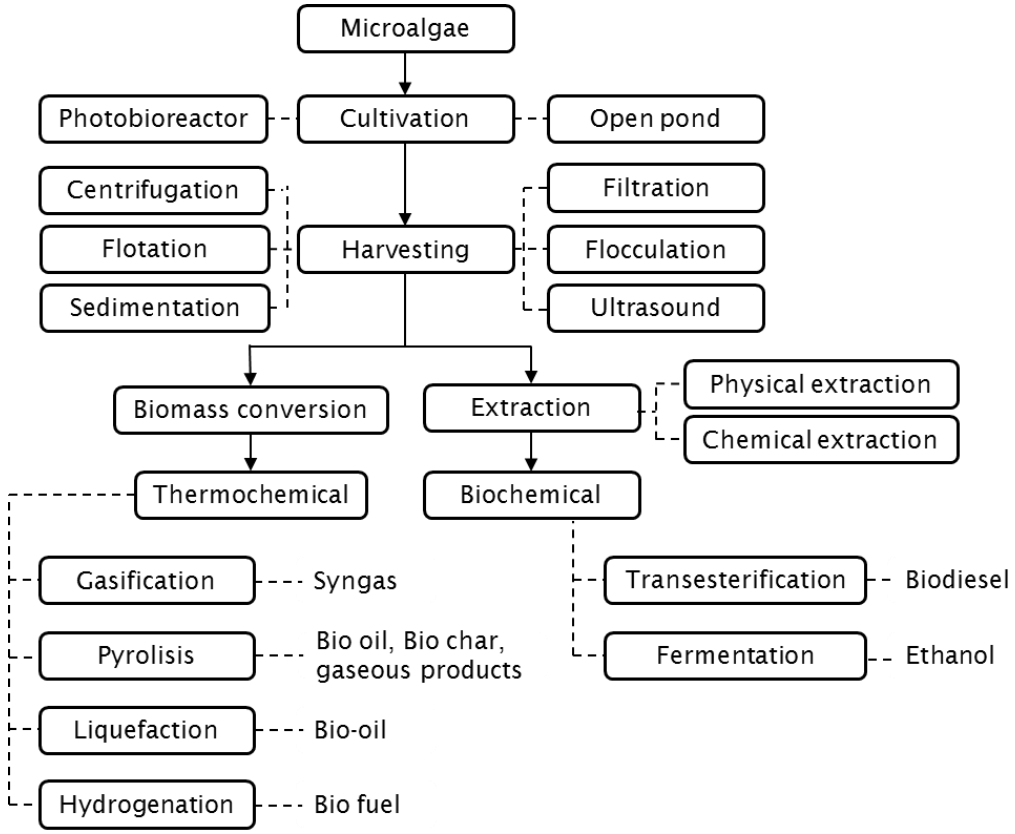

Figure 2.- A summary of microalgal transformations into biofuel. The main product of each process is shown at the end of the transformation route (Suali & Sarbatly, 2012)

Despite the multiple possibilities that microalgae derived biofuels offer, the industry faces major challenges to its competitiveness in the energy market, such as the high energy inputs required in all the steps necessary from the cultivation to the production of the biofuel (harvesting, dewatering of biomass, lipid extraction and conversion processes), or the dependence on fertilizers to maintain biological activity and growth. Any effective industrial process must reduce or eliminate these overheads associated with the biofuel production cycle, trying to combine high efficiency technologies with new production systems. The use of wastewater as a nutrient source in microalgae cultures, linked to chemical or physical separation processes, could help to overcome the obstacles associated with biofuels production, and this has been specially studied in the production of biodiesel and biogas (Chisti, 2007; de la Noie et al., 1992; Schenk et al., 2008; Sialve et al., 2009).(Pittman et al., 2011).

2.3.1 Biodiesel

The technology for producing and using biodiesel has been known for more than 50 years (Chisti, 2007). It is based on the transesterification reaction (Figure 3) in which 1 mol of triglycerides is reacted with 3 mol of alcohol (usually methanol), producing 3 mol of methyl esters of fatty acids (biodiesel) and 1 mol of glycerol as co-product, although industrial processes use 6 mol of methanol for each mol of triglyceride to ensure that the equilibrium in the reaction is driven in the direction of the products (Fukuda et al., 2001). Some authors describe the possibility of using different substances as catalysts in the reaction: acids, alkalis (Fukuda et al., 2001; Meher et al., 2006) and lipase enzymes (Sharma et al., 2001). It is expected the same process will be used for algal biodiesel, since some authors have reported lipids concentrations in specific microalgal species in the laboratory up to 60-70 % (Chisti, 2007; Liang et al., 2010; Metzger & Largeau, 2005; Pienkos & Darzins, 2009) , although the more commonly quoted figure is below 25 % (Becker, 1994; Becker, 2007; Brown et al., 1997; Ketheesan & Nirmalakhandan, 2012). From this total lipid composition, up to 70 % corresponds to triglycerides (TAG) that can potentially be used for biodiesel production (Eichenberger & Gribi, 1997; Sun et al., 2011).

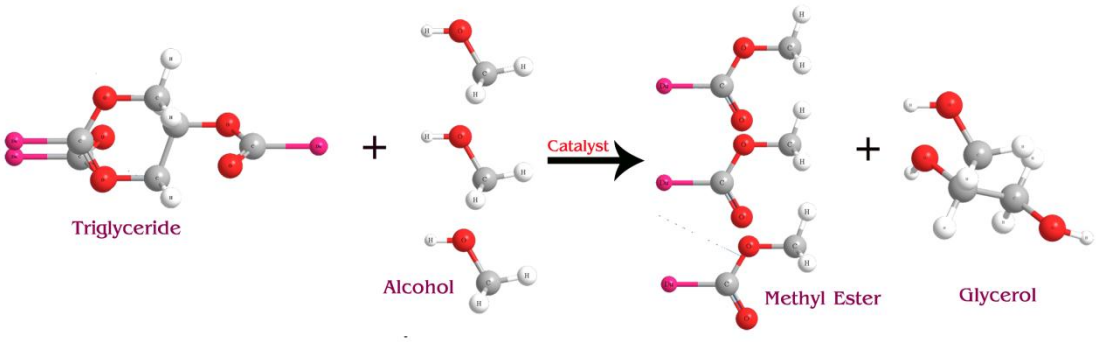

Figure 3.- General transesterification reaction of triglycerides (UI)

An estimate of the potential of microalgae as a source of lipid is shown in Table 3, where a comparison was made with other traditional oil sources (Chisti, 2007). In column 2 the oil yield in litres per hectare is presented for different crops and for two scenarios in the case of microalgae, with 70 % and 30 % of oil in weight. Following Chisti, between the presented crops, oil palm seems to have the better oil yield but this yield is 10 times lower than the yield of microalgae with only 30 % oil. Column 3 shows the land area needed to meet 50 % of current transport fuel needs in the United States and column 4 it is possible to see what percentage this land is of the total existing cropping area in the country. According to this study, using oil palm would require 24 % of the existing US cropping area, while for microalgae this percentage decreases to less than 3 %. This optimistic scenario presented by reputed scientists in the field shows up the potential of microalgae as oil source, although it seems difficult to meet the current transport fuel requirements with the sum of all the biodiesel produced from different sources: oil crops, waste cooking oil, animal fat and microalgae. In addition, the high biomass productivity in photobioreactors in which is based the calculation showed in Table 3 do not take into account the costs of biodiesel production in comparison to fossil fuels. The confluence of high productivities and low cost production is a challenge for the microalgae based technologies today and, at the same time, it is an opportunity for the scientific community to make new contributions to knowledge. Thus, even though its future is promising, the widespread cultivation of algae for energy purposes has a long way to go.

Table 3.- Yields and land area requirements of some sources of biodiesel

Crop	Oil yield (L ha^{-1})	Land area needed (M ha)[a]	Percent of existing US cropping area[a]
Corn	172	1540	846
Soybean	446	594	326
Canola	1190	223	122
Jatropha	1892	140	77
Coconut	2689	99	54
Oil palm	5950	45	24
Microalgae[b]	136900	2	1,1
Microalgae[c]	58700	4,5	2,5

[a] For meeting 50% of all transport fuel needs of the United States
[b] 70 % oil (by wt) in biomass
[c] 30 % oil (by wt) in biomass

Source: (Chisti, 2007)

Some researchers believe that the high productivity of microalgae per square metre and the possibility of selecting strains and modifying the cultivation characteristics to obtain a biomass rich in lipids, could potentially reduce the competition for land with other crops used in human nutrition (Fenton & hUallacháin, 2012; Schenk et al., 2008). Thus, it could be eliminated the ethical problems associated with the use of land for crops cultivation used as a raw material for fuel production in a global scenario where millions of people suffer poverty and famine. Furthermore, it has been suggested that algae farms could be located in areas not suitable for crops like deserts where the availability of water is reduced but with possibility of use sea water for marine strains of microalgae, emerging the possibility of create employment and wealth in those economically depressed areas and allowing greater access to fuel resources for all nations (Hannon et al., 2010; Moody et al., 2014).

The production cost of microalgae as a biofuel feedstock is high in relation to the final yield of the product, however, since microalgae need specific techniques for cultivation, harvesting, extraction and biomass conversion (Suali & Sarbatly, 2012). The microalgal biomass used in biodiesel production is based in its lipid content. Among the huge variety of microalgal species, the strains able to produce more lipids have a lower specific growth rate due to the cell biological configuration which uses available resources for producing secondary metabolites rather than for microalgae growth. This is an inevitable consequence of producing secondary metabolites rather than growth-related materials (Beardall & Raven, 2013).

2.3.2 Anaerobic digestion of microalgae: biogas production

The anaerobic digestion process is currently one of the most attractive possibilities available for creating a renewable source of energy from algal biomass (Ward et al., 2014). The solar energy converted and stored by the microalgal cells as a result of their photosynthetic activities can be transformed into usable energy through digestion of the microalgae to produce methane (Gouleke et al., 1956). Where the algae are grown on wastewater or other wastes, this is therefore part of the third generation of biofuels which are produced from non-food crops (Fenton & Ohuallachain, 2012). One of the main drawbacks of conventional activated sludge treatment is the high energy requirement of this technology, mainly in the oxygen supply for the degradation of organic matter and nutrient removal. Microalgae-bacteria mixotrophic cultures can produce by themselves the oxygen needed for the digestion of organic matter and the nitrification process, reducing the energy consumption (Figure 4) (de Godos et al., 2013). Some of the challenges of this technology are related to the low concentration of digestible biodegradable substrate, recalcitrant substrate constituents, cell wall degradability, low carbon to nitrogen ratio, ammonia toxicity and effects form salinity and associated metal ions (Ward et al., 2014).

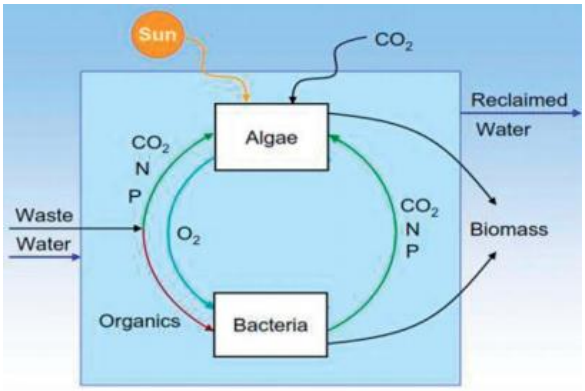

Figure 4.- Mixotrophic culture microalgae-bacteria (All-gas, 2010)

A number of different approaches to anaerobic digestion from microalgal biomass are possible depending on the overall biofuel production process to be carried out (Figure 5): direct anaerobic digestion after the concentration of the biomass, the digestion of disrupted biomass where the cell wall is broken to obtain some intracellular substances (generally lipids); and digestion of the

residual biomass obtained from biomass conversion of these intracellular substances into biofuel.

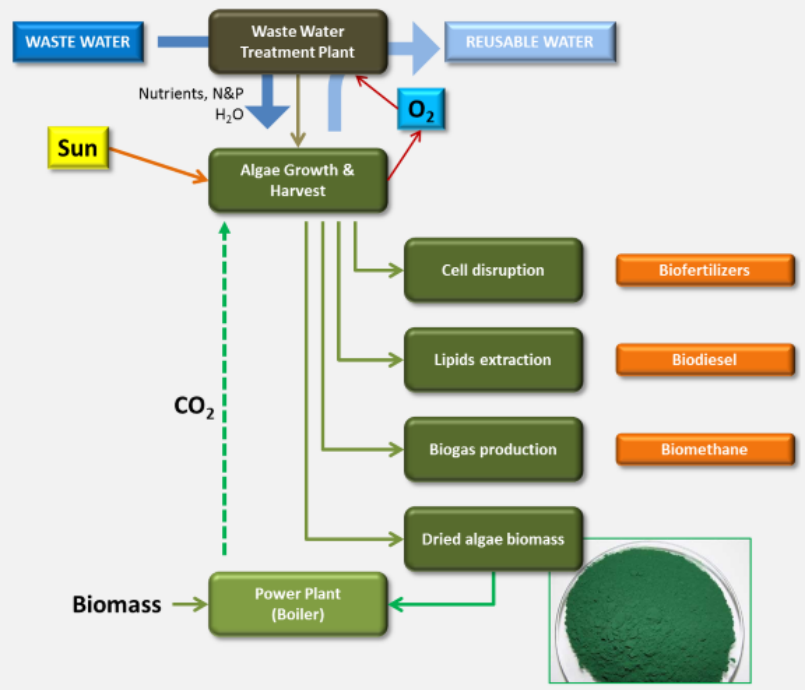

Figure 5.- Conceptual visualisation of anaerobic digestion incorporation into microalgal biofuel production (All-gas, 2010)

2.3.3 Nutrient requirements

Microalgae need inorganic nutrients to maintain their biological processes and to grow. A wide variety of recipes for fresh medium can be used, depending on the requirements of the microalgal strain or the desired conditions in the culture. For this purpose, it is possible to use ingredients from commercial fertilizers of agricultural quality to high purity substances (Jiménez et al., 2003), whose use is limited to laboratory scale or to the production of some high value compounds, as in the case of pure CO_2. At a large scale, fertilizers are normally used in closed photobioreactors for the growth of pure microalgal strains with special applications or containing valuable substances that can be isolated with applications in the fields of food, cosmetics and pharmacology (Spolaore et al., 2006).

The reduction of costs in microalgal production for energy purposes is essential for the success of this technology, however, and the use of fertilizers is associated with high production costs and, therefore, high disequilibrium

between algal-fossil energy sources. The use of microalgal-bacterial consortia for nutrient removal in the secondary treatment of wastewaters and biomass production with energy purposes (mainly biogas and biodiesel production) has being studied extensively during the last century, mainly in stabilization lagoons (Sutherland et al., 2013). In these processes, bacteria primarily decompose the organic constituents of the wastes. Then microalgae take these constituents to growth and, by means of photosynthesis, release oxygen to the culture medium that can be potentially used by the bacteria to oxidize wastes (De Schamphelaire & Verstraete, 2009). Some authors describe the use of industrial, agricultural or urban waste water as a source of ammonium, nitrate and phosphate for microalgae cultures (Craggs et al., 2012; Christenson & Sims, 2011; Gomez et al., 2013; Moo-Young & Chisti, 1994; Muñoz et al., 2009; Park & Craggs, 2010; Park et al., 2011; Sialve et al., 2009; Sutherland et al., 2013).

Whatever the origin of the nutrients or the use of the microalgae, the composition of any medium for microalgae cultivation must take into account the following points (Grobbelaar, 2004):

1. The total salt content determined by the original habitat of the microalgae species.
2. The cell ionic composition in components such as K^+, Mg^{2+}, Na^+, Ca^{2+}, SO_4^- and Cl^-.
3. The nitrogen sources: nitrate, ammonia and urea.
4. The carbon source: CO_2 or HCO_3^-.
5. pH.
6. Trace elements.
7. Vitamins.

In general, a complete recipe with all the necessary nutrients for microalgae growth should have about 30 different elements, including macronutrients and micronutrients. If the composition of the medium is adequate and the nutritional requirements of mass cultured microalgae are satisfied, mixing design to create a turbulent flow is the most important requirement to achieve high productivities of microalgal mass (assuming that other environmental conditions are not growth-limiting) (Grobbelaar, 2004). In addition, one of the main strategies to increase the concentration of lipids in the microalgae is based on the algae capacity for storage of lipids under

nutrient limitation when there is no requirement for the synthesis of new membrane compounds (Guschina & Harwood, 2006; Thompson, 1996).

2.3.4 Carbon supply

The mixture of gases in the atmosphere contains only 0.04 % CO_2.. Photosynthetic organisms use this carbon dioxide to obtain energy and maintain the biological processes involved in the production of cellular material, i.e. carbohydrates. In contrast to land plants, atmospheric CO_2 cannot satisfy carbon requirements of high yielding autotrophic microalgal production systems because microalgae are usually in an aqueous medium where the CO_2 has to be dissolved prior to its entrance into the algal cells. The solubility of CO_2 in water is approximately 1600 mg L^{-1} at ambient air temperatures (20 ºC) in a CO_2-saturated atmosphere and, taking into account the low concentration of CO_2 in air, there is a very low carbon input in the aquatic medium which at most can sustain productivities of around 10 g TSS m^{-2} day^{-1}; while rates as high as 70 g TSS m^{-2} day^{-1} have been reported by bubbling a gas enriched with CO_2 (Grobbelaar, 2004). Therefore, the low CO_2 concentrations present in atmospheric air are not sufficient for cell reproduction with high productivities. The optimum CO_2 supplementation and concentration in the medium depends on the strain of microalgae, and is an important factor because of its influence on the final composition (i.e. lipid concentration and lipid composition) and on biomass yield (Widjaja et al., 2009).

Once CO_2 is dissolved in water, a reaction takes place in which carbonic acid is formed. This weak acid is later dissociated into the hydrogen and bicarbonate ions following the reaction:

$$CO_2 + H_2O \leftrightarrows H_2CO_3 \leftrightarrows H^+ + HCO_3^- \quad (2)$$

Therefore, in aqueous environments, the inorganic carbon in water is present in the form of both CO_2 and HCO_3^-. CO_2 can enter the cells by diffusion across the plasmalemma, while cell membranes are essentially impermeable to HCO_3^- (Beardall & Raven, 2013). Only certain microalgae can also take up HCO_3^- (Giordano et al., 2005; Korb et al., 1997). During the photosynthesis reaction, microalgae take the CO_2 from the aqueous medium, increasing the pH of

culture. This will produce a decrease in the ratio of CO_2/bicarbonate as well as a reduction in absolute CO_2 concentration. Thus, a bicarbonate-carbonate buffer system is established from the equilibrium reactions that describe the interaction between CO_2 and H_2O shown in the following equations, of which Eq(5) and Eq(6) correspond to the first and second dissociation of carbonic acid, respectively:

$$CO_2 + H_2O \leftrightarrows H_2CO_3 \quad (3)$$

$$H_2CO_3 \leftrightarrows H^+ + HCO_3^- \quad (4)$$

$$CO_2 + H_2O \leftrightarrows H^+ + HCO_3^- \quad (5)$$

$$HCO_3^- \leftrightarrows H^+ + CO_3^= \quad (6)$$

Then, the inorganic C exists in the water in four different forms: CO_2, H_2CO_3, HCO_3^- and $CO_3^=$. These species are the main buffering system in water and their relative presence or concentration in equilibrium is highly dependent of the pH of the medium, as is represented in Figure 6. Therefore, the proportion of ionic species from carbon dioxide is significantly altered by pH: at pH <6 CO_2 is the dominant specie, while at pH values between 7-9 HCO_3^- is dominant and $CO_3^=$ increases considerably at pH >9.

The consumption of CO_2 by microalgae is linked to the subsequent increase in pH of the medium. Thereby, when pH 8-9 is achieved, there is no available CO_2 in the medium and if algae cannot take up HCO_3^- the photosynthesis reaction will be stopped. Taking into account that most of the common algae species grow at this pH, the low CO_2 concentration could potentially stop the growth. For this reason they have adapted to these conditions by developing a system called the carbon concentrating mechanism used when the CO_2 concentration in the environment is very low and is not enough to saturate the Rubisco enzyme involved in the first phase of photosynthetic carbon fixation. In these conditions, they are able to take bicarbonate and convert it into CO_2 which enters the cells and, if it does not go straight to the chloroplast, is converted again into bicarbonate and is stored. Therefore, the rubisco cannot convert inorganic carbon into organic carbon if

the source is bicarbonate because it requires CO_2, but the algae can use bicarbonate that is inside the cell and convert it into CO_2 that can be used in photosynthesis. This pathway requires more energy than using CO_2, however, and therefore a high concentration of CO_2 will enhance growth (Borowitzka, 2013). Thus, the addition of an extra supplement of CO_2 is necessary in high density cultures and the best strategy for this is the direct bubbling on demand of a gas rich in CO_2 into the culture medium to maintain the pH at the desired level and, at the same time, for the addition of CO_2 used in the photosynthesis reaction. It has been also reported that the implementation of an advance system for pH control allows improvements in the efficiency of the CO_2 exchange by diminishing the carbon input and losses (Berenguel et al., 2004). In this connection, Pawlowski noted that the use of Model Predictive Control (MPC) allows minimization of the pH gradients to which the cells are exposed in the reactor, increasing the biomass concentration by around 30% and obtaining better biomass productivities than the on/off control scheme (Pawlowski et al., 2014).

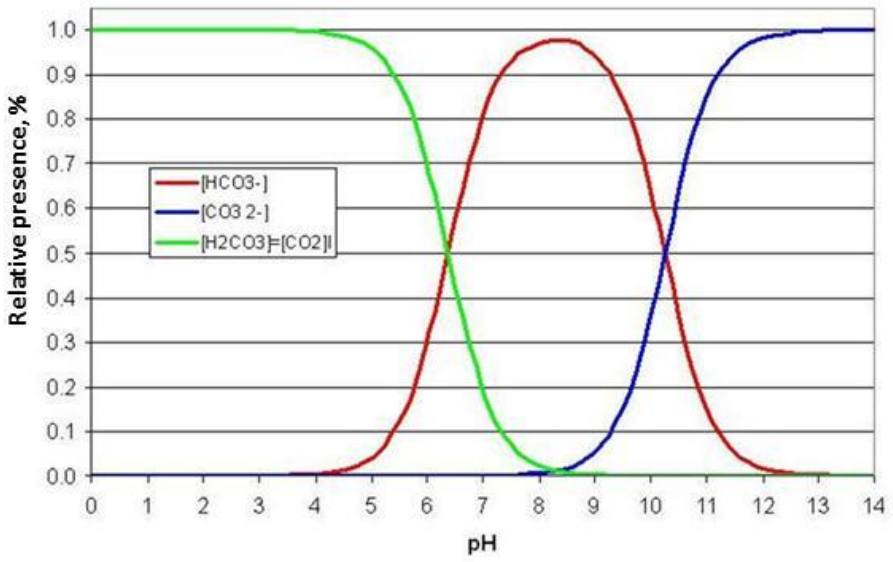

Figure 6.- Chemical equilibrium of dissolved inorganic carbon species as a function of culture medium pH

In the photosynthesis reaction, water is broken down into H^+ and OH^- to produce a series of biochemical reactions aimed at the reduction of CO_2 to organic carbon (carbohydrates) by means of the energy contained in the light. This process is divided in two stages: light and dark reactions. In the light reactions, the light energy harvested by chlorophyll molecules is converted to

chemical energy providing a biochemical reductant $NADPH_2$ and a high energy compound ATP. In the dark reactions, this reductant and ATP are used in the reduction of carbon dioxide to carbohydrates. To fix one molecule of CO_2 two $NADPH_2$ molecules and three ATP are needed, as shown in Figure 7. The necessary energy for this mechanism, is provided by the absorption of 8 light photons (Park et al., 2011). This means light is essential in the photosynthesis reaction and, in situations when there is no light to maintain biological activity, microalgae obtain the energy from organic reserve compounds kept inside the cellular structure (Masojidek, 2004). This is the respiration process. Those compounds are oxidized to produce CO_2, water and energy as ATP to supply the cell's physiological necessities in the so-called cellular photorespiration process.

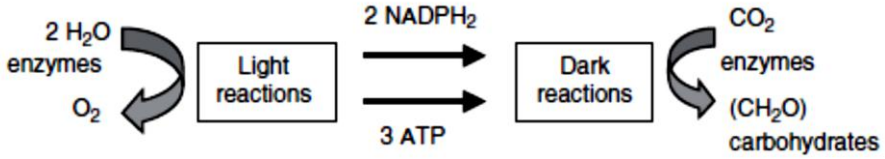

Figure 7.- Major reactions and products in photosynthesis (Masojidek, 2004)

Microalgae fix CO_2 by means of the enzyme Rubisco (ribulose bisphospate carboxylase/oxygenase) in the dark reaction using the $NADPH_2$ and ATP produced in the light reaction of photosynthesis (Eq(7)). The process consists of a series of chained equations that constitutes the Calvin Cycle.

$$CO_2 + 4\ H^+ + 4\ e^- \xrightarrow{2\ NADPH_2, 3\ ATP, enzymes} (CH_2O) + H_2O \qquad (7)$$

The enzyme Rubisco has two competing functions: carboxylase and oxygenase. This means that, depending on the situation, this enzyme can catalyse the photosynthesis reaction using CO_2 as substrate to produce energy or, on the other hand, catalyse the opposite photorespiration process in which organic carbon is converted into CO_2 without any metabolic gain. Competition between both functions is regulated by the relative concentration of oxygen and carbon dioxide present in the culture. Thus high O_2/CO_2 ratios promote the photorespiration process, whereas low ratios favour carboxylation. The affinity of rubisco to CO_2 is low and under high irradiance, high oxygen concentration

and low CO_2 concentration, the equilibrium in the reaction is shifted towards photorespiration (Masojidek, 2004). This explains the use of gases rich in CO_2 in microalgae cultures, since a high ratio CO_2/O_2 promotes the photosynthesis reaction and enhances algal growth. Furthermore, photosynthetic oxygen tends to accumulate in the culture at supersaturated concentrations, favouring the photorespiration process and causing an inhibitory effect in cell growth. For this reason, oxygen is usually stripped from the culture to minimize this phenomenon.

2.3.5 Mixing

Mixing or turbulence is one of the major external parameters directly related to the productivity and energy consumption in photobioreactors for microalgal culture (Soeder & Stengel, 1974). A high degree of mixing generally stimulates growth due to better distribution of nutrients in the culture, and to promotion of the interchange of cells between dark and light zones. High mixing is usually linked to high energy consumption, however, since elements that introduce mixing in the system at the same time produce head losses that must be compensated by the mechanical device used for culture circulation. Therefore, it is necessary to study both phenomena together to optimize an intermediate solution where mixing is enough to stimulate the productivity but, on the other hand, must not be associated with a non-acceptable power requirement that could adversely affect the energy balance of the system.

Although mixing and velocity are two concepts that are not necessarily linked, the term mixing speed has been suggested in the literature (Benemann & Oswald, 1996) as a minimum velocity needed in the reactors to prevent the sedimentation of microalgae. The energy necessary to achieve this speed will therefore be the minimum, and an increase of velocity will produce an exponential increase in the power consumption with no guaranteed improvements in the mixing. Mixing is created in the reactors by the turbulence of the fluid when circulating, and it has several consequences (Oswald & Gouleke, 1960):

- It breaks down possible diffusion barriers that may limit microalgal cell metabolism and, therefore, promotes nutrient uptake.

- Prevents thermal stratification and allows gas exchange with the atmosphere (mainly oxygen release), and prevents bottom anaerobiosis.
- Increases the frequency of dark/light cycles in the cells, potentially improving photosynthetic efficiency by reducing the adverse effects of photoinhibition and photolimitation phenomena.

Despite the fact that the large influence of mixing in microalgae growth has been observed, it has not been studied exhaustively at large-scale in outdoor cultures (Gates & Borchardt, 1964; Persoone et al., 1980; Weissman et al., 1988). Recent studies based on a particle tracing methodology have been conducted to predict and examine the distribution and mixing of algae cells in algae ponds, pointing out the effectiveness of the adequate raceway design and operation (paddlewheel, water depth, raceway size, etc.) in the mixing (Ali et al., 2014). On the other hand, Prussi (Prussi et al., 2014) used Computational Fluid Dynamic analysis to investigate the flow field of the culture in the raceway and define the level of vertical mixing by sections. It was found that algae tend to settle in long straight sections due to the poor vertical mixing, while in bends the changes in flow direction caused vortexes that increased the mixing. No experimental information is given, however, about the effect of paddlewheel in the flow and the use of sumps and baffles to increase the mass transfer efficiency of the system is obviated. The use of air-lift driven raceways for liquid circulation and mixing has also been suggested (Ketheesan & Nirmalakhandan, 2011; Ketheesan & Nirmalakhandan, 2012), although in this kind of system in which the turbulence is provided by means of air bubbling mass transfer phenomena take place between the culture medium and the air bubbles causing a loss of CO_2 from the medium to the air bubbles reducing the CO_2 mass transfer efficiency (Rodríguez-Maroto et al., 2005). Nevertheless, the choice of culture circulation and mixing system is a parameter that still needs to be evaluated (Prussi et al., 2014) and the introduction of new devices in the system with the aim of increasing the productivity have to be carefully evaluated in terms of mixing and power consumption. Recently, the All-gas project (All-gas, 2010) co-financed by the EU Commission within the FP 7 programme and led by the Spanish company Aqualia with the participation of the University of Southampton among others, is looking at this issue as part of the demonstration of sustainable production of bio-fuels based on low cost microalgae cultures at a large scale. The deep

study of current technologies and the development of new efficient systems for water motion in raceways is a challenge that, definitively, has to be analysed for the success of this technology.

2.3.6 Light, temperature and pH

Energy for photosynthesis is based on the capability of microalgae cells to capture light. From the whole electromagnetic spectrum, only a small fraction between 380 and 750 nm corresponds to the visible part (Figure 8). A section of this range of visible light between 400 to 700 nm, delivered in the form of photons, corresponds to the photosynthetically active radiation (PAR). The radiation outside this range is not used in photosynthesis. Light is often measured as total energy per unit of area, e.g., W m^{-2} or J m^{-2} s^{-1}. This parameter is called irradiance, and the conversion to number of photons incident on a surface, which is the parameter that determines the photochemical reactions, is 1 W m^{-2} equals about 4.5 µmol photon m^{-2} s^{-1} (Masojidek, 2004).

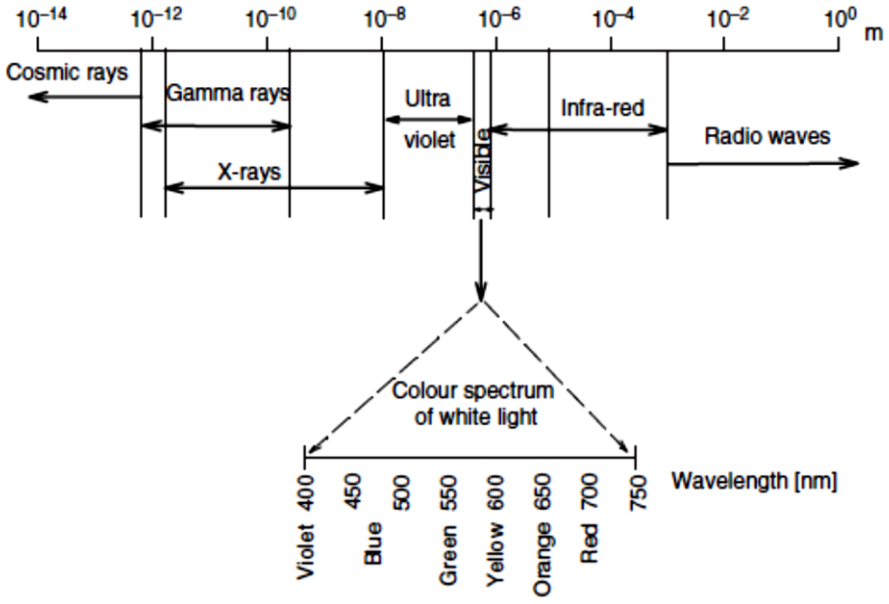

Figure 8.- Spectra of electromagnetic radiation and spectral pattern of visible light (Masojidek, 2004)

The use of sunlight as free natural energy source is limited by its availability due to weather conditions, diurnal cycles and seasonal variations. For this reason, outdoor commercial facilities must be located in high solar

radiation areas, since light is generally the limiting factor (Dismukes et al., 2008). Covered reactors would result in high temperatures, which would kill all but the most heat tolerant microalgae species, in addition to the expensive cost of the cover (Benemann & Oswald, 1996). Depending on the strains and the conditions of the culture, the optimal light intensity is variable but, in general, is in the range 50-600 μmol m^{-2} s^{-1} (Hsieh & Wu, 2009; Illman et al., 2000). In this range, the final condition of light and temperature determines the composition of the microalgal biomass obtained. Temperature affects the degree of fatty acid saturation, with low temperatures generally increasing the proportion of unsaturated fatty acids in microalgae, although the response is different for every strain (Harwood, 1998). On the other hand, high light intensities usually cause oxidative damage of polyunsaturated fatty acids (Fabregas et al., 2004) and lead to reduced photosynthesis, increased respiration and reduction in productivity. This is the photoinhibition process, which produces photo-damage in the cells that must be repaired and has a metabolic cost to the microalga (Borowitzka, 2013). Figure 9 shows the influence of sunlight intensity on specific growth rate of a microalgal culture. It is possible to see how the photoinhibition phenomena take place at light intensities only slightly higher than the intensity at which the specific growth rate peaks. Therefore, the reduction of the photoinhibition process and the exposure of microalgae cells to a light intensity close to this that gives the maximum specific growth rate could potentially increase the productivity of the microalgae culture.

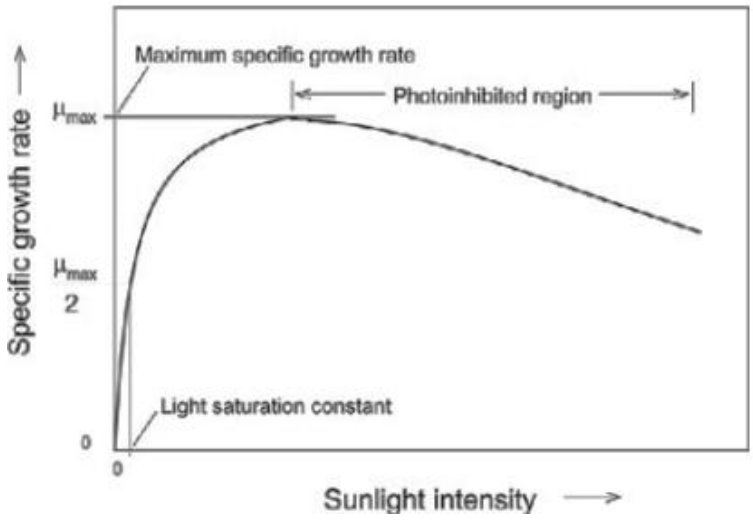

Figure 9.- Effect of light intensity on specific growth rate of microalgae

The concentration of cells determines the optimal light intensity, since in cultures with high concentrations self-shading occurs which considerably reduces the amount of effective light arriving in deeper zones of the culture. For this reason, the light distribution is a critical aspect that must be taken into account in the design of reactors for algae growth. In tubular photobioreactors, for example, criteria such as the orientation or size of the tubes are very important in order to maximize the light distribution in the reactor and improve the efficiency of light capture. In raceway reactors, the operational depth is the main variable that influences the use of light by microalgae, since there is a light profile from the surface of the culture, where the radiation is at a maximum, to the bottom of the channel, where there is a dark zone. The depth of this dark zone depends on the concentration of the microalgae, since the penetration of light is lower when the cell concentration is high. Beardall et al. (Beardall & Raven, 2013) found that in optically dense cultures with concentrations around 1 g m^{-3}, approximately 90 % of the photons would be absorbed in the first 10 mm by algae suffering severe light inhibition, and so using photons very inefficiently. That means that the rest of the culture could use the rest of the light very efficiently, since they are not affected by photoinhibition phenomena. In practice, however, since most of the photons are absorbed in the low efficiency upper layer, the remaining cells are in darkness and are therefore light limited despite their high photons absorption potential. The level of photoinhibition in an algal culture outdoors can be reduced to some degree by managing the cell density (i.e. the average irradiance received by the cells), but some degree of photoinhibition during the day is inevitable (Kromkamp et al., 2009; Lu & Vonshak, 1999; Richmond, 2004a).

The objective in a dense culture is to ensure efficient light utilization by reduction of photoinhibition phenomena and improvement of light distribution in the cell broth. To achieve this, different approaches have been studied (Beardall & Raven, 2013):

- Reducing the self-shading in the culture by using short optical pathways. This is to reduce dark zones in low depth cultures. This is not a solution for the photoinhibited upper layer, but it has been demonstrated that it is possible to achieve high density and production.

- Microalgae are able to adapt their characteristics to the environment in which they are growing. In high light situations, microalgae can reduce the size of their light harvesting antennae to attenuate the effect of photoinhibition in the cell. This situation allows more light to penetrate into the culture, increasing the efficiency of use of incident photons and therefore the areal productivity.
- Optimization of turbulence in cultures could potentially also increase the productivity of reactors. The CO_2 fixation process is much slower than the photon capture in microalgae, so only a part of the photon flux that arrives to cells in high irradiance situations is effectively used in CO_2 fixation processes, the rest of the photons being wasted. Therefore, high efficiency in light capture is linked to the capacity of algae of use this energy effectively, i.e. linked to CO_2 fixation, by means of optimization of dark/light periods for cells in well mixed systems.

At laboratory scale, lamps are often used to provide artificial light to cultures. Thus, it is possible to have a complete control of the light intensity applied to the algae, the proportion of the light/dark cycle and the temperature of the culture, at every moment and whatever the conditions of the culture (Suali & Sarbatly, 2012). In pilot and industrial plants, however, the reactors are located outdoor and the external conditions influence the culture. The temperature and light are dependent on the weather and change from day to day. Although microalgae have the capacity of adaptation to seasonal characteristic parameters, it must be accepted that mild temperatures during the whole day (including daylight and night) and longer daylight periods, favour algal growth and the achievement of high productivities. Thus, generally, spring and the end of the summer are typically the periods of the year with better climatic conditions for the culture of algae, while in summer (due to its high temperatures, depending on the location of the reactor) and mainly in winter microalgal production decreases drastically. Depending on the geographical location, the algae must be able to tolerate a range of temperatures that may reach 35-40 ºC in outdoor ponds or even higher in closed photobioreactors unless cooled, with great differences between maximum and minimum temperatures during the day. For example, an experiment carried out with *Spirulina* in a 450 m^2 open raceway pond located

in southern Spain between September and July revealed a maximal temperature of the culture at mid-day of 28 ºC in July (20 ºC average between spring and autumn), while the minimal recorded temperature was 9 ºC in December (12 ºC average in winter) (Jiménez, 2003). For this, the identification of local strains or other strains whose optimal growth physicochemical parameters fit well with local climate conditions could help in resisting the extreme conditions achieved, taking into account that the lethal and optimum temperatures usually do not differ significantly (Borowitzka, 1998). Jimenez studied in an earlier work the viability of the industrial production of *Spirulina* in the same area (Jiménez et al., 2003), finding that the cultivation of this strain in open raceway ponds was satisfactory above 15 ºC and that its commercial production may be feasible at this location at least 9 months per year. This author revealed the importance of the strain selection for a particular culture system at a definite geographical location and its implication in the profitability of the production. This is more important in large-scale outdoor culture where temperature control is technically difficult and economically unfeasible. Beyond local algae, there are some identified algae which tolerate a broad temperature range, including the temperature achieved in warm areas during daylight hours and its adaptation to lower temperatures during the coldest months of the year (Borowitzka, 1998; Goldman, 1977).

2.3.7 Accumulation of dissolved oxygen

During the photosynthesis reaction, oxygen is produced as a product and competes with CO_2 as substrate for Rubisco (Badger et al., 1998). This oxygen is released by the algal cells into the aqueous medium that contains them, and in dense cultures oxygen supersaturation rapidly occurs where photosynthesis is significantly inhibited by the high O_2 concentration, especially at non-optimal temperatures (Raven, 1997; Ugwu et al., 2007; Vonshak et al., 1994). Once the oxygen is in the medium, the net rate of desorption from the liquid phase (the culture) to the gas phase (the atmosphere) is low, as the production of oxygen in the photosynthesis reaction is higher. As a result, there is a process of oxygen accumulation in the reactor which has an inhibitory effect on the microalgal growth. Depending on the reactor configuration, the exposure of the surface of the culture to the atmosphere favours the outgassing of this dissolved oxygen (DO). It may be thought that raceway open reactors have a

high capacity for DO desorption, since they have a high surface area per volumetric unit of culture which allow the outgassing of oxygen from the liquid phase to the atmosphere. It is true that this desorption capacity is necessarily higher in raceways than in closed systems like tubular reactors, where this culture/atmosphere contact does not exist. This reactor configuration, however, is not enough for desorption of high amounts of photosynthetic oxygen produced, mainly at midday when the solar radiation is higher and the rate of the photosynthesis reaction is accelerated. High oxygen concentration in raceways and photobioreactors is a major limiting factor on algal productivity (Kliphuis et al., 2011; Ogawa et al., 1980). Thus, if high productivities are desired, it is absolutely necessary to design devices for an efficient oxygen removal whatever the configuration of the reactor, and to try to find strains whose Rubisco is less sensitive to oxygen.

2.3.8 Harvesting

Harvesting is one of the technical challenges of microalgal cultivation, since it is an important percentage of the total production costs (Uduman et al., 2010). This is due to the huge volume of culture that must be treated to separate its biomass content, typically around 1,000,000 L ha^{-1} day^{-1} (Benemann & Oswald, 1996); and due to the added difficultly caused by the microscopic size of the algae and its low concentration in the culture. Therefore, the design of an efficient harvesting process with high concentration factors allows the adequate scale-up of the required equipment.

Microalgae flocculation and followed by a settling process seems to be a good option for microalgae harvesting. The use of chemical flocculants induces the formation of aggregates called flocs, formed when the solute particles collide and adhere to each other. A wide variety of flocculants are available on the market, with different properties to fit the requirements of the flocculation process. In general, it has been observed that the use of metal salts or chitosan was not efficient, whereas polyelectrolytes used in wastewater treatment processes allow the efficient recovery of biomass, at doses of 2-25 mg g^{-1} biomass (Granados et al., 2012).The required doses depend on the particular polyelectrolyte and microalgae strain, but cationic polyelectrolytes are generally recommended, with concentration factors higher than 35 in most cases (Granados et al., 2012). This is because microalgae can generally be

considered as particles whose stability is due to surface charge, which is electronegative for pH values of 2.5-11.5 (Uduman et al., 2010). Other characteristics also affect the stability of the flocculation process such as steric effects (due to water molecules bound to the microalgal surface), or the presence of absorbed macromolecules or extracellular organic matter, making it difficult to name a single technique as the best for microalgal recovery (Vlaski et al., 1997). The stability of these microalgal suspensions is, therefore, dependent on the interactive forces between the particles themselves and the particles and water. Other techniques used for dewatering are (Uduman et al., 2010):

- Centrifugation: Use of centrifugal forces to separate solids and liquids based on the particle size and density difference of the medium components. It is possible to obtain high separation rates in a short period but it requires high investment and operating costs.

Figure 10.- Continuous centrifuge Alfa Laval Clara 15. University of Almeria, Spain

- Filtration: Use of a permeable medium which retains the solids and allows the liquid to pass through. It requires a pressure drop to be applied across the system in order to force the fluid through the filter and regular backwashes of the filter. There are different filters made of different materials and with different pore sizes depending on the size of the cells that have to be retained. Some examples are diatomaceous earth, sand or cellulose fibre filters.
- Gravity sedimentation: Separation in lamella separators or sedimentation tanks by natural gravity to obtain a concentrated slurry and clear liquid from the original culture. The feeding and

the exit of clear liquid are continuous while slurry is removed discontinuously, the energy needed to pump the slurry being the only energy required in the process. The addition of flocculants improves the efficiency of separation, as well as the presence of algae cells with high densities.

Figure 11.- Gravity sedimenter. Blue column is a mixing column where the culture broth is previously mixed with the flocculants. University of Almeria, Spain

- Flotation: the opposite process to sedimentation. A gas is bubbled in the culture and the cells attach to the gas bubbles. Therefore, solid particles are driven by the gas to the top, where they accumulate and the sludge containing the biomass is separated from the clear liquid. In that case, the lower the particle size is the higher separation efficiency.
- Electrophoresis techniques: The use of chemicals to help biomass flocculation has the disadvantage of potential contamination of the medium, which in most cases should be recirculated to the culture after the separation process. For this, the use of electrolytic methods offers an alternative based on the ability of the microalgae to act as colloidal particles which can be separated from water-based medium solutions by movement in an electric field.

2.4 Culture systems

2.4.1 Photobioreactors

Microalgae are produced in special reactors equipped with the necessary instrumentation and characteristics for the growth of photosynthetic microorganisms. These consist of a device able to give adequate conditions for algae grown from a small volume to be used as inoculum up to the entire volume of the reactor. In general, all reactors include a vessel containing the culture and constituting the reactor itself; an agitation system to ensure mixing in the reactor; a control system for maintenance of the pH in the desired range; a nutrient input system including both fertilizers in liquid medium and gaseous phase; and a culture output system which must pass the culture and biomass to the subsequent harvesting system to separate the microalgae from the liquid medium. Usually, reactors for microalgal growth are called photobioreactors because the term 'photo' makes reference to the capacity of the reactor to receive light from its surrounding, as is necessary for the processes taking place inside. On the other hand, the term 'bio' refers to the biological nature of the processes taking place inside, some of them competing with the algal growth and reducing the productivity of the system. In large-scale algal culture, there is a risk of contamination by parasitic organisms which can become predators of the microalgae. These are animals and plants without chlorophyll which do not have the ability to form organic matter by photosynthesis, and have to live at the expense of green plants like algae that make their own food. Therefore, photobioreactors do not usually contain only algae, but also a wide variety of microscopic animals called protozoa, microscopic aquatic plants such as moulds, and yeast and bacteria that may limit biomass productivity due to their competing requirement for organic carbon (Burlew, 1976). Various different types of photobioreactor are used, with different configurations and characteristics. Parameters such us the final use of the biomass, its quality or the production costs, determine the selection of the suitable reactor in each case.

Open systems: these are open to the atmosphere, with no material covering the culture surface to separate it from its surroundings. The main advantage of this reactor type is its low cost, both in construction and operation. The power consumption is low in comparison with other reactors

and the solar radiation availability is high, since there is no separation from the ambient light, avoiding attenuation in the construction material itself or due to the accumulation of dust on the surface. On the other hand, precisely because the reactors are open, they are more exposed to possible external contamination. Moreover, climatic variations have a considerable effect on the culture conditions, making control very complicated and decreasing the damping capacity of the system to adapt to changes. Some examples of this kind of reactors are raceways ponds, thin layer reactors and inclined or cascade systems where mixing is achieved through pumping and gravity flow.

Figure 12.- Examples of open systems for microalgae cultures (University of Almería, Spain). Left: thin layer raceway. Right: cascade raceway

Closed systems: In practice, the term photobioreactor is normally used for this type of reactor, and uncommon for open systems. Unlike open reactors, cultures contained in closed systems are isolated from the outside in special vessels (photobioreactors). Thus, the main advantage of this reactor type is the possibility of working with pure culture with lower risk of contamination and better control of culture parameters. This results in a more stable culture and in higher productivities. The cost of biomass production is much higher, however, due to the higher construction costs and power consumption. As a result, this type of reactor is only suitable for the production of high value biomass for pharmaceutical, nutrition or cosmetic purposes looks suitable for production in this kind of reactors. These reactors receive light in two ways: one part is directly lit while the other part receives diffuse radiation. This is another important difference from open reactors that receive only direct light, and the design of closed reactors must pay special attention to diffuse radiation in terms of the configuration and final orientation of the reactor. Typical examples of closed reactors are tubular reactors (vertical

and horizontal) and flat panels, although bubble columns are also commonly used, mainly for the growth of inoculum.

Figure 13.- Examples of closed systems for microalgae cultures (University of Almería, Spain). Left and right up: bubble bag column and vertical tubular photobioreactors. Right down: Horizontal tubular photobioreactor

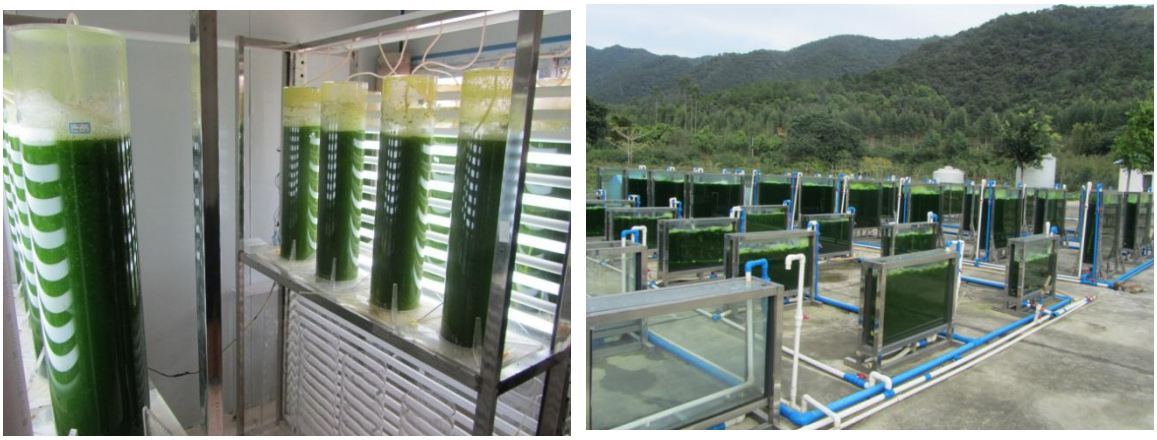

Figure 14.- Examples of closed systems for microalgae cultures (Foshan Innovation & Incubation Center of Renewable Energy Technology, China). Left: Indoor bubble column for inoculum growth. Right: Outdoor flat panels

The design and operation of the reactor has an enormous influence on the characteristics of the final biomass and, therefore, on the energy and economic balance of the process. It is estimated that around 25 % of the recoverable energy yield depends on the cultivation approach (Suali & Sarbatly, 2012). Obtaining a microalgal biomass with high lipid content is not a guarantee of economic success in the biofuel production process, since the capital cost is high. Some authors says that in energy terms the direct anaerobic digestion of the whole biomass may be more effective than other processes based on the concentration, drying and extraction of suitable compounds of the microalgae cell to produce other kind of biofuels, since it omits a processing step being a more straightforward process of producing energy (González-Fernández et al., 2012; Gouleke et al., 1956; Ward et al., 2014). In summary, the costs are today a huge obstacle to the development of this technology and the production of algal biofuel (Alabi et al., 2009; Sheeman et al., 1998).

Besides optimal engineering and design of the reactor, there are other techniques which could increase the biomass and, if desired, the lipid production ratio by more than 10-fold. These techniques are based on changing the phycological metabolism of the microalgal cells by manipulating the culture conditions and nutrient feed in order to achieve firstly a high concentration of biomass (high number of cells in the culture) and, once the culture is concentrated, increase the lipid content in the cells by means of nutrient limitation or excess in the culture medium (Suali & Sarbatly, 2012).

A variety of different reactor types can be used for a successful microalgae production, from tubular to flat panels or raceways (Posten, 2009). At a commercial scale, however, raceway reactors are the most common and have been used for the large-scale production of *Spirulina* and *Dunaliella*, as well as at smaller scale for other strains, due to their flexibility and easy scale-up (Jiménez, 2003; Moheimani & Borowitzka, 2007; Moreno, 2003; Radmann et al., 2007; Richmond & Cheng-Wu, 2001). Despite the development of many alternative systems for algal cultivation, including tubular and flat plate photobioreactors, bubble columns and thin layer culture systems, the raceway reactor still remains the only large-scale engineered system capable of biomass production at a commercial scale, especially for microalgal energy production (Grobbelaar, 2012; Jorquera et al., 2010; Mata et al., 2010).

2.4.2 Raceways

The use of raceways or high-rate algal ponds for algal production was suggested by Oswald and Gouleke more than fifty years ago (Oswald & Gouleke, 1960; Oswald & Gouleke, 1968) and, although engineering aspects of the design were evaluated by Weissman (Weissman et al., 1988), current reactors still follow the principles established then. In fact, these reactors are sometimes known as Oswald ponds, in honour of their inventor who started to use them for wastewater treatment which is one their main applications, besides the production of edible biomass (Craggs et al., 2012; Richmond et al., 1990). The aim of raceways is to imitate the processes that occur in lakes and ponds where microalgae grow by themselves, but modifying the necessary parameters in order to accelerate the natural process and to enhance the productivity of the system.

Figure 15.- Different raceway reactors (University of Almería, Spain)

The low initial financial investment necessary in the construction and operation of raceways compared to other photobioreactors has triggered the popularity of raceways as 'low cost' reactors. They are suitable for microalgal production with relatively low construction costs and a small energy requirement for mixing, which may be on the order of 4 W m^{-3} (Jorquera et al., 2010). For these reasons, raceways have been proposed as the most feasible system for microalgal energy production (Jorquera et al., 2010). In fact, it is calculated that in 2013 more than 99 % of microalgae produced commercially were cultivated in open ponds, with raceway types being the dominant cultivation system (Benemann, 2013). Water velocities of between 20 and 30 cm s^{-1} are most commonly used (Borowitzka & Moheimani, 2013), since the

energy input must provide adequate mixing for the maintenance of cells in suspension, and prevent thermal stratification in the reactor with the minimum power consumption.

The concentration of cells in the culture causes turbidity producing, thereby, different light conditions depending on the depth. Thus, the surface is the zone where the light is more intense and the phenomenon of photoinhibition could occur due to excess light, which passes through the culture being progressively absorbed (depending on the turbidity of the culture) until reaching a dark zone at the bottom of the channel. In consequence, the working depth of raceways is an important parameter that has to be considered, since an adequate light distribution will increase the productivity of the system. Raceways usually work with depths between 10-30 cm (Weissman & Goebel, 1987). Mixing has an important role also in light distribution because a suitable mixing will favour the radial movement of the cells from the bottom of the reactor to the surface, where the light is available, and vice versa. This movement is repeated continuously producing light/dark cycles in the cells. This cycling in the culture broth is important for the exposure of all cells to at least some light and, more importantly, to prevent or reduce photoinhibition of those at the top. Therefore, mixing has a key role in the performance of the system and, consequently, in the productivity of the reactor.

As with all open reactors, raceways have some drawbacks that may limit their performance, including the risk of culture contamination, low final biomass concentrations that lead to high harvesting costs, lack of temperature control and poor gas/liquid mas transfer (Carvalho et al., 2006; Posten, 2009; Richmond, 2004b). Although raceway reactors theoretically have the potential to produce more than 40 g m^{-2} day^{-1} of algal biomass, equivalent to 146 tonne ha^{-1} $year^{-1}$ (Brennan & Owende, 2010), reported productivities are in general much lower. Richmond estimated that annual productivity in raceways was between 16 and 19 g m^{-2} day^{-1} (Richmond et al., 1990). A maximum productivity of 21 g m^{-2} day^{-1} has been reported for *Spirulina* (Vonshak & Guy, 1992) and of 13.2 g m^{-2} day^{-1} for *Chlorella* (Hase et al., 2000). Despite this, the current interest in energy production from microalgae is now leading to re-examination of raceway cultivation systems in order to improve their performance in terms of energy and materials inputs (Chiaramonti et al., 2013;

Sompech et al., 2012). Moreover, the selection of adequate strains for the conditions presented in outdoor open cultures may be critical, since there is a high risk of contamination with competitive strains and protozoa. Thus, if a selected strain is growing under optimal conditions in the reactor, the possibility of contamination with other strains for which these conditions are not optimal is reduced considerably (Borowitzka, 2013). The selection of natural local strains *in situ* in large scale cultures is also an option, since the strain is probably adapted to local climate conditions making its growth easier under optimal conditions (Borowitzka, 1998). If the desired strain is different to 'wild' alga which may compete and become the predominant strain, a regular re-establishment of the culture with fresh pure inoculum is usually necessary in order to reduce the risk of colonization risk. On the other hand, if the strain is not important or the desired strain corresponds to the algae with better growth rates under the reactor conditions, the strategy to follow is to maintain the natural selection of species in the reactor and, at the end, the predominant alga will be the strain growing under optimal (or almost optimal) conditions compared to other strains (Borowitzka, 2013). This is the case of reactors fed with wastewater where it is very difficult to control the strains and contaminants that may arrive with the inflow. In this case, the natural selection is the approach to adopt in the culture.

Some engineering aspects of the design of the raceway have been previously studied(Weissman et al., 1988), but in-depth analysis of the fluid dynamic behaviour of this type of reactor is of current interest (Labatut et al., 2007; Wang et al., 2008). A theoretical approach to modelling microalgae growth in raceway reactors, taking into account the biological and hydrodynamic phenomena occurring in the reactor, has also been reported (James & Boriah, 2010). The fluid dynamics of the system is an important factor in the behaviour of any type of photobioreactor as it influences phenomena such as mass transfer and nutrient distribution.

At present, the overall design for raceway reactors for microalgal production does not differ greatly from Oswald's original proposal. This consisted of a shallow pond (0.1-0.4 m deep) divided into either two or four channels joined by bends, in which the liquid is mixed and circulated generally by means of a paddlewheel, and with a gas exchange device to improve the mass transfer between gas and liquid phases (Figure 16).

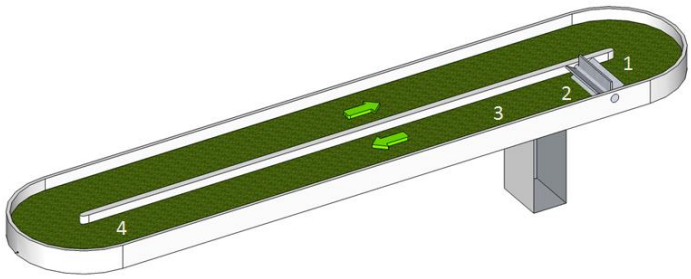

Figure 16.- Schematic of a raceway reactor. The parts in which consisted are: two shallow channels joined by bends (1 and 4, 180º bends), a device for mixing and liquid circulation (2, paddlewheel) and a device for gas exchange (3, sump).

2.4.2.1 Shallow ponds

A raceway pond consists of a close loop recirculation channel where the culture is continuously circulated and mixed. The most widespread configuration for raceways is two straight channels connected by two 180º bends usually provided with semi-circular flow deflectors or baffles to assist the turning of the fluid and avoid dead zones.

Figure 17.- Raceways in Foshan Innovation & Incubation Center of Renewable Energy Technology. Guangzhou Institute of Energy Conversion, China. Left: Detail of the channels. Right: Detail of the bends

Some authors describe raceways ponds with multiple channels for a better use of the space and to reduce the construction costs (Sompech et al., 2012). The higher the number of channels, however, the greater the number of curved sections necessary to link the channels and, therefore, the higher the

power consumption is, since the presence of bends is one of the main factors producing energy dissipation in the reactor (Mendoza et al., 2013). For a better energy balance, the number of bends must be a minimum and attention must be paid to its design in order to reduce the head loss in this part of the raceway.

It has been reported that there may be significant differences in the flow behaviour depending on the bend configuration (Sompech et al., 2012). The study assessed the occurrence of dead zones (zones with low velocity) in the bend section using computational fluid dynamics (CFD) and it was concluded that there is a reduction in dead zones when the number of bend deflectors increases (Figure 18). Using three bend deflectors the dead zones disappear; but there is no experimental data in raceways to show how the power consumption is affected by the elimination of dead zones in the bend. This is essential in order to assess the potential benefits of increasing the number of baffle bends in the raceway design stage. The more baffle bends there are, the higher the construction costs will be and this potential increase in the capital cost has to be linked to a reduction in power consumption.

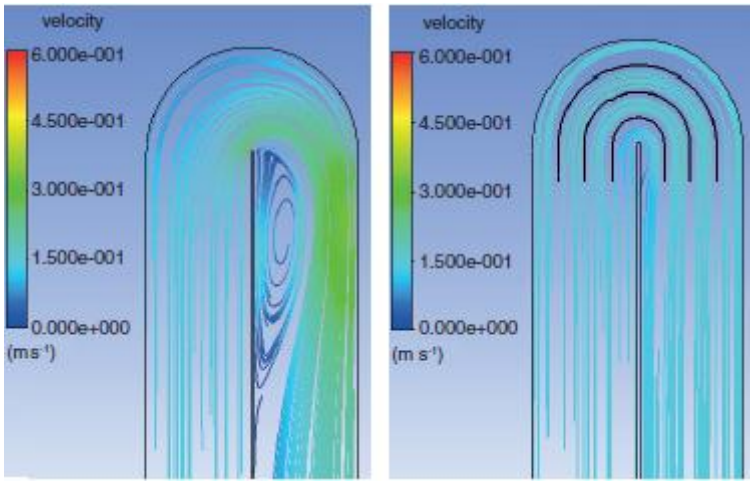

Figure 18.- CFD simulation of velocity profiles in bends (Sompech et al., 2012). Left: standard configuration. Right: three end baffles.

Raceway construction materials are typically low cost. At a large scale, raceways can be directly excavated into the ground and lined with impermeable material, or can be constructed on the surface of the ground and made of earth of blocks lined covered with a thin layer of a polymeric material , such us polyethylene, polypropylene and polyvinyl chloride (PVC), to prevent

seepage. The characteristics of the area where the raceway is to be installed determine the construction method and cost but, generally, excavated ponds are considerably cheaper to construct than raceways with concrete walls (Borowitzka & Moheimani, 2013). In addition, concrete is not recommended for growth of microalgae in saline media, unless it is lined. The polymer used as liner must be resistant to ultraviolet light to prevent its deterioration, and special attention must be paid to avoid materials that leach chemicals which can contaminate the culture. For example, in the fabrication of PVC some substances are used which are potentially harmful to humans, such us lead or mercury (Borowitzka, 2005). Microalgae can accumulate these heavy metals very efficiently and, therefore, its use is not recommended for microalgal production with food or feed purposes. The correct selection of the liner material taking into account parameters like operational and climate conditions, determines the life of the material and, ultimately, the life of the reactor. It has been proven that, with the right choice of liner material and when laid carefully and correctly, these liners have a life of at least 20 years (Borowitzka & Moheimani, 2013). The guarantee of a long life for the liner is essential, since this material is the most expensive component of the raceway construction. For instance, most commercial plants use long-life plastic membranes of 1-2 mm thick UV-resistant PVC or polyethylene sheets, whose cost can vary from 10 € to more than 25 € m^{-2}.

2.4.2.2 Circulation-mixing system

Mixing in raceways is essential to prevent settling of cells and avoid thermal, nutrient and oxygen stratification. For this, a turbulent flow is needed to ensure a stable system with high productivity. Different devices have been proposed for microalgal culture mixing such as air-lifts (Acién Fernández et al., 2001; Babcock et al., 2002; Ketheesan & Nirmalakhandan, 2011; Ketheesan & Nirmalakhandan, 2012; Persoone et al., 1980); propellers (Chiaramonti et al., 2013); and paddlewheels (Chisti, 2012; Mendoza et al., 2013; Oswald & Gouleke, 1960; Sompech et al., 2012). Some of these proposals are relatively recent but they have to overcome some serious drawbacks that may make the use of some of these devices unsuitable at a large scale. For instance, propellers have only been tested in small ponds and the power demand of those devices is similar to paddlewheel, while air-lift systems have low efficiency and high power requirements (Borowitzka & Moheimani, 2013).

The traditional way to circulate the fluid in the raceway is using a paddlewheel (Figure 19). The use of paddlewheels in raceways was proposed when these reactors first appeared, and is still accepted as the most effective way to circulate the culture with the lowest power requirements for the system. In fact, most of the raceways producing microalgae at a large scale around the world work with paddlewheels. The paddlewheel rotates by a geared motor which is connected to the shaft of the wheel, and is responsible for the main energy consumption in the reactor. Although this power consumption is much lower in comparison with other reactor configurations (Mendoza et al., 2013), this is one of the most important parameters to be optimized to achieve the goal of making microalgae production competitive in the field of energy production.

Figure 19.- Paddlewheel for fluid circulation and mixing (Foshan Innovation & Incubation Center of Renewable Energy Technology. Guangzhou Institute of Energy Conversion, China)

2.4.2.3 Gas exchange device

One area requiring particular attention is the supply of carbon, due to the limitations on mass transfer and the potential for losses when CO_2 is bubbled. Some authors have pointed out the importance on improving the efficiency of carbon dioxide addition to culture (Ketheesan & Nirmalakhandan, 2011), since its supply and transfer could potentially account for nearly 1/3 the cost of algal cultivation (Benemann et al., 1987).Open ponds are limited by

the poor gas/liquid mass transfer between the surface of the broth and the atmosphere. During sunlight hours, the pH in algae culture increases unless it is controlled by CO_2 injection. This is evidence of the limitation of direct CO_2 absorption from the atmosphere and the necessity of increasing the carbon dioxide input into the reactor. CO_2 absorption in the liquid phase by direct gas injection at the bottom of the channel is insufficient, however, due to the characteristic shallowness of raceway cultures.

Low depth is a prerequisite in raceways to ensure light penetration in the culture and reduce power consumption (Benemann & Oswald, 1996); but, on the other hand, the contact time between gas and liquid in a 20 cm depth culture is not enough to ensure efficient CO_2 absorption in the liquid phase. That is why raceways are frequently equipped with devices such as sumps and mixing columns to increase the gas/liquid contact time and the efficiency of CO_2 absorption (Azov & Shelef, 1982; Park et al., 2011; Putt et al., 2011; Weissman & Goebel, 1987; Weissman et al., 1988). The use of sumps (Figure 20) is one of the simplest ways to improve carbonation in raceways, as they can be easily constructed within the raceway and do not need an external energy supply. When sumps are used, the provision of a baffle has also been suggested to direct the flow down one side, around the bottom, and then up and out the other side of the sump. This baffle allows also a counter-current injection of CO_2 as a means of increasing the mass transfer (Weissman et al., 1988). Although the presence of this baffle is often regarded as improving the raceway performance, its effect in power requirements for mixing has not been fully studied before. Moreover, the use of a sump with central baffle and continuous gas injection can provide a means of circulating the liquid round the raceway by the gas-lift pump principle (Ketheesan & Nirmalakhandan, 2011; Ketheesan & Nirmalakhandan, 2012). Therefore, although sumps of different configurations have been proposed, the behaviour of the liquid and the influence of the hydraulic operating conditions on the hydrodynamics of the entire reactor have not been studied.

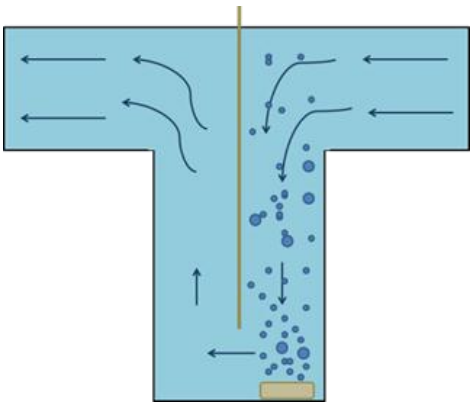

Figure 20.- Schematic of the gas bubbling when using sump baffle to give counter-current contact between gas and liquid phases

Improvements in the design of devices for gas exchange are linked to the development of new kinds of reactors like thin layer reactors, where the depth is very low, making the direct injection of gas into the shallow channel impossible. It has been reported that the use of a 1.5 m deep sump in raceways can potentially produce CO_2 removal efficiencies in the gas phase of 86 % in flue gas (15 % CO_2) and up to 95 % in pure CO_2 (Weissman & Goebel, 1987). In any case, the design of the carbonation system must be studied carefully, since incorrect estimation of parameters such as size of the carbonation device or concentration of CO_2 in the gas phase could produce a low mass transfer efficiency and, therefore, the CO_2 would be released to the atmosphere.

If flue gas is used, the source of the gas determines its characteristics: not only the CO_2 concentration, but also the presence of other compounds such as SO_x, NO_x, CO or even heavy metals in concentrations which may vary widely (Acien Fernandez et al., 2012). Depending on the situation, some pre-treatment steps could be necessary to modify the physic-chemical properties of the flue gas to those which are suitable for microalgal growth (e.g. cooling operations in hot gases or pressurization to inject the gas in the culture). Some typical sources of gases that may be suitable for use in microalgae cultures could be from the combustion of coal or natural gas, to flue gases from the cement or chemical industries.

The development of technology for growth of microalgae as a biomass feedstock for energetic purposes depends on the reduction of production costs. Therefore, the use of pure CO_2 as the carbon source is only viable in

closed reactors where it is possible to control all the parameters to produce a determinate strain of algae with a high value component used in cosmetics or pharmaceuticals. The alternative is the use of flue gases from highly polluting plants and factories, with a double economic and social benefit: on the one hand a reduction of cost in the production of microalgal biomass using a free CO_2 source and, on the other, the utilisation of CO_2 emissions wherever they are produced. Their elimination from the exhaust gases in the industrial sector is an environmental benefit, the value of which is much more difficult to calculate. The installation at large scale of photobioreactors has, however, some drawbacks in developed areas with suitable climate conditions for microalgal growth like the European shores of the Mediterranean Sea, in comparison with other zones with similar climate conditions. The most important is the price of land, which is much higher in Europe than in areas like the north of Africa. Nevertheless, the industrialized world in general and the European Union in particular has to make a definite commitment to sustainable development. The countries of Southern Europe, which are the nations most affected by the recent economic crisis in our continent, are called upon to have a major role in the energy revolution, due to the enormous possibilities that their natural resources offer. Thus, it is possible to think that in the near future the strategic location of industries could be influenced by the potential for installation of algae farms due to the local climatic conditions, taking into account the economic profits derived from the reduction of taxes for no pollutant industries in the carbon market established in the Kyoto Protocol in 1997 (UN). The total sequestration of CO_2 by microalgae in highly polluting plants, however, seems difficult due to the huge amount of CO_2 produced. A closer examination of some figures reveals that, for example, a medium-size cement plant produces 100.000 tonnes CO_2 $year^{-1}$ (Oilgae, 2015). Taking into account the conversion coefficient 1.8 g CO_2 g^{-1} biomass and a raceway productivity of 30 g biomass m^{-2} day^{-1} the area necessary to capture all the CO_2 produced is 463 hectares. This means that microalgae by themselves cannot satisfy global requirements for the total elimination of current CO_2 emissions, but they have the potential to reduce the net amount of CO_2 released to the atmosphere, among other benefits previously described.

In addition to the transfer of CO_2 to the culture, the removal of photosynthetically generated oxygen is necessary. The adverse effects of

dissolved oxygen are widely reported, as its accumulation is one of major problems in the design and operation of closed photobioreactors (Camacho Rubio et al., 1999). It is has often been assumed that in raceway reactors the oxygen produced will be released to the atmosphere along the channels, with no major accumulation in dissolved oxygen: this is considered to be one of the advantages of this type of reactor. In practice, however, seasonal differences in the accumulation of dissolved oxygen in raceway cultures have been described in southern Spain with concentrations ranging between 10 mg L^{-1} in winter (115 % of O_2 saturation) and 30 mg L^{-1} in summer (375 % of O_2 saturation) and a clear decrease in biomass concentration when dissolved oxygen was higher than 25 mg L^{-1} (Jiménez, 2003). Dissolved oxygen concentrations as high as 500 % saturation have been also reported, causing inhibition of photosynthesis and growth, and eventually leading to culture death (Márquez et al., 1995; Singh et al., 1995; Vonshak, 1997). It is, therefore, necessary to provide mechanisms for the removal of dissolved oxygen, and to consider these when designing raceway reactors and establishing operational protocols. To develop an oxygen control strategy, a knowledge of the mass transfer capacity of each section of the raceway reactor is needed (Camacho Rubio et al., 1999).

2.5 Conclusions from the literature review

From the above study of the published literature, it is clear that according to the current state of knowledge raceways remain the most suitable microalgal biomass cultivation system for energy production purposes. Some key areas of knowledge are missing, however, or need improvement to achieve the goal of having profitable microalgae culture systems with competitive production costs in the energy market. Thus, while the basic principles of raceway technology are known, the possibility of obtaining a more efficient system for microalgal cultivation based on this knowledge is hypothesized. Several key issues can be studied to achieve this goal, since there is still work to do on reducing unit production costs, enhancing the efficiency of the input utilization (nutrients, energy), enlarging the knowledge of the parameters involved in productivity (fluid dynamic characterization, mixing, CO_2/O_2 gas exchange phenomena, influence of each section in the overall behaviour of the raceway) and improve the overall energy balance of the system (power consumption). Therefore, it was decided to carry out a programme of

experimental work to fill in some of these gaps in knowledge, focused on 4 main tasks:

1. A complete fluid dynamic characterization of a pilot-scale raceway reactor taking into account the different sections in which the raceway is divided and analyzing the mixing and power consumption at different liquid depths, liquid circulation velocity, number of baffles in the bend and sump configuration with and without baffle.

2. A close analysis of the carbonation process in microalgae, with special attention paid to the sump as a device to enhance the efficiency of CO_2 removal from different carbon sources.

3. An examination of the complexity of the oxygen mass transfer phenomena taking place in the raceway. Evaluation of dissolved oxygen accumulation in the raceway, study the possibility of oxygen desorption by sections in comparison to experimental measurement of photosynthetic oxygen production rate in real microalgae culture, pointing the effect of oxygen accumulation on biomass productivity.

4. The study and testing of new devices for liquid circulation in raceways with the aim of reducing the power consumption of the paddlewheel and, therefore, helping to achieve a final energy net balance positive in microalgae cultures as a source of biomass for biofuel production.

All this work aims at adding to the knowledge of raceway systems for microalgae cultivation in the hope of opening new opportunities for the definitive implementation of this technology globally to fight against climate change by means of the production new green biofuels.

Chapter III

3. MATERIALS AND METHODS

3.1 Location

Unless noted, all the experimental work was carried out in two identical raceway reactors located at the Estación Experimental Las Palmerillas of Fundación CAJAMAR in El Ejido, in the province of Almeria, south-east of Spain (36˚48'00.9"N 2˚43'15.4"W). As can be deduced from Figure 21, Almeria has a Mediterranean climate determined by its geographical location with mild temperatures during all the year between 9-17 ˚C in January and 24-33 ˚C in August, and an annual average temperature above 19 ˚C (Table 4).

Figure 21.- Location of Almería in Europe, red mark (GoogleMaps, 2015)

It is one of the areas of Europe with most sunlight, with almost 3.000 hours per year. The average number of rainy days, defined as having more than 1 mm of rainfall, is 26 per year, with a total annual precipitation of 196 mm. These climatic conditions make this location suitable for microalgal

growth throughout the year. This is the reason why other works regarding outdoor microalgae cultures had been carried out in the province of Almeria (Acién Fernández et al., 2001; Camacho Rubio et al., 1999; Sierra et al., 2008) or in nearby provinces like Malaga (Jiménez, 2003; Jiménez et al., 2003).

Table 4.- Average climate parameters in Almeria between 1971-2000

Month	T ˚C	T_{max} ˚C	T_{min} ˚C	Rain, mm	Rainy days	Sunlight, h
January	12.5	16.9	8.2	23	3	191
February	13.2	17.7	8.8	21	3	191
March	14.7	19.2	10.1	15	3	228
April	16.4	21.0	11.9	20	3	250
May	19.1	13.6	14.6	14	2	299
June	22.7	27.3	18.2	10	1	322
July	25.7	30.3	21.1	1	0	338
August	26.4	30.7	22.0	1	0	312
September	24.0	28.3	19.6	12	1	257
October	20.0	24.3	15.7	28	3	221
November	16.2	20.4	12.0	28	3	187
December	13.7	17.9	9.4	23	3	176
Annual	18.7	23.1	14.3	196	26	2965
Source: (AEMET)						

Since it was founded in 1975, the Experimental Station Las Palmerillas (Cajamar) has been characterized by the applied nature of their projects and for their dedication to knowledge transfer activities as a technology centre for Southeast agriculture. In 2003, in collaboration with the Chemical Engineering department of the University of Almeria, the Experimental Station decided to open a new research line in the field of microalgae biotechnology and its commercial applications. At present, Las Palmerillas is a reference in this area, being a place with a strong scientific productivity and counting on high technology facilities where different researches are carried out.

The Experimental Station has maintained its own weather station since 1985, which records: dry and wet temperatures (ventilated psychrometer Thies); soil temperature at 15 and 30 cm deep (resistive sensor PT100); global/diffuse radiation (CM-11, Keep & Zonen) and PAR radiation (LI-190S Quantum Sensor, Lycor); wind speed and direction at 10 m high (vane anemometer, 05103-5, Young), rain intensity (pluviograph Hellmann with transmitter Reed 0.1mm resolution, Thies); evaporation by means of an

evaporimetric tank (1 m^2 surface with 0.1L precision micrometer screw). The updated information can be consulted and downloaded by all the researchers working there from the central computer where all the data is continuously registered. A part from that, solar radiation was directly measure on-site in the raceway by means of a light sensor (Li-Cor, Pyranometer, PY 61654, USA), allowing to have all the information given by the rest of the probes related on-line to the solar radiation in the control computer.

Figure 22.- General view of the Experimental Station Las Palmerillas. It is possible to see some of the microalgae facilities belonging to the Biotechnology Research Area

3.2 Raceway reactors

Two identical raceways were specially designed and built for the present work. Each reactor consisted of two 50 m length channels, 1 m wide and connected by 180º bends at each end (Figure 23). The dimensions the raceway were selected based on a number of factors. Firstly they were chosen to fit the available space in the Experimental Station and to allow transportation of the raceway components by truck from the UK where it was built, to Almeria (Spain) where it was installed. In addition, it was considered that at the planned velocities and operating depths, a width of 1 m was to ensure the effect of the channel walls was small and the behaviour of the raceway could be considered as approximating that of a strip of a wider channel; the priority was therefore to maximise the length within the space The entire reactor, including the

sump, was made of white 3 mm thick fibreglass. The mixing in the system determines the productivity of the reactor and the cost of construction and operation, so it was a key issue in the design process. After analysis of the available alternatives, finally the most common system in open raceways of mixing by a paddlewheel was implemented to maintain the liquid circulation velocity.

The paddlewheel used in the main experimental work had 8 blades, although in the final experiments on improved paddlewheel designs a 12-blade wheel of similar construction was used. Each paddlewheel was made of marine plywood and has a diameter of 1.2 m. It was driven by a three-phase electric motor (W12 35 kW, Ebarba, Barcelona, Spain) with gear reduction (I=25 0.37 kW 90º; 0.50 HP, WEG Ibérica, S.A., Barcelona, Spain). The velocity of the motor was controlled by a frequency inverter (CFW 08 WEG Ibérica, S.A., Barcelona, Spain).

Figure 23.- Pictures of the construction process of the raceways

3.2.1 Sump and bends configuration

Biomass production in photobioreactors requires a source of carbon to maintain high algal growth rates. The amount of CO_2 necessary for optimal growth of a particular microalgae depends on the way the system provides this CO_2 to the culture (Carvalho et al., 2006). The usual way to add the CO_2 is by direct bubbling into the reactor, with the drawback of low efficiency in CO_2 capture produced by the inefficient gas to liquid transfer in shallow channels. To overcome this situation, a sump was located part of the way down one channel with the aim of increasing the liquid-gas contact time and improve the efficiency of CO_2 capture of the system. The dimensions of the sump were 0.65 m long, 0.9 m wide and 1.0 m deep (Figure 24). The effect of the sump and other parts of the reactor in the hydrodynamic is an issue that has to be carefully studied since the head loss produced may increase the energetic requirements for mixing and make the system potentially unaffordable from an economic point of view. In addition, the benefit produced in the gas exchange phenomena by the sump must be also evaluated, taking into account what is the mass transfer dynamic in other parts of the reactor.

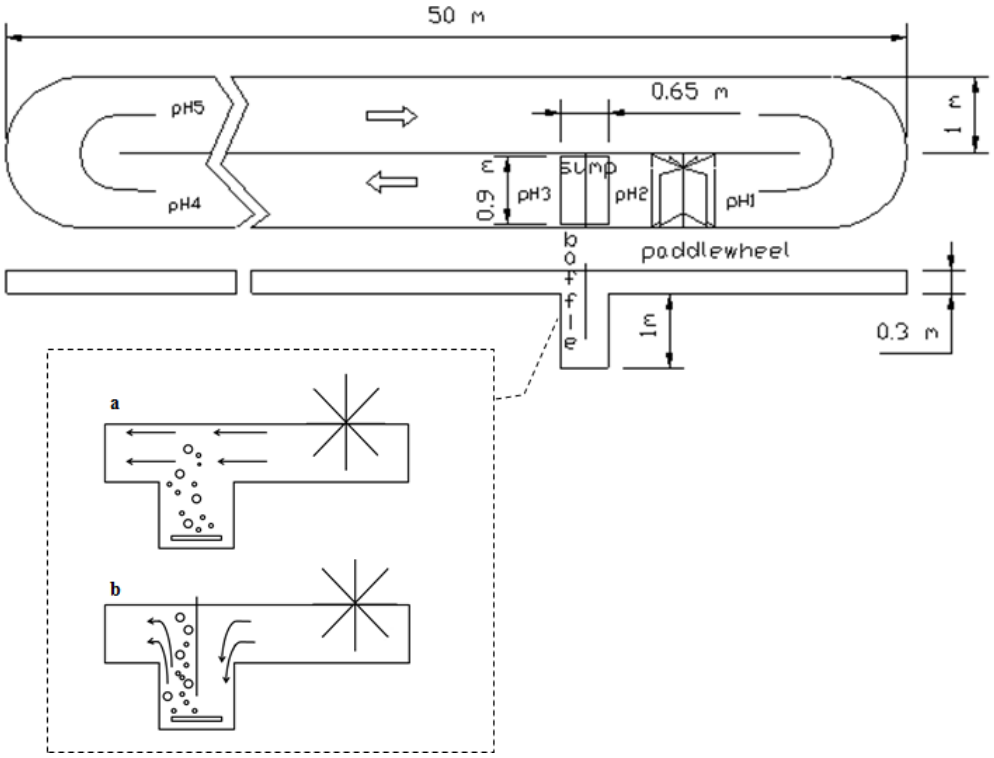

Figure 24.- Schematic of the raceway reactor showing its dimensions and operation of the sump: A) without baffle, B) with baffle.

The design of the raceway was intended to allow testing of a wide range of operating conditions and parameters. The sump was fitted with a removable baffle made of marine plywood (Figure 25); when in place this forced the liquid to flow through a gap of 0.3 m at the bottom of the sump (Figure 24).

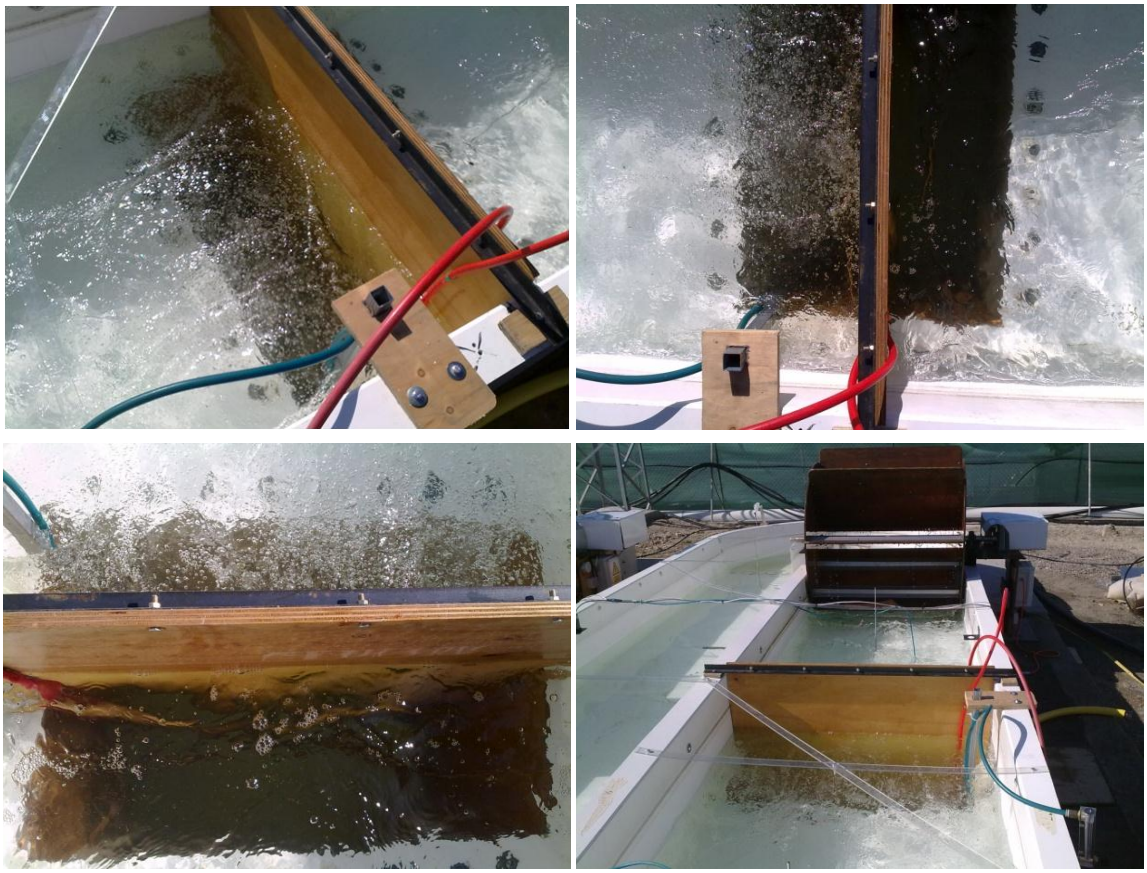

Figure 25.- Images of the sump baffle and the bubbling zones during a mass transfer experiment with fresh water into the raceway

3.3 Probes and control system

3.3.1 Probes

The raceway reactors were provided with a variety of probes and electrodes to measure the parameters used in this study. Thereby, pH and Dissolved oxygen (DO) were monitored using 5083T and OD5120 probes (Crison, Barcelona, Spain) calibrated and maintained in accordance with the manufacturer instructions and connected to transmitters (MM44, Crison, Barcelona, Spain) (Figure 26). The gas flow rate entering the reactor was

measured by flow meters (PFM 725S-F01-F, SMC, Tokyo, Japan and FR4500, Key Instruments, USA).

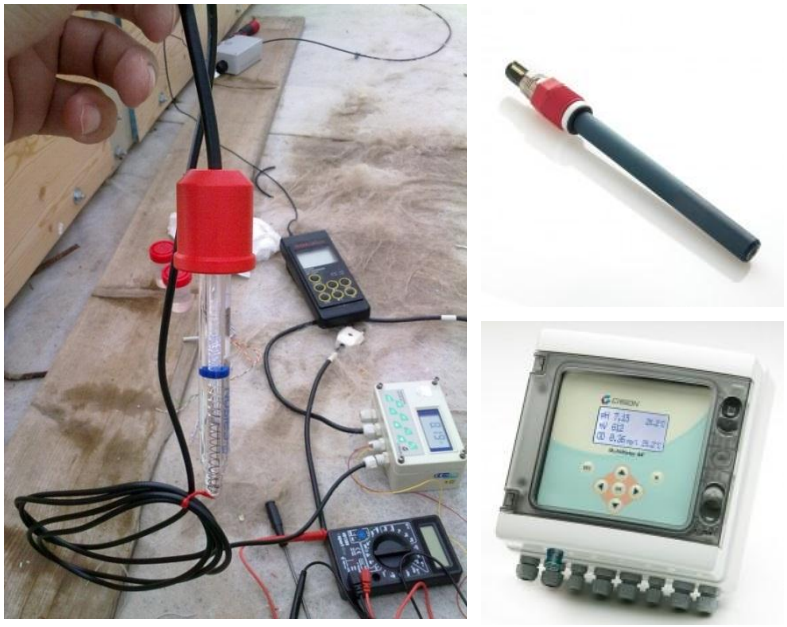

Figure 26.- Left: dissolved oxygen probe (OD5120). Right: pH probe (5083T) and transmitter (MM44) (pictures obtained from www.crisoninstruments.com)

In carbonation studies, the gas reaching the surface above the sump was collected via a fume hood made of polyethylene and attached to a steel bar (Figure 27, left). The hood was provided with holes at the top to allow the insertion of the probes to measure the gas composition inside. The hood was fitted with a CO_2 probe (Carbocap, Vaisala) connected to transmitter (GMT220, Vaisala) (Figure 27, right) and an O_2 probe as described in the paragraph above.

Figure 27.- Left: Detail of the fume hood which collected the gas reaching the surface for the measurement of its CO_2 concentration. Right: CO_2 probe located inside the fume hood and transmitter (picture obtained from www.vaisala.com)

All of the probes were connected to a 36 Core Industrial Cable (0.22 mm² CSA 1 A, 300 V Screened PVC Sheath, 10.8mm OD, 100m, RS) (Figure 28, left) which carried the signals from the cabinets, installed next to the reactor to protect the electronic equipment and connections of probes and transmitters (Figure 28, right), to two dataloggers (LabJack U3, Colorado, USA) located in a control room.

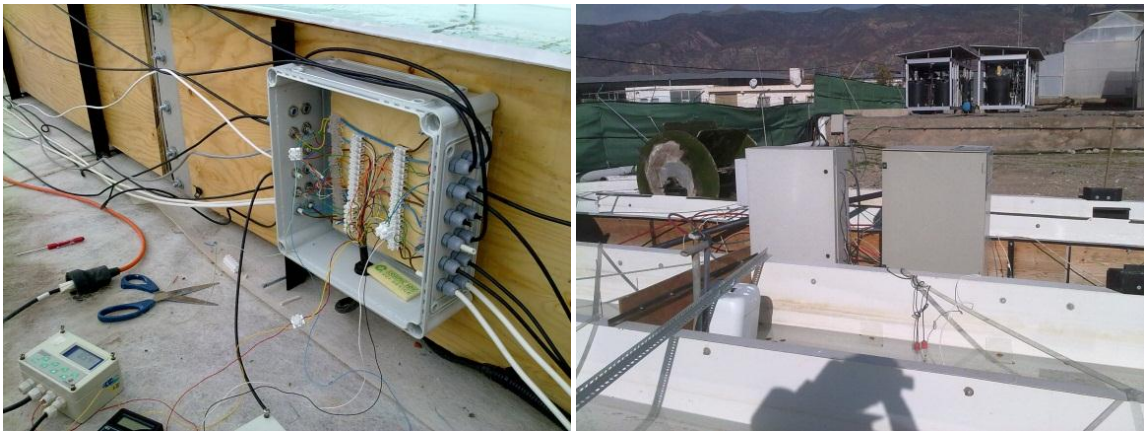

Figure 28.- Left: Detail of the connection box installed in the wall of one of the raceways where the 36 wires cable collected the electrical signals of probes to send it to the control room. Right: Cabinets where all the probes were connected to the transmitters to protect the electronic equipment

3.3.2 Control system

Logged data were collected and processed in real time in the control room by means of a computer. The computer was equipped with the data acquisition software Daqfactory (Azeotech, Arizona, USA) (Figure 29), which allowed not only the collection of data, but also the design and implementation of automatic control systems to maintain pH, OD, depth and dilution rate under the desired conditions, depending on the experimental requirements in each case. In Figure 29, the grey box above shows all the parameters and variables recorded in both raceways and the two small grey boxes below show the pH, dilution, DO and depth control systems. The white box on the right shows the workspace where: all the variables and parameters are defined with its signal to real value conversion, the channels are configured, the control sequences are programmed and the information sent by probes is logged. The sampling time for all the experiments was 0.2 s and they were averaged every 5 values in order to have one piece of data per second. This sampling time was

increased to once per minute in microalgal culture experiments due to its long duration which achieved several months.

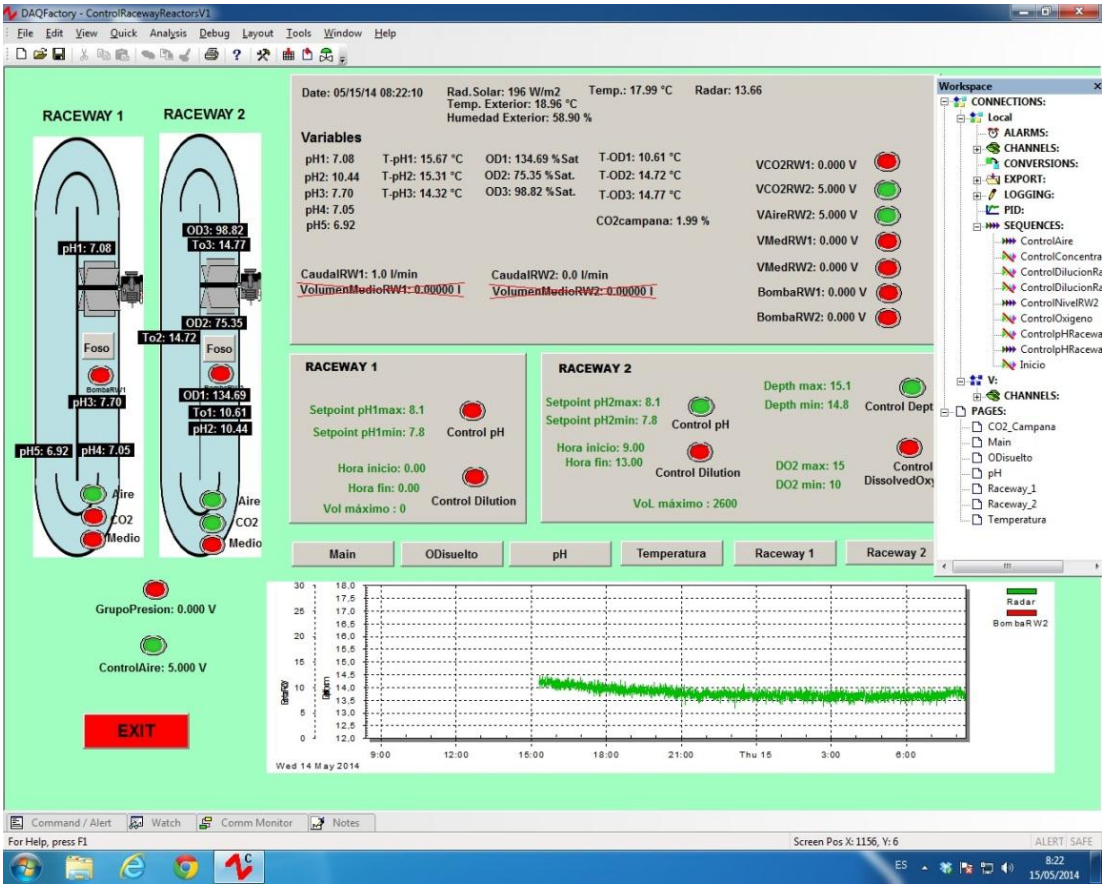

Figure 29.- Screenshot of control computer

3.3.2.1 Dissolved oxygen and pH

In microalgae cultures, the pH was controlled by means of CO_2/flue gas supply on demand. Maximum and minimum pH values of 8.1-7.8 were chosen as set-points. When the pH in the culture was higher than the set-point, a solenoid on/off valve was switched automatically trough the computer control system allowing the CO_2 be bubbled in the culture until the pH achieved the minimum set. This occurred only during daylight periods (solar radiation >50 W m^{-2}) as no CO_2 demand was exerted by the algae during the night. The same strategy was also used, in some experiments, to control the dissolved oxygen. When its concentration achieved the maximum allowed, air was bubbled into the sump for O_2 desorption until the concentration achieved the minimum set, although the control was subject to the activation of pH control, i.e. when microalgae demanded CO_2, the pH control prevailed over dissolved oxygen

control and, therefore, air for oxygen desorption was bubbled only when no carbonation was required by microalgae.

3.3.2.2 Dilution rate and harvesting

The volume of culture medium added was continuously measured by means of a digital flow meter (PF3W740-F06-FT-M, 5-40 L min^{-1}, SMC, Japan) (Figure 30, left). A desired dilution rate was set in the control system together with the time at which the dilution had to start. The control system regulated the operation of a solenoid on/off liquid valve. This valve was opened when the time was the same than the time set and was closed when the volume added to the raceway arrived to the set-point.

For harvesting, the depth of liquid in the raceway was also measured (radar sensor Vegaplus WL 61, Vega, Germany) (Figure 30, right), and the liquid depth increase produced by the addition of fresh medium was compensated by the removal of culture from the reactor by means of a submersible pump (Jardín & Natura DW7500, 400W, Hmax 5m, Qmax 8.000 L h^{-1}) located at the bottom of the sump. In this way, maximum and minimum allowed liquid depths were set, and when the maximum was exceeded the submersible pump was automatically activated until the minimum set point in the control system was reached. The medium pumped out of the raceway was not recycled into the reactor, but was reused for the irrigation of gardens and trees onsite. This is acceptable in experimentation but at industrial level the reuse of water and nutrients contained in the harvested flow after the separation of biomass is mandatory in order to reduce costs. In addition, evaporation was not compensated with fresh water. This can potentially led to accumulation of salts and other recalcitrant products that may inhibit growth or cause other issues in the system. In this case, the accumulation of bicarbonate also may reach a concentration above the optimal for several microalgae species. In practice, however, to maximise the amount of harvestable biomass the aim was to operate the system at high dilution rates on the order 20-50 %, thus limiting the accumulation of these compounds. A safety overflow was installed in the raceway to allow the culture to escape from the raceway in case of failure of harvesting control or heavy rain.

Figure 30.- Left: digital flow meter PF3W740-F06-FT-M, (SMC). Right: Liquid depth sensor Vegaplus WL 61

3.4 Gas supply system

3.4.1 Diffusers

Gas was supplied at the bottom of the sump by means of different types of diffusers. Three different spargers widely used in the water industry were tested (Figure 31), to study the differences in the mass transfer capacity of the sump and the power requirements for gas supply through the diffuser. The diffusers all had the same surface area of 0.20 m^2, and were of the following types:

1. Membrane tube 2.5 m length and 25 mm diameter. It gave small bubble size but with a high pressure drop.
2. Membrane plate 0.3 m diameter (three plates to give the same surface area than other diffusers). It gave a small bubble size with a low pressure drop.
3. Porous tube 2.5 m length and 25 mm diameter. It gave medium-size bubbles with a low pressure drop.

Figure 31.- Diffuser types used. From left to right: Membrane tube (type 1), membrane plate (type 2) and porous tube (type 3)

3.4.2 Carbon source: Pure CO_2 & Flue gas

The carbonation source used was chosen depending on the purpose of the experiment. Pure CO_2 was obtained from the general supply system available in the Experimental Station and was supplied to the raceway from the local distribution point through a 200 m polyethylene pipeline of 25 mm diameter.

Flue gas was taken from a diesel-fuelled heating boiler (Tradesa, MOD SF 20, RA-GTI, TRADE, Italy) and had an average gas composition of: 10.6 % CO_2, 18.1 ppm CO, and 38.3 ppm NO_x, and 0.0 ppm SO_2. The flue gas was cooled to air temperature, compressed to 2 bar (BUSCH, Mink MM 1104 BP, model C-1000 compressor, Barcelona) and stored in a 1.5 m^3 pressure vessel regulated with a SMC pressure control valve (ISG 230-031) (Figure 32, left) which allowed the automatic ignition of boiler and compressor to maintain the pressure in the desired range. The flue gas was supplied from the pressure vessel to the raceway by a 150 m polyethylene pipeline of 25 mm diameter and bubbled in the sump through the diffusers previously described in 3.4.1 (Figure 32, right).

Figure 32.- Flue gas supply to the raceway. Left: flue gas production system with diesel boiler (white), gas compressor (black) and gas pressure vessel (blue). Right: sump view with flue gas bubbling in a microalgae culture.

3.4.3 Nitrogen and air

Nitrogen was used in the dynamic method described in section 5.1 for sump mass transfer characterization. For this, the sump was filled with water, and nitrogen gas was bubbled through a diffuser at the bottom of the sump

until the dissolved oxygen concentration reached zero. Nitrogen was obtained in commercial gas cylinders provided by Abelló Linde, Spain.

Compressed air was used in the raceway for the mass transfer characterization and for oxygen desorption in microalgal cultures. It was obtained from the general line that provides this gas to the Experimental Station.

3.5 Culture medium

The culture medium was prepared by an automatic irrigation and fertilization device (Nutritec N-9000, Ritec, Murcia, Spain) (Figure 33, left) and kept in a 10.000 litres tank. When the harvesting automatic control system was activated, the medium was pumped (Husqvarna AB, S-561 82, Hmax 36 m, Qmax 3.1 m^3 h^{-1}, Huskvarna, Sweden) from this tank to the raceways, after being filtered through two 10 µm wound depth water filter cartridges (Parker M19R10A-RS) (Figure 33, top right) to remove solid particles and prevent obstructions in pipes and equipment.

Figure 33.- Left: automatic irrigation and fertilization device (Nutritec N-9000) used for the preparation of fresh culture medium. Right: water filter cartridge used to eliminate solid particles before fresh medium addition to the raceway and tanks with nutrients solutions used by the automatic irrigation device to prepare the culture medium.

The tank was equipped with a depth sensor (characteristics not provided by the company) able to detect when the liquid level is decreasing and therefore to activate the production of more culture medium. The automatic irrigation machine took the fertilizers from four 10,000 litre tanks (Figure 33, bottom right), each one containing a different solution of nutrients. Thus, it was programmed to take and mix the nutrients from these tanks in the desired proportion to produce the culture medium with the required ionic concentration.

The algal culture medium was prepared in fresh water using commercial fertilisers and supplements to give the additional ionic concentrations to those naturally present in the fresh water source shown in Table 5.

Table 5.- Composition of the algae culture medium prepared using commercial fertilisers

Chemical ion	Concentration (mmol L^{-1})
NO_3^-	9.49
NH_4^+	0.59
$H_2PO_4^-$	1.00
K^+	1.60
Ca^{2+}	5.00
Mg^{2+}	3.25
$SO_4^=$	1.20
HCO_3^-	2.80
Na^+	8.20
Cl^-	11.10
Fe^{3+}	2.00
Mn^{2+}	0.84
Zn^{2+}	0.56
B^{3+}	0.49
Cu^{2+}	0.08

The fresh medium for the cultures in the inoculum room (500-mL and 5-litres flasks) was previously prepared and sterilized in the laboratory, using high quality chemical products with laboratory purity. In the outdoor facilities, the medium was automatically prepared by means of a commercial irrigation machine and fertilizer quality chemical products widely used in greenhouses for crop cultivation. The composition of this culture medium was checked periodically in the lab to confirm that it contained the correct proportion of chemical ions presented in Table 5. The culture medium was chosen so that there was no limitation on any of the nutrients (San Pedro et al., 2013), as it

was observed from the analysis of the samples of culture medium taken directly from the raceway before the addition of fresh medium.

3.6 Microalgal cultures

3.6.1 Feedstock material and inoculum

The strain selected from the microalgae collection held by the University of Almeria was *Scenedesmus* sp. This was recommended by experts in the field from this University, based on its adaptation to local conditions, since it is widespread in the region. The microalgal species present in the raceway culture after its inoculation, however, were diverse. The strain brought from the University was maintained in the inoculum room located at the experimental facilities under light and agitation conditions in 500-mL flasks (Figure 34, left). Light was provided by fluorescent tubes attached to the shelves where the flasks were maintained and agitation was obtained by means of direct air bubbling in the flasks, allowing at the same time the desorption of photosynthetic oxygen. Fresh medium was added periodically to the flasks in order to maintain the strain in an optimal growth environment, and sterile conditions were assured by using the autoclave for all the instrumentation and the medium used in this room. The purity of the culture in the inoculum room was periodically checked using a microscope. In case of contamination by other strains or predators the culture was eliminated and new inoculum was brought from the University of Almeria.

The volume of the culture was increased progressively to obtain the amount necessary to inoculate the raceway. Different reactor configurations available in the Experimental Station were used for this purpose: from 500 mL to 5-litres flasks, later in a 200-litres bubble column and finally in 4 m^3 tubular reactors. For the inoculation of the raceway, it was filled with fresh medium until the desired depth and then 3 m^3 of culture from the tubular reactor was added to the reactor (Figure 34, right).

Figure 34.- Left: Flasks with different microalgae strains in the inoculum room. It is possible to see the illumination structure with fluorescent tubes and the agitation system with means of air bubbling. Right: Inoculation of the 100 m^2 raceway with 3 m^3 of microalgae culture obtained from the tubular reactors

The purity of the mono-strain culture was maintained as far as possible in all steps in the inoculation process from 500 mL flasks to the raceways, although the bigger the size of the reactor the higher the contamination risk, especially since the bubble column and tubular reactor were located outdoors. In any case, the raceway was inoculated with cultures of *Scenedesmus* sp. that were as pure as possible, although the open conditions present in the raceway may subsequently change the microalgal population dynamics in the culture as a result of on multiple factors, some of which like the perturbations produced by weather conditions were not controlled in the current work. Figure 35 shows the raceway before and after the inoculation with *Scenedesmus* sp.

Figure 35.- Left: raceway before inoculation and without sump baffle. Right: raceway inoculated with *Scenedesmus* sp. with sump baffle in position

The composition of harvested algae was not studied in detail in the current experimental work. Only sporadic analyses were made for other reasons not related to the experiments shown in the thesis. For this reason, this information is not presented in the document. Additional analyses including elemental composition of a sample of algae was carried out by Khanh Tran and is reported in his thesis (in review) and in a joint paper (Tran et al., 2014).

3.7 Laboratory and pilot plant practice

All laboratory operations were carried out using good laboratory practice, and having first carried out the appropriate risk assessments and, where necessary, COSSH assessments. All equipment, laboratory apparatus, and analytical instruments were operated in accordance with the manufacturer's instructions. All glassware was washed using washing detergent followed by rinsing with tap water and deionised water. All the operation in the pilot plant was also carried out according to the risks prevention protocol, following the safety instructions and using the appropriate personal protection equipment.

3.7.1 Characterization of mixing in the raceway.

Reactor mixing was characterized using the method described by Verlaan (Verlaan et al., 1989) who described mixing in terms of the Bodenstein number (Bo). This parameter describes the degree of back mixing in the raceway and is defined as the ratio of transport by convection to that by axial diffusion in the liquid phase. When Bo is equal to 0, there is complete mixing and the reactor is equivalent to a continuously stirred tank reactor, while when Bo value tends to infinity corresponds to ideal plug flow. In practice, complete mixing was taken as Bo≤20 and plug flow as Bo≥100 (Brechtelsbauer & Ricard, 2001). The intermediate range is considered as a transition regime. Bo is a dimensionless number which is a function of the liquid velocity v (m s^{-1}), the length of the section $L_{section}$ (m) and the dispersion coefficient D_z (m^2 s^{-1}) (Eq(8)). Verlaan calculated Bo as a function of attenuation of output signal with respect to input signal, with both signals in the current work being experimentally determined pH values. According to this methodology, the Automation, Robotics and Mechatronics Group of the University of Almeria (ARM) implemented a code in Matlab 6.5 (The MathWorks, Inc.) for the calculation of

the Bodenstein number (Bo) (see Appendix I). Once Bo is known, the dispersion coefficient can be calculated from Eq(8). Therefore, the experimental work must provide clear input and output pH signals in the sections studied in the raceway in order to study the attenuation of the signal in the software.

$$Bo = \frac{vL_{section}}{D_z} \tag{8}$$

The locations of the probes were selected to allow characterization of the different sections of the reactor: paddlewheel, sump, channel 1, bend 1, and channel 2 + bend 2 (Figure 36).

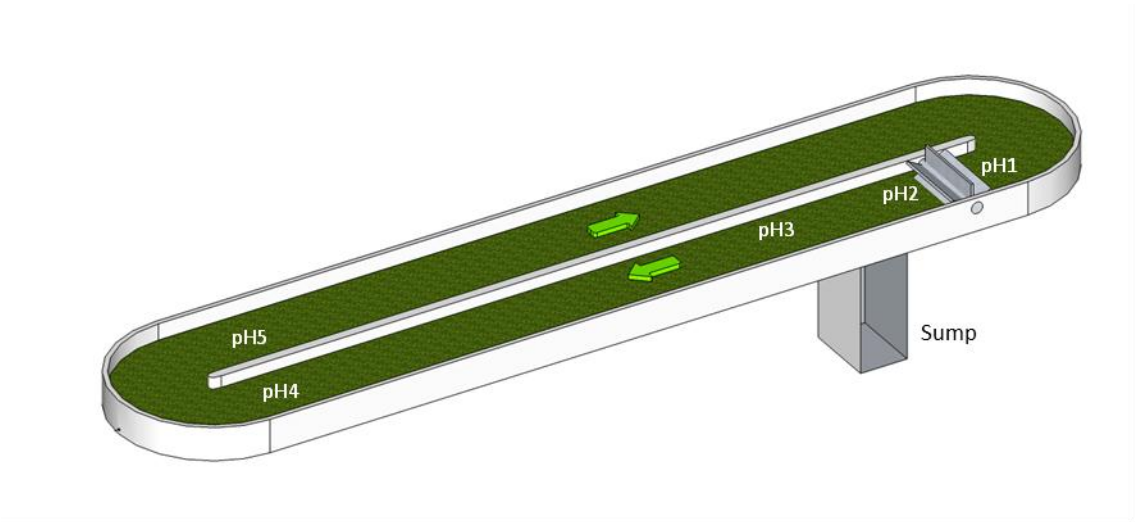

Figure 36.- Schematic showing position of the pH probes used during the experiments (not to scale)

3.7.2 Total Suspended Solids (TSS) and ash content

Total suspended solids (TSS, g L^{-1}) content was measured by passing a known volume (0.25 L)of culture broth through a 1 µm pore size glass fibre filter paper (GF/C, Whatman, UK) of known dry weight (W_1). Samples were weighed to an accuracy of ± 0.001 g and placed in an oven (LTE Scientific Ltd., Oldham UK / Heraeus Function Line series, UK) for drying overnight at 105 ± 1 °C. After 24 hours drying, the samples were transferred to a desiccator to cool for at least 40 minutes. Samples were then weighed (W_2) again with the same balance and finally TSS was determined according to the following equation:

$$TSS = \frac{W_2 - W_1}{0.25} \quad (9)$$

If the desired parameter was the ash content (%), an additional step was necessary. Samples were transferred to a muffle furnace (Carbolite Furnace 201, Carbolite, UK) and heated to 550 ± 10 ºC for two hours in accordance with Standad Method 2540 G (APHA, 2005). After this ashing step, samples were again cooled in a desiccator for at least one hour before weighing a third time (W_3). Then, ash content was calculated as:

$$Ash\ content = \frac{W_3 - W_1}{W_2 - W_1} 100 \quad (10)$$

3.7.3 Total Inorganic and Organic Carbon determination (TIC and TOC).

TIC and TOC were determined using the test kits LCK-381(Hach-lange, Germany) (Figure 37). In this test, total carbon (TC) and TIC contained in a liquid sample are converted to CO_2 by, respectively, oxidation and acidification. The CO_2 passes from the digestion cuvette through a membrane and into the indicator cuvette. The change of colour of the indicator is photometrically evaluated. TOC is determined as the difference between the TC and TIC values. The samples where carefully prepared following the manufacturer instructions.

Figure 37.- Tests kits LCK-381(picture obtained from http://www.hannainst.es/)

3.7.4 Chlorophyll fluorescence: Fv/Fm

The chlorophyll fluorescence was evaluated as the parameter Fv/Fm, which is the ratio of variable fluorescence to maximal fluorescence. After dark adaptation, minimum fluorescence is measured using a modulated light source (too low to drive photosynthesis). When an intense saturation pulse of light is applied, all the available reaction centres are closed and maximum fluorescence is measured. The difference between maximum and minimum fluorescence is Fv, which is normalized dividing it by maximum fluorescence to obtain the ratio Fv/Fm. This represents the maximum potential quantum efficiency of PSII if all capable reaction centres were open, and is used to estimate the potential efficiency of PSII by taking dark-adapted measurements. This parameter, therefore, tests whether or not microalgae stress affects photosystem II.

Experimentally, a sample of culture was introduced in a cuvette (10x10x45 mm) under dark conditions for 10 minutes. After this time, the Fv/Fm ratio was immediately measured by means of a fluorometer (AquaPen AP 100, Photon Systems Instruments, Czech Republic) (Figure 38).

Figure 38.- AquaPen AP 100 (picture obtained from www.psi.cz)

3.7.5 Turbidity

Turbidity in the culture was measured as a function of microalgae concentration in the reactor. It is created by suspension particles presented in the culture broth that produced light absorption or dispersion. To measure it, a sample is illuminated by an artificial light emitted by a light source whose intensity is known. The dispersion of light produced by particles is analysed by a photo-detector, usually in a 90° angle. This principle is called nephelometry,

and the results are expressed in Nephelometric Turbidity Units (NTU) or the equivalent Formazine Turbidity Units (FTU) defined in the standard ISO 7027.

In practice, turbidity was measured by means of a Portable HI 93703 C Turbidimeter-Nephelometer (Hanna Instruments, Italy) (Figure 39), which measured turbidity in the range 0-1000 NTU.

Figure 39.- Turbidimeter-Nephelometer Portable HI 90703 C (picture obtained from www.hannainst.es).

3.7.6 Absorbance

Absorbance was measured at 680 nm, which is the wavelength at which the chlorophyll absorbs light energy in the PSII. The device used was a double-beam Helios Alpha Spectrophotometer (Figure 40) which measures in the UV-Visible range. When the measured absorbance was above 1.5 the sample of culture was diluted in order to obtain a reliable value.

Figure 40.- Helios Alpha Spectrophotometer (picture obtained from www.ifj.edu.pl).

Chapter IV

4. FLUID-DYNAMIC CHARACTERIZATION OF RACEWAY REACTORS

In this part of the work an analysis was carried out of the fluid dynamics of a real-scale raceway reactor under various configurations and conditions. For this purpose, the raceway was operated at different water depths (which in turn determined the volume of water in the reactor) and liquid velocities, both with and without a sump baffle. Fluid dynamic parameters such as liquid velocity and circulation time, mixing time and Bodenstein number were determined, in addition to the specific power consumption. Circulation time defined the liquid velocity, which is a parameter of interest since, as described in the literature review, it must be maintained within a range to ensure the circulation of liquid at a low power requirements in order to prevent cells settling and stratification. Bodenstein number and mixing time were the parameters used to study the amount of mixing present in each part of the raceway, and the residence time in each section was used to evaluate the effect of the mixing properties in each specific section regarding the time for which every portion of liquid is exposed to these characteristics. These critical parameters are discussed in relation to the optimal conditions to operate this type of reactor for algae growth, and practical information for raceway design is provided.

4.1 Liquid depth

4.1.1 Objective

To determine the effect of water depth on power consumption of the raceway. To define the water depth that gives the minimum power consumption in W m^{-3} of fluid.

4.1.2 Methodology

Experiments were performed in the raceway described in section 3.2, operated with and without sump baffle. An air gas flow of 25 L min^{-1} gas was continuously injected in the sump through the diffuser type I described in section 3.4.1. Water depth was modified (from 10 to 30 cm in 5 cm

increments) and the paddlewheel rotation speed (i.e. the liquid circulation velocity) was modified by means of a device to control the electric frequency fed to the motor (from 10 to 40 s^{-1} in 10 s^{-1} increments). Specific power consumption was measured directly from the electrical power consumption of the converter-motor-gear box-paddlewheel unit and expressed in W m^{-3} of fluid to take account of the variation in the volume of water in the raceway. Three measurements were taken in each experiment, and the averaged value was presented as the final result.

4.1.3 Results

Table 6 shows the results of the experiments carried out, which are represented graphically in Figure 41 A) with and B) without the sump baffle. Without the sump baffle, the minimum specific power consumption was observed at a water depth of 20 cm, and ranged from 1.5 to 8.4 W m^{-3}. Higher specific power consumptions were recorded at a depth of 10 cm, ranging from 7.7 to 17.4 W m^{-3}; and also at 30 cm, from 2.6 to 12.2 W m^{-3}. In percentage terms, the power consumption at a water depth of 20 cm was 30 % lower than power consumption at 10 cm, and around 50 % lower than at 30 cm. With sump baffle in position, however, the differences in power consumption between 20, 25 and 30 cm depth were not significant, ranging from 2.4 to 2.9 W m^{-3} at motor frequency 10 s^{-1} and from 12.2 to 15.1 W m^{-3} at motor frequency 30 s^{-1}. In this case, power consumption at 10 and 15 cm were clearly higher than other depths.

Table 6.- Power consumption (W m^{-3}) at different water depths and motor frequencies with and without sump baffle

	Motor Frequency, s^{-1}	LIQUID DEPTH (cm)				
		10	15	20	25	30
Without sump baffle	10	7.7	5.0	1.5	3.0	2.6
	20	9.9	7.2	2.6	4.7	4.3
	30	13.2	12.5	5.2	8.4	7.6
	40	17.4	19.8	8.4	13.6	12.2
With sump baffle	10	7.3	5.0	2.9	3.0	2.4
	20	10.3	8.4	5.4	5.2	4.4
	30	15.0	14.2	9.7	9.0	7.9
	40	20.5	22.7	15.1	13.8	12.2

Figure 41 shows that specific power consumption increased at higher paddlewheel speeds (as measured by increased motor frequency), as a result of the higher liquid velocities. Specific power consumption also depended on water depth. Therefore, careful selection of a suitable water depth could significantly improve the energy efficiency of the system by reducing the power consumption.

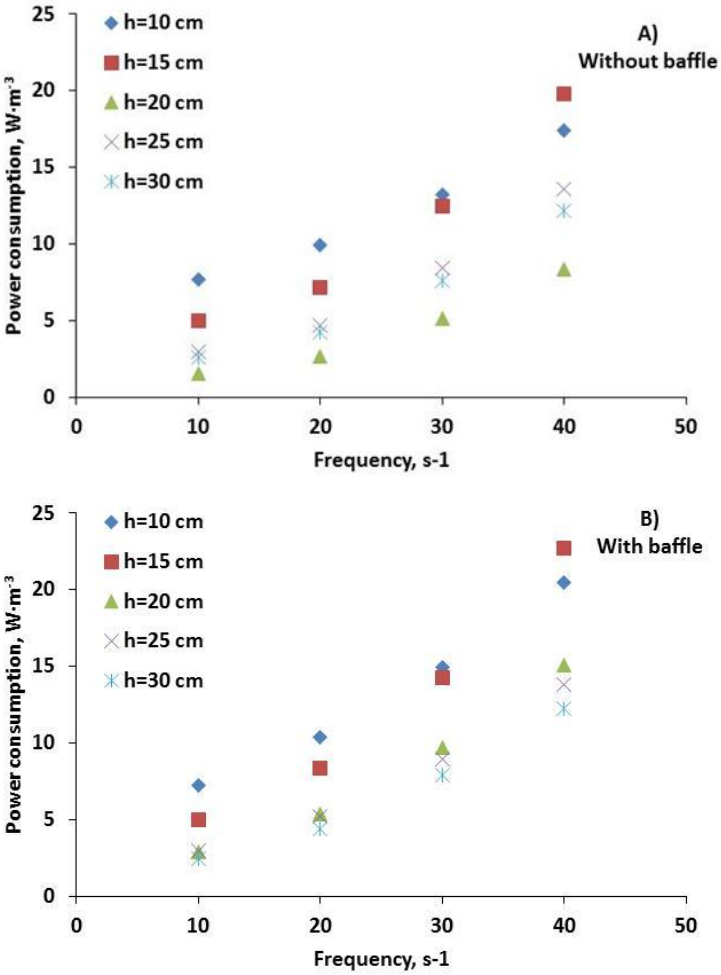

Figure 41.- Influence of motor frequency and water depth on specific power consumption in the paddlewheel in the raceway (a) without baffle and (b) with baffle

4.2 Preliminary tracer experiments

4.2.1 Objective

To determine the amount of tracer to be used in the investigation of mixing properties of the raceway and the location at which it should be added to the raceway.

4.2.2 Methodology

Preliminary tests were carried out to determine the amount of tracer to be used and the location where this should be added to the raceway in the stimulus-response experiments. The tracer used was NaOH and the response to the resulting pulse was measured by pH probes distributed in the raceway as described in section 3.7.1 to divide the raceway in 5 sections with the following length: paddlewheel (2 m), sump (2 m), channel 1(46), bend 1 (2 m) and channel 2 + bend 2 (52 m). The data collected by the probes was used to calculate the cycling time t_c (s) in the reactor from the time intervals between consecutive pH peaks in one location, i.e. time of pH1 in the first peak $tpH1_{Peak1}$ (s), and time of pH1 in the second peak $tpH1_{Peak2}$ (s) (Eq(11)). Cycling time was measured between cycles 1 and 2 in each of the 5 sections in which the raceway was divided plus an additional measurement for the all raceway in position 1. The final value of cycling time was calculated as an average of these 6 measurements. The residence time in each section (t_r) was also calculated during the first cycle as the time between recorded peaks in consecutive pH probes (Eq(12)). The liquid velocity in the channel v (m s^{-1}) was calculated as the ratio of the travel distance in the reactor (L=100 m) to the cycle time (Eq(13)). The velocities tested were obtained by means of the motor frequency controller, which was set between 15 and 40 s^{-1} with 5 s^{-1} increments. Mixing time t_m (h) was defined as the time required for variations in pH to reach less than 5 % of the final stable value. Thus, the number of cycles necessary for mixing (C_m) were obtained as Eq(14). Experiments were carried out with and without sump baffle, where an air gas flow of 25 L min^{-1} was continuously injected.

$$t_c = tpH1_{peak2} - tpH1_{peak1} \quad (11)$$

$$t_r = tpH1_{peak1} - tpH2_{peak1} \quad (12)$$

$$v = \frac{L}{t_c} \quad (13)$$

$$C_m = \frac{t_m}{t_c} \quad (14)$$

4.2.3 Results

Figure 42 shows the results of one of the preliminary tests carried out to determine the amount of sodium hydroxide and the injection point. As can be seen, the pulse method for determining mixing, cycling and residence times in the reactor appeared to be very effective: although the amplitude of the peaks decreases as mixing occurs, their definition is sufficient to allow quantification of these parameters.

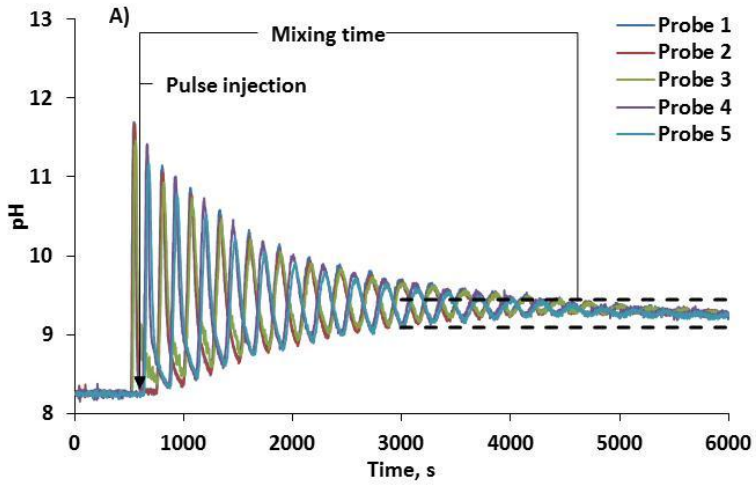

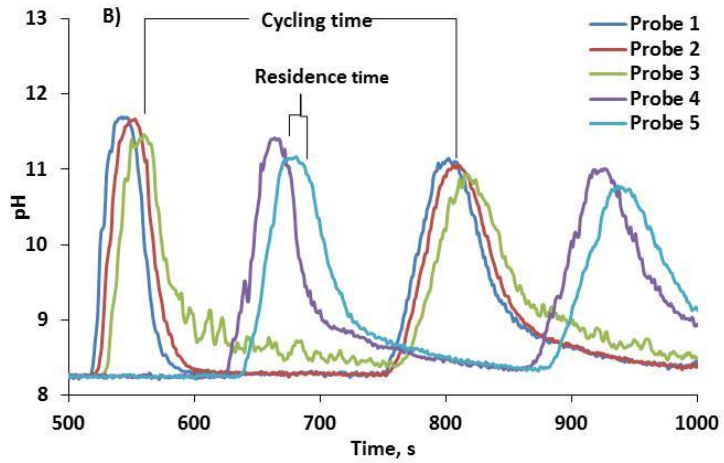

Figure 42.- Results from an experiment at 20 cm water depth without a baffle at a motor frequency of 40 Hz, indicating how the values are used to characterize the fluid dynamic in the reactor are derived. A) Pulse injection and mixing time, B) cycling time and residence

The liquid velocity achieved in the raceway with and without the baffle at different motor frequencies is presented in Table 7. In the experiments carried out without the baffle, the velocity was in the range of 0.22-0.40 m s^{-1}, while when baffle was used the velocity achieved was in the range 0.14-0.23 for the same motor frequencies. This was a 63 % and 58 % reduction in the minimum and maximum liquid velocity achieved when baffle was in position, respectively. Regarding mixing, 1.4-2.0 h and between 16-20 cycles were needed to mix the pulse of NaOH added, while without the baffle this range was 4.8-5.9 h and 31-41 cycles. Therefore, mixing time without the baffle was around 70 % lower than mixing time when a sump baffle was used.

Table 7.- Cycle time, mixing time, number of cycles for mixing and velocities in the raceway with and without sump baffle at different motor frequencies

	Motor Frequency, s^{-1}	tc, min	tm, h	C_m cycles	v, m s^{-1}
Without baffle	15	7.66	2.0	16	0.22
	25	4.98	1.6	19	0.34
	35	4.60	1.5	20	0.36
	40	4.33	1.4	19	0.40
With baffle	15	11.61	5.9	31	0.14
	25	8.88	5.2	35	0.19
	35	7.83	5.1	39	0.21
	40	7.13	4.8	41	0.23

The residence time was calculated in the raceway at different motor frequency with and without baffle (Table 8). In short sections like the paddlewheel, sump and bends the residence time was very similar in all the motor frequency tested. Mayor differences were found, however, in channel sections where small differences in liquid velocity produced big changes in residence time due to the longer size of these sections.

Table 8.- Residence time (s) at different motor frequency in the 5 sections of the raceway, with and without baffle

	Without baffle				**With baffle**			
Motor Frequency s^{-1}	15	25	35	40	15	25	35	40
Paddlewheel	11	6	9	11	2	19	12	10
Sump	8	1	9	7	42	30	21	27
Channel 1	196	132	109	104	280	200	190	181
Bend 1	16	15	18	17	40	26	12	8
Channel 2 + Bend 2	220	140	133	121	323	263	225	205

Based on the results of these preliminary experiments it was concluded that pulses of 1 L of saturated sodium hydroxide solution (10 mol L^{-1}) added before the bend preceding the paddlewheel gave a clear and well-defined response in the pH probes which could be used for investigation of mixing properties. This decision was based on the mixing properties of each section of the raceway; the pulse is added immediately before the set bend-paddlewheel where it was previously predicted that most of the mixing take place. Therefore, the NaOH pulse added in the straight section had time enough to acquire the same velocity than the liquid in the raceway before arriving at the section with higher turbulence. The final degree of mixing in this part in comparison to others in the raceway had to be confirmed by this fluid dynamic study.

4.3 Bend configuration: effect of number of deflectors

4.3.1 Objective

To determine the effect of the number of bend deflectors on power consumption for raceway mixing. To define the optimal number of bends in terms of power consumption.

4.3.2 Methodology

The raceways were operated without the sump baffle at a water depth of 20 cm and with motor frequencies from 10 to 40 s^{-1} corresponding to the maximum range that could be achieved. Three independent removable deflectors made of stainless steel were designed with the aim to be placed in the bends at intervals of one quarter of the channel width. Thus, four different bend configurations were tested: 3 bend deflectors, 2 bend deflectors, 1 bend deflector and without bend deflector. Specific power consumption was also measured directly from the electrical power consumption of the paddlewheel motor and the velocity was obtained by stimulus-response experiments with NaOH previously explained in section 4.2.2. Three measurements were taken in each experiment, and the averaged value was presented as the final result.

4.3.3 Results

The results showed that as the number of deflectors in the bends increased, the liquid velocity also increased for the same motor frequency (Figure 43A), and the power consumption for the same liquid velocity reduced (Figure 43B). Without deflectors the maximum liquid velocity achievable was less than 0.3 m s^{-1}, whereas with one or more deflectors the maximum velocity was 0.47 m s^{-1} (Table 9). Introduction of a single baffle had a major effect, whereas the effect of adding further baffles was relatively small at around 0.20-0.25 m s^{-1}, which is the typical operating velocity in raceway reactors. Subsequent experiments were therefore run with a single baffle positioned at a distance of one quarter of the channel width from the central wall, and at a channel depth of 20 cm.

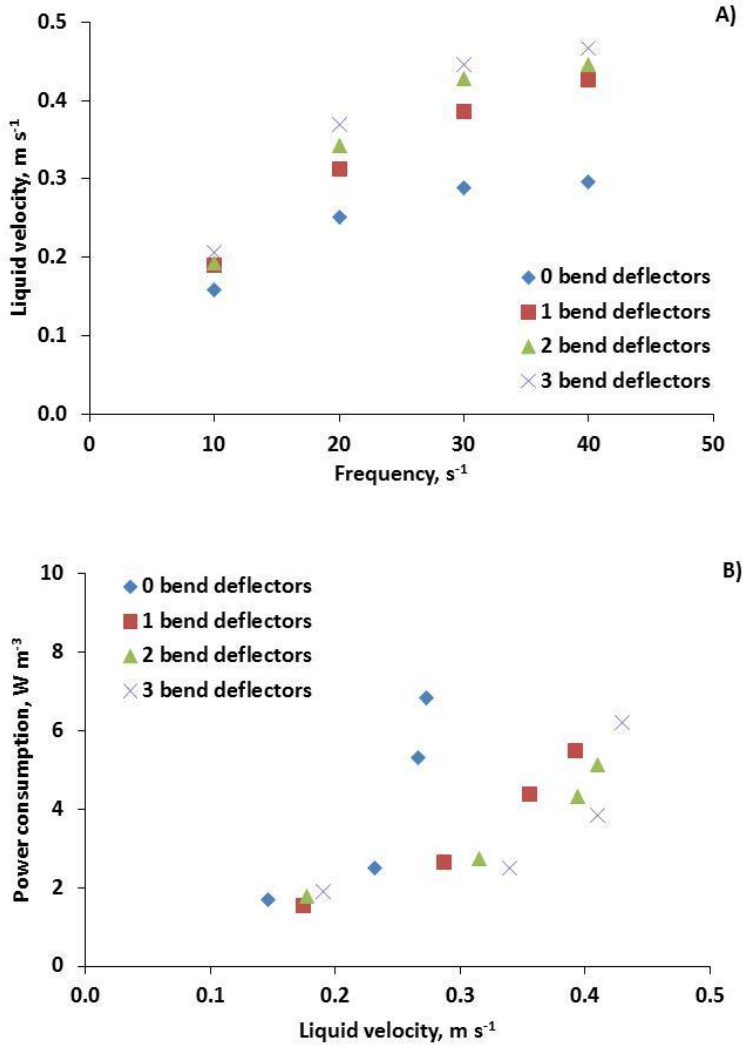

Figure 43.- Influence of bends deflectors on: A) liquid velocity at different motor frequency; B) power consumption at different liquid velocities

Table 9.- Liquid velocity and power consumption obtained at different motor frequencies with 0, 1, 2 and 3 bend deflectors

	Motor frequency, s^{-1}	Liquid velocity, m s^{-1}	Power consumption, W m^{-3}
0 Bend deflectors	10	0.16	1.69
	20	0.25	2.49
	30	0.29	5.33
	40	0.30	6.85
1 Bend deflectors	10	0.19	1.54
	20	0.31	2.64
	30	0.39	4.40
	40	0.43	5.50

	Motor frequency, s^{-1}	Liquid velocity, m s^{-1}	Power consumption, W m^{-3}
2 Bend deflectors	10	0.19	1.78
	20	0.34	2.74
	30	0.43	4.32
	40	0.45	5.12
3 Bend deflectors	10	0.21	1.91
	20	0.37	2.49
	30	0.45	3.86
	40	0.47	6.20

4.4 Sump configuration: effect of the sump baffle

4.4.1 Objective

To determine the effect of sump baffle on the liquid velocity in the raceway and to define its effect in the power consumption.

4.4.2 Methodology

The raceways were operated at a depth of 20 cm and motor frequencies from 10 to 40 s^{-1} (with 5 s^{-1} increments) with and without the sump baffle. The sump by itself may influence the fluid dynamic behaviour in this section of the raceway, but it can be influenced at the same time by the turbulence produced by the gaseous phase when it is bubbled at the bottom of the sump. Therefore, the culture conditions were simulated in the sump using fresh water and air bubbled at 25 L min^{-1}. The methodology to determine liquid velocity, residence time and mixing time by means of stimulus-response experiments with NaOH was developed in section 4.2.2, and the power consumption was directly measured as the electric power needed in the motor for paddlewheel rotation.

4.4.3 Results

The results shown in Figure 44A indicate that motor frequency is directly related to the paddlewheel rotational speed, and hence to the liquid velocity. As the liquid velocity increases, however, frictional losses in the channel increase exponentially. Therefore, specific power consumption increases exponentially with velocity due to the exponential relationship between the

velocity of the liquid and its kinetic energy, giving the curve seen in Figure 44B. This effect is more pronounced when the baffle is present as the frictional losses are greater.

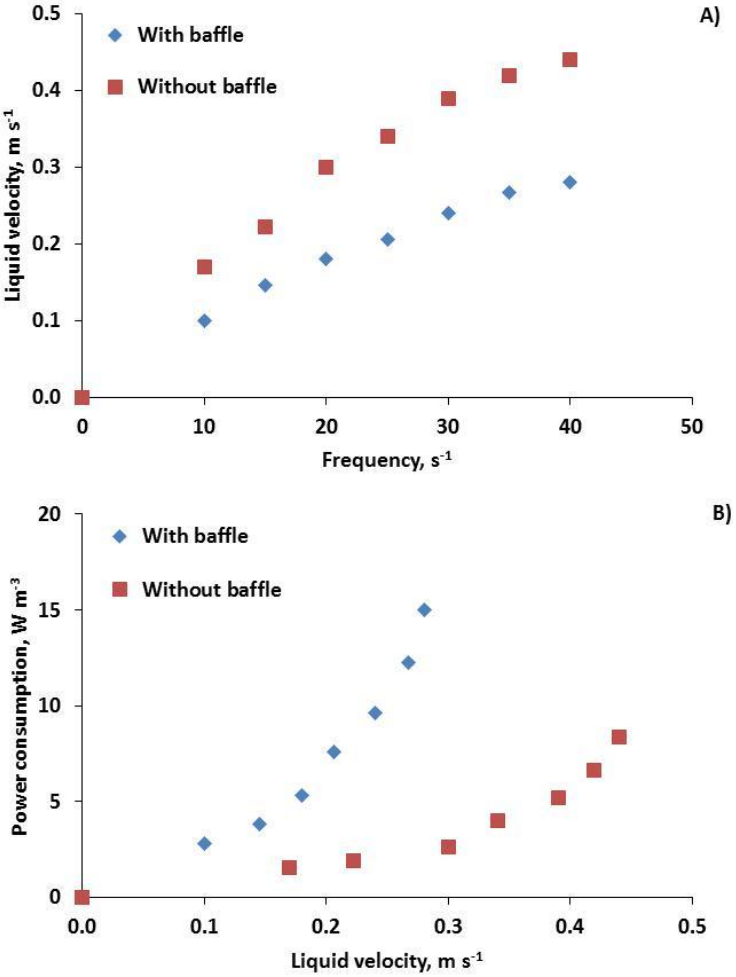

Figure 44.- Influence of sump baffle on: A) liquid velocity at different motor frequencies; B) power consumption at different liquid velocities

Table 10 shows the results obtained from these experiments. Without the baffle, the highest liquid velocity achieved was 0.44 m s^{-1}, while with the baffle in place it was 0.28 m s^{-1}. Over the range of liquid velocities tested, the specific power consumption was up to 8.36 W m^{-3} without the baffle and up to 15.07 W m^{-3} with the baffle in place i.e. 79 % higher. Thus the maximum liquid velocity when the baffle is in place was 37 % lower than without the baffle, and, at the same time, the presence of the baffle greatly increased the specific power consumption over the range of liquid velocities tested.

Table 10.- Liquid velocity and power consumption for different motor frequencies tested with and without sump baffle

	With sump baffle		Without sump baffle	
Motor frequency, s^{-1}	**Liquid velocity, m s^{-1}**	**Power consumption, W m^{-3}**	**Liquid velocity, m s^{-1}**	**Power consumption, W m^{-3}**
10	0.10	2.86	0.17	1.54
15	0.15	3.89	0.22	1.92
20	0.18	5.39	0.30	2.64
25	0.21	7.64	0.34	3.97
30	0.24	9.68	0.39	5.17
35	0.27	12.31	0.42	6.64
40	0.28	15.07	0.44	8.36

Residence time is another important fluid dynamic variable that determines the total time necessary to complete the course along the entire reactor, and thus affects reactor performance. It is widely accepted that a liquid velocity of 0.2 m s^{-1} is suitable for the growth of microalgal cultures in raceway reactors (Weissman et al., 1988), the specific power consumption at this velocity being relatively low. According to the experimental results, this velocity was obtained in the raceway without the baffle at a motor frequency of 15 s^{-1}, whereas at the same frequency with the baffle in place, the liquid velocity was only 0.12 m s^{-1}. The residence times determined experimentally in each section under these conditions are shown in Figure 45. As can be seen, the residence time in the channels is much higher than in the paddlewheel, sump and bend sections due to their smaller volumes, i.e. due to the shorter length of these sections. For the reactor without the baffle, the total residence time in each channel is around 200 s, whereas the residence times in bends, paddlewheel and sump were 16, 11 and 8 s, respectively. The presence of the baffle increased the residence time in all the studied sections. The total residence time, as the sum of the individual residence time of every section, in the reactor with baffle, therefore, increased from 450 to 700 s. This total residence time was the time necessary to complete the liquid one lap around the raceway.

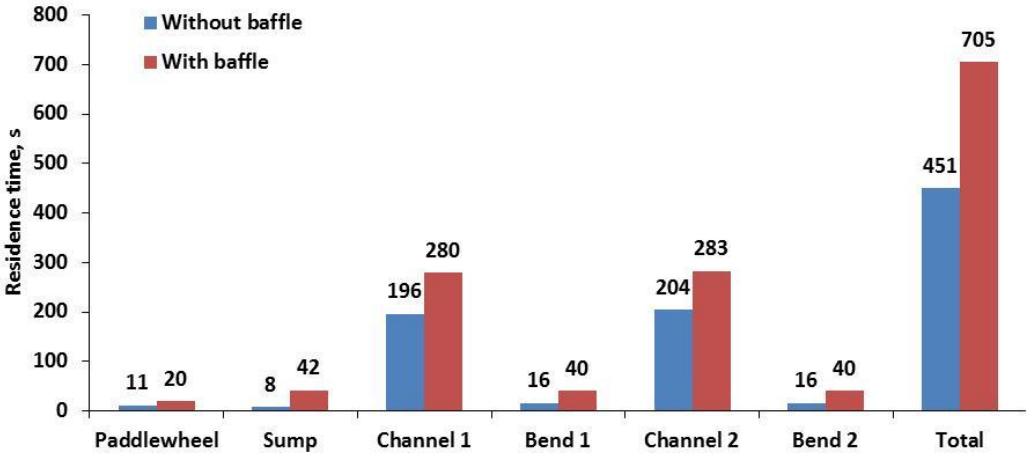

Figure 45.- Residence time of liquid in each section of the raceway reactor for an experiment carried out at a motor frequency of 15 s^{-1} giving a velocity of 0.22 m s^{-1} without a baffle and 0.12 m s^{-1} with sump baffle

Mixing time in the reactor reduced when the liquid velocity increased, both with and without the baffle (Figure 46). The presence of the baffle extended the mixing time considerably, however, even at the same liquid velocity. For the velocities studied, the mixing times ranged from 1.4 to 2.0 h without the baffle, and from 4.8 to 5.9 h with the baffle. The presence of the baffle had a greater influence than the liquid velocity on the time needed for complete mixing. In terms of cycles (circuits around the reactor), these data indicate that to achieve complete mixing, 15-20 cycles were needed without the baffle compared to 30-40 cycles with the baffle.

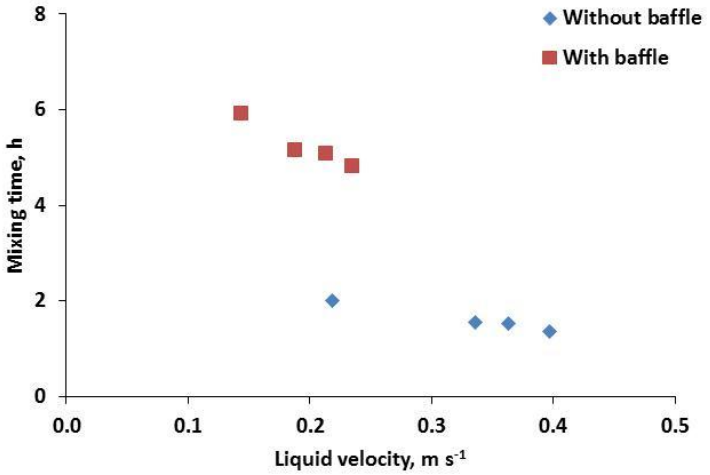

Figure 46.- Variation of mixing times in the reactor against liquid velocity, with and without a baffle

4.5 Mixing

4.5.1 Objective

To determine the contribution of every section of the raceway to global mixing. To study the effect of sump baffle in the mixing.

4.5.2 Methodology

The raceways were operated at a depth of 20 cm and liquid velocity was again modified from the minimum producing water circulation until the maximum allowed. The tests were carried out with and without sump baffle, where an air flow of 25 L min^{-1} was continuously injected during the experiment to simulate algae culture conditions. The mixing was studied by means of the Bodenstein number (Bo), which was calculated as described in section 3.7.1. Dispersion coefficient was calculated from Bo, liquid velocity and section length as Eq(8) showed also in section 3.7.1.

4.5.3 Results

Analysis of the results showed similar behaviour in all experiments, regardless of liquid velocity and the presence, or absence, of the baffle (Table 11): the paddlewheel, sump and bends presented low Bo values of less than 7, whilst the straight stretches, which account for 93 % of the total reactor volume, showed high Bo values ranging from 151 to 406. In the channels there are no features that cause disturbance to the flow and therefore the pattern corresponded to plug flow. As can be seen in Figure 47 and Table 11, there was a clearly defined difference between low and high values of Bo, demonstrating the usefulness of this non-dimensional number to indicate poor or good mixing. Liquid velocity did not show a strong influence on the Bo values for the channel sections when the baffle was presented (Figure 47B); whereas removal of the baffle increased the Bo values in the channel sections, and increasing the velocity in these conditions further increased the degree of plug flow (Figure 47A). In the other sections (sump, paddlewheel and bend), however, the behaviour as indicated by Bo values was independent of the sump arrangement. It is not possible, however, to use small differences in Bo value to compare the degree of mixing in zones with similar values. For this reason, as can be seen in Table 11, the final experimental value obtained for the whole

raceway does not always increase with velocity, but it is clear that all values are much higher than 100 and the raceway therefore behaves like a plug flow reactor.

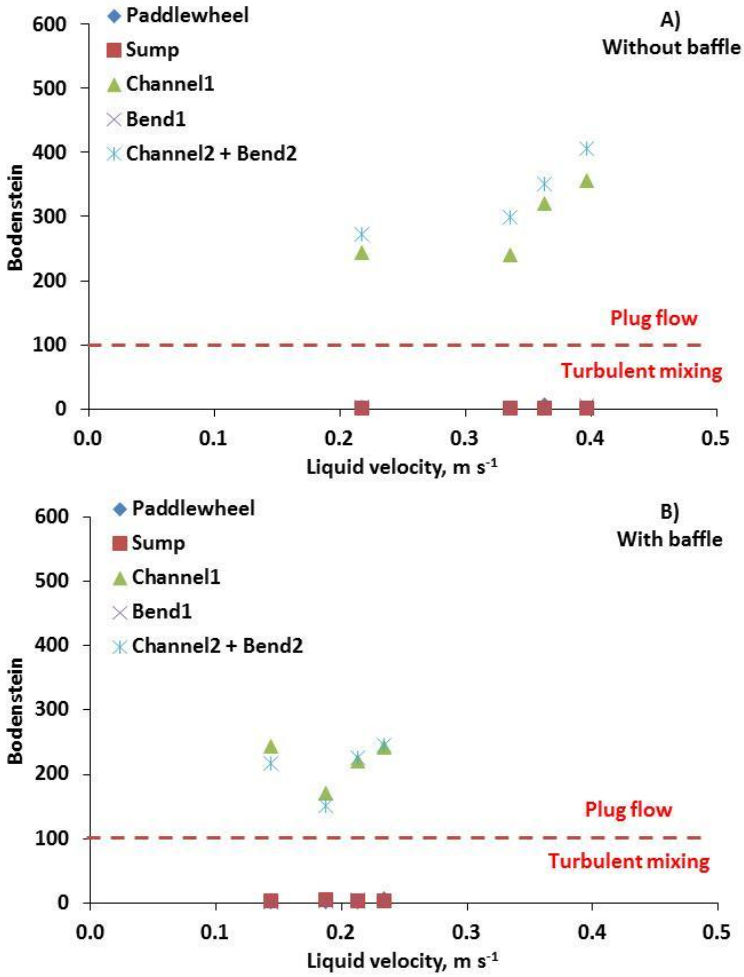

Figure 47.- Variation of the Bodenstein number in each section of the reactor against liquid velocity: A) without a baffle, B) with a baffle

Table 11.- Bodenstein number by raceway section and in the whole raceway at different liquid velocities with and without sump baffle

	Velocity m s^{-1}	Paddle-wheel	Sump	Channel 1	Bend 1	Channel2 + Bend2	Raceway
Without baffle	0.22	4	1	244	3	272	329
	0.34	1	1	240	1	298	399
	0.36	7	1	321	1	350	328
	0.40	1	1	357	5	406	432
With baffle	0.14	1	2	244	1	217	370
	0.19	1	4	170	2	151	463
	0.21	2	3	220	4	226	386
	0.23	7	4	242	3	245	406

Regarding the dispersion coefficient, Figure 48 shows the results obtained by sections at different liquid velocity with and without baffle (A) and B), respectively). The main differences were found in the sump, where the dispersion coefficient was between 0.44-0.72 m^2 s^{-1} without baffle and between 0.09-0.14 m^2 s^{-1} when baffle was used (Table 12). The dispersion coefficient in the other sections of the raceway was maintained under 0.2 m^2 s^{-1}, without significant differences found when using or not the sump baffle.

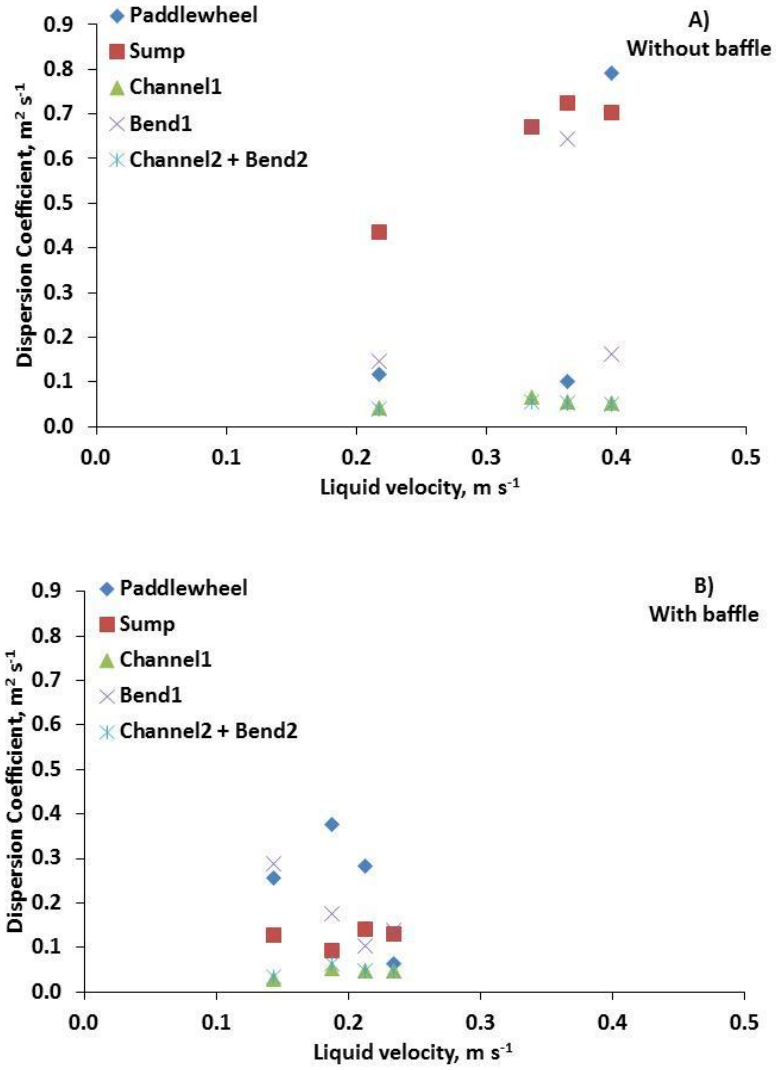

Figure 48.- Variation of the Dispersion coefficient (m^2 s^{-1}) in each section of the reactor against liquid velocity: A) without a baffle, B) with a baffle

Table 12.- Dispersion coefficient (m^2 s^{-1}) by raceway section and in the whole raceway at different liquid velocities with and without sump baffle

	Velocity, m s^{-1}	Paddle-wheel	Sump	Channel1	Bend1	Channel2 + Bend2	Raceway
Without baffle	0.22	0.12	0.44	0.04	0.15	0.04	0.07
	0.34	0.67	0.67	0.07	0.67	0.06	0.09
	0.36	0.10	0.72	0.05	0.64	0.05	0.11
	0.40	0.79	0.70	0.05	0.16	0.05	0.10
With baffle	0.14	0.26	0.13	0.03	0.29	0.03	0.04
	0.19	0.38	0.09	0.05	0.18	0.06	0.04
	0.21	0.28	0.14	0.05	0.10	0.05	0.06
	0.23	0.06	0.13	0.05	0.14	0.05	0.06

4.6 Discussion and conclusions

Fluid-dynamic characterization of the reactor showed that the water depth, liquid velocity and presence or absence of deflectors in the bends or of a baffle in the sump all influenced the behaviour of the entire system. The optimum water depth for this paddlewheel was determined as 0.2 m, based on the specific power consumption. The paddlewheel must therefore be carefully designed to match the planned liquid depth for the raceway reactor, otherwise its efficiency will be decreased: this supports the findings of Weissman and Goebel (Weissman & Goebel, 1987). The presence of deflectors in the bends improved the performance of the reactor by reducing the power consumption for the same liquid velocity. Similar findings have recently been reported from data obtained by CFD simulations (Labatut et al., 2007), which recommended the use of asymmetric islands to minimize the existence of dead zones and maximize the energy yield. Sompech et al. (Sompech et al., 2012) also reported based on unvalidated CFD simulations the existence of dead zones in curves and the possibility of reducing them by means of bend deflectors. They found that three bend deflectors eliminated almost the all dead zones in raceway bends. In practice, it was observed that major differences in power consumption and liquid velocity were obtained when configurations with and without bend deflectors were compared, independently of the number of deflectors used. The current work provides real data for the first time to support this view that one deflector is enough to achieve the desired improvement in the hydraulic performance of the bend. Whatever the

configuration, the results showed that specific power consumption increases significantly with liquid velocity, and this increase is higher when the baffle is in place as it offers a direct obstacle to the flow even at low liquid velocities.

It is interesting to compare the measured specific power consumption with the theoretical potential energy yields from the system based on maximum photosynthetic efficiency (Figure 49). On the site where the reactor is located the daily mean value of solar radiation is 17.58 MJ m^{-2} day^{-1} and, assuming a photosynthetic efficiency of 5 % (Carvalho et al., 2006), the maximum amount of energy that can be fixed is 0.88 MJ m^{-2} day^{-1}. If the energy consumption to run the system is limited to 20 % of this maximum energy production, this means 0.18 MJ m^{-2} day^{-1} is available for parasitic or self-uptake demand (Acien et al., 2012). Using the baffle, the specific power consumption is higher than the acceptable self-uptake demand of the system at liquid velocities above 0.24 m s^{-1} (V_{max} for the system with sump baffle); whereas without the baffle, the specific power consumption is less than the acceptable self-uptake demand over the entire range of liquid velocities tested. From these data it can be concluded that the use of a baffle potentially represents an important disadvantage in the net energy performance of these systems. Figure 49 shows that, at a typical velocity of 0.2 m s^{-1} as used in large-scale raceways, both configurations with and without sump baffle have power consumptions below the self-uptake of energy. It should be noted that power consumption without the baffle at this velocity was considerably lower than with the baffle, so the elimination of this device could potentially improve the total energy balance of the system as tested. It is important to remark, however, that the dimensions of the baffle used were not optimised. Recent work based on CFD modelling of the current system (Musgrove & Heaven, 2015) suggests that the power requirement for circulation of fluid around the sump can be reduced by up to 73 % through modifications to the sump and baffle design. These results emphasise the power of combining CFD approaches with real experimental data.

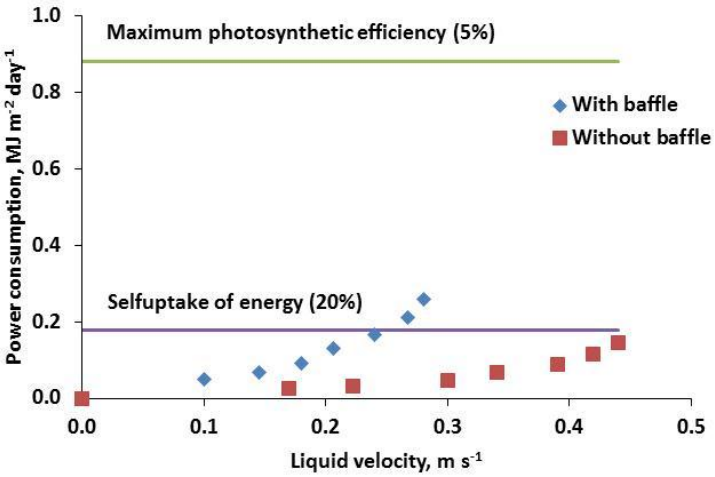

Figure 49.- Power consumption and liquid velocity, with and without a baffle. Comparison with maximum allowable values based on photosynthetic efficiency

In addition to the baffle, other features of the channel design also influence power consumption in the raceway reactor. The power requirement to circulate liquid at different velocities in large-scale raceways has previously been reported (Oswald & Borowitzka, 1988; Weissman et al., 1988). Weissman et al. (Weissman & Goebel, 1987) described the mixing power requirements in raceways as the variation of the Manning´s formula showed in Eq(15), where the power consumption P (W) of a raceway can be calculated as a function of the pond area A (m^2), the mean channel velocity v ($m\ s^{-1}$), the Manning's roughness n ($s\ m^{-0.3}$) which was 0.012 for smooth plastic, the depth of liquid d (m) and the overall mixing system efficiency e which included both the hydraulic efficiency of the pumping device and that of the drive (30 % is typical for paddlewheels). Dividing Eq(15) by the volume of liquid in the raceway, it is possible to obtain the specific power consumption in $W\ m^{-3}$.

$$P = \frac{9810 A v^3 n^2}{d^{0.3} e} \qquad (15)$$

Alternatively, once the liquid is in regime and the kinetic energy remains constant the power consumption per volumetric unit can be calculated from the mechanical energy balance (Bernoulli equation) as a function of the head loss in the system ΣF ($J\ kg^{-1}$) and the total volume of liquid into the reactor V

(m^3) (Eq(16)). In this equation, volumetric flow Q ($m^3\ s^{-1}$) and liquid density ρ (kg m^{-3}) represented the conversion factors to obtain the power consumption in the desired units (W m^{-3}).

$$P = \frac{\sum FQ\rho}{V} \tag{16}$$

The head loss is a function of the reactor length L (m), the liquid velocity v (m s^{-1}) and the equivalent diameter D (m) which is an approximation of the diameter for non-circular sections in addition to the Fanning friction factor f_F, which takes account of turbulence and relative roughness (Fanning Equation(17)). Fanning friction factor was obtained from Chen's equation (Eq(18)), which is valid for any friction factor and roughness, and for transition and turbulent flows. In this equation, the absolute roughness (ε) used for glass fibre was 0.01, D was the equivalent diameter (m) and N_{Re} was the non-dimensional Reynolds number. The equivalent diameter was calculated as 4 times the hydraulic radio (Eq(19)), where w and d were channel width and water depth respectively. The Reynolds number was calculated as Eq(20), where μ was the water viscosity (10^{-3} Pa s). The advantage of using Eq(21) is that the head loss associated with different features (e.g. bends and sump baffle) can be calculated and added to that in the channels to determine the contribution of different components to the overall head loss under different operating conditions. The head loss in a bend and sump baffle was calculated as a function of the loss coefficient for the feature $K_{feature}$, which is a characteristic coefficient that depends on the feature. This was obtained by fitting the experimental data to Eq(21).

$$\sum F = 2f_F \frac{Lv^2}{D} \tag{17}$$

$$\frac{1}{\sqrt{f_F}} = -4\log_{10}\left\{\frac{1}{3.7065}\left(\frac{\varepsilon}{D}\right) - \frac{5.0452}{N_{Re}}\log_{10}\left[\frac{1}{2.8257}\left(\frac{\varepsilon}{D}\right)^{1.1098} + \frac{5.8506}{N_{Re}{}^{0.8981}}\right]\right\} \tag{18}$$

$$D = 4R_h = 4\frac{wd}{w + d + d} \tag{19}$$

$$N_{Re} = \frac{Dv\rho}{\mu} \tag{20}$$

$$\sum F_{feature} = K_{feature}\frac{v^2}{D} \tag{21}$$

Experimental data were compared with the values obtained using the above equations. The results obtained using the Manning's Equation (15) and Bernoulli's Equation (16) for the raceway without features were very similar (Table 13), with specific power consumption increasing exponentially with liquid velocity.

Table 13.- Specific power consumption obtained theoretically using Manning's and Bernoulli's Equations ((15) and (16), respectively), at different liquid velocities

	Theoretical Power consumption W m^{-3}			
Velocity, m s^{-1}	**Manning**	**Bernoulli**	**Bernoulli+Bends**	**Bernoulli+Bends+Baffle**
0.10	0.04	0.04	0.10	0.67
0.20	0.31	0.33	0.79	5.36
0.30	1.03	1.12	2.66	18.09
0.40	2.44	2.65	6.31	42.88

By fitting the experimental data to Equation (21), including head loss in the bends, a bend loss coefficient of 11.4 was obtained (10 times the equivalent diameter, 20 times if both bends are considered). The results obtained here show the head loss in the bends and sump baffle were 1.5 and 13.5 times the head loss in the straight channel, respectively. When only channel length was used in the calculation, calculated values for power consumption were lower than experimentally measured results, both with and without the baffle (Table 14).

Table 14.- Specific power consumption obtained experimentally at different liquid velocities with and without sump baffle

Without sump baffle		With sump baffle	
Velocity, $m\ s^{-1}$	Power Consumption, $W\ m^{-3}$	Velocity, $m\ s^{-1}$	Power Consumption, $W\ m^{-3}$
0.17	1.54	0.10	2.86
0.22	1.92	0.15	3.89
0.30	2.64	0.18	5.39
0.34	3.97	0.21	7.64
0.39	5.17	0.24	9.68
0.42	6.64	0.27	12.31
0.44	8.36	0.28	15.07

Experimental data shown in Table 14 for specific power consumption without the baffle agreed with the value calculated using Eq(21) and including the head loss in the bends, thus confirming the adequacy of the method used (Figure 50). Because of the known effect of bends on power consumption, it has been recommended that raceway reactors have a maximum of four parallel channel sections (Weissman & Goebel, 1987). No data have previously been reported, however, on the influence of the baffle on the specific power consumption. Equation (21) was used to calculate the loss coefficient in the baffle based on experimental data and gave a value of 114 (200 times the hydraulic diameter).

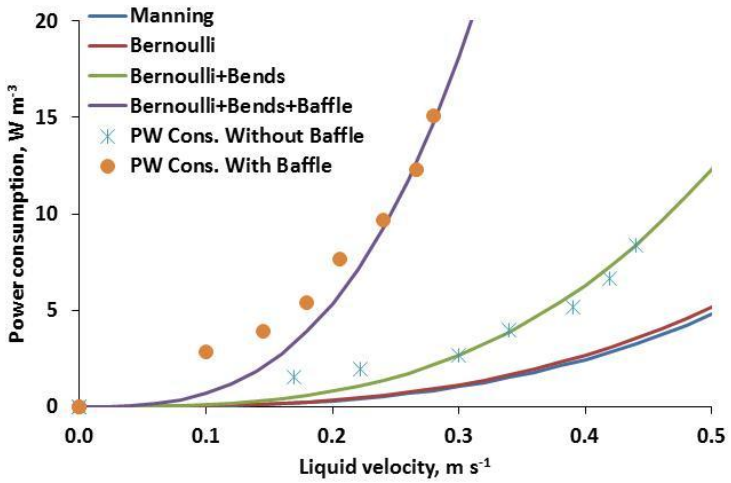

Figure 50.- Power consumption and liquid velocity. Comparison between experimental data and previously reported models

The low specific power consumption required for mixing shows one important advantage of raceways over other types of microalgae culture reactors. The raceway design was intended to allow a wide range of operating depths and liquid velocities to be tested, rather than being optimised to reduce head losses, and the measured specific power consumption was higher than reported values for large-scale units, which range from 0.5 to 1.5 W m^{-3} (Weissman et al., 1988). For smaller reactors the power consumption is likely to be even higher, with values of 9.0 W m^{-3} being reported for a 20 m^2 raceway reactor (Wang et al., 2008). The specific power consumption was nevertheless much lower than reported values for other types of reactor at similar biomass productivities e.g. 53 W m^{-3} in flat plates, 40 W m^{-3} in bubble columns and 2000 W m^{-3} in tubular photobioreactors (Acién Fernández et al., 2001; Hall et al., 2003; Sierra et al., 2008).

When culturing microalgae for biofuel production, energy inputs must be minimized in order to achieve a positive energy balance (Lundquist et al., 2010): this is particularly important due to the low anticipated profit margin of these systems (Hall & Benemann, 2011; Stephenson et al., 2011). Net energy yields in raceway reactors could be enhanced by improving the efficiency of the paddlewheel system (Chapter VII) or possibly by replacing it with alternative systems (Wang et al., 2008). There is scope also for optimisation of sump design (Musgrove & Heaven, 2015). Previous researchers have looked at the effect of raceway velocities on power consumption, as this is one of the major contributing factors to energy demand (James & Boriah, 2010; Weissman et al., 1988). The results from this study demonstrate the effect of higher velocities, and confirm the importance of optimising velocity in relation to algal productivity. The work also shows that the presence of a baffle can have a great impact on the specific power consumption. Potential benefits that might offset this, in terms of increased overall productivity due to enhanced gas transfer and mixing, need to be evaluated using the sump in both co-current and counter-current mode. A significant improvement in productivity would be required, however, to compensate for the increase in power consumption produced by the sump baffle in the current case.

An efficient algal cultivation system should avoid gradients in water chemistry, light, temperature and nutrient concentration, all of which may damage or limit growth. Turbulence moves the liquid and thus the algal cells

between the 'light' volume near the surface and the 'dark' volume at the bottom. Light/dark cycles at frequencies of 0.3-1.0 s^{-1} may stimulate growth rates, but these cannot easily be achieved in large reactors (Posten, 2009). In raceway reactors dead-zones and areas of low turbulence exist due to non-optimized designs (Labatut et al., 2007; Stephenson et al., 2011; Wang et al., 2008). In this system, results show the strong influence of the baffle configuration on the total mixing time: for the same flow velocity of 0.22 m s^{-1}, the presence of the baffle increased the mixing time by 3 hours. Mixing times without the baffle (2.0 h), and with it (5.1 h), are of the same order of magnitude as the period of high solar radiation (6-8 h). Thus, the reactor must be operated in continuous mode to avoid nutrient gradients that may reduce the biomass yield; or alternatively in semi-continuous mode, provided that nutrient addition occurs in the late afternoon after harvesting to allow complete mixing of the culture before dawn.

In large raceways with long channels and a high degree of plug flow, mixing could be even more important, and for this reason it is useful to know the contribution of each section to mixing in the reactor. The results showed that dispersion in the system took place mainly in three sections: the sump, paddlewheel and bends, which showed complete mixing. Figure 47 shows that the greatest mixing (Bodenstein < 20) with and without sump baffle took place in the paddlewheel and sump, where energy was added to the system; and also in the bends, where high head loss occurs. As 93 % of the reactor volume is in the straight channels with Bodenstein values >150 in all conditions, the overall characteristics of the reactor are best described as plug flow and mixing only occurs in a short part of the section of the entire raceway.

The dispersion coefficient (D_z) was calculated as a function of liquid velocity (v), the Bodenstein number (Bo) and the length of the section ($L_{section}$) according to Eq(22):

$$D_z = \frac{vL_{section}}{Bo} \tag{22}$$

For experiments performed at a liquid velocity of 0.22 m s^{-1}, the dispersion coefficient in the channels and the bends is the same with or

without the baffle, but changes considerably in the paddlewheel and sump sections as Figure 51 shows.

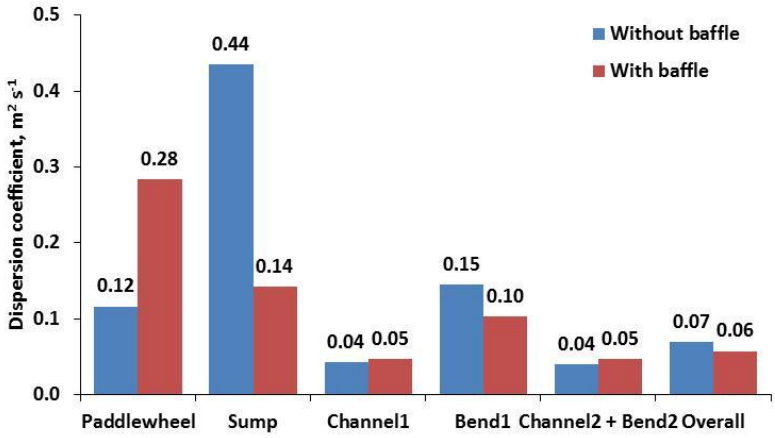

Figure 51.- Influence of a baffle on the dispersion coefficient in each section of the reactor at a liquid velocity of 0.22 m s^{-1}

The dispersion coefficient for the paddlewheel section is higher with a baffle because, under these conditions, the liquid depth in this section increases, causing increased mixing. For the sump, the opposite is observed. When the baffle is present, the liquid flow through the sump is similar to that through a closed pipe, and the dispersion coefficient is lower than when there is no baffle in place and the whole liquid column is mixed by aeration. Dispersion coefficients for the paddlewheel, sump and bends were in the range 0.10-0.44 m^2 s^{-1}, higher than the calculated values for the channels, which ranged from 0.04 to 0.05 m^2 s^{-1}. As the channels make up the main volume of the reactor, the overall dispersion coefficients for the raceway at 0.22 m^2 s^{-1} were 0.06-0.07 m^2 s^{-1} with specific power consumptions of 1.8 W m^{-3} and 6.8 W m^{-3} for operation with and without a baffle, respectively.

In flat panels and bubble columns, dispersion coefficient values of 0.02-0.04 m^2 s^{-1} have been reported, with specific power consumptions ranging from 40 to 200 W m^{-3} (Carvalho et al., 2006; Sierra et al., 2008). In tubular photobioreactors, dispersion coefficients ranging from 0.008 to 0.021 m^2 s^{-1} have been reported (Davies, 1972). Moreover, in tubular photobioreactors, the power demand is up to 2000 W m^{-3} but the value of the dispersion coefficient is similar to flat panels and bubble columns, ranging from 0.01 to 0.04 m^2 s^{-1} (Acién Fernández et al., 2001; Hall et al., 2003). In this respect, raceway reactors are demonstrated to be highly efficient in the use of energy; but at the

same time, if operated correctly, are able to provide enough mixing to avoid concentration gradients that can limit the growth of microalgae cultures.

4.7 Summary conclusions for Chapter IV

In conclusion, the work in this chapter has shown the following:

- The one-baffle bend configuration was identified as the best option at a typical operational liquid velocity. The addition of one bend produced a significant reduction in power consumption and increase in liquid velocity, with relatively little further benefit from the addition 2 or 3 bends at this velocity.
- The maximum liquid velocity at which the use of only 1 baffle in the bend was recommended was 0.25 m s^{-1}. If the liquid velocity is higher, the energy saving using additional baffle(s) may be worthwhile, although higher velocities are out of the range of typical values found in the literature for liquid circulation in raceway reactors.
- Over the range of velocities tested, the specific power consumption increased with the sump baffle. The maximum velocity achieved when the baffle was in place was 37 % lower than without the baffle, with the power consumption 79 % higher. Mixing time also increased by 3 hours when using the sump baffle.
- With the baffle, the specific power consumption was higher than the acceptable self-uptake demand of the system at liquid velocities above 0.24 m s^{-1}, whereas without the baffle it was lower over the entire range of liquid velocities tested.
- The use of the sump baffle in the studied configuration is not recommended from an energy point of view, unless its hydrodynamic characteristics are improved to reduce the head loss produced. The hypothetical improvement in mass transfer produced by the sump baffle must be evaluated (section 6.2).
- The greatest mixing took place in the paddlewheel, sump and bends. The general behaviour of the raceway, however, was considered as plug flow, since 93 % of the reactor is composed of straight channels with poor mixing.

Chapter V

5. OXYGEN MASS TRANSFER ASSESSMENT IN RACEWAY REACTORS

One of the main advantages of open reactors in comparison to closed is the direct contact with the atmosphere which, in theory, facilitates mass transfer for oxygen desorption from a supersaturated algal culture to the air where the concentration is lower. However, this mass transfer phenomenon has not been extensively studied in raceway reactors at large scale. Dissolved oxygen (DO) must be removed from the culture to avoid the damaging effects of photo-oxidation on cells, photorespiration, and suppression of photosynthesis (Vonshak, 1997) producing a decrease in the overall performance of the system. As the mass transfer of CO_2 and O_2 are closely related both must be considered in a good design (Camacho Rubio et al., 1999). The oxygen released into the culture medium by microalgae as a product of the photosynthesis reaction and its accumulation in the broth depends on the reactor configuration. For this reason, the work in this part of the thesis was focused in the analysis of oxygen transfer capability of the raceway provided with a gas transfer sump through which gas injection could be controlled by varying the flow rate and diffuser type.

The mass transfer capacity for oxygen was determined for the whole reactor at different liquid velocities, and also for specific sections of the reactor, including straight and curved channel sections, the paddlewheel section, and sump section. Different diffusers commonly used in waste-water treatment plants were also tested, studying the overpressure needed to allow the bubbling of gas (characteristic pressure needed to pass through the diffuser plus the pressure produced by the column of water present in the sump), the compression work necessary to achieve this overpressure and the mass transfer coefficient of each diffuser at different gas flow rate. Microalgal culture experiments were also carried out to study the effect of DO accumulation.

5.1 Mass transfer characterization of sump and diffusers

5.1.1 Objective

To determine the oxygen mass transfer capacity in the sump of three gas diffusers commonly used in wastewater treatment plants. To define the most suitable diffuser based in its performance in terms of mass transfer efficiency and power consumption.

5.1.2 Methodology

Oxygen mass transfer was determined at different gas flow rate using a dynamic method in which the sump was filled with fresh water (Figure 52, left), and nitrogen gas was bubbled through a diffuser at the bottom of the sump until the DO concentration reached zero. At this point the gas flow was switched to air which was bubbled until the water became saturated with dissolved oxygen in equilibrium with the air (Figure 52, right). DO concentration was measured at the liquid surface, and it was assumed that the sump was well mixed due to the turbulence produced by gas bubbling. Therefore, readings taken at this point were considered representative of the sump contents. Different gas flow rates were tested from 0 to 3.6 m^3 h^{-1}.

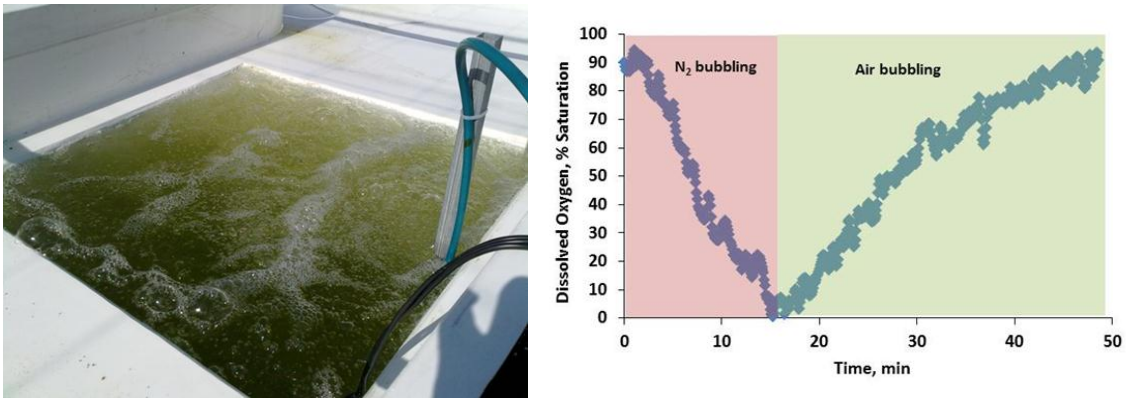

Figure 52.- Left: Sump filled with water for sump and diffusers characterization. Right: Results from a DO desorption/absorption experiment at 18.6 L min^{-1} gas flow with membrane plate diffuser (type 2). Oxygen desorption and absorption was obtained by bubbling nitrogen and air, respectively

The variation in DO with time is assumed to be a function of the mass transfer coefficient (K_la_l) and the driving force ($[O_2^*]$-$[O_2]$) (Eq(23)), where K_la_l is the overall volumetric mass transfer coefficient (s^{-1}), $[O_2]$ is the DO concentration (mg L^{-1}), $[O_2^*]$ is the equilibrium DO concentration (mg L^{-1}) and t is time (s).

$$\frac{d[O_2]}{dt} = K_l a_l \cdot ([O_2{}^*] - [O_2]) \tag{23}$$

By integrating this equation between time zero and time t the mass transfer coefficient can be obtained (Eq(24)). This equation is valid only when the reactor is fully mixed, and K_la_l may be influenced by electrode delays that are a function of the fluid hydrodynamics near its measuring surface (Chisti et al., 1987). This may be accounted for by defining the fractional approach to equilibrium (E) (Eq(25)), and the mass transfer coefficient can be obtained as a function of E and time (Eq(26)).

$$\ln\left(\frac{[O_2{}^*] - [O_2]_{t=0}}{[O_2{}^*] - [O_2]}\right) = K_l a_l \cdot t \tag{24}$$

$$E = \left(\frac{[O_2] - [O_2]_{t=0}}{[O_2{}^*] - [O_2]_{t=0}}\right) \tag{25}$$

$$K_l a_l = \frac{\ln(1-E)}{t} \tag{26}$$

Three different types of diffuser commonly used in wastewater treatment and previously described in Chapter III-3.4.1 were tested at different pressure. The power consumption for gas transfer is calculated as the work required to compress air from atmospheric pressure to overpressure under isothermal conditions at 20 ºC using Eq(27), where P is the power consumption (J s^{-1}), N is the gas molar flow (mol s^{-1}), R is the ideal gas constant (8.31 J K^{-1} mol^{-1}), T is temperature (293 K), p_1 is the atmospheric pressure (1 atm) and p_2 is the overpressure in the diffuser (atm) required to bubble the gas in the sump. This

is determined by passing different gas flows through the diffusers and measuring the pressure using a standard glycerine manometer.

$$P = NRT \ln\left(\frac{p_2}{p_1}\right) \tag{27}$$

5.1.3 Results

Figure 53 shows the differential pressure (overpressure) required to obtain different gas flow rates for each type of diffuser, including the 0.10 atm of hydrostatic pressure at the bottom of the sump (1 m depth). The type 1 diffuser clearly needs a higher overpressure to work in comparison to the other two diffusers tested. To reach the highest gas flow rate tested of 3.6 $m^3\ h^{-1}$, the type1 diffuser required an overpressure of 2.94 atm, whereas the type 2 and 3 diffusers attained the same gas flow rate with only 0.67 and 0.95 atm of overpressure, respectively (Table 15). This means it is possible to achieve this gas flow with diffusers 2 and 3 at only 19-27 % of the pressure needed with diffuser 1, and this pressure is directly related to the required power consumption for gas supply in the system. Irrespective of the type of diffuser, the gas flow rate showed a linear relationship to the overpressure with slopes of 0.84, 0.28 and 0.21 atm h m^{-3} for types 1, 2 and 3, respectively. This highlights the big difference in overpressure between the membrane tubing diffuser and, on the other hand, the membrane plate and porous tubing diffuser whose overpressure were quite similar and much lower than the type 1 diffuser.

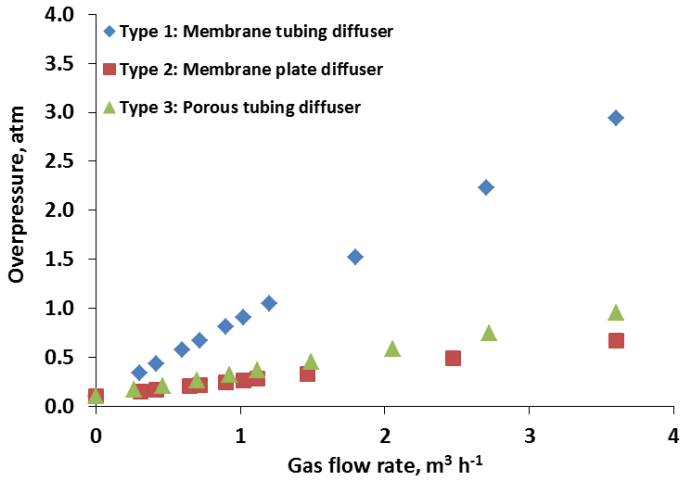

Figure 53.- Variation of overpressure with gas flow rate and diffuser type

The power consumption necessary to achieve the required pressures was also determined and compared for all diffusers. Figure 54 shows an exponential relationship between gas flow rate and compression work, with power consumption using the membrane tubing diffuser clearly higher than using diffusers 2 and 3 at all gas flow rates tested. Due to the exponential relationship, the difference in power consumption between diffuser 1 and diffusers 2 and 3 increased sharply with increasing gas flow. To obtain the maximum gas flow tested in the system, a power consumption of up to 149.12 W was required when using membrane diffuser type 1 (Table 15). This decreased to 72.71 and 55.86 W when using the porous tube and plate diffuser, equivalent to 46 % and 37 % of the energy used with diffuser type 1, respectively. Therefore, from a power consumption point of view, diffusers type 2 and 3 seem suitable to be used in raceway reactors for microalgae cultivation.

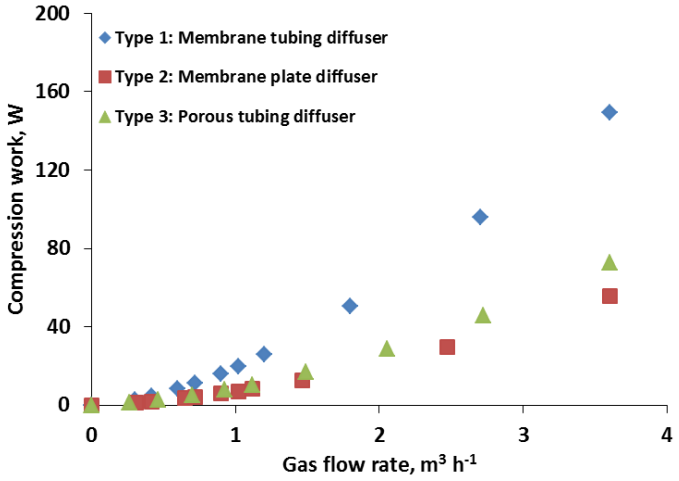

Figure 54.- Variation of compression work with gas flow rate and diffuser type

It is also important, however, to know which of the diffusers studied gives a better performance in terms of mass transfer, since the higher power consumption may be compensated by an increment in the gas transference capacity of the system due to the gas flow pattern and bubble size produced by the diffuser. Figure 55 shows that the membrane diffusers (types 1 and 2) gave a higher gas transfer coefficient than the porous tube (type 3). This is due to the material used to fabricate these membrane diffusers, which are usually made of teflon. This material gives a smaller bubble size than the porous

tubing at the same gas flow rate, clearly demonstrating that the mass transfer coefficient is only a function of bubble size and gas flow rate and is independent of pressure drop. Mass transfer coefficients of 32.40 and 29.16 h^{-1} were obtained for type 1 and 2 diffusers, compared to 10.80 h^{-1} (3 times lower) for the type 3 diffuser when operated at the highest gas flow rate of 3.60 m^3 h^{-1} (Table 15). In conclusion, the membrane plate diffuser (type 2) seems to be the most suitable of the diffusers studied for gas bubbling in raceway reactors since it is able to provide a gas flow with small bubbles that enhances the mass transfer and, at the same time, requires a lower overpressure to work i.e. low power consumption.

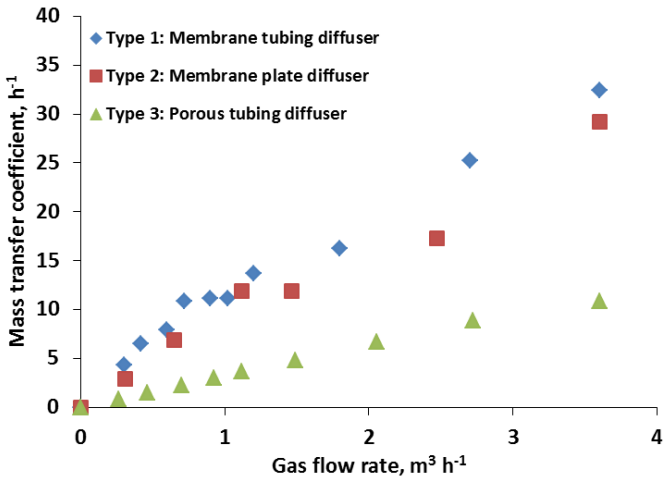

Figure 55.- Variation of mass transfer coefficient with the nitrogen gas flow rate and diffuser type

Table 15.- Overpressure, compression work and mass transfer coefficient at different gas flow rates

	Qair, m^3 h^{-1}	Overpressure, atm	Compression work, W	Kla, h^{-1}
Type 1: Membrane tubing diffuser	0.00	0.10	0.00	0.00
	0.30	0.34	2.63	4.32
	0.42	0.43	4.55	6.48
	0.60	0.57	8.21	7.92
	0.72	0.67	11.13	10.80
	0.90	0.81	16.13	11.16
	1.02	0.90	19.85	11.16
	1.20	1.05	25.96	13.68
	1.80	1.52	50.26	16.20
	2.70	2.23	95.64	25.20
	3.60	2.94	149.12	32.40

	Qair, m^3 h^{-1}	Overpressure, atm	Compression work, W	Kla, h^{-1}
Type 2: Membrane plate diffuser	0.00	0.10	0.00	
	0.31	0.15	1.30	2.88
	0.42	0.17	1.96	
	0.65	0.20	3.64	6.84
	0.72	0.21	4.22	
	0.90	0.24	5.91	8.64
	1.02	0.26	7.17	
	1.46	0.33	12.69	11.88
	1.12	0.28	8.25	11.88
	2.47	0.49	29.85	17.28
	3.60	0.67	55.86	29.16
Type 3: Porous tubing diffuser	0.00	0.10	0.00	0.00
	0.26	0.16	1.20	0.86
	0.46	0.21	2.64	1.49
	0.70	0.27	5.00	2.28
	0.92	0.32	7.72	2.99
	1.12	0.36	10.46	3.62
	1.49	0.45	16.79	4.83
	2.05	0.59	28.57	6.65
	2.72	0.74	45.72	8.82
	3.60	0.95	72.71	10.80

To clarify this, the mass transfer coefficient obtained was compared to the calculated power consumption (Eq(27)) for each of the three diffusers used, and gave the relationships shown in Figure 56. This figure shows a potential relationship between mass transfer coefficient and compression work, which can be described by the empirical equations showed in Table 16, where *P/V* is the power consumption per unit volume (W m^{-3}) taking into account the sump volume of 0.549 m^3 and the 0.10 atm sump pressure produced by the column of water over the diffuser.

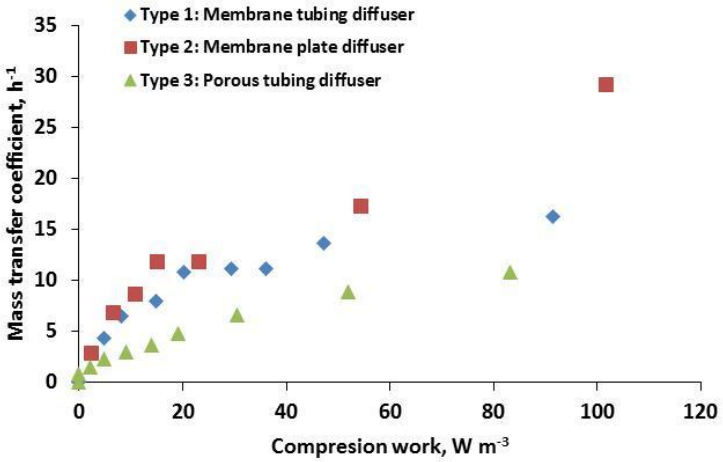

Figure 56.- Relationship between mass transfer coefficient and compression work for each of the three diffusers used

Table 16.- Potential adjustment of mass transfer coefficient and compression work

Diffuser	Potential relationship	R^2
Type 1 Membrane tubing	$K_l a_l = 0.00063 \left(\frac{P}{V}\right)^{0.4635}$	0.9802
Type 2 Membrane plate	$K_l a_l = 0.00057 \left(\frac{P}{V}\right)^{0.5707}$	0.9666
Type 3 Porous tubing	$K_l a_l = 0.00016 \left(\frac{P}{V}\right)^{0.6209}$	0.9975

5.2 Mass transfer characterization of the raceway

5.2.1 Objective

To define the oxygen mass transfer capacity in the raceway determining how much oxygen is absorbed/desorbed in each section of the reactor.

5.2.2 Methodology

A steady state method was used in which the reactor was filled with fresh water to the test depth of 20 cm determined in Chapter IV-4.1 as the optimal depth in terms of power consumption, and liquid circulation at

different velocities was achieved by adjusting the rotational speed of the paddlewheel. The tests were carried out by bubbling nitrogen into the sump at a gas flow rate of 6 m^3 $hour^{-1}$, using the membrane plate diffuser identified as having the best performance in terms of bubble size and pressure drop in section 5.1. For the purposes of the analysis the reactor was considered to have four zones: the paddlewheel, the sump, the first channel, and the second channel including the two bends. Dissolved oxygen measurements were taken at the beginning and end of each zone from DO probes (described in 3.3.1) located at the inlet to the paddlewheel, inlet of the sump, outlet of the sump, and end of the first channel. Raceway characteristics and size can be consulted in Chapter III-3.2.

From these measurements the mass flows of oxygen transferred in each section were calculated from the difference in oxygen concentration at the inlet and outlet to the section and the flow of water in the channel. This was expressed in terms of the oxygen transfer coefficient, driving force and volume in each zone (Eq(28)) where $mO_{2,zone}$ is mass flow of O_2 into the zone (mg s^{-1}), Q is the water flow in the channel (L s^{-1}), $[O_2]_{in/out}$ is the DO concentration entering and leaving the zone respectively (mg L^{-1}), $K_l a_{l_{zone}}$ is the O_2 transfer coefficient for the zone (s^{-1}), $([O_2] - [O_2{}^*])_{zone}$ is the average driving force in the zone (mg L^{-1}), and V_{zone} is the volume of the zone (L). The mass of oxygen transferred in each section was confirmed by the overall steady state mass balance (Eq(29)).

$$mO_{2,zone} = Q([O_2]_{in} - [O_2]_{out})_{zone} = K_l a_{l_{zone}}([O_2] - [O_2{}^*])_{zone} V_{zone} \quad (28)$$

$$mO_{2,sump} + mO_{2,paddlewheel} + mO_{2,channel1} + mO_{2,bends+channel2} = 0 \quad (29)$$

5.2.3 Results

Results from steady state reactor characterisation at a liquid velocity of 0.2 m s^{-1} are shown in Table 17. This velocity was selected as typical of velocity usually found in raceway cultures. The total oxygen desorption in the sump was -171.88 g $hour^{-1}$, and oxygen absorption occurred mainly in the paddlewheel section at 105.78 g $hour^{-1}$. Oxygen transfer into the channel 1 straight section was 27.15 g $hour^{-1}$, and in the channel 2 straight section +

bends was 38.94 g $hour^{-1}$. This indicates that the oxygen transfer capability of the two bends was 11.7 g $hour^{-1}$, equivalent to 0.43 of the capability of the straight channel 1 despite being only 0.06 of its length. The sections of the reactor where gas transfer is most effective are thus the sump and the paddlewheel, with the straight section and bends in the channel contributing 16 % and 7 % respectively. The mass transfer coefficient determined for the sump using the steady state method was 63.66 $hour^{-1}$ which is higher than the 32.4 $hour^{-1}$ measured previously using the dynamic method due to the higher driving force for gas exchange in the sump produced by DO desorption in channels, bends and paddlewheel during the steady state method. Mass transfer was also influenced by gas flow rate in the dynamic method and by liquid flow in the steady state method, two parameters that defined the liquid-gas ratio in the sump. The value obtained using the steady state method at a flow rate of 6 m^3 $hour^{-1}$ also fitted the empirical correlation obtained for this diffuser (Table 16, diffuser type 2, membrane plate). The highest mass transfer coefficient (164.48 $hour^{-1}$) was determined for the paddlewheel section and the lowest for the channel (0.87 $hour^{-1}$).

Table 17.- Experimentally-obtained steady state values of volume, dissolved oxygen concentration, mass flow, driving force and mass transfer coefficient for each section of the raceway

	Paddle-wheel	**Sump**	**Channel 1**	**Bends + Channel 2**
Volume, m^3	0.20	0.59	8.00	11.26
DO, % Sat.	63.98	50.42	52.56	55.63
mO_2, g $hour^{-1}$	105.78	-171.88	27.15	38.94
Driving force, g m^{-3}	3.22	-4.58	3.88	3.67
K_la, $hour^{-1}$	164.48	63.66	0.87	0.94

The reactor was operated at a liquid depth of 0.2 m and velocity of 0.22 m s^{-1} with nitrogen flow rate of 6 m^3 $hour^{-1}$

To determine the influence of liquid velocity on the mass transfer capacity of the reactor, experiments were performed using the steady state method at different velocities. The results showed that mass transfer coefficients in all sections of the reactor increased with increasing liquid velocity (Figure 57, Figure 58). The percentage change was similar in each section: in the paddlewheel section it increased from 132.72 to 189.73 $hour^{-1}$ (30 %) and in the sump from 62.96 to 94.72 $hour^{-1}$ (34%) as the liquid velocity increased from 0.17 to 0.39 m s^{-1} (Table 18).

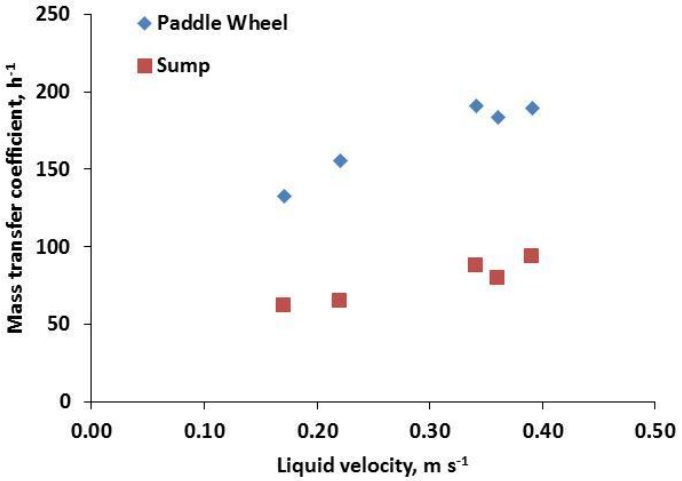

Figure 57.- Variation of mass transfer coefficient in paddle wheel and sump with liquid velocity

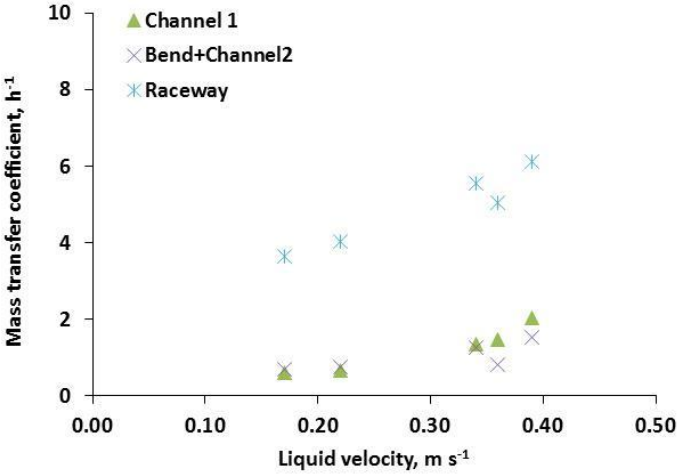

Figure 58.- Variation of mass transfer coefficient in channel 1, bend+channel 2 and the entire raceway with liquid velocity

Values in the channels and bends were much lower and ranged from 0.61 to 2.03 h^{-1}. Overall the mass transfer coefficient for the entire reactor increased from 3.66 to 6.13 h^{-1} with the increase in liquid velocity (Table 18). In an experiment where no gas was bubbled into the sump, the mass transfer coefficient of the reactor was reduced to 1.8 h^{-1}. The experiment at 0.22 m s^{-1} was repeated and not relevant differences were found regarding the experiment previously reported (Table 17). This confirmed the accuracy of the described method for the study of oxygen mass transfer in raceway reactors.

Table 18.- Mass transfer coefficients ($hour^{-1}$) at different liquid velocities in each section of the raceway and in the whole reactor

Liquid velocity, m s^{-1}	Paddle-wheel	Sump	Channel 1	Bends + Channel2	Raceway
0.17	132.72	62.96	0.61	0.69	3.66
0.22	155.61	65.68	0.68	0.75	4.02
0.34	190.83	88.76	1.36	1.27	5.57
0.36	183.80	80.08	1.47	0.82	5.05
0.39	189.73	94.72	2.03	1.53	6.13
Nitrogen flow rate of 6 m^3 $hour^{-1}$					

5.3 Microalgae growth experiments

5.3.1 Objectives

To determine whether the mass transfer capacity of the reactors is sufficient to prevent DO accumulation above inhibitory concentrations (300 % Sat) during cultivation of *Scenedesmus* spp.. To determine the effect of different carbonation gases on DO desorption and microalgae productivity.

5.3.2 Methodology

In this case, both of the raceway reactors were operated simultaneously with the aim to maintain them under the most similar external conditions (Figure 59). The first raceway was inoculated with 3 m^3 of *Scenedesmus* sp. grown in the culture medium under aseptic conditions in a tubular photobioreactor at a dilution rate of 0.3 day^{-1}, temperature 25-30 ˚C and pH 8.0. The raceway was operated as a batch reactor until a biomass concentration of 0.7 g total suspended solids L^{-1} (TSS) was reached. At this point half of the volume of the first raceway was transferred into the second raceway reactor as inoculum. Culture medium prepared as described in section 3.5 was then added to both reactors to reach the working volume and they were again operated in batch mode until a biomass concentration of 0.7 g TSS L^{-1} was achieved.

Figure 59.- Raceway reactors used simultaneously in this experiment. The setting-up of two reactors allowed pairs of experiments to be carried out under the same external conditions (wind, ambient temperature, solar radiation, etc.)

Once both raceways had achieved the desired biomass concentration, reactor operation was switched from batch to semi-continuous by daily additions of culture medium to give a dilution rate of 0.25 day^{-1}. Raceway pH was controlled between set points of 7.8 and 8.0 by bubbling pure CO_2 at 0.6 $m^3\ h^{-1}$ in the first reactor, and flue gas from a diesel boiler containing 10 % CO_2 (6 % O_2, 150 ppm NO_x, 0 % SO_x) at 6.0 $m^3\ h^{-1}$ in the second raceway. The liquid velocity in the reactors was 0.22 m s^{-1} and the operational depth was maintained at 0.2 m by means of the dilution rate and harvesting control described in section 3.3.2.2. Temperature was dependent on ambient air temperature and incident solar radiation. The experiment was carried out for a period of 7 days starting from 26th of March 2012.

5.3.3 Results

Both reactors were operated under the same external conditions. Table 19 shows the information registered on-site by the weather station. The temperature was also the same in the raceways (Figure 60), since both were exposed to the same weather conditions. The different source of carbon used in the raceways did not influence the capacity of controlling the pH around 8 by on-demand injection.

Table 19.- Weather conditions during the experimental period

	Ambient Temperature, ºC			Wind Speed, m s^{-1}			Humidity, %			Solar Radiation, W m^{-2}	
Day	Max	Min	Aver	Max	Min	Aver	Max	Min	Aver	Max	Aver
1	19.1	14.5	16.3	8.1	2.2	4.3	51.0	32.0	41.1	923.0	272.0
2	19.7	14.5	16.8	7.1	2.8	4.3	48.0	29.0	39.9	918.0	274.5
3	18.5	13.4	15.7	7.6	0.5	3.2	78.0	36.0	53.5	927.3	263.8
4	17.3	10.6	13.9	3.4	0.2	1.6	83.0	46.0	59.5	935.5	237.1
5	17.3	10.8	14.2	4	0.4	1.6	85.0	42.0	58.6	951.3	191.1
6	19.6	9.5	14.3	7.4	0.1	3.0	85.0	46.0	71.5	1165.9	71.8

Maximum, minimum and daily average values are shown, except minimum solar radiation which was 0 W m^{-3}. There was no rain in this period

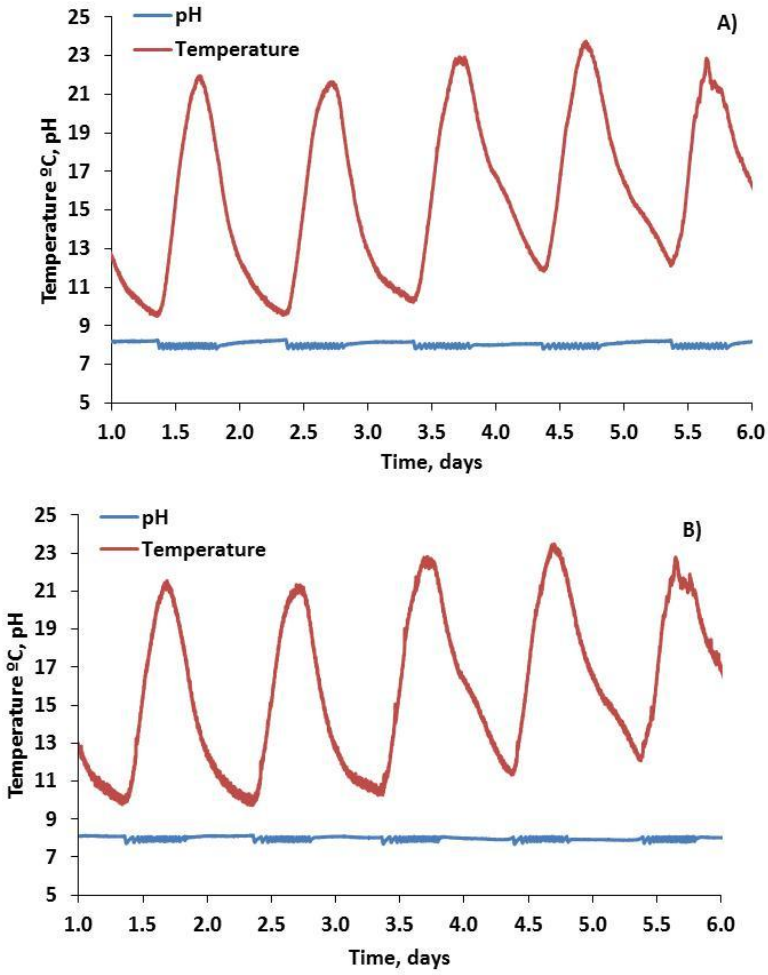

Figure 60.- Temperature and pH evolution in raceway reactor (A) with on-demand injection of pure CO_2 and B) with on-demand injection of flue gas (10 % CO_2)

The main difference was in relation with the carbon injection time needed to control the pH. The raceway operated with pure CO_2 needed a higher injection time to control de pH due to the lower mass flow used in comparison to the raceway with flue gas (Figure 61). Since the gas flow was different for each raceway, Figure 62 shows the net volume of gas injected every day to control the pH and the fraction of CO_2 that included in the flue gas.

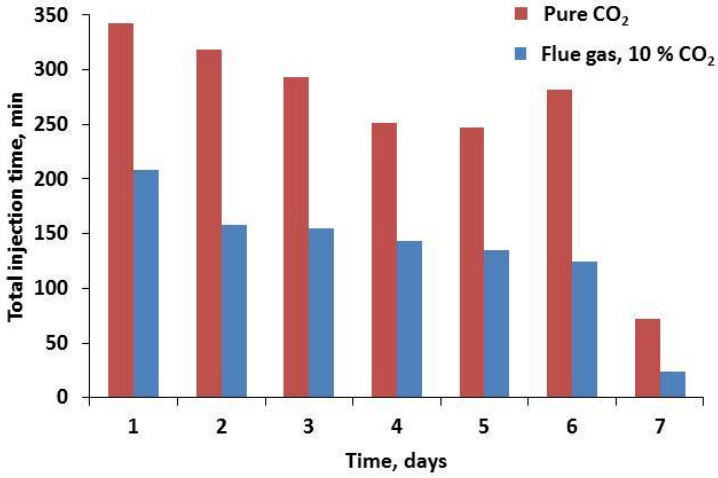

Figure 61.- Total gas injection time in the raceways operated with flue gas and pure CO_2

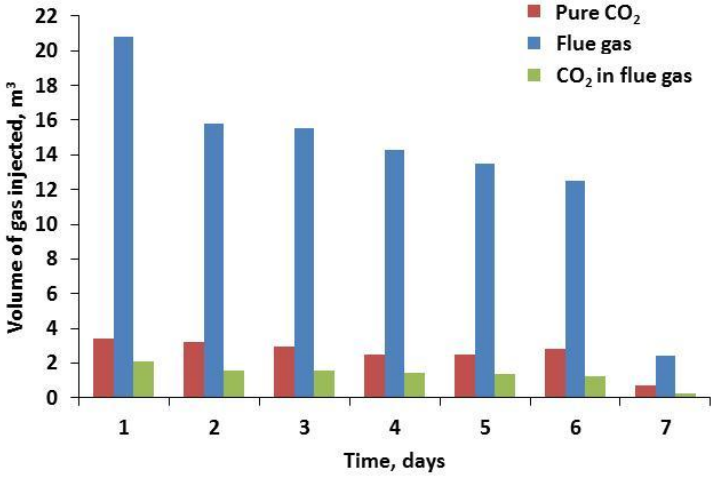

Figure 62.- Daily volume of gas injected during the culture experiment in the raceway operated with pure CO_2 and with flue gas. The CO_2 in the flue gas was calculated as the 10 % of the total flue gas added

Dissolved oxygen concentrations in the reactor with pure CO_2 reached 25-30 mg L^{-1} around noon (Figure 63A), but were lower in the reactor using flue gas at 20-25 mg L^{-1} (Figure 63B). This is a remarkable difference, taking into

account that both raceways were maintained under the same operational and weather conditions, and clearly indicates that the source of carbonation in microalgae cultures may determine the maximum oxygen accumulation peak during the day.

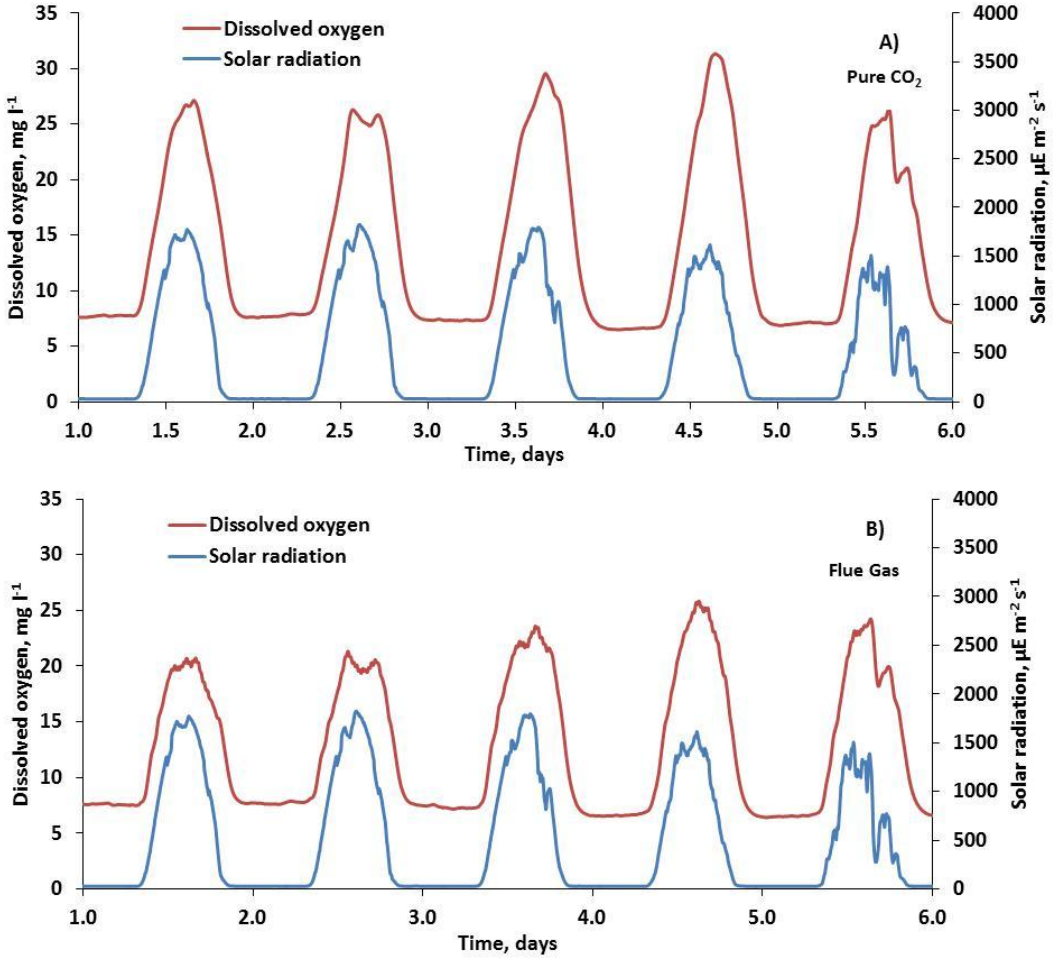

Figure 63.- Variations in DO and solar radiation over a 6-day experimental period in 2 raceway reactors A) with pH controlled by on demand injection of pure CO_2 and B) with on-demand injection of flue gas with 10 % CO_2

Using the mass transfer coefficients ($K_l a_l$) calculated in the raceways for pure CO_2 and flue gas bubbling, it was possible to calculate the oxygen production by photosynthesis $RO_{2_{phot}}$ based on the rates of oxygen desorption $K_l a_l([O_2] - [O_2^*])$ and accumulation $\frac{d[O_2]}{dt}$ in mg O_2 L^{-1} h^{-1} (Eq(30)).

$$\frac{d[O_2]}{dt} = RO_{2_{phot}} - K_l a_l([O_2] - [O_2^*]) \quad (30)$$

When pure CO_2 was used, the results showed that the desorption capacity of the reactor was low, with a maximum value of 37 mg L^{-1} h^{-1} despite the high dissolved oxygen concentrations (Figure 64A): this was due to the low mass transfer coefficient (1.53 h^{-1}). The low mass transfer can be attributed to the low gas flow rate of 0.6 m^3 h^{-1} in the sump when using pure CO_2. When flue gas was used, the mass transfer coefficient increased to 4.0 h^{-1} because of the greater volume of gas injected, giving a desorption capacity of 70 mg L^{-1} h^{-1} (Figure 64B). If the photosynthetic oxygen productivities based on oxygen accumulation and desorption are considered (Eq(30)), a much higher value of 65 mg L^{-1} h^{-1} is obtained with flue gas (Figure 64B) compared to the 35 mg L^{-1} h^{-1} when pure CO_2 was used (Figure 64A).

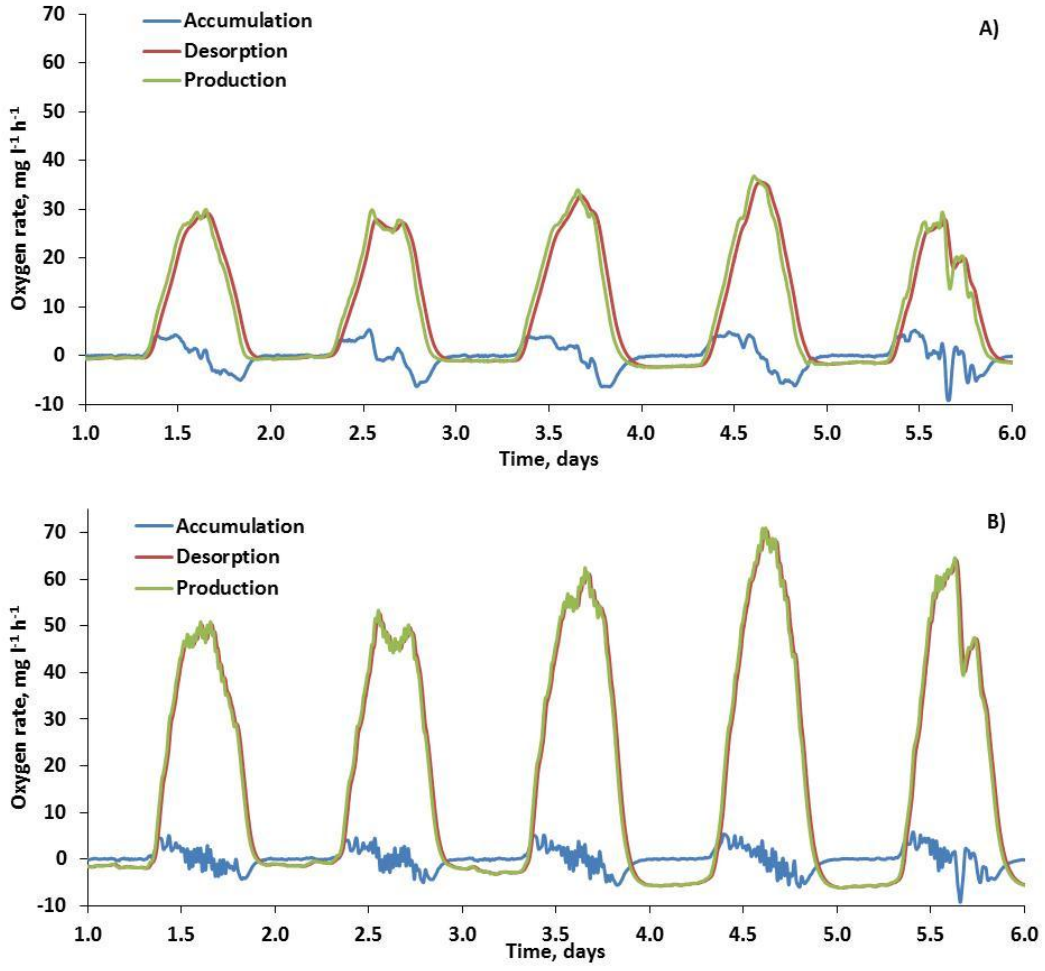

Figure 64.- Photosynthesis production, desorption and accumulation of oxygen calculated by mass balance in the reactor: A) with on-demand injection of pure CO_2 and B) with on demand flue gas (10 % CO_2)

These results strongly support the view that an accumulation of dissolved oxygen has a negative effect on photosynthesis, since other external parameters were similar in both raceways as shown in Table 19. To verify this, the overall yield of the cultures grown in the two reactors was analysed over 6 days. For this, a daily sample was taken in each reactor to check the culture status and determine the algae growth and biomass productivity. The results of the analysis made are shown in Table 20, and included the absorbance at 680 and 760 nm, dry weight, turbidity and quantum yield (Fv/Fm) which is a parameter used to evaluate the fluorescence of the chlorophyll to give an idea of the health of photosynthesizing organisms and the associated variables that indirectly or directly affect them and describes how well microalgae can assimilate light.

Table 20.- Results of analyses (absorbance, dry weight, FV/FM, turbidity) for samples taken in the raceways with pure CO_2 and with flue gas

	Abs 680-760 nm		Dry weight, g L^{-1}		Fv/Fm		Turbidity, FTU	
Day	Pure CO_2	Flue gas	Pure CO_2	Flue gas	Pure CO_2	Flue gas	Pure CO_2	Flue gas
1	1.34-1.81	2.13-2.87	0.86	1.47	0.70	0.70	133	294
2	1.48-2.05	2.06-2.83	0.87	1.46	0.70	0.70	195	395
3	1.57-2.17	2.31-3.15	0.85	1.37	0.68	0.70	192	391
4	1.45-2.00	1.87-2.62	0.80	1.25	0.66	0.70	188	352
5	1.49-2.05	1.92-2.68	0.86	1.30	0.66	0.70	200	380
6	1.53-2.10	1.97-2.74	0.92	1.35	0.66	0.70	211	408

In addition, daily values during daylight period for photosynthesis rate, O_2 to biomass ratio and photosynthetic efficiency were calculated and shown in Table 21. The average biomass yield of 0.33 g TSS L^{-1} day^{-1} in the reactor using flue gas was higher than the 0.24 g TS L^{-1} day^{-1} using pure CO_2. Using flue gas, the average oxygen-to-biomass ratio was 1.46 O_2 g^{-1} biomass while using pure CO_2 the ratio was 0.99 g O_2 g^{-1} biomass. The photosynthetic yield was 61.0 E mol^{-1} O_2 when using pure CO_2 and 31.1 E mol^{-1} O_2 when flue gas was used.

Table 21.- Influence of solar radiation on cultures grown using pure CO_2 and flue gases for pH control

Day	Solar radiation, μE m^{-2} s^{-1}	Photosynthesis rate, mg L^{-1} h^{-1}		Biomass productivity, g L^{-1} day^{-1}		O_2 to biomass, g O_2 g^{-1} biomass		Photosynthetic efficiency, E mol^{-1}	
		Pure CO_2	Flue gas	Pure CO_2	Flue gas	Pure CO_2	Flue gas	Pure CO_2	Flue gas
1	544	9.3	16.8	0.26	0.41	0.85	0.98	67.1	37.2
2	549	9.4	17.6	0.24	0.37	0.95	1.13	67.6	35.9
3	528	10.3	19.7	0.28	0.35	0.87	1.33	58.9	30.8
4	474	9.8	20.4	0.26	0.31	0.91	1.57	55.8	26.8
5	382	7.9	17.9	0.14	0.19	1.36	2.26	55.5	24.6

Values are average for daylight period based on experimental values recorded at one minute intervals

5.4 Productivity versus consumption simulation

5.4.1 Objective

To establish a model describing the overall oxygen transfer in the system. To use the equations obtained to calculate mass transfer requirements and associated power consumption, which can potentially be used in the design of raceway reactors.

5.4.2 Methodology

To predict energy productivity in different conditions, a set of simulations was carried out using empirical data and the following assumptions. The culture is assumed to have a biomass concentration C_b of 1 g TSS L^{-1} and a biomass extinction coefficient K_a of 0.18 m^2 g^{-1} biomass. Hourly values for solar radiation I_0 (μE m^{-2} s^{-1}) are available for the raceway location, and from these data the average irradiance inside the culture I_{av} (μE m^{-2} s^{-1}) can be calculated for a constant culture depth d of 0.2 m using Eq(31).

$$I_{av} = \frac{I_0}{K_a d C_b}\left(1 - exp(-K_a d C_b)\right) \quad (31)$$

The rate of photosynthetic oxygen production $RO_{2\ phot}$ is a function of I_{av} and specific maximum photosynthesis rate $RO_{2\ max}$ (mg L^{-1} h^{-1}), and is assumed to fit a hyperbolic model with n=2 and I_K=60 μE m^{-2} s^{-1} (Camacho Rubio et al., 1999) (Eq(32)).

$$RO_{2phot} = \frac{RO_{2\,max} I_{av}^n}{I_k^n + I_{av}^n} \tag{32}$$

RO_{2max} can be calculated from Eq(33), using the experimentally-obtained mass transfer coefficient values and assuming a maximum acceptable DO concentration in the raceway of 250 % saturation.

$$\frac{d[O_2]}{dt} = RO_{2_{phot}} - K_l a_l([O_2] - [O_2^*]) \tag{33}$$

The overall biomass productivity in the raceway can then be calculated based on the daily total oxygen production, using a conversion factor of 1.33 g O_2 g^{-1} biomass. This factor was a stoichiometric value deducted from the basic photosynthesis reaction (Eq(34)) and obtained as Eq(35) considering that the C content in the biomass is 50 %. The energy potential of the biomass is calculated based on a typical calorific value of 20 kJ g^{-1} biomass. The biomass potential energy yields can then be compared with the additional energy consumption required to achieve this mass transfer capacity in the sump using the obtained empirically-derived equation presented in Table 16 for type 2-membrane plate diffuser, which relates the mass transfer coefficient (K_la_l) with the power consumption per unit volume (P V^{-1}, in W m^{-3}) for the three tested diffusers.

$$6\ CO_2 + 6\ H_2O \quad C_6H_{12}O_6 + 6O_2 \tag{34}$$

$$\frac{6\ \text{mol}\ O_2}{\text{mol biomass}} \frac{\text{mol biomass}}{6 \cdot 12\ \text{g C}} \frac{32\ \text{g}\ O_2}{\text{mol}\ O_2} \frac{0.5\ \text{g C}}{\text{g biomass}} = 1.33\ \frac{\text{g}\ O_2}{\text{g biomass}} \tag{35}$$

5.4.3 Results

The power consumption required to increase the mass transfer coefficient in the sump from 0 to 150 h^{-1} increased exponentially, with a power requirement of 1800 W m^{-3} in the sump to achieve the maximum value. As the volume of the sump is small in comparison with the entire raceway, however, the impact on the overall power consumption is relatively small. Thus, the overall power consumption increases from 4 W m^{-3} when no gas is supplied into the sump (only liquid circulation), to 13 W m^{-3} when gas is supplied into the sump at maximum flow rate of 200 m^3 h^{-1} to achieve the maximum mass transfer coefficient into the sump of 150 h^{-1}. The results of the simulation (Figure 65A) indicated that the increased mass transfer should allow an increase in biomass productivity from 0.17 g L^{-1} day^{-1} without gas supply into the sump, up to 0.50 g L^{-1} day^{-1} with a mass transfer coefficient of 150 h^{-1}. On the basis of an energy value of 20 kJ g^{-1} biomass, there is a substantial increase in potential net energy production from 3400 to 9700 kJ m^{-3} day^{-1} (Figure 65B). The increase of mass transfer coefficient linked to an increment of productivity, however, is limited by other values that start to control biomass productivity and thus energy potential. For example, above certain productivity per m^2 light availability will become limiting and improvements in mass transfer do not necessarily imply better productivities.

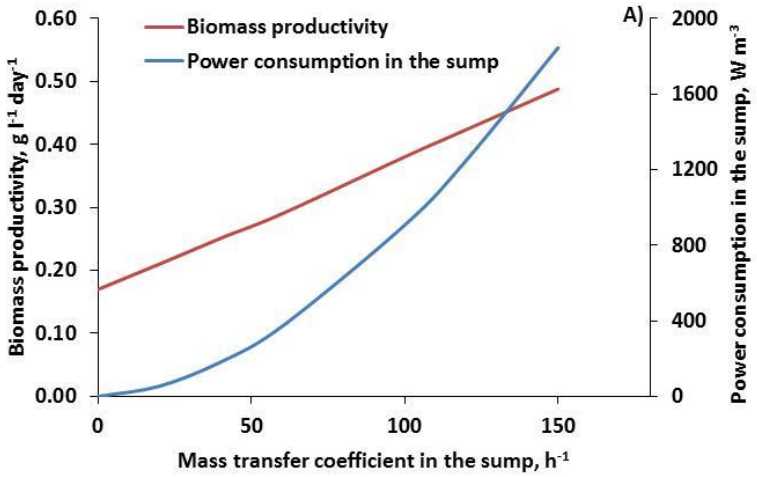

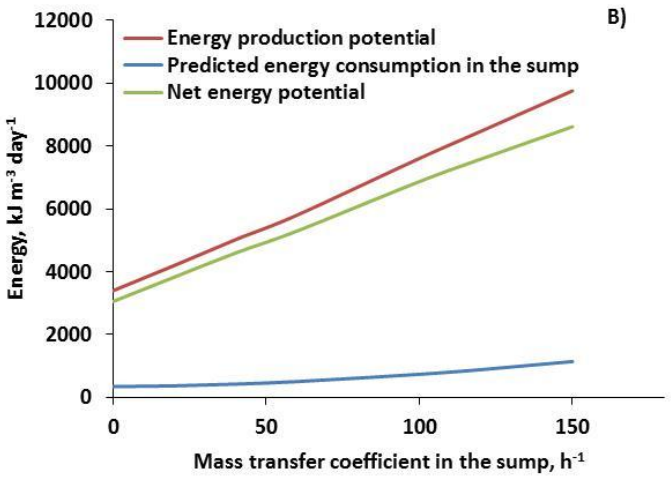

Figure 65.- Variation of A) biomass productivity, power consumption and B) energy balance with mass transfer into the sump. Values obtained from simulations performed considering a hyperbolic photosynthesis model (mO_{2max}=190 mg O_2 L^{-1} h^{-1}, n=2, I_k=60 UE m^{-2} s^{-1}) for a raceway of 0.2 m depth operated at 0.22 m s^{-1}, biomass concentration of 1.0 g TS L^{-1} and biomass extinction coefficient of 0.18 m^2 g^{-1}

5.5 Discussion and conclusions

High DO concentrations have previously been found in raceway reactors of the scale used in the current experiments. Values from 25 to 40 mg DO L^{-1} were reported in 100 m^2 raceway reactors used for the production of *Chlorella* sp. (Weissman et al., 1988). In 450 m^2 raceway reactors producing *Spirulina platensis* the DO concentration ranged from 10 mg L^{-1} in winter (115 % of O_2 saturation) to 30 mg L^{-1} in summer (375 % saturation); a decrease in biomass concentration was found when the DO concentration was higher than 25 mg L^{-1} (Jiménez, 2003). DO concentrations as high as 500 % saturation have also been reported in large ponds with limited mixing (Márquez et al., 1995; Singh et al., 1995; Vonshak, 1997). In the current experiments the raceway to which pure CO_2 was added showed higher DO concentrations and reduced biomass productivity compared to the raceway receiving flue gas. The lower productivity was probably a result of photorespiration, which has been well documented (Eckardt, 2005). The US EPA (EPA, 1985) quotes values for the oxygen yield from algal biomass production from 1.24 to 1.8 g O_2 g^{-1} biomass from various studies. In the current work the average value for the flue gas reactor was 1.46 g O_2 g^{-1} biomass, which was considerably higher than the 0.99 g O_2 g^{-1} biomass

for pure CO_2. Both values suggest that some of the CO_2 is being diverted from assimilative growth, and the photorespiration mechanism could account for this difference. Similarly in ideal conditions the theoretical photosynthetic conversion efficiency can be as high as 10 E mol^{-1} O_2: in the current work the efficiency of the culture using pure CO_2 was only 16 % of this theoretical value, compared to 32 % for the flue gas.

The results reported here showed that the mass transfer coefficient was high where the mixing between gas and liquid was effective, and this occurred mainly in the sump and paddlewheel sections, with values of up to 90 and 160 h^{-1}. This compares to 0.7 h^{-1} in the channel where the mixing between liquid and gas phases is poor: this result agrees well with (Weissman et al., 1988) who found a value of 0.5 h^{-1} for CO_2 released from the surface of a 100 m^2 raceway pond. In general, where gas is bubbled through the water the overall value of the mass transfer coefficient K_la_l is higher than for diffusion alone, although a wide range of K_la_l values between 0.4 and 350 h^{-1} has been reported for aerated systems of different designs (Carvalho et al., 2006). In tubular photobioreactors a typical value for the mass transfer coefficient in the closed loop is 1.1 h^{-1}, but can be as high as 90 h^{-1} in the degassing section where air is bubbled (Camacho Rubio et al., 1999). These values are similar to the values found in this study for the raceway, taking the loop as equivalent to the channel sections and the degassing column equivalent to the sump; the major difference lies in the volume ratios of these coupled sections in each type of reactor, and hence their overall ability to release oxygen. In the raceway only 4 % of total liquid volume is aerated at any one time compared to a minimum volume of 15 % in tubular photobioreactors.

The mass transfer capacity for removing oxygen from the raceway appeared to be directly related to volume of gas injected into the raceway in order to satisfy the carbon requirements, as all other components in the system were the same. Recently, the relation between mass transfer and gas injection properties has been studied (Nock, 2015), and it has been demonstrated that in bubble swarms of with different CO_2 concentrations mass transfer is higher than in single bubbles with the same CO_2 concentration, despite the volume reduction were approximately the same. This may influence DO desorption rate since if CO_2 transfer is higher in bubble swarms and the volume is the same, that means that the bubble composition changed and

there is an absorption/desorption phenomena at the same time in the liquid for CO_2 and O_2, respectively. In the raceway, even when flue gas was used, however, the volume of gas bubbled was not sufficient to reduce the DO to concentrations below an inhibitory value in the middle of the day. Using the data on the contribution made to the mass transfer in each of the sections, the maximum photosynthetic rate and hence the productivity were modelled, on the basis of allowing a maximum DO concentration of 250 % saturation to accumulate. When mass transfer occurred at the culture surface only, the maximum photosynthesis rate ranged from 8.4 to 27.6 mg O_2 L^{-1} h^{-1}, equivalent to biomass productivities of 6-20 g m^{-2} day^{-1}, similar to the values usually found in raceway reactors. This result is further supported by the work of Boussiba (Boussiba et al., 1988) who found that under the same culture conditions the productivity of *Isochrysis galbana* cultures was 30 g m^{-2} day^{-1} when using a 2.5 m^2 raceway reactor, whereas in a 100 m^2 raceway reactor, in which the mass transfer contribution of the paddlewheel is reduced, productivity decreased to 22 g m^{-2} day^{-1}.

To improve productivity, measures to enhance mass transfer are needed, which requires improved mixing between gas and liquid phases. This could be by increasing the volume of the sump or even using additional sumps, improving the performance of the diffuser, or increasing the gas flow to the sump. An alternative is to increase the gas transfer at the water surface, or to improve the mass transfer capacity of the paddlewheel section, both of which are likely to have a significant effect on the raceway fluid dynamics and energy consumption. In the short term, major improvements therefore appear to be best focussed on the sump, and as a first measure the choice of a small bubble size diffuser is essential, preferably one with a low pressure drop. The oxygen desorbed will also depend on the gas flow rate, and the capacity for oxygen removal may be more rate-determining than the supply of CO_2. The experimental results showed that, even when using flue gas bubbling with 10 % CO_2 coupled to carbon demand through pH control, the volume of gas used was insufficient to reduce DO concentrations to <20 mg L^{-1}. It may therefore be necessary to continue bubbling gas into the culture to reduce the concentration of oxygen even when there is no demand for carbon, and this might be done by switching the gas stream to air rather than flue gas when there is sufficient dissolved carbon in the system. Special attention must be

paid to the possibility of CO_2 stripping by bubbling air in cultures with a high concentration of bicarbonate (see equilibrium Eq(2) in section 2.3.4), so the possibility of reducing the concentration of oxygen in dense microalgae cultures using this technique should be studied regarding the effect on CO_2 losses. The bubbling of larger volumes of gas leads to greater power consumption, which will depend on the type of diffuser used, sump depth and other characteristics. Under the conditions considered the benefits in biomass productivity achieved by increasing the mass transfer rate appear, however, to give a net gain in energy production up to the point at which other limiting factors take over.

In the experiments carried out with microalgae cultures, the reactor operated with pure CO_2 needed a higher injection time (Figure 61) and net volume of CO_2 injected (Figure 62) than using flue gas, despite being more productive the raceway operated with flue gas than the raceway operated with pure CO_2, As example, Figure 66 shows the cumulative volume of gas injected in each reactor to control the pH during daylight time in day 2. It is possible to see that the total volume of flue gas injected was 15.5 m^3 of which only 1.5 m^3 (10 %) was CO_2. The reactor operated with pure CO_2, however, needed the injection of only 2.9 m^3 of CO_2 to control the pH. This justifies the necessity of doing an exhaustive study of the CO_2 mass transfer in raceway reactors to determine the amount of CO_2 injected with the gas phase that is effectively absorbed in the liquid phase.

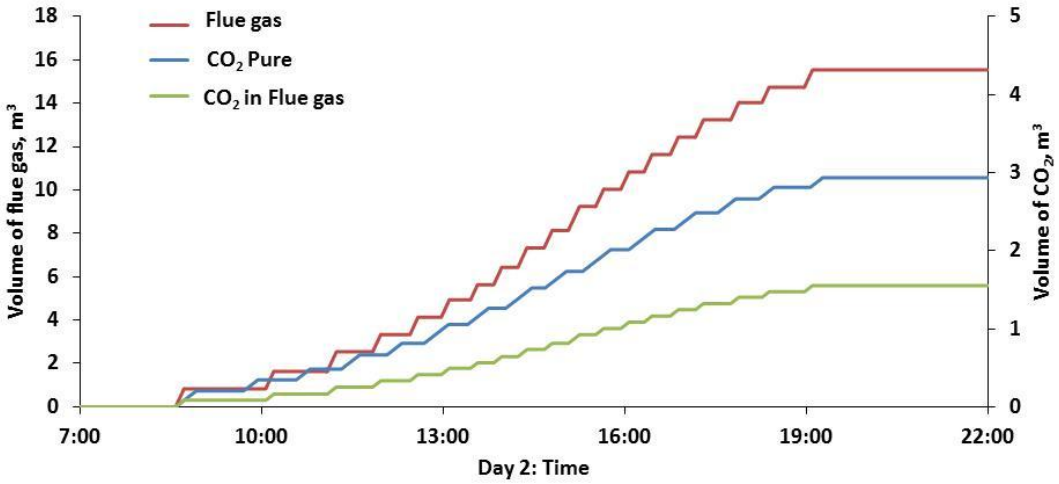

Figure 66.- Cumulative volume of gas injected to control the pH during day-2. It was also represented the volume of CO_2 injected with the flue gas (10 % CO_2)

5.6 Summary conclusions for Chapter V

In conclusion, the work in this chapter has shown the following:

- The type of diffuser selected may have a high impact on the mass transfer efficiency and power consumption. The membrane plate diffuser was the best option among the diffusers tested due to the small size of the bubbles generated (enhancing mass transfer) and the low pressure drop produced for gas bubbling (reducing power consumption).
- Oxygen mass transfer took place mainly in the sump and paddlewheel, where the mixing between gas and liquid was effective and, therefore, the mass transfer coefficients were higher.
- Inhibition caused by oxygen accumulation is potentially a major problem for growth of algae cultures in raceway systems. Carbonation with flue gas reduced the maximum DO concentration compared to the use of pure CO_2.
- The flow of gas in the sump was directly related to mass transfer capacity for removing oxygen from the raceway. Special attention, however, must be paid when using gas for DO desorption because there is a risk of CO_2 stripping in cultures with high concentration of bicarbonates.

Chapter VI

6. CO_2 MASS TRANSFER ASSESSMENT IN RACEWAY REACTORS

In addition to the requirement for DO accumulation in raceways to avoid the damaging effects of photo-oxidation on cells, photorespiration, and suppression of photosynthesis (Vonshak, 1997), CO_2 mass transfer efficiency must also be studied in microalgae cultures. The mass transfer of CO_2 and O_2 are closely related, and both must be considered in a good design (Camacho Rubio et al., 1999). The work in this part of the thesis investigated the CO_2 mass transfer phenomena between gas and liquid phases in the pilot-scale raceway reactor described previously, using real flue gases from a diesel boiler (10 % CO_2). Mass transfer was quantified under two sump configurations, with and without a baffle, at different liquid velocities and gas flow rates. The measurements were made first in fresh water (in vitro assessment) to allow quantification of the different phenomena and modelling of the optimal operational conditions. Measurements were then made using algal cultures (in vivo assessment) under the optimum conditions found previously, to allow determination of a carbon balance for the system based on the net CO_2 flows and taking biological fixation into account. The results thus provide basic information that can be used in the design of carbonation systems and methodology to evaluate the gas-liquid mass transfer in raceway reactors is presented, besides the assessment of the improvement of the carbon supply mechanism to the raceway.

6.1 CO_2 mass transfer in the raceway

6.1.1 Objectives

To establish a methodology to evaluate the gas-liquid mass transfer in raceway reactors. To quantify the CO_2 mass transfer capacity of the raceway (especially of the sump) using pure CO_2 and flue gas. To determine the carbon requirements for pH control through CO_2 injection on demand.

6.1.2 Methodology

All the experimental work was carried out in the same raceway reactor as described in Chapter III, 3.2. The raceway was operated without a vertical sump baffle. In the experiments, flue gas was be injected through three plate membrane diffusers at the bottom of the sump which were located so as to give counter-current gas injection when the baffle is in place (Figure 67). The membrane plate diffuser was previously identified, between three kinds of diffusers, as the most suitable in terms of mass transfer yield and power requirements (

Chapter V, 5.1).

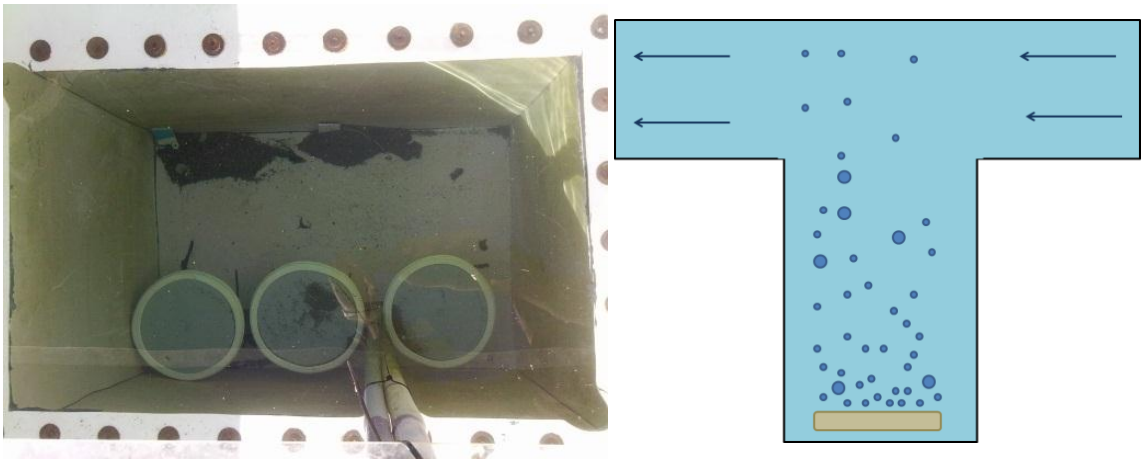

Figure 67.- Left: Three plate membrane diffusers used for gas bubbling located at the bottom of the sump (view from the top of the sump). Right: Schematic of the gas bubbling when using sump baffle to give counter-current contact between gas and liquid phases.

To determine the CO_2 mass transfer into the reactor via the carbonation sump, flue gas was injected at constant flow rate and the composition of the gas entering and leaving the sump was measured with the gas hood and probes previously described in Chapter III, 3.3.1. These experiments used only fresh water without microalgal cells to avoid interferences due to biological activity. The dissolved oxygen concentration and pH of the liquid phase were also monitored at different locations in the raceway using appropriate electrodes as described in section 3.3.1. The concentration of CO_2 dissolved in the liquid phase was determined using test kits (LCK-381, Hach-lange, Germany) described in 3.7.3.

In the first set of experiments, carbonation was evaluated using a liquid velocity of 0.22 m s^{-1}. This velocity was chosen because it is in the range of typical liquid velocities in raceways. A constant gas flow of 100 L min^{-1} was used, which corresponded to the calculated maximum likely carbon demand, based on an assumed maximum productivity of 5 g biomass m^{-2} h^{-1} and 100 % efficiency of transfer of CO_2 from the flue gas to the water. In a second set of carbonation experiments, the gas flow rate was adjusted to 50, 100, 200 and 280 L min^{-1} while other parameters remained constant and at optimum values as determined in the first set of experiments. The CO_2 removal and O_2 desorption efficiency in the sump were calculated using Eq(36) and Eq(37), respectively, where y_{inlet} is the molar fraction of each compound in the gas entering the sump and y_{outlet} is the molar fraction in exhausted gas leaving the sump in steady stable conditions. A parameter L/G was calculated to give the ratio between liquid and gas flows (Eq(38)).

$$CO_2 removal\ Eff. = \frac{y_{CO_2\ inlet} - y_{CO_2\ outlet}}{y_{CO_2\ inlet}} \quad (36)$$

$$O_2 stripping\ Eff. = \frac{y_{O_2\ outlet} - y_{O_2\ inlet}}{y_{O_2\ outlet}} \quad (37)$$

$$\frac{L}{G} = \frac{Liquid\ flow}{Gas\ flow} \quad (38)$$

6.1.3 Results

Table 22 shows the molar fraction of CO_2 and O_2 in the gas injected at the bottom of the sump through the diffuser and in the exhausted gas collected in the gas at the top of the sump. The liquid flow was maintained and different gas flows were tested. Therefore, the ratio liquid to gas in the sump was changed in every experiment. It is possible to see that the liquid/gas (L/G) ratio strongly influenced the mass transfer in the sump: when this ratio decreased, the CO_2 removal and O_2 stripping efficiencies also decreased.

Table 22.- CO_2 and O_2 molar fraction in gas entering and leaving the sump, and removal or stripping efficiency, at different gas flow rates

Q_{gas}, l min^{-1}	L/G	CO_2, %			O_2, %		
		y_{Inlet}	y_{Outlet}	Removal Efficiency	y_{Inlet}	y_{Outlet}	Stripping Efficiency
276	10	11.24	6.02	46	6.09	7.95	23
198	13	11.04	3.98	64	6.09	8.28	26
98	27	10.69	3.02	72	6.09	15.03	59
51	51	10.61	0.66	94	6.09	15.49	61

The liquid to gas ratio was calculated taking into account the liquid velocity (0.22 m s-1) and the sump surface (0.55 m2).

Figure 68 shows the gas phase data from one experiment carried out at a liquid velocity of 0.22 m s^{-1} and a gas flow of 100 L min^{-1}, without a sump baffle.

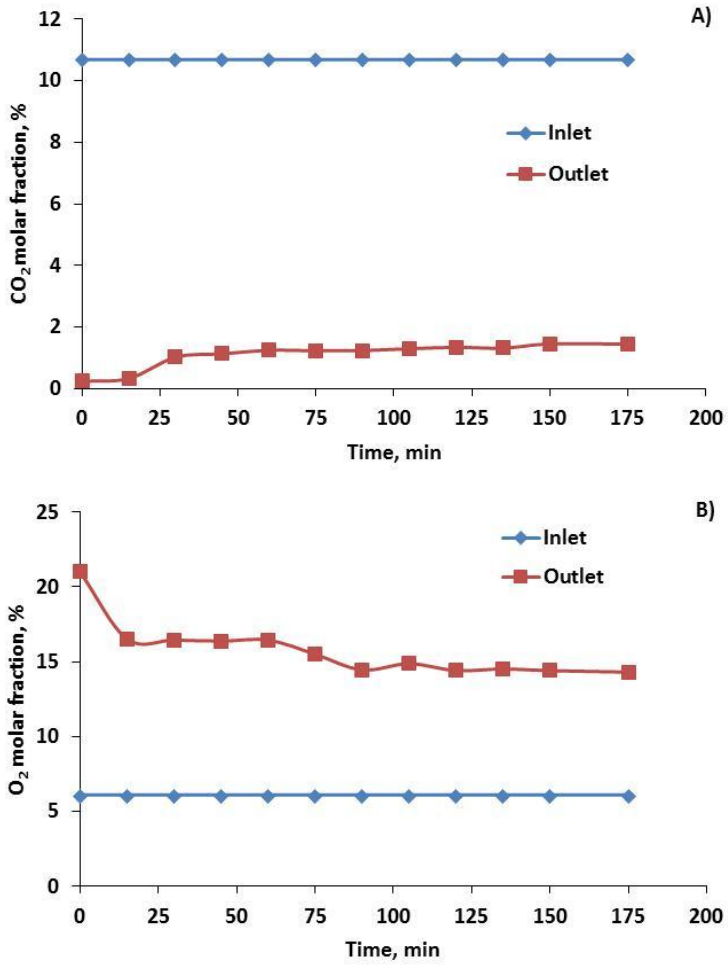

Figure 68.- Variation over time of parameters measured during a carbonation assay performed at a liquid velocity of 0.22 m s^{-1} and flue gas flow rate of 100 L min^{-1} using a sump without a baffle. A) CO_2 molar fraction at the inlet and outlet of the sump. B) O_2 molar fraction at the inlet and outlet of the sump

It can be seen that CO_2 is efficiently absorbed into the liquid, as the CO_2 molar fraction reduces from an initial 10.7 % in the inlet gas to stabilise at around 1.3 % after 60 minutes in the outlet gas; as time passes the CO_2 molar fraction in the exhaust gas increases due to saturation of the liquid phase and reduction in pH (Figure 68A). The data also shows that oxygen is stripped from the liquid to the gas phase, as the oxygen molar fraction in the flue gas increases from 6.1 %, as supplied at the diffuser, to between 21 % at the beginning of the experiment and an average of 14.5 % when the system was stable after 100 min (Figure 68B). These percentages were measured in the gas captured in the gas hood above the sump. Differences in the stripping efficiency could be related to the L/G ratio, as seen in Table 22. Equilibrium between the liquid and gas phases was achieved after 150-200 min of continuous flue gas addition, depending on the conditions in the raceway.

Figure 69 shows the variation in dissolved inorganic carbon, dissolved oxygen and pH in the liquid phase for the run shown in Figure 68. The dissolved inorganic carbon in the liquid phase increased with time due to absorption of CO_2 from the gas phase whilst at the same time the pH and dissolved oxygen decreased. The pH decreased from 8.6 to a final value of 6.7 and as a result of this the ratio of dissolved carbon species also changed, as the initial pH was due to the alkalinity of the fresh water used, whereas final pH value was a function of the CO_2 molar fraction in the flue gas used. Dissolved oxygen in the liquid decreased with time as oxygen was desorbed from the water, resulting in an equilibrium value of dissolved oxygen of 80 % with respect to saturation with air.

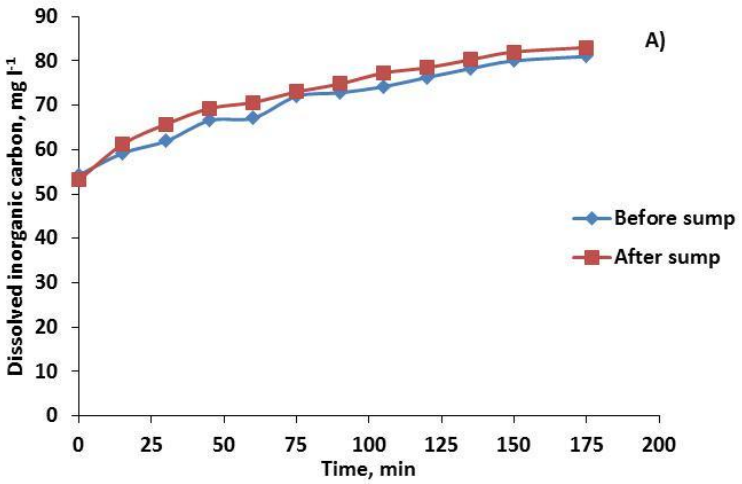

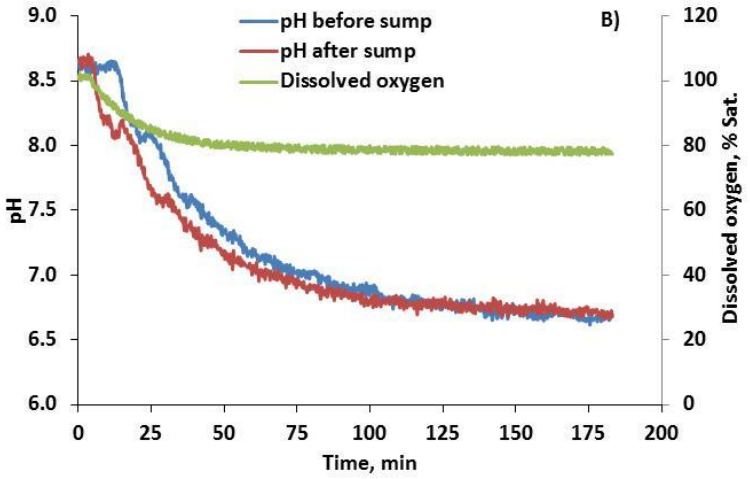

Figure 69.- Variation over time of parameters measured during a carbonation assay performed at a liquid velocity of 0.22 m s^{-1} and flue gas flow rate of 100 L min^{-1} using a sump without a baffle. A) Dissolved inorganic carbon before and after the sump. B) pH of the liquid before and after the sump, in addition to dissolved oxygen after the sump

To confirm these values, pH and dissolved inorganic carbon measurements were made at different positions in the raceway, at the beginning and end of the experiments when stable conditions had been achieved (Table 23). The data shows large differences in dissolved inorganic carbon between the beginning and end of the experiment, but only small differences between the different sampling points, including those immediately before and after the sump. The pH showed a similar pattern, with large differences between the start and end of the experiment but only small variations between sampling positions at any one time. The data clearly shows CO_2 absorption is a function of pH, and this justifies the use of pH as a useful measurement in studying the behaviour of the system.

Table 23.- Variation of pH and dissolved total inorganic carbon (TIC) at different positions in the reactor at the beginning and end of the experiment

Position	pH		TIC, mg L^{-1}	
	Initial	Final	Initial	Final
Before paddlewheel	8.6	6.7	53.3	81.2
Before sump	8.6	6.7	53.2	83.0
After sump	8.4	6.7	58.1	83.9
End of channel	8.5	6.7	56.2	82.0

Performed at a liquid velocity of 0.22 m s^{-1} and a flue gas flow rate of 100 L min^{-1} using a sump without a baffle

A mass balance approach was used to calculate the mass flow of inorganic carbon absorbed ($C_{absorbed}$, g C min^{-1}) from the gas to the liquid phase based on the flue gas flow rate (Q_{gas}, L gas min^{-1}) and the difference in CO_2 molar fraction at the inlet ($y_{CO2\ \ inlet}$) and outlet to the reactor ($y_{CO2\ \ outlet}$), considering the ratio mass of carbon to mol of CO_2 ($M_{C/CO2}$, g C mol^{-1} CO_2) and the molar volume at the operating conditions (V_{mol}, L gas mol^{-1} gas) (Eq(39)). Similarly, measurement of concentration of total inorganic carbon (TIC) in the liquid phase over time allowed the mass of inorganic carbon accumulated ($C_{accumulated}$, g C min^{-1}) to be calculated by considering the rate of change in TIC concentration ($d[TIC]\ dt^{-1}$, g C L^{-1} min^{-1}) in the known liquid volume ($V_{reactor}$, L) of the raceway (Eq(40)). The difference between the mass of inorganic carbon absorbed ($C_{absorbed}$, g C min^{-1}) and accumulated ($C_{accumulated}$, g C min^{-1}) allowed the mass of inorganic carbon desorption ($C_{desorbed}$, g C min^{-1}) or decarbonation to be calculated (Eq(41)):

$$C_{absorbed} = Q_{gas}\left(y_{CO_2\ inlet} - y_{CO_2\ outlet}\right)\left(\frac{M_{C/CO_2}}{V_{mol}}\right) \tag{39}$$

$$C_{accumulated} = V_{reactor}\frac{d[TIC]}{dt} \tag{40}$$

$$C_{desorbed} = C_{absorbed} - C_{accumulated} \tag{41}$$

The mass flow of inorganic carbon absorbed is a function of the mass transfer coefficient in each zone, represented by the volumetric mass transfer coefficient ($K_l a_l$) expressed as min^{-1}, the driving force or gradient between the CO_2 concentration in the liquid phase ($[CO_2]$), and that in equilibrium with gas in contact with the liquid ($[CO_2^*]$), expressed as g L^{-1} and determined by Henry's law, and the overall volume of the zone, V in litres (Eq(42).

$$C_{absorbed} = K_l a_l([CO_2] - [CO_2{}^*])V \tag{42}$$

For the experimental run shown in Figure 68, the results showed that the absorption rate was a maximum at the beginning of the experiment

and reduced with time due to saturation of the liquid phase with CO_2 (Figure 70A). In addition, accumulation was a maximum at the beginning and was equal to absorption, indicating that under these conditions all the CO_2 transferred was absorbed and remained in the liquid phase. At the beginning there was no desorption but with time the rate increased and by the end of the experiment, when the water had become saturated and acidified, the desorption was close to the absorption rate.

Figure 70B shows the calculated CO_2 concentration in the liquid phase based on experimental values for dissolved inorganic carbon and pH, and the calculated CO_2 concentration in equilibrium with the gas phase in each section of the reactor (sump and channel). As the CO_2 concentration in equilibrium with the flue gas in the sump (81.3-90.3 mg L^{-1}) is much higher than the CO_2 concentration in equilibrium with air (0.5 mg L^{-1}), the concentration of CO_2 in the liquid increases with time, from 1.2 to 99.6 mg L^{-1}, due to absorption of inorganic carbon and acidification. The results also suggest that as the water becomes saturated at the end of the experiment all of the CO_2 absorbed from the gas phase via the sump will be released to the air along the raceway channels as a result of outgassing.

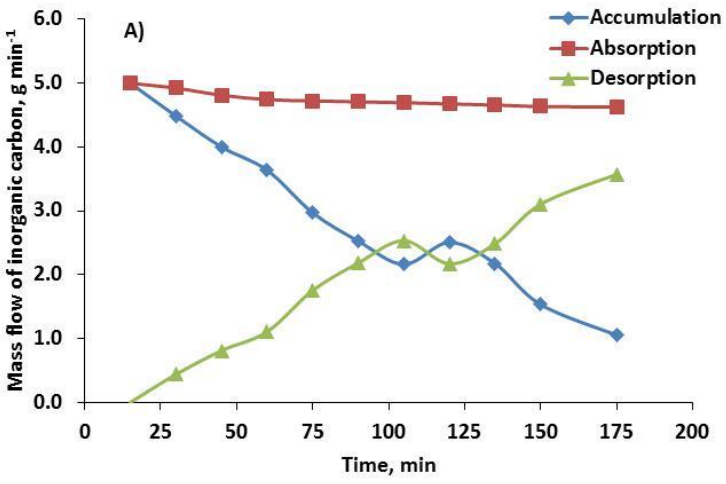

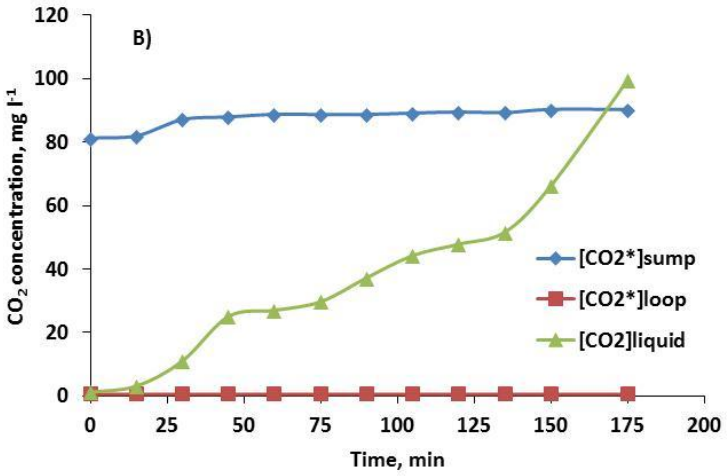

Figure 70.- Variation over time of A) mass flow of inorganic carbon, and B) CO_2 concentration in the liquid and saturation concentration at different positions, for the experiment performed at a liquid velocity of 0.22 m s^{-1} and a flue gas flow rate of 100 L min^{-1} using a sump without a baffle

6.2 Influence of sump baffle and pH in CO_2 mass transfer

6.2.1 Objective

To determine CO_2 mass transfer in the sump with and without baffle under different liquid and gas flow. To quantify the influence of pH in CO_2 mass transfer.

6.2.2 Methodology

As pH was known to have a large influence on the CO_2 mass transfer, experiments were carried out at pH 8 and pH 6 to assess this effect, although it must be stressed that in typical microalgal culture conditions CO_2 transfer normally takes place at pH 8. Sump configurations with and without a baffle were tested (Figure 71), and the effect of liquid to gas ratio (L/G) on gas transfer efficiency was also assessed by using different liquid velocities in the channel. These were between 0.15 and 0.23 m s^{-1} when operating with the baffle, and between 0.22 and 0.44 m s^{-1} without the baffle, as previously determined in the fluid dynamic experiments (Chapter IV, 4.4). The measurement of CO_2 concentration was carried out using the gas hood and

probes previously described in Chapter III, 3.3.1 The results were expressed as the percentage of CO_2 removed from the gas phase (Eq(36)) and the CO_2 mass transfer (amount of CO_2 transferred to the liquid phase) was calculated as Eq(43).

$$CO_2 absorbed = Q_{gas}\left(y_{CO_2\,inlet} - y_{CO_2\,outlet}\right) \quad (43)$$

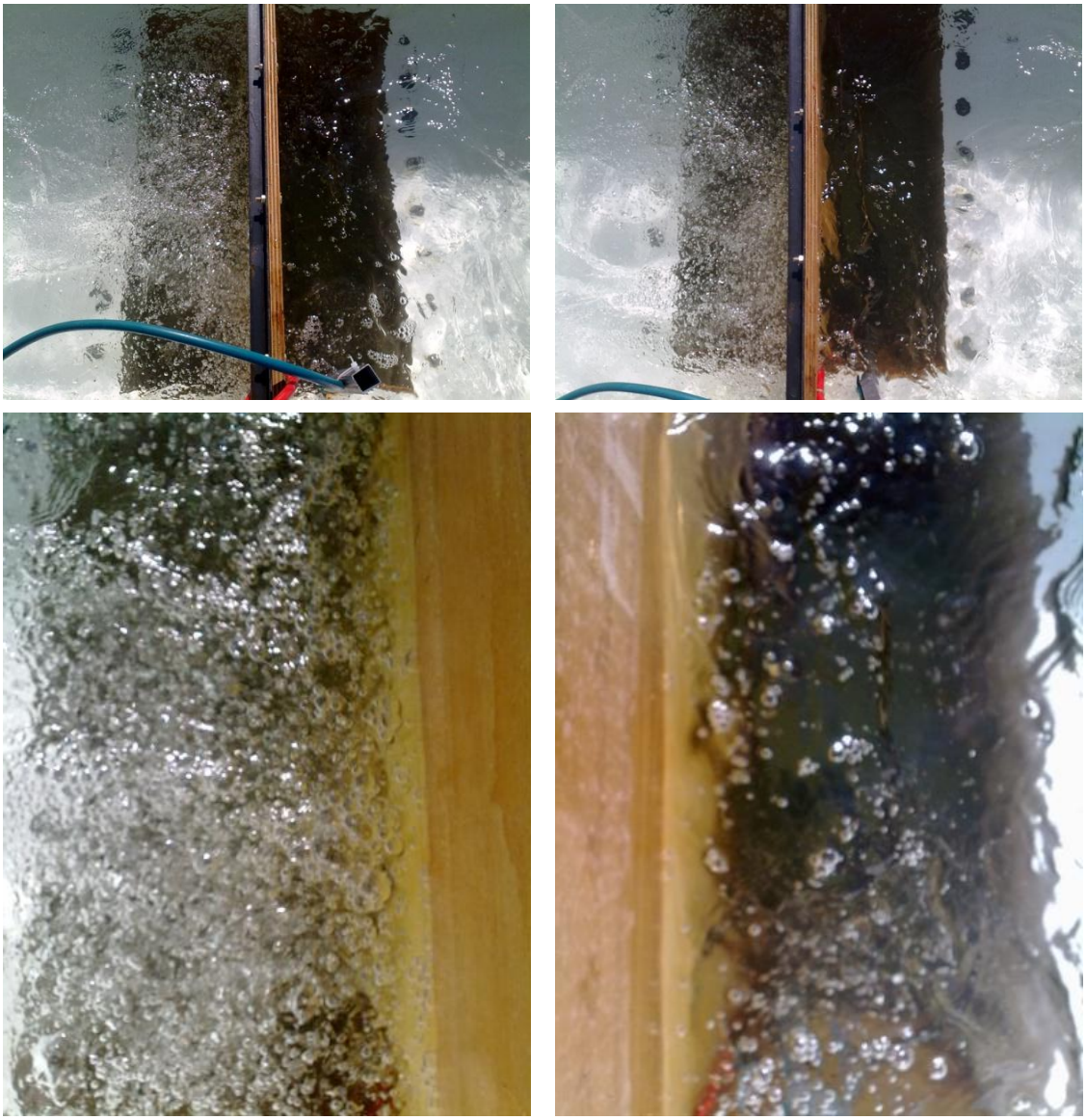

Figure 71.- Images of the bubbling zones inside the sump during the experiment performed in counter-current flow of gas and liquid with baffle

6.2.3 Results

Results obtained at a constant gas flow of around 100 L min^{-1} showed that the removal of CO_2 from the flue gas was over 94 % at pH 8 when operating at liquid velocities greater than 0.22 m s^{-1} and without a baffle in the sump (Table 24). Reducing the liquid velocity, decreased the liquid to gas ratio and, therefore, decreased the removal of CO_2 from the gas phase indicating that the driving force for mass transfer was reduced.

Table 24.- CO_2 removal efficiency at the beginning (pH=8) and at the end (pH=6) of the experiment at different liquid/gas ratios without sump baffle

Q_{gas}, L min^{-1}	Liquid velocity, m s^{-1}	L/G	pH=8			pH=6		
			y_{Inlet}, %	y_{Outlet}, %	CO_2Removal Eff. %	y_{Inlet}, %	y_{Outlet}, %	CO_2Removal Eff. %
118	0.17	17	10.81	1.44	87	10.81	4.27	61
110	0.22	24	11.14	0.70	94	11.14	3.00	73
101	0.34	41	11.56	0.32	97	10.56	1.21	89
113	0.36	38	11.09	0.28	97	11.09	0.51	95
115	0.39	41	11.15	0.31	97	11.15	0.45	96

When using a baffle (Table 25), CO_2 removal greater that 94 % could be obtained at liquid velocities higher than 0.19 m s^{-1}, but removal was reduced at a lower liquid velocity, although less so than had been observed when not using a baffle. The CO_2 removal from the gas phase was also higher at pH 8 than 6 with and without baffle, due to the greater driving force at the higher pH value.

Table 25.- CO_2 removal efficiency at the beginning (pH=8) and at the end (pH=6) of the experiment at different liquid/gas ratios with sump baffle

Q_{gas}, L min^{-1}	Liquid velocity, m s^{-1}	L/G	pH=8			pH=6		
			y_{Inlet}, %	y_{Outlet}, %	CO_2Removal Eff. %	y_{Inlet}, %	y_{Outlet}, %	CO_2Removal Eff. %
94	0.10	13	11.86	1.25	89	11.86	2.98	75
95	0.15	18	11.46	1.00	91	11.46	2.70	76
96	0.19	24	11.55	0.74	94	11.05	2.42	78
107	0.22	25	11.86	0.24	98	11.86	1.89	84
112	0.24	26	11.11	0.65	94	11.11	1.99	82

Figure 72 shows the CO_2 removal efficiency at pH 8 and 6 when the raceway is operated with and without sump baffle. The main differences appeared at different pH values, while no significant difference in the CO_2 removal efficiency was observed due to the presence or absence of a baffle.

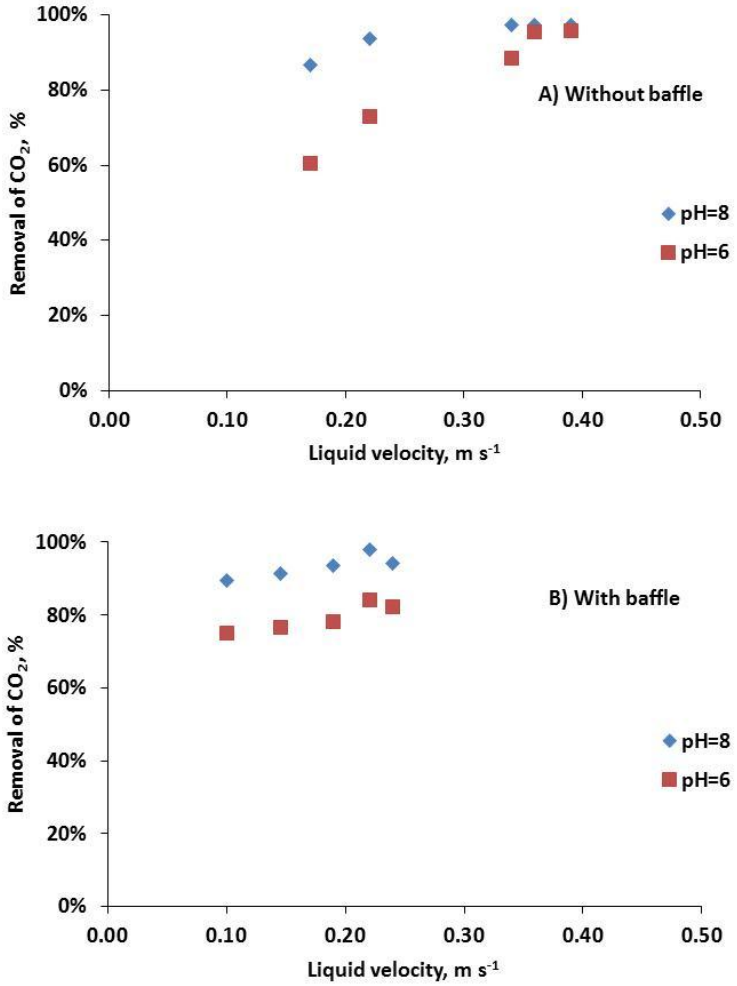

Figure 72.- Influence of liquid velocity, pH and presence of a baffle in the removal of CO_2 from flue gas when using a constant gas flow of 100 L min^{-1}

To verify this, CO_2 mass transfer as estimated from the CO_2 transferred from the gas to the liquid was calculated in Table 26. CO_2 transference without baffle in the sump increased with liquid velocity from 20.28 to 22.79 g min^{-1} and from 14.16 to 22.49 g min^{-1} at pH 8 and 6 respectively. Using sump baffle it ranged from 18.22 to 21.45 g min^{-1} at pH=8 and from 15.25 to 18.71 g at pH=6.

Table 26.- CO_2 mass transfer (g min^{-1}) with and without sump baffle at different gas-liquid flow rates at pH 8 and 6

Without baffle				With baffle			
Q_{gas}, L min^{-1}	v_{liquid}, m s^{-1}	CO_2 mass transfer, g min^{-1}		Q_{gas}, L min^{-1}	v_{liquid}, m s^{-1}	CO_2 mass transfer, g min^{-1}	
		pH=8	pH=6			pH=8	pH=6
118	0.17	20.28	14.16	94	0.10	18.30	15.32
110	0.22	20.97	16.35	95	0.15	18.22	15.25
101	0.34	20.75	18.89	96	0.19	19.01	15.87
113	0.36	22.47	21.99	107	0.22	22.77	19.55
115	0.39	22.79	22.49	112	0.24	21.45	18.71

Although it was intended to maintain the gas flow at 100 L min^{-1}, there were slight variations due to differences in gas pressure in each experiment. In addition, achievable liquid velocities were different depending on the sump configurations (with or without baffle), so the CO_2 mass transfer was also evaluated regarding the normalized ratio liquid to gas in every experiment (Figure 73). This figure confirmed that the net CO_2 transferred from gas to liquid depended on liquid to gas ratio and pH, the influence of sump baffle in mass transfer being negligible.

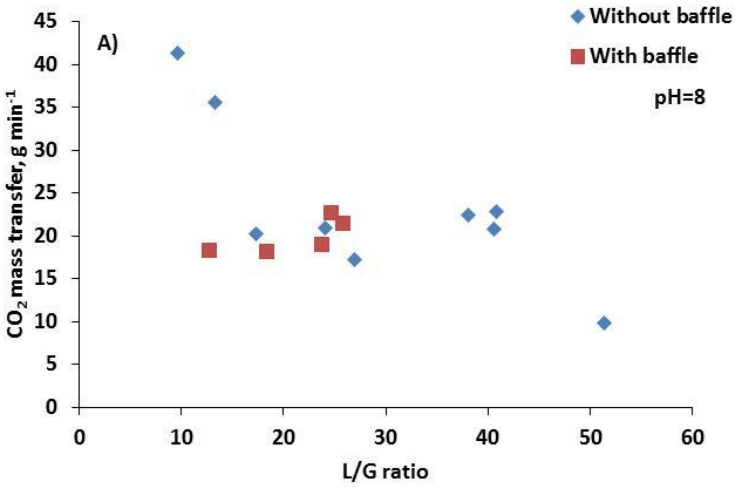

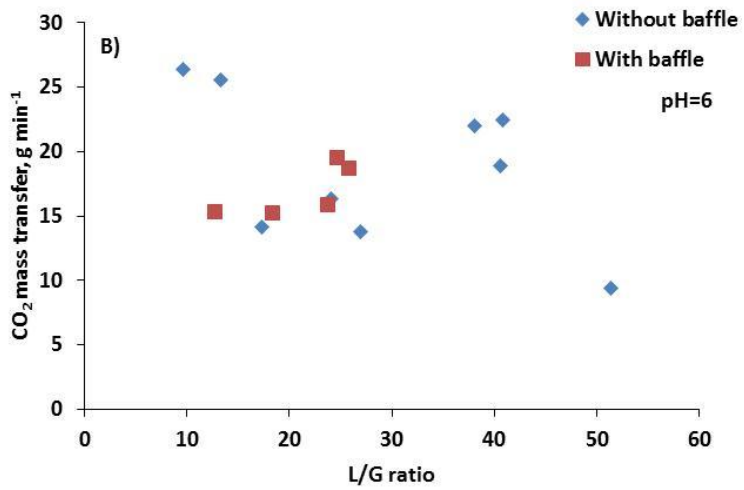

Figure 73.- Influence of liquid to gas ratio and presence of sump baffle on the net CO_2 transfer at a gas flow 100 L min^{-1} at A) pH 8 and B) pH 6

Figure 74 shows CO_2 removal efficiency with and without baffle at pH 8 and 6. It is possible to see that best performance was obtained when the ratio of liquid flow to gas flow was increased. As noted in the analysis of previous figure, pH and L/G ratio influenced the CO_2 removal efficiency to a greater extent than baffle presence.

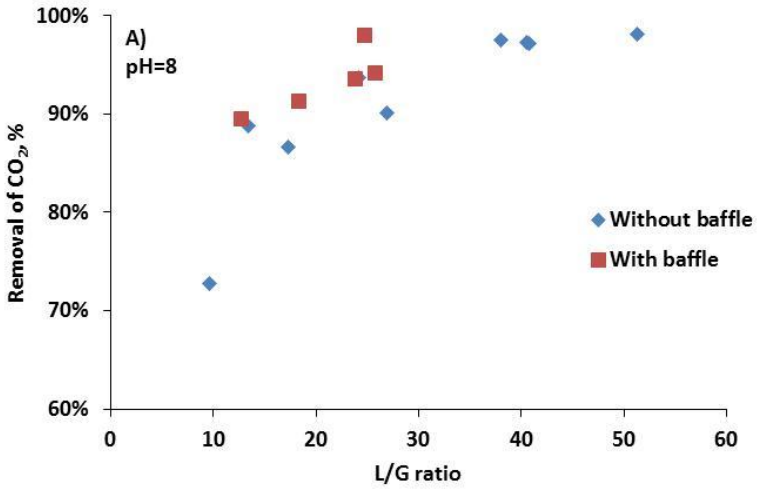

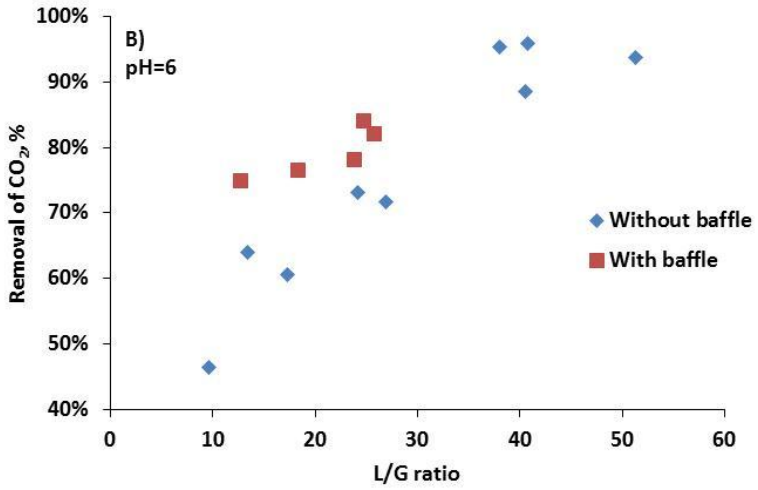

Figure 74.- CO_2 removal efficiency with and without baffle. A) pH 8 B) pH 6

Selected values of CO_2 mass transfer and CO_2 removal efficiency with and without baffle are shown Table 27. These values were the values showed in Figure 73 and Figure 74 at pH 8, which is the pH usually set in microalgae cultures.

Table 27.- CO_2 mass transfer and CO_2 removal efficiency at different L/G ratios with and without baffle at pH 8

	L/G	CO_2 mass transfer, g min^{-1}	Removal of CO_2, %
Without Baffle Sump	10	41.33	0.73
	13	35.56	0.89
	17	20.28	0.87
	24	20.97	0.94
	27	17.30	0.90
	38	22.47	0.97
	41	22.79	0.97
	41	20.75	0.97
	51	9.81	0.98
With baffle sump	13	18.30	0.89
	18	18.22	0.91
	24	19.01	0.94
	25	22.77	0.98
	26	21.45	0.94

As the presence of the sump baffle did not appear to influence the removal of CO_2 from the gas stream or its mass transfer, experiments to determine the influence of gas flow rate were carried out without a baffle and at a constant liquid velocity of 0.22 m s^{-1}. The results at pH 8 showed that CO_2 removal from the flue gas was reduced when the gas flow increased (Figure 75). The maximum removal of 98 % was achieved at the minimum gas flow rate of 50 L min^{-1}, and the minimum removal of 73 % was found at 280 L min^{-1}, which was the highest gas flow tested (Figure 75A). When tested at pH 6, the CO_2 removal at the highest gas flow rate was 46 % and there was no significant difference at the lowest gas flow tested. In contrast, however, the net amount of CO_2 transferred to the liquid was higher when the gas flow rate increased; at pH 8 net values ranged from 9.8 to 41.3 g min^{-1} (Figure 75B). These results demonstrated that gas flow rate has a stronger influence than liquid velocity on CO_2 removal from the bubbled gas stream in the current sump configuration.

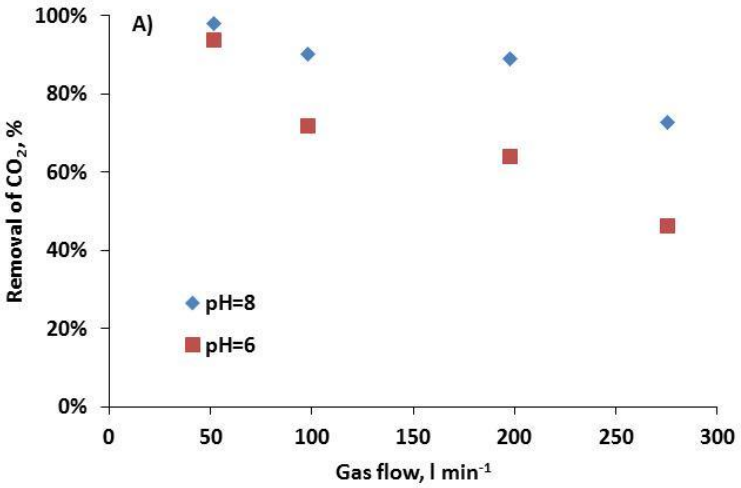

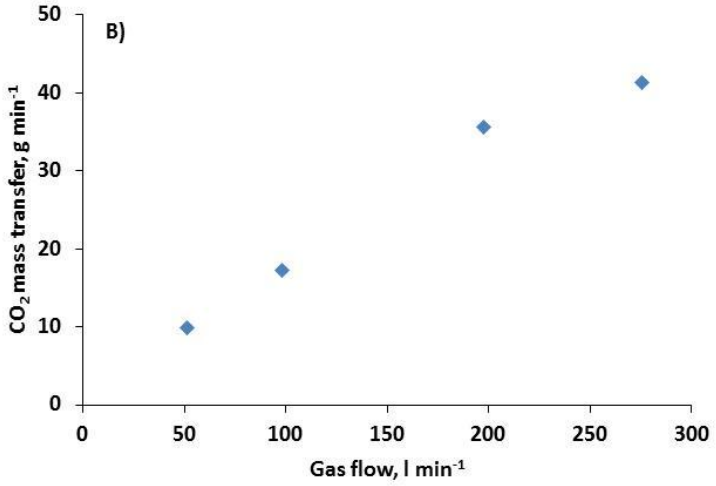

Figure 75.- Influence of gas flow rate in CO_2 mass transfer at the same liquid velocity of 0.22 m s^{-1}, without sump baffle: A) Removal of CO_2 at pH 6 and 8 pH; B) Net CO_2 mass transfer at pH 8

6.3 Effect of CO_2 mass transfer and seasonal changes on microalgae production

6.3.1 Objectives

To maintain an active microalgal culture in the raceway using flue gas as carbon source. To identify the biomass productivity at different dilution rates. To determine the CO_2 removal efficiency in the sump when the raceway was operated with a microalgae culture and flue gas. To determine the effect of seasonal changes in climate and culture conditions.

6.3.2 Methodology

The raceway was operated without a baffle, at a liquid velocity of 0.22 m s^{-1}, a depth of 0.2 m and with flue gas supplied on demand at a flow rate of 100 L min^{-1}. The measurement system described in Chapter III, 3.3.1 was used to determine the CO_2 mass transfer from flue gas to the culture and to measure DO and temperature. The pH was controlled between set points of 7.8 and 8.1 as described in Chapter III, 3.3.2.1. The experiments were carried out in the raceway with an actively metabolizing microalgal culture. For this, the reactor was inoculated with 3 m^3 of *Scenedesmus* sp. culture previously grown in a tubular photobioreactor at a dilution rate of 0.3 day^{-1}. The raceway was

initially operated in batch mode for 11 days until the total suspended solids (TSS) concentration of the biomass reached 0.7 g TSS L^{-1}, at which point the culture was switched from batch to semi-continuous operation in which pre-determined amounts of culture medium were added each day (during light hours) for 5 days per week to give the desired dilution rate. The culture medium was prepared from commercial fertilizers and fresh water as described in Chapter III, 3.5. Biomass concentration was measured daily, and mean daily production (g m^{-2} day^{-1}) was calculated based on this concentration and the harvested volume, taken over weekly time intervals. Harvesting was carried out as described in Chapter III, 3.3.2.2, and fresh culture medium was added to restore the raceway to its normal working depth. Evaporation was obtained from the weather station located at the Experimental Station. The culture status was checked daily by measuring the absorbance at 680 nm, the turbidity and the chlorophyll fluorescence as specified in section 0, where the method to evaluate the ash content was also described. The culture health was also observed by microscope to determine possible contamination with predators causing cell death.

The raceway was operated over a 6-month period from December to May to provide information on algal growth during winter and spring periods, and during this time the dilution rate was varied to control the biomass growth rate in relation to raceway conditions. To determine the optimum dilution rate a trial-and-error approach was adopted, hence the dilution rate was modified weekly.

6.3.3 Results

During the batch start-up the average water temperature was 13.6 °C, with a maximum daytime temperature of 18.4 °C. As shown in Figure 76A, the temperature increased in the transition from winter to spring conditions and this had a pronounced effect on the evaporation rate. In December the average air temperature was around 15 °C with an evaporation rate of around 100 L day^{-1}; whilst by the end of the experimental period in May the temperature had risen to 25 °C with an evaporation rate of 700 L day^{-1}. The evaporation rate was therefore between 2 % and 7 % of total reactor volume and a significant fraction of the total daily volume removed for harvesting: this loss was taken into account when calculating the biomass yield. Figure 76B shows the total

suspended solid concentration in the raceway culture, which remained around 0.75 g L^{-1} for the first 6 weeks of operation when the average water temperature was fairly constant. Once the temperature started to rise there was a corresponding increase in culture density, reaching 1.4 g TSS L^{-1} by early April. Further increases in temperature did not increase culture density, which in fact declined slightly as temperatures rose further in May. Figure 76B shows the chlorophyll fluorescence evaluated as Fv/Fm and TSS. Fv/Fm was in the range 0.6-0.7, although small seasonal variations were observed coinciding with changes in TSS concentration. The higher temperatures seen at the end of the study period may have resulted in a reduction in Fv/Fm and TSS concentration as a result of photoinhibition in part of the culture. Other possible factors that may have contributed to this reduction are the accumulation of certain ions linked to the increase of evaporation (which was not compensated with fresh water although the dilution factor at the end of the period also increased), the older microalgae presented in the broth, the accumulation of dissolved oxygen or inadequate harvesting ratio, Turbidity and absorbance at 680 nm (Figure 76C) were related to the culture concentration (R^2=0.613, n=111 and R^2=0.775, n=108, respectively; $p<0.001$ in both cases) showing that, as expected, absorption of light in the culture increased with the culture density. It should be noted that when the concentration of the culture was high, the sample was diluted in order to reduce the density of cells and to maintain the measured value below 1.5. This dilution may affect the accuracy of the result since not only pigments in cells absorb light: other structures such as membranes, dust etc, also cause light scattering. Although the value of some measurements may be affected by dilution, however, it is interesting to observe the trend in absorbance and its close relationship with turbidity (Figure 76C).

Figure 76D shows the dilution rate expressed as the amount of fresh medium added as a percentage of the total reactor volume; and the productivity as the mass of algae produced per unit area per day. The results indicate that 43 % of the variation in productivity can be attributed to the dilution rate (R^2=0.43, n = 23, $p < 0.001$), and also how productivity increased during the spring period from late February through to the end of May, reflecting the higher temperatures and longer days with more solar radiation. When averaged over weekly periods, estimated productivities of 10-15 g TSS m^{-}

^{2} day^{-1} was achieved in winter (December - February) and of 20-25 g TSS m^{-2} day^{-1} during spring (April-May) (Figure 76D). The highest productivity was obtained in Spring at a dilution rate of 20-25 %.

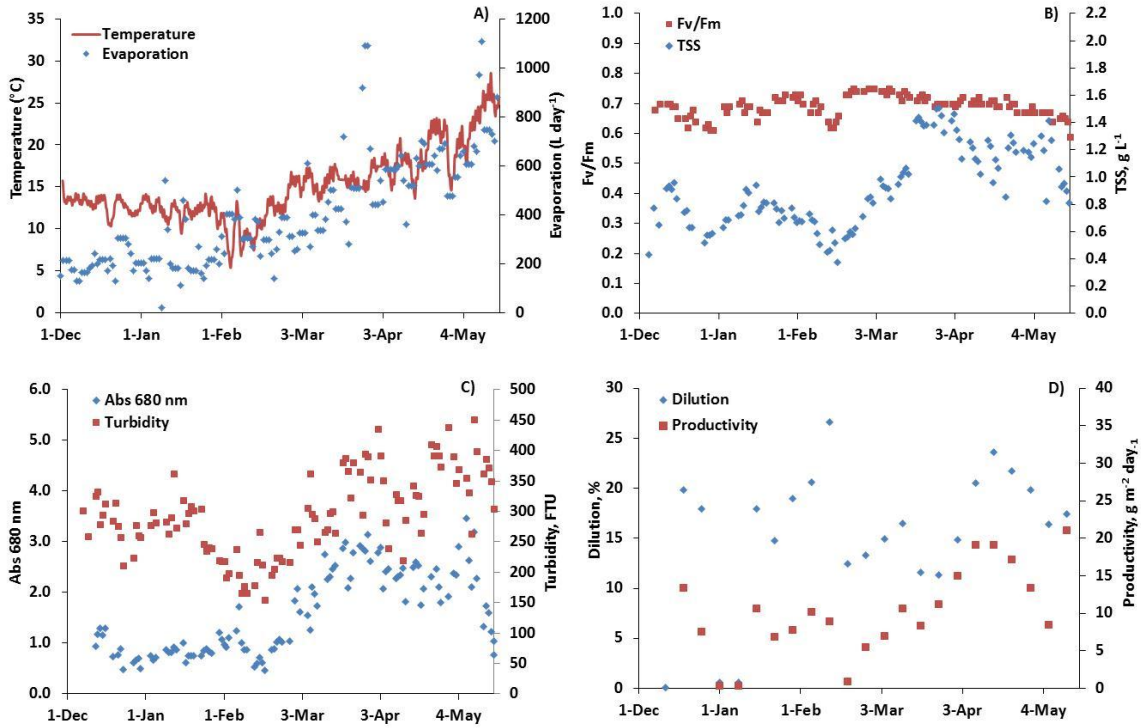

Figure 76.- Parameters studied during the culture period on the raceway reactor operated in semi-continuous mode growing *Scenedesmus* sp. A) Online culture temperature registered and daily evaporation in the raceway. B) Daily analysis of total suspended solids and quantum yield. C) Daily analysis of absorbance at 680 nm and turbidity. D) Weekly average dilution and productivity in raceway algal culture

Figure 77 shows mean daily pH and DO concentration in the culture during the experimental work. It is possible to see where the pH of the reactor was controlled at 7.95 ± 0.07 (timing time 1 s) by automatically switching on and off the flue gas supply to the sump based on the pH reading. The CO_2 molar fraction of flue gas added was 10.05 %, whereas in the gas collected over the sump it was 0.22 ± 0.09 %, corresponding to a CO_2 removal of 98 %. DO tended to accumulate in the second half of the study period, coinciding with higher productivities during Spring, when frequency of flue gas additions increased. Therefore, the volume of CO_2 injected in the raceway to cover

microalgae demand increased with solar radiation in Spring (Figure 78). In this figure is also possible to see the relationship between Fv/Fm values and CO_2 injection in the raceway. This indicated that when cell stress was reduced due to seasonal weather conditions microalgae CO_2 demand increased and, therefore, photosynthetic efficiency was higher until the end of the studied period when photoinhibition occurred.

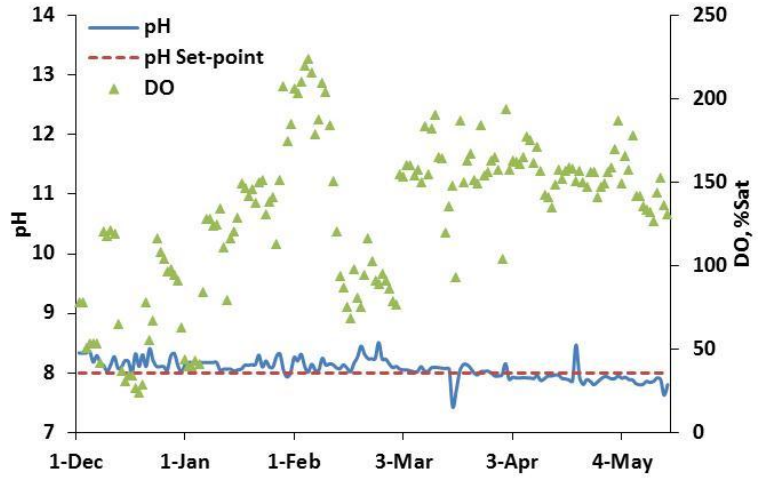

Figure 77.- Mean daily pH and DO in the culture during the experimental work on the raceway reactor operated in semi-continuous mode growing *Scenedesmus* sp. The pH set-point is also represented

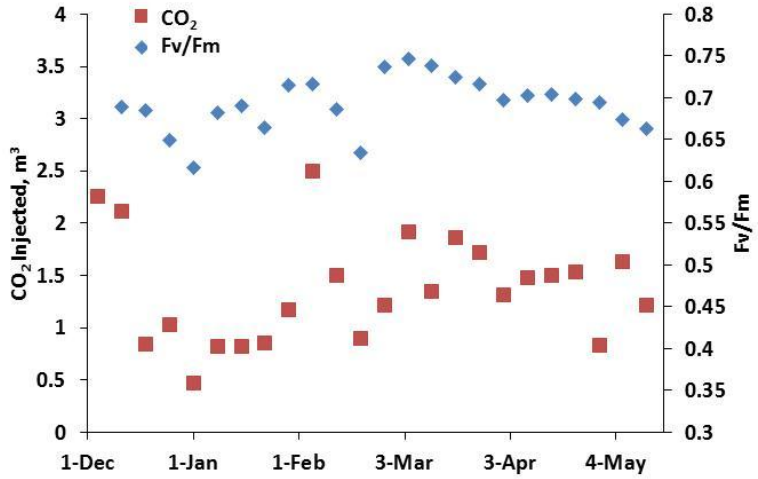

Figure 78.- Weekly average CO_2 injected and Fv/Fm in raceway reactor operated in semi-continuous mode growing *Scenedesmus* sp.

Figure 79 shows continuous monitoring data for selected periods of operation corresponding to batch start-up, first week of semi-continuous operation, period of maximum productivity and the onset of reduced productivity in early summer conditions (Figure 79 A, B, C and D respectively). During the batch start-up period (Figure 79A) peak daily solar radiation was between 300-550 W m^{-2} and both water temperature and DO concentrations showed diurnal fluctuation, with day and night temperatures varying by up to 10 ˚C. A similar pattern was reflected in the first week of continuous operation (Figure 79B), and during December DO concentrations never rose above 200 % saturation. In the maximum productivity period (Figure 79C), peak solar radiation was between 800-900 W m^{-2}, and water temperature peaked between 25-30 ºC falling to around 15 ºC at night. By May water temperature had increased to over 30 ºC in the middle of the day. This was associated with reduced productivity and lower peak DO concentrations of 200-250 % saturation (Figure 79D). In all cases temperature and DO peaks lagged behind peak solar radiation.

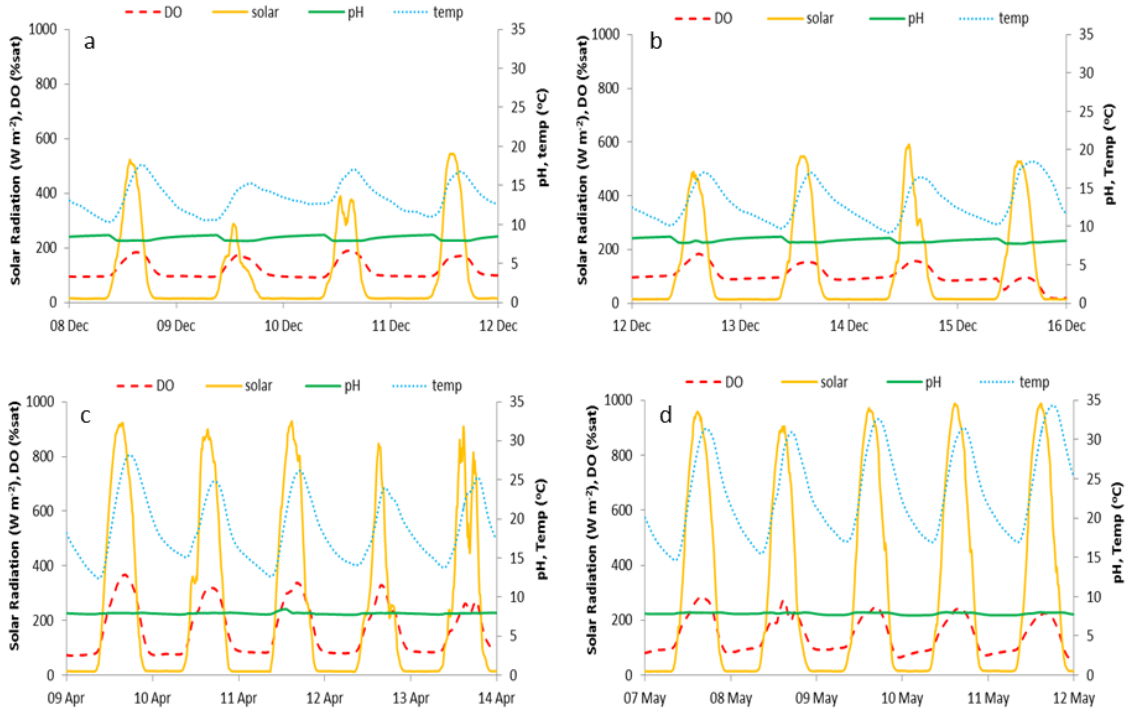

Figure 79.- Selected results from continuous monitoring of raceway culture during the experimental period: A) batch start-up, B) first week semi-continuous, C) maximum productivity, and D) reduced productivity

To study the seasonal differences in depth, two days were selected as example of typical behaviour of all runs. These were a low productivity day in Winter (14th February - Day A) and a high productivity day in Spring (28th March – Day B). Table 28 shows the culture conditions during these two days. Longer daylight periods and higher ambient temperatures in Spring increased the mean solar radiation and culture temperature. In the examples shown, the daily average solar radiation and culture temperatures increased from 186.48 to 274.48 W m^{-2} and from 8.65 to 15.04 ˚C for day A and B, respectively. As a result of the better weather conditions on day B, microalgal cell stress was lower in comparison to day A as indicated by the parameter Fv/Fm (0.62 in day A and 0.70 in day B). TSS concentration increased from 0.46 to 1.51 g L^{-1}, as did biomass productivity from 5.52 to 21.27 g m^{-2} day^{-1}. Oxygen accumulation as a consequence of high photosynthetic activity was previously evaluated in

Chapter V, and in this example daily mean DO concentration increased from 86.41 to 158.83 % Sat. The double advantage of using flue gas as carbon source in microalgae culture and, at the same time, to reduce DO accumulation in the culture was also reviewed in

Chapter V. Figure 80 shows the effect of flue gas injection in pH and DO concentration in days A and B. In both situations, pH was controlled around the desired set-point 8 by flue gas injection on demand and, at the same time, DO concentration in the raceway was reduced with every flue gas injection. Other parameters such as evaporation, dilution rate, absorbance at 680 nm and turbidity are also compared in Table 28.

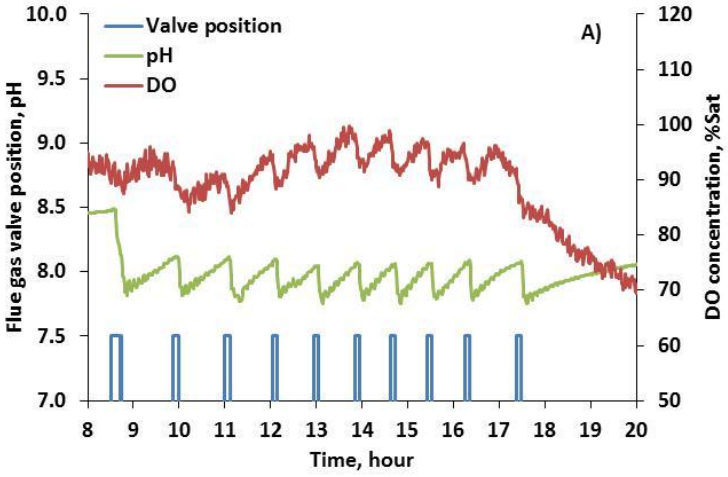

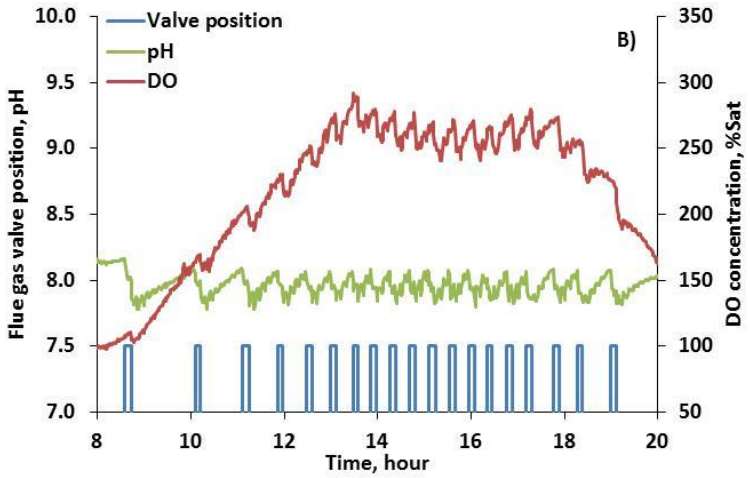

Figure 80.- Influence of flue gas injections (7.5 is flue gas valve opened) in pH and DO concentration over the daylight period on the raceway reactor operated in semi-continuous mode growing *Scenedesmus* sp. A) 14th February - Day A, B) 28th March – Day B

Table 28.- Culture conditions on the raceway reactor operated in semi-continuous mode growing *Scenedesmus* sp. for two days with low and high microalgae productivity (14th February – Day A and 28th March – Day B, respectively)

	Low productivity, 14 Feb – Day A	**High productivity, 28 March – Day B**
Solar Radiation (average), W m^{-2}	186.5	274.5
Culture temperature (average), ˚C	8.65	15.04
DO concentration (average), %Sat	86.4	158.8
Evaporated volume, L	380	1090
Dilution rate, %	12.30	14.10
Abs 680 nm	0.59	2.87
Fv/Fm	0.62	0.70
Turbidity, FTU	216.6	395.3
TSS concentration, g L^{-1}	0.46	1.51
Productivity, g m^{-2} day^{-1}	5.52	21.27

Figure 81 shows the CO_2 demand on the sump during the daylight period in days A and B. In both days, flue gas supply on demand made it possible to control the raceway pH in the desired range of 7.8-8.1 even during peak carbon demand in the mid-day period when solar radiation was at its most

intense. In day A 10 injections during a total time of 78 minutes were necessary to control the pH, while in day B 19 injections and 155 minutes were needed. Table 29 shows the CO_2 balance to the gas phase in the raceway in day A and B. During day A 32.46 mol of CO_2 in total were injected from which 0.30 mol were not absorbed in the liquid phase and were released to the atmosphere with the exhaust gas. During day B in Spring, however, a total of 64.65 mol of CO_2 were injected and 0.74 mol did not pass to the liquid phase to be used by microalgae. In both days, therefore, the CO_2 removal efficiency in the sump was 99 % and CO_2 content in the exhaust gas leaving the sump was lower than 0.5 %.

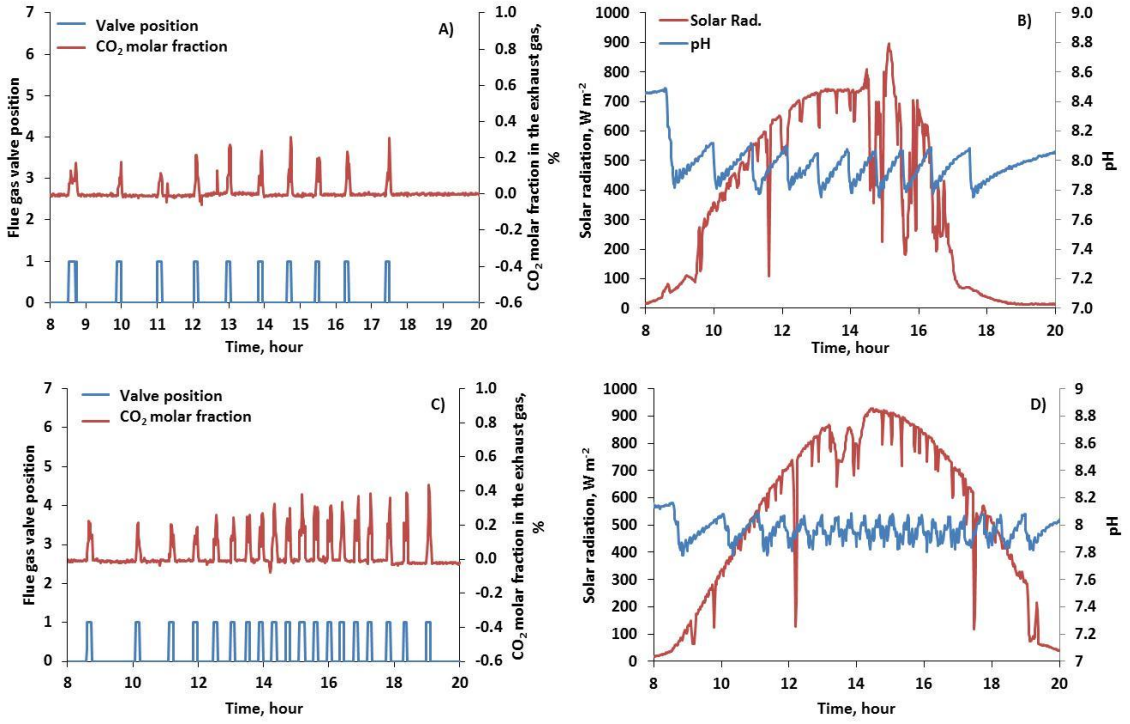

Figure 81.- CO_2 demand on the sump over the daylight period on the raceway reactor operated in semi-continuous mode growing *Scenedesmus* sp. Figures A) and B) corresponds to low productivity day (Day A) and figures C) and D) corresponds to high productivity day (Day B), being 14th February – Day A and 28th March – Day B, respectively. Figures on the left represented timing of flue gas injections and % of CO_2 in gas exhausted to atmosphere. Figures on the right represented the pH control hysteresis in the range of 7.8-8.1 as maintained by flue gas injection (0 is flue gas valve closed and 1 is flue gas valve opened) and solar radiation

Table 29.- CO_2 balance in the gas on the raceway reactor operated in semi-continuous mode growing *Scenedesmus* sp on days A and B

	Low productivity, 14 Feb – Day A	High productivity, 28 March – Day B
Total injection time, min	78	155
Number of injections	10	19
Time per injection, min	7.8	8.2
Flue gas injected, mol	325	647
CO_2 injected, mol	32.5	64.7
CO_2 exhaust gas, mol	0.30	0.74
CO_2 removal Efficiency, %	99.1	98.9

6.4 Carbon balance in microalgae cultures

6.4.1 Objective

To determine the carbon balance in a raceway microalgae culture operated with flue gas.

6.4.2 Methodology

The raceway reactor was operated without a baffle at 0.2 m depth in semi-continuous mode, growing *Scenedesmus* sp. at a dilution rate of 0.3 day^{-1}. Liquid velocity was 0.22 m s^{-1} and flue gas flow was 100 L min^{-1}. TSS, ash content, biomass productivity, Fv/Fm, absorbance at 680 nm and turbidity were obtained as explained in Chapter III, 0. Flue gas injection was made on demand to maintain the pH at 7.8-8.1, and pH, DO and temperature were recorded using the probes as described in Chapter III, 3.3. A carbon balance for the raceway was made taking into account the net amount of carbon supplied in the flue gas and liquid medium used and the outlet of carbon with the biomass, liquid and gas phases (flue gas into the sump and decarbonization along the channels). Carbon content in the inlet and outlet gas was measured using the CO_2 probe and gas hood described in the Materials and Methods, section 3.3. In the liquid phase, TC, TIC and TOC content were obtained in the inlet fresh medium and the harvested culture using the kits described in Chapter III, 3.7.3.

6.4.3 Results

The experiment was carried out on the 18th April, so moderate climate conditions were present in the raceway, typical of the Spring season in this location. The average solar radiation, culture temperature and DO concentration on this day were 270.84 W m^{-2}, 17.36 ˚C and 160.64 % Sat, respectively. The TSS concentration was 0.96 g L^{-1}, giving a biomass productivity of 22.82 g m^{-2} day^{-1}. Other culture parameters such as evaporated volume, absorbance at 680 nm, Fv/Fm and turbidity are shown in Table 30.

Table 30.- Culture conditions for the raceway reactor operated in semi-continuous mode growing *Scenedesmus* sp.

Solar Radiation (average), W m^{-2}	271
Culture temperature (average), ˚C	17.4
DO concentration (average), %Sat	161
Evaporated volume, L	600
Dilution rate, day^{-1}	0.3
Abs 680 nm	2.53
Fv/Fm	0.71
Turbidity, FTU	325
TSS concentration, g L^{-1}	0.96
Productivity, g m^{-2} day^{-1}	22.82

The pH of the reactor was controlled at 7.95 ± 0.07 (Figure 82A) by automatically switching on and off the flue gas supply to the sump based on the pH reading. This happened 17 times during the daylight period, with an average duration of 7.8 ± 0.8 min on each occasion, which is analogous to a cycling time of 7.6 min. The CO_2 molar fraction of flue gas added was 10.05 ± 0.09 % (measured hourly during daylight period) whereas in the gas collected over the sump it was 0.22 ± 0.09 %, corresponding to a CO_2 removal of 98 %. The frequency of flue gas additions increased as the solar radiation increased, and the total cumulative time the sump flue gas valve was open was 149 min day^{-1} (Figure 82B).

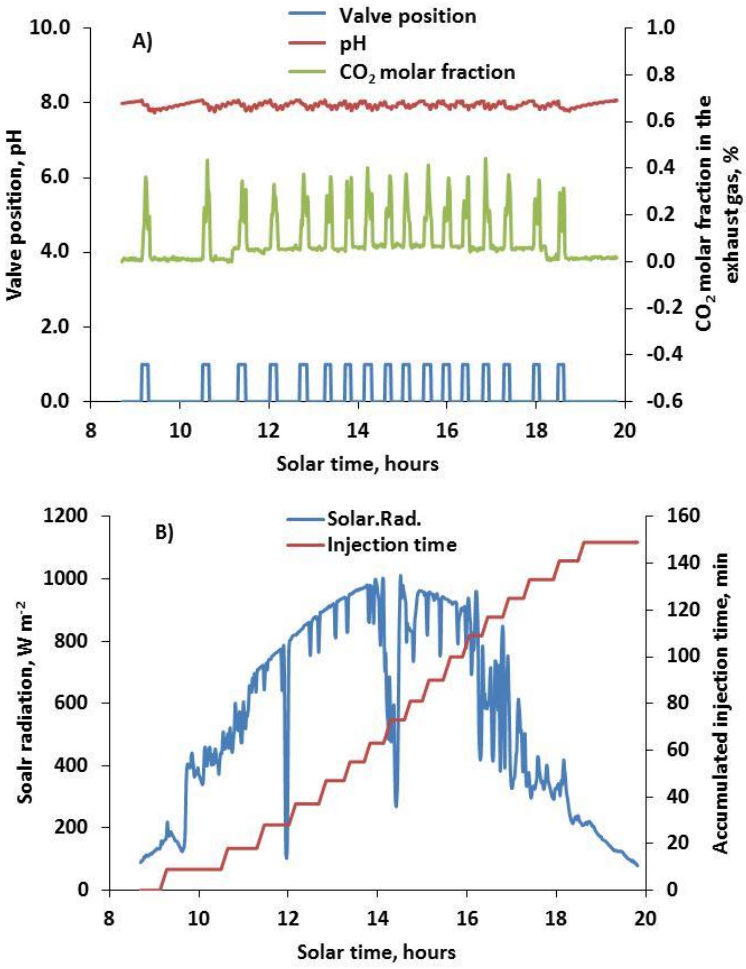

Figure 82.- Variation of solar radiation and variables related with CO_2 injection A) valve position, pH, CO_2 molar fraction in the exhaust gas, and B) accumulated injection time, over the daylight period on the raceway reactor operated in semi-continuous mode growing *Scenedesmus* sp.

Effluent from the raceway had a higher dissolved bicarbonate concentration than the fresh medium (0.66 g L^{-1} vs 0.32 g L^{-1}) and this was taken into account in the carbon balance, as was the loss of water by evaporation which was estimated to be 6 L m^{-2} day^{-1}. Under these conditions the CO_2 removal from the injected flue gas was 96 %, which was higher than the predicted 90 % based on the fresh water study. The carbon balance showed that 1010 g C day^{-1} (86 % of total carbon inlet) was injected with the flue gas, and a further 165 g C day^{-1} (14 % of total carbon input) was supplied as a result of the alkalinity of the culture medium (Table 31). From this inlet carbon, 43, 285 and 777 g C day^{-1} were present in the outlet flue gas, liquid and biomass corresponding to 4, 24 and 66 %, respectively. The remaining 70 g C day^{-1}

necessary to close the balance corresponded to decarbonisation losses in the raceway, accounting for 6 % of the total carbon output.

Table 31.- Carbon balance in the raceway divided into gas, liquid and biomass balance in the inlet and outlet

	Inlet		Outlet	
	g C day^{-1}	Percentage (%)	g C day^{-1}	Percentage (%)
Flue gas	1010	86	43	4
Liquid	165	14	285	24
Biomass	0	0	777	66
Decarbonization	0	0	70	6
Total	1175	100	1175	100

6.5 Discussion and conclusions

Although raceway reactors have been the most common system for large-scale algal biomass cultivation for the last 50 years, recent studies have shown there is still scope to improve their performance by an improved understanding of the fluid dynamics (Chiaramonti et al., 2013; Chisti, 2012) and mass transfer characteristics of gases (Bao et al., 2012; Li et al., 2013). Understanding how to optimize CO_2 mass transfer is therefore critical to efficient and economic operation if energy costs and CO_2 usage are to be reduced. As most previous studies have used pure CO_2 gas as the carbon source, there has been no data to show how flue gases interact in the supply of CO_2 and in the desorption of O_2. The results are therefore very pertinent to algal biofuel production, as flue gases have been suggested as the only sustainable way of providing carbon for this purpose (Jonker & Faaij, 2013; Mata et al., 2010).

The composition of flue gases varies depending on the source and fuel used, with the CO_2 molar fraction ranging from 4 % in natural gas boilers, up to 15 % in coal boilers, or even as high as 30 % in cement kilns. Not only does the composition of the flue gas have a major role in determining the mass transfer of gases, but it will also affect the equilibrium pH if gas is added in an uncontrolled manner. This is an important consideration as control of pH is a major factor influencing carbon availability and determining the productivity of microalgal cultures. It has been reported that gas containing 3 % CO_2 allowed maximum productivity of *Chlorella* at pH 8 (Fulke et al., 2010); whereas injection of 15 % CO_2 produced a culture with a pH in the range 6.2-7.2 (Li et

al., 2013). In this study using flue gas with ~10 % CO_2 from the diesel boiler gave a final equilibrium pH of 6.5 (Figure 69B). This is too low for optimal growth of most algal strains, which occurs between pH 7.0 and 8.0. Operating at a higher pH would improve CO_2 absorption and minimize decarbonation, but a balance must be found that will promote growth without dramatically reducing CO_2 mass transfer. The current work demonstrated that operation at pH 8 gave a driving force for absorption of CO_2 from flue gas of 37 mg L^{-1} with mass transfer in the sump of 65 h^{-1} , whereas the driving force for desorption to the air was 0.7 mg L^{-1} in the channels with a mass transfer coefficient of 0.9 h^{-1}. These differences allowed sustained absorption of CO_2 with minimum losses in this type of system (Figure 70). The mass transfer is in good agreement with those of Weissman who found a value of 0.5 h^{-1} for CO_2 released from the surface of a 100 m^2 raceway pond (Weissman & Goebel, 1987; Weissman et al., 1988). Reported mass transfer values for CO_2 absorption by bubbling gas through the liquid phase range from 0.4 to 350 h^{-1} (Carvalho et al., 2006) and are very dependent on the system used. Taking into account the volume of the sump and the entire reactor it was estimated that the maximum net CO_2 absorption rate in the sump was around 33.6 g min^{-1}, compared with a maximum desorption rate within the channels of around 0.2 g min^{-1}. In the current experiment, the concentration of dissolved oxygen found in the raceway culture was as high as 32 mg L^{-1} at midday; injection of flue gas would help to desorb some of this, as the large differential between this peak concentration and the low values found in the flue gas (6 % v/v) would provide a strong driving force for oxygen stripping in the sump.

The absorption capacity was experimentally evaluated in different operational conditions, with and without a sump baffle and at different liquid and gas flows (Table 22, Table 24, Table 25, Table 26). The use of a sump with a middle baffle with counter-current injection of gases has been widely reported as a means of maximizing CO_2 absorption (Craggs et al., 2012; Weissman et al., 1988; Weissman et al., 1998). This recommendation is based only on the improvement in mass transfer that could be obtained by increasing the gas liquid contact time through reducing the bubble rise velocity under counter-current conditions (Camacho Rubio et al., 1999; Chaumat et al., 2005; Singh & Majumder, 2011). The result from the current study demonstrate that although the presence of the baffle in the sump increased the CO_2 transfer

from the gas phase compared to that obtained without a baffle, the difference was very small. The high gas transfer found in this system without a baffle, better than predicted previously (Weissman et al., 1988), appears to raise questions over the need for a sump baffle in the configuration studied. Furthermore, as the power requirement when using the sump baffle was 4-fold higher that without a baffle at the same flow velocity of 0.22 m s^{-1} (see Chapter IV, 4.4) the disadvantages of using a baffle with the studied configuration may far outweigh any advantages, unless the hydrodynamic performance of this type of baffle can be improved. It is important to note that the results presented were obtained for a particular system in which neither sump nor baffle dimensions were optimised. There is a lot of scope for improvement in design of gas transfer and of mixing systems in raceways since general knowledge about gas transfer for bubbles is still limited, especially for more complex systems like CO_2 in mixed gases (flue gas). This is important as energy is critical in fuel applications of microalgae and excessive power consumption is one of the key factors in the design of cultivation systems for algae-based biofuels, where the net energy profits are relatively small (Acien et al., 2012).

Any CO_2 supply system must satisfy carbon demand while minimizing CO_2 losses to the atmosphere. This is important even when using flue gas, which is often regarded as a 'free' source of carbon, as there are still costs and restrictions associated with its use. These are influenced by the length of gas pipeline and type of injection system, with penalties for the release of large amounts of CO_2 at ground level. The CO_2 supply system should therefore be designed to provide enough carbon to meet the maximum demand, normally associated with midday conditions, but also be regulated to meet any lower demand conditions. In an optimum productivity scenario, the CO_2 demand in a raceway reactor is estimated to be around 10 g CO_2 m^{-2} h^{-1}, corresponding to productivity of 25 g biomass m^{-2} day^{-1}. This is based on the assumption that the productivity will be concentrated in five central hours and a ratio of 1.8 g CO_2 g^{-1} biomass will be required. From the current study the net CO_2 transfer rate was 17.3 g CO_2 min^{-1} (Figure 75) which is equivalent to 10.4 g CO_2 m^{-2} h^{-1}, assuming 90 % of efficiency in the use of CO_2 contained in the flue gas supplied. The supply of CO_2 to the raceways was therefore considered to be

sufficient to meet the demand at times of high productivity, whilst at the same time addition was regulated by linking its supply to a pH control algorithm.

6.5.1 Microalgal culture

An active microalgal culture of *Scenedesmus* sp. was maintained for 6 months from December to May. During this period, increases in temperature in the culture during cold seasons like Winter were linked to increases in TSS concentration, although there was a limit above which further increases in temperature did not increase culture density, which in fact declined slightly as temperatures rose further in May (Figure 76). This decrease in TSS concentration may be explained by photoinhibition phenomena taking place, which increased cell stress and reduced productivity. This was confirmed by measuring the parameter Fv/Fm, which is linked to the performance at which microalgae carry out the photosynthesis reaction. This parameter was maintained between 0.6-0.7, in the range for culture that is photosynthetically active (Molina Grima et al., 1997). Small variations, however, in this parameter could be explained by changes in the average irradiance due mainly to variation in weather conditions from winter to spring, while some variations may also be explained as a result of changes in the cell size and concentration or pigment content (Gomez et al., 2013). In any case, the higher temperatures seen at the end of the study period resulted in a reduction in solar efficiency and TSS concentration as result of different factors: photoinhibition in part of the culture, concentration of inhibitory substances (ions, salts, recalcitrants) due to evaporation which was not compensated with fresh water or the increase of cells age in the broth due to the maintenance of the culture for a long period of time.

Maximum biomass productivity in the studied period of 18-20 g TSS m^{-2} day^{-1} (Figure 76D) was obtained in Spring due to the increasing intensity of irradiance and the duration of daylight periods. This productivity was comparable to that reported in the literature, with values of 19 g TSS m^{-2} day^{-1} obtained in an airlift-driven raceway (Ketheesan & Nirmalakhandan, 2012) and in outdoor cultivation with natural sunlight and a culture depth of 10 cm (Vonshak & Guy, 1992). In a nearby facility in the same region as the raceways used in this work and, therefore, with similar Mediterranean climate conditions, a productivity peak of 14 g TSS m^{-2} day^{-1} was obtained in July in a

450 m^2 raceway inoculated with *Spirulina platensis* and grown during a 10-month trial (Jiménez et al., 2003). Minimum productivity was obtained in winter, with values ranging between 3-5 g TSS m^{-2} day^{-1} comparable to those achieved in January and February by Jimenez et al. in the cited paper. A part from climate conditions, the raceway design may also have affected productivity during the winter period as the angle of inclination of the sun during these months is low, and the relatively narrow width of the raceway resulted in more than half of the culture surface being in the shadow of the freeboard of the channel at mid-day; this area was reduced as the sun's angle of inclination increased throughout the experimental period.

During the entire study period, pH remained within narrow limits with only small increases during the dark period which were more pronounced in winter than spring (Figure 79). The control of raceway pH by the addition of flue gas CO_2 addition thus proved very effective, and the single carbonisation sump was adequate for its purpose. DO concentrations during the day could reach 350 % saturation. DO concentrations as high as 45 mg l^{-1} have been reported in raceways (Márquez et al., 1995; Vonshak, 1997), causing inhibition of photosynthesis and growth. The accumulation of photosynthetic oxygen in raceways during operation at high irradiancies was one of the main potential problems observed, as this can lead to a loss of productivity due to inhibition. The use of flue gas minimised DO accumulation as can be seen in Figure 80 as a result of the high volume of gas passing through the sump, which in turn stripped oxygen out of the culture medium. The sump proved to be one of the main zones in the raceway where oxygen could effectively be removed, as was shown in

Chapter V. The other major problem was the increase in temperature between spring and summer. As air temperatures increased in late May the water temperature in the raceways rose above 35 ^oC (Figure 79) resulting in very marked effects on productivity as a result of thermal inhibition. This was apparent as the dissolved oxygen concentration in the raceway was reduced during the mid-day period along with a reduced demand for CO_2, both strongly indicating inhibition or even death of the culture. As the summer progressed it became increasingly difficult to maintain the raceways in a stable condition.

6.5.2 Carbon balance

In the studied conditions, the CO_2 removal from the injected flue gas was 96 %, which was higher than the predicted 90 % based on the fresh water study. This was due to the influence of biological reactions which through fixing CO_2 increase the driving force for absorption in the sump, and decrease the driving force for desorption in the channels. Of the total carbon supplied to the raceway, 66 % was assimilated into the biomass. Carbon losses with flue gases were identified as a minor problem accounting for only 4 % of the injected carbon, and it was estimated this could be further reduced by increasing the L/G ratio (Figure 73, Figure 74). In addition, decarbonation represented only 6 % of total carbon supplied; although CO_2 outgassing has been described as an important factor in raceway design and operation if mixing is too energetic and pH too low (Weissman et al., 1989), the carbon balance calculated from this study indicated that it was almost negligible. According to Weissman et al., at pH 7.5-7.8 25 % of the CO_2 absorbed in the carbonation sumps was lost to the atmosphere by outgassing through the pond surface. Operating at pH 8-8.3 can reduce this to less than 10 %. Therefore, pH should be maintained above 8 to reduce outgassing losses to less than 10 %, a value that agrees with the results presented in this work. The two factors that affect outgassing the most are the concentration in the liquid and the resistance to movement through the gas-liquid interface. Both are unfavourable. Low mixing systems as in the raceway studied in this work have lower outgassing rates, since the rate at which the pond surface is renewed with CO_2-rich water is low. The mass transfer coefficients between liquid and atmosphere for this raceway are, therefore, very low, and this could explain the absence of outgassing observed at this scale of operation.

The major carbon loss from the raceway was through the liquid phase via total inorganic carbon leaving the reactor along with the harvested algae. This was higher than that entering the raceway with the culture medium, which represented 25 % of the total carbon entering the raceway. Specific growth rates in *Nannochloropsis salina* cultures were reduced by bicarbonate addition, whereas bicarbonate addition had no significant effect on the growth rates of *Tetraselmis suecica* cultures, suggesting species specific responses to bicarbonate addition (White et al., 2012). The carbon balance made to the raceway revealed that the bicarbonate concentration was 660 mg L^{-1}, while for

Chlorella vulgaris the optimum level of sodium bicarbonate addition is 1.000 mg L^{-1} (Yeh et al., 2010). In any case, the optimum bicarbonate concentration is highly dependent on the microalgae specie, and in open raceways where the microalgae population is heterogeneous and changing this issue seems to be difficult to control.

In order to avoid the continuous release of carbon when harvesting the culture, the supernatant after cell harvesting could be recycled to return non-consumed nutrients and carbon to the raceway: this strategy has already been proposed in laboratory-scale culture systems (González-López et al., 2012). This could, however, potentially lead to a build-up of undesirable recalcitrant or even inhibitory compounds (Igou et al., 2014). It should be noted, however, that the fresh water used in preparation of the culture medium has its natural inorganic carbon content increased through the addition of fertilizers (which contain carbonates), so carbon loss through the liquid effluent could also be reduced by changing the composition of the culture medium. The recycle of the supernatant after cell harvesting may need an additional step to avoid environmental problems. The storage of this medium in a pound with O_2 bubbling in order to accelerate the oxygenation of the organic matter can be considered as a potentially feasible alternative.

The experimentally determined value of 96 % utilization of CO_2 from the flue gas stream was notably higher than previously found in many reported studies. In laboratory-scale closed raceway reactors, the maximum carbon recovery was 46 % when using *Chlorella,* and 35 % when using *Spirulina* grown in batch mode while maintaining 10 % of CO_2 in the atmosphere over the culture (Ramanan et al., 2010). In these experiments the pH of the culture was 10, possibly to enhance CO_2 absorption, and this could in part compensate for the reduced growth rate (Ramanan et al., 2010). The maximum efficiency of CO_2 absorption was 82 % when a 3.1 m high bubble column was used, compared to 36 % when using a sump in the same raceway reactor (Putt et al., 2011). This type of approach, however, introduces complexity into the system and has higher power consumption as the culture must be circulated between the bubble column and raceway. Even when closed photobioreactors are used, reported values of CO_2 transfer efficiency are lower than those observed in this study. With a 15 % rich-CO_2 gas a removal efficiency of 16 % was reported for *Chlorella* sp., whereas this increased to 56 % when a 2 % rich-CO_2 gas was

substituted (Chiu et al., 2008). Cheng et al. (2006) demonstrated that increasing retention time of CO_2 in a photobioreactor significantly enhanced the CO_2 fixation efficiency (Cheng et al., 2006). When the entire liquid surface of a raceway was covered with a plastic sheet, the maximum CO_2 efficiency when 15 % rich-CO_2 gas was added continuously was reported to be 64 %. This efficiency increased to 95 % when intermittent injection was used to better match the carbon requirements of the microalgal culture (Li et al., 2013). The current study strongly indicates that CO_2 addition to meet carbon demand coupled with control over the ratio of gas to liquid addition can lead to very effective carbon utilization from flue gas, and the key to this is optimisation of this ratio and carbon addition regulated through pH control.

The results showed that a number of parameters under the control of the operator can influence the mass transfer of CO_2. For the raceway studied, the ratio of gas flow to liquid volume in the sump was an important factor in the removal of CO_2 from the flue gas, and determining this ratio should be the first step in the optimisation. The results showed that by operating at high liquid/gas ratio, the removal of CO_2 from the flue gas was maximized, but the overall rate of CO_2 transfer to the culture medium was reduced. The latter parameter is less important provided that sufficient CO_2 is transferred to meet the demand of the culture. When growing an algal culture, this can best be achieved by controlling the flue gas injection to maintain pH at ~8, as for most cultures this will be a reasonable compromise between maximizing CO_2 absorption and maintaining suitable algal growth conditions.

6.6 Summary conclusions for Chapter VI

In conclusion, the work in this chapter has shown the following:

- Flue gas (10 % CO_2) bubbling was effective for pH control at around pH 8 and for effective carbonization of the microalgal culture, with CO_2 mass transfer efficiencies above 96 %.
- The use of flue gas reduced DO concentration peaks at midday by oxygen stripping in the sump.
- The presence of the sump baffle increased the CO_2 transfer from the gas phase to the liquid, although the difference was very small. The power consumption when the baffle was used increased considerably

(see section 4.4), therefore its utilization is not recommended unless the hydrodynamic performance of this type of baffle can be significantly improved.

- The maintenance of an active microalgal culture for a period of months was achieved using flue gas as carbon source.
- Only 66 % of the total carbon supplied to the raceway was assimilated into the biomass, with carbon losses in the flue gases accounting for only 4 % of the injected carbon.
- CO_2 outgassing in the raceway was almost negligible, representing only 6 % of the total carbon supplied. The major carbon loss was, therefore, through the liquid phase with the harvested algae. For this reason, nutrient recycling is a key issue to be taken into account in the design of industrial plants for microalgal biomass production.

Chapter VII

7. HYDROSTATIC PRESSURE WHEEL FOR WATER LIFTING IN RACEWAY REACTORS

In Chapter IV, the power consumption associated with different operations and configurations of the reactor was studied and it was concluded that the configuration of every section of the raceway affected the energy requirements of overall system. One key section in raceways is the paddlewheel which is where energy enters into the system. This energy is transformed to produce the circulation of liquid but there are no in-depth studies on new designs and technologies for the improvement of paddlewheel efficiency. It is necessary, therefore, to investigate new low-energy technologies for water motion in the raceway and overcome the drawbacks linked to its operating costs. A new low-power paddlewheel design could potentially produce a considerable change in the final energy balance of the system due to the necessity to maintain the circulation of the culture all year round (Rogers et al., 2014).

This research started from the traditional paddlewheel configuration used during the previous experiments as a starting point, and compared this with a new energy-efficient design based on the theory of the hydrostatic pressure wheel for water lifting (HPW). This idea was first developed by Dr Gerald Muller of the University of Southampton, and he kindly gave guidance during this part of the work.

7.1 Operating principles

The idea of the HPW as a water lifting device in raceway reactors emerged from the studies carried out by Senior et al. (Senior, 2009; Senior et al., 2010). These authors described the use of a special wheel and a platform as a device for hydropower conversion at very low head differences, between 0.2 and 2.5 m. They predicted high theoretical energy efficiencies in the system (ranging from 0.5 to 0.9) at very low head differences, similar to those occurring in raceway reactors. Figure 83a presents the principles on which the HPW is based. It consists of a wheel with radius R whose blades act as a weir, producing a water depth d_1 upstream and d_2 downstream. To maintain this head difference $H = d_1 - d_2$ and reduce leakage losses in the gaps between

wheel and bed, Senior et al. described a curved bed under the wheel. The hydrostatic force F produced by the head difference is therefore responsible for the power generation in the system. Figure 83b shows the experimental and theoretical efficiencies versus d_2/d_1 in a test carried out at 15 l/s by Senior et al. A high experimental efficiency was observed, close to the theoretical value, which increased with the reduction in the head loss. The slight difference between theoretical and experimental values was explained by the gap losses. From this study, information about the wheel and shoe construction was extracted: the design of a 12-blade paddlewheel, the design of a curved section at the bottom to close the space between two blades, the importance of matching wheel lifting capacity to headloss upstream/downstream and the necessity to reduce leakage to achieve high efficiencies.

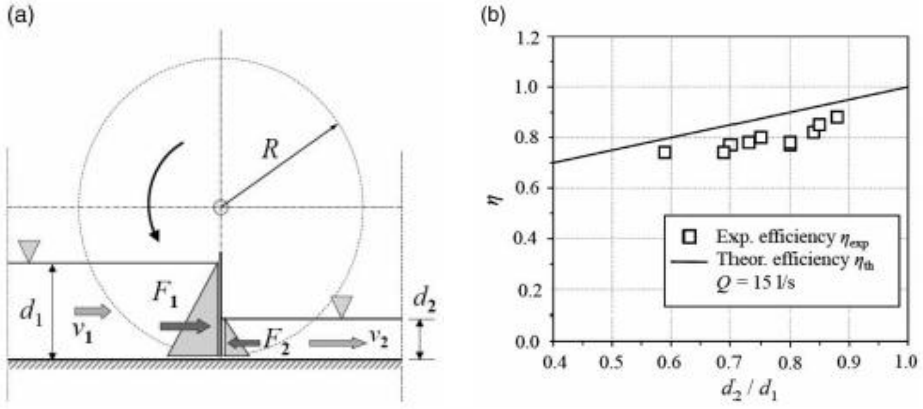

Figure 83.- Hydrostatic Pressure Wheel: (a) principle, (b) efficiencies, (Senior et al., 2010)

In the case of raceways, the HPW concept is expected to work in reverse mode: this means that instead of using the head loss to transform the hydrostatic power into mechanical power which may be used efficiently to produce energy, the system has to use energy efficiently to transform the mechanical power into hydrostatic power to make the water circulate in the reactor. For this purpose, a platform called a 'shoe' was designed to raise the bed of the channel downstream of the wheel by a vertical distance $\Delta h = d_1 - d_2$, as shown in Figure 84. In Figure 84a is possible to see the movement of the blade from position 1 to position 2, when water is pushed forward and lifted by the vertical distance d_1-d_2. Figure 84b shows that once the water is lifted to position d_1, it can flow around the raceway under gravity until it reaches the upstream position just before the paddlewheel, which is the shallowest point in

the raceway. Then, in position number 1 again, the next blade of the paddlewheel is ready to make the same movement and lift more water into position 2, with this process repeating for all of the blades while the wheel is maintained in rotation.

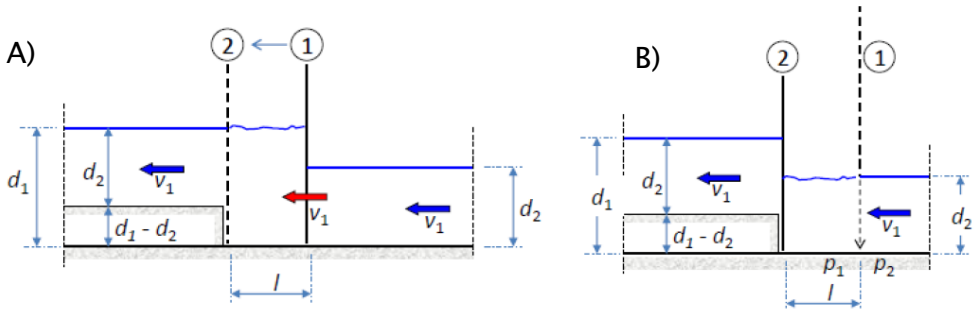

Figure 84.- Hydrostatic water lifting wheel for raceways: A) pumping stroke, B) filling and entry of next blade

The ideal situation occurs if there is no leakage of water from position 2 where the water is at the higher level, to position 1 where the water level is lower. If leakage occurs, the efficiency of the wheel will be lower and, therefore, the power consumption will increase. For this reason it is important to reduce gaps to the minimum and 'close off' the portion of water that is lifted by each blade, ensuring that water does not flow back.

7.2 Hydrostatic pressure wheel for water lifting in flumes

7.2.1 Objectives

To determine the hydraulic power and efficiency of the HPW in a flume at laboratory scale. To define the power requirements of this system under different conditions and compare it with the traditional paddlewheel for water circulation. To establish a start point for the design of an efficient HPW system to be tested in the raceways in pilot plant at a larger scale.

7.2.2 Methodology

7.2.2.1 Flume and paddlewheel

The experimental work was carried out using existing facilities in the Hydraulics laboratories at the University of Southampton. These consisted of a

12.0 m long, 0.3 m wide and 0.37 m high flume (Figure 85, left) in which was installed a 12-blade paddlewheel with a diameter of 1.0 m (Figure 85, right), driven by a 24 V DC electric motor (CM808-71B-TW03, 0.280 kW, Stannah International, UK) which was attached to the wall of the flume by a metal frame and connected, at the same time, to the shaft of the wheel by means of a chain belt. The paddlewheel was fixed to the wall of the flume using a metal frame in both sides of the shaft. The wheel was designed to fit as well as possible to the flume walls and bottom, although careful attention was paid to avoid possible friction between the paddlewheel and the channel.

Figure 85.- Left: Flume. Right: Detail of paddlewheel, motor and shoe

The inflow was maintained by pumping water into the flume, with the pumped flow controlled by means of a valve. An adjustable weir was located at the end of the flume to control the downstream level. The head difference was therefore influenced by the pumped water flow, the height of the weir and paddlewheel rotation. Once the water passed the weir, it was collected in a tank and pumped back to the beginning of the flume in a closed circuit. Different depths and paddlewheel rotation speeds were tested in order to simulate a wide range of conditions in the raceway: for every height of weir (200, 175, 150 mm), the power supply in the paddlewheel was progressively increased from the minimum required for wheel rotation to the maximum allowed for efficient water lifting in the system. In addition, different water flows were tested for each power supply position. These experiments were designed to provide data on the behaviour of the water lifting wheel under different conditions and flow regimes.

The depth of water was measured upstream and downstream of the wheel and upstream of the weir. Waves and other disturbances can make it difficult

to measure depth directly in the flume with any precision. For this reason, a hole was made at each measurement position along the channel and PVC tubes were inserted connecting the flume to three damping cylinders (400 mm height, 80 mm diameter). The damping cylinders were provided with a measuring tape where the 'zero' position matched the bottom of the channel, i.e. the level in the damping cylinder was zero when the flume was empty. In this way, the water depth in the flume could be measured directly in the cylinder, regardless of the influence of waves, once the flow conditions had stabilised.

7.2.2.2 Shoe

A device called a 'shoe' was specially designed as an artificial channel bed. It was located at the bottom of the flume, just under the paddlewheel (Figure 86, left). The aim of the shoe is to allow water to pass the wheel smoothly and efficiently, maintaining the required head loss upstream/ downstream and reducing the backflow produced by the difference of heights (Lucas, 2011). The reduction of turbulence and counter flow (leakage) are essential since these directly affect the performance of the system. For this reason, the shoe had the same curvature as the paddlewheel and the curved section had exactly the same length as the distance between two blades (πD/12) (Figure 86, right). In this way, there was always at least one blade in the curved position of the shoe and the leakage was kept as low as possible.

Figure 86.- Left: Detail of shoe and the attachment system to the channel bed. Right: Detail of the curvature of the shoe: it is possible to see how the curvature fits the gap between two blades

Two different shoes were tested in the flume. The difference between the designs was the upstream lifting ramp section to allow the device to work in deeper channels (Figure 87A). This part of the shoe elevates the bed of the channel, allowing the wheel to work in a higher position without backflow in the gaps between shoe and wheel. Figure 87B shows the configuration for shallow channels in which the wheel lifts water directly from the bed of the channel. The downstream section had a similar shape in both shoe configurations, taking into account that the discharge ramp was longer in Figure 87A due to the greater depth provided by its configuration. Finally, the efficiency of water lifting of both shoes was compared with the traditional flat configuration.

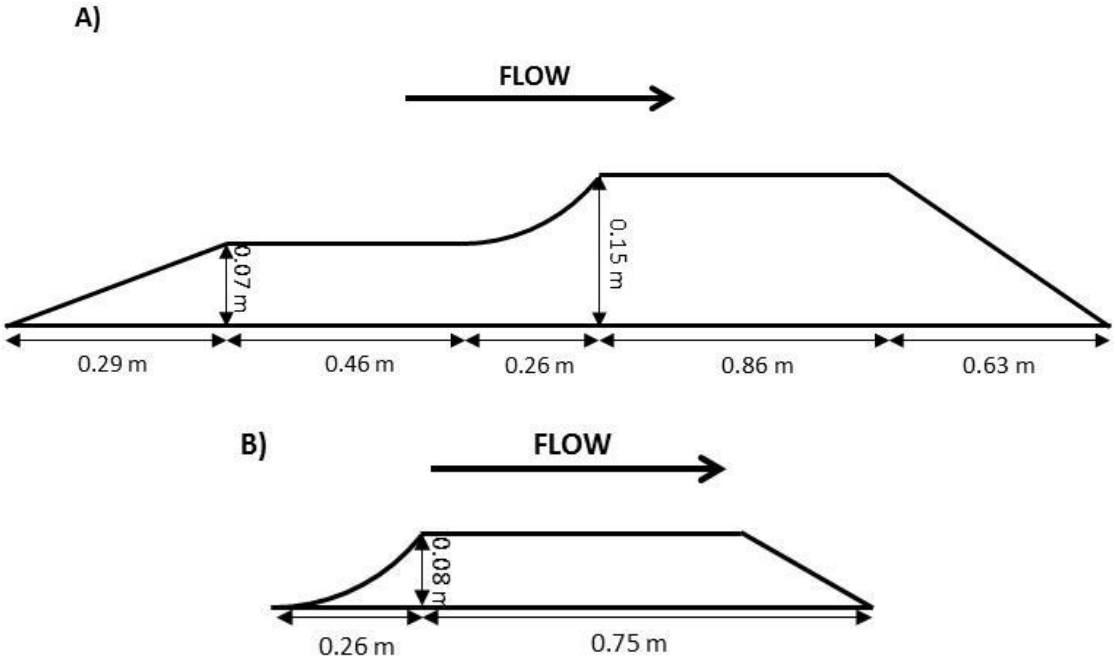

Figure 87.- Vertical cross-section through the shoes tested (not to scale): A) Shoe design for deep flumes (shoe 1), B) Shoe design for shallow flumes (shoe 2)

7.2.2.3 Power calculations

Electrical energy is supplied to the paddlewheel motor to produce its rotation. This is the main energy input in the system and, therefore, is responsible for the main electrical power consumption (P_{elec}, W). For this reason, in every test carried out, the electrical current (I, A) and voltage (V', V) were recorded and the electrical power was measured as:

$$P_{elec} = IV' \tag{44}$$

The mechanical power (P_{mech}, W) needed to maintain a constant rotation of the paddlewheel was measured by means of a load cell with a capacity of 100 kg (Low profile aluminium load cell, Model 1042, Tedea Huntleigh, USA). The mechanical power developed by the engine torque (T, N m), which is the moment of force exerted on the motor shaft power to lift the water, is proportional to the angular velocity (ω, rad s^{-1}) of the shaft (Eq(45)). The angular velocity was calculated using Eq(46), by measuring the time it taken for the paddlewheel to complete 5 rotations, then calculating the duration of one rotation, i.e. the period of the wheel (t_{wheel}, s).

$$P_{mech} = \omega T \tag{45}$$

$$\omega = \frac{2\pi}{t_{wheel}} \tag{46}$$

The load cell was calibrated to determine the correlation between torque and mechanical power. For this, a known mass (m, kg) was located at the end of the blade and the torque was calculated as the weight force (W, N) times the distance between the place where the weight force is acting and the shaft of the wheel, i.e. the radius (r, m) (Eqs(47) and (48)).

$$W = mg \tag{47}$$

$$T = Wr \tag{48}$$

This torque was related to the electrical signal provided by the load cell and recorded in the computer. This was repeated with different masses from 0 to 3.5 kg, with increments 0.5 kg, giving the calibration curve shown in Figure 88, and the calibration Eq(49).

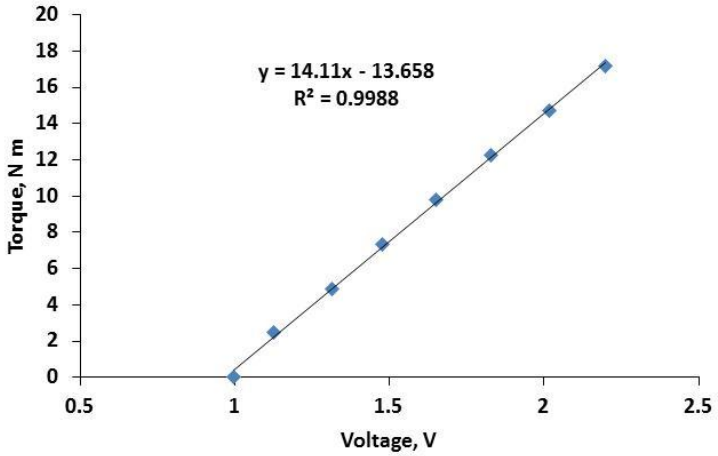

Figure 88.- Load cell calibration curve

$$T = 14.11V' - 13.658 \tag{49}$$

The hydraulic power (P_{hyd}, W) is the power stored in the water due to the action of the paddlewheel. The mechanical power in the wheel is transformed into hydraulic power which is responsible for the circulation of water into the raceway from the deepest section immediately after the wheel (d_2, m) until the shallowest section before the wheel (d_1, m). The difference between downstream and upstream depths is the head difference (H, m) (Eq.(50)) and the hydrostatic pressure (p, N m^{-2}) at a point in the fluid due to the weight of the fluid above it increases linearly with head difference (Eq.(51)), where ρ is the density of the fluid (water ~1000 kg m^{-3}) and g is the gravitational acceleration (9.81 m s^{-2}).

$$H = d_2 - d_1 \tag{50}$$

$$p = \rho g H \tag{51}$$

The force (F, N) is calculated in Eq.(52) as the product of the hydrostatic pressure multiplied by the area of the blade (A_b, m^2). Assuming that the liquid has the same velocity as the blades to maintain a constant depth, the hydraulic power (P_{hyd}, W) is then calculated as in Eq. (53).

$$F = pA_b = \rho g H A_b \tag{52}$$

$$P_{hyd} = Fv = \rho g H A_b v = \rho g H Q \tag{53}$$

The water flow downstream (Q, $m^3\ s^{-1}$) was calculated using Eq.(54), obtained from the British Standard for open channel flow measurement using thin-plate weirs (BS-ISO-1438:2008), where Q is the flow in $m^2\ s^{-1}$ per m width of the channel, g is the acceleration due to gravity (9.81 $m\ s^{-2}$), d_3 is the height of water upstream of the weir (m) measured with a damping cylinder, z is the height of the weir (m) and C is the discharge coefficient calculated as Eq.(55).

$$Q = \frac{2}{3} C \sqrt{2g} (d_3 - z)^{1.5} \tag{54}$$

$$C = 0.602 + 0.083 \frac{d_3 - z}{z} \tag{55}$$

Experimental efficiency (η_{Exp}, %) of the paddlewheel can be obtained as the ratio:

$$\eta_{Exp} = \frac{P_{hyd}}{P_{mech}} \tag{56}$$

7.2.3 Results

For each of the three weir height used in this experimental work, an average of 5 power supply positions in the paddlewheel motor were tested, and for each power supply position between 4-8 different flow values were tested by controlling the degree of opening of the inlet valve to the flume. This was repeated for the two shoe types described above and for the flat configuration. This gave a total of 274 experiments whose results are given in detail in Appendix II (Table 34, Table 35 and Table 36). In Figure 90, Figure 89 and Figure 91, mechanical and hydraulic power are presented for shoe 1, flat and shoe 2 configuration, respectively, divided by the three weir heights tested (200, 175 and 150 mm). To facilitate the presentation of results, they were

averaged in groups of three and the error was calculated and presented in the figure as the standard deviation of these three points.

The results obtained with the flat configuration (Figure 89) showed maximum head differences of 148, 132 and 117 mm at weir heights 200, 175 and 150 mm, respectively. The highest hydraulic power (10.2, 9.1 and 7.4 W) was obtained at head differences 96, 75 and 55 mm, which corresponded to mechanical power of 22.1, 14.5 and 10.6 W at the three weir heights studied. In this case, a bell-shaped curve was found for hydraulic power at intermediate head differences. Mechanical power, however, increased with head difference during the experiment.

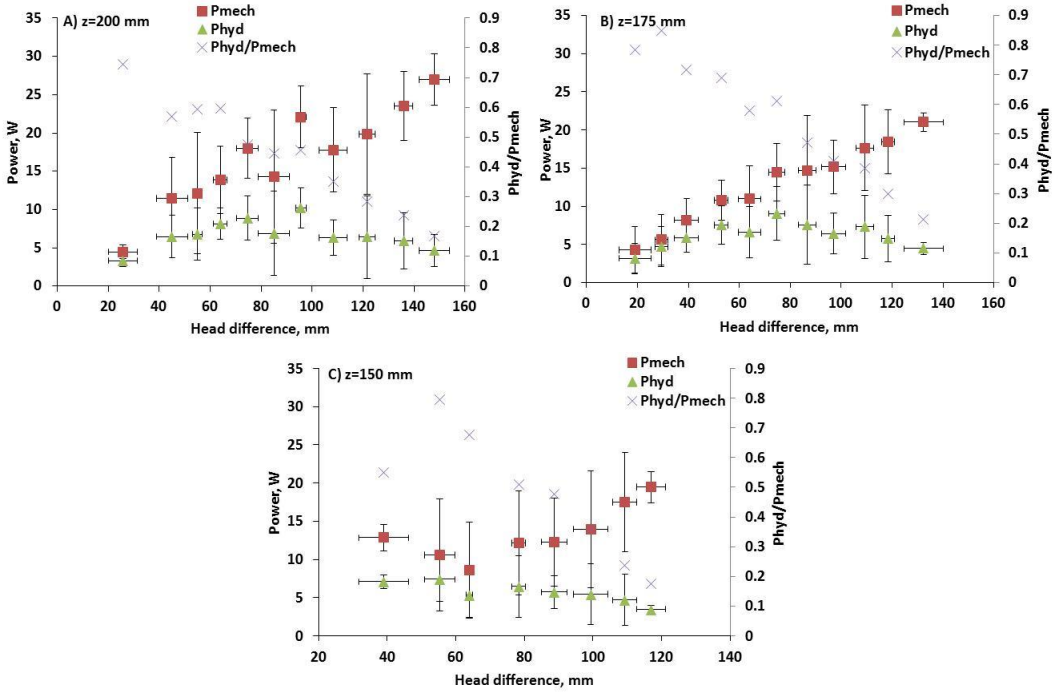

Figure 89.- Variation in mechanical power, hydraulic power and hydraulic efficiency (P_{hyd}/P_{mech}) with head difference using flat configuration at weir heights of: A) 200 mm, B) 175 mm and C) 150 mm

In the flat configuration, as can be seen for shoe 1 (Figure 90) and shoe 2 (Figure 91) the head differences were not major factors in the determination of hydraulic and mechanical power, since the variability of the results gave high standard deviations which produced overlapping error bars. At high head differences, however, it was observed that low hydraulic power and high mechanical power were obtained due to the back flow through the gaps between channel and paddlewheel. In this case, mechanical power in the wheel and hydraulic power in the channel

do not follow the same trend and, as a consequence, hydraulic efficiency is negatively affected. Highest efficiencies obtained at very low head difference were consequence of the similar values of hydraulic and mechanical power obtained, but the low hydraulic power achieved difficult the operation in raceways in terms of liquid velocity at this head difference.

With shoe 1 (Figure 90) a maximum head difference of 113 mm was obtained with the weir at 200 mm high, while 87 and 63 mm were obtained with weir at 175 and 150 mm high, respectively. Maximum mechanical power achieved was 13.3, 10.6 and 8.0 W at weir positions 200, 175 and 150 mm, while the maximum hydraulic power was 8.9, 8.0 and 3.8 W in these weir positions at head differences of 72, 58 and 46 mm. This maximum hydraulic power corresponded to a mechanical power of 13.3, 10.6 and 8.0 W. In all the case, the same behaviour was observed: low mechanical power, hydraulic power and hydraulic efficiency were obtained at low and high head differences, while the maximum peak in power and efficiency was achieved at an intermediate value of head difference of 73, 58 and 46 mm in the three weir positions.

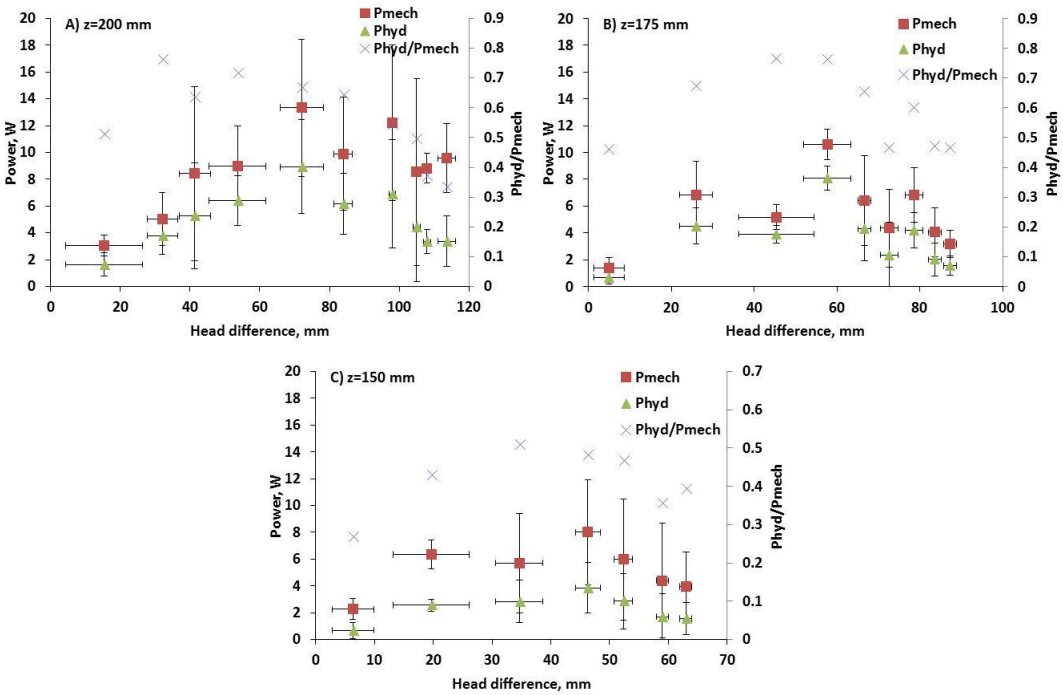

Figure 90.- Variation in mechanical power, hydraulic power and hydraulic efficiency (P_{hyd}/P_{mech}) with head difference using shoe 1 at weir heights of: A) 200 mm, B) 175 mm and C) 150 mm

Figure 91 shows the result obtained using the shoe 2 described in 7.2.2.2. Maximum head differences were 158, 151and 128 mm at weir height 200, 175 and 150 mm, respectively. In this case, hydraulic power followed the bell shape, with maximum values of 13.1, 11.5 and 9.4 W obtained at head differences 100, 72 and 76 mm, higher than the flat configuration showed in Figure 89. These hydraulic powers required a mechanical power of 20.0, 17.3 and 13.2 W, respectively. Shoe 2 configuration required a lower mechanical power to achieve higher hydraulic power compared to the flat configuration, so the water lift effect produced by the shoe and its benefit in hydraulic performance due to leakage reduction was evident. Compared to shoe 1 (Figure 90), the head difference with Shoe 2 is much higher even at low weir heights. Shoe 2 configuration, therefore, seems to work better than shoe 1 in the range of head differences studied.

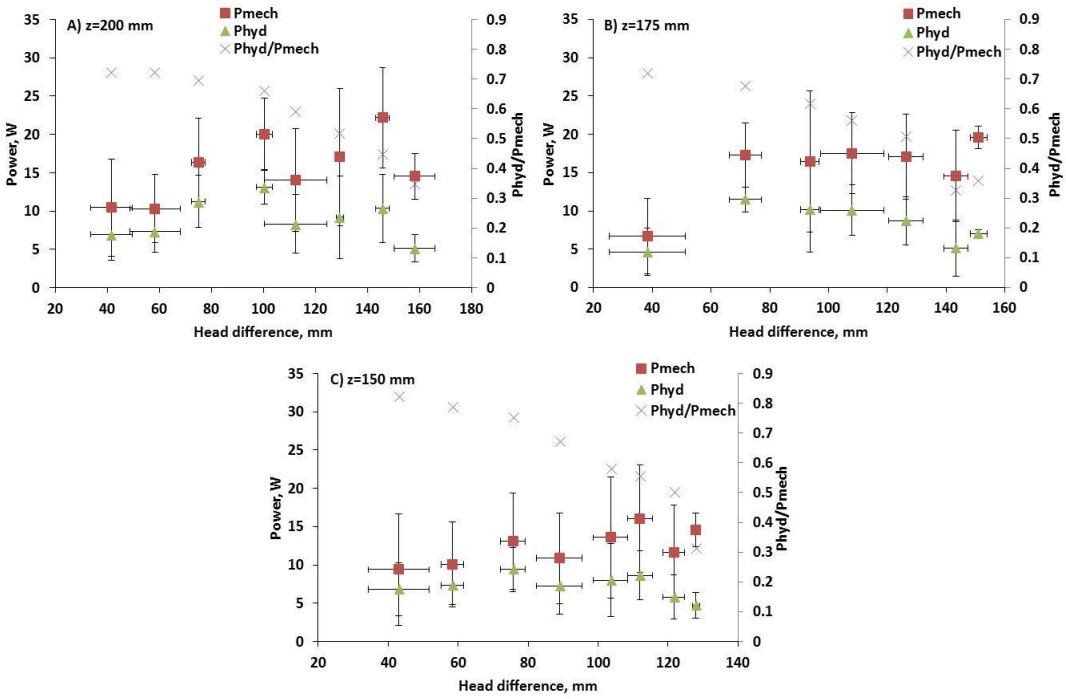

Figure 91.- Variation in mechanical power, hydraulic power and hydraulic efficiency (P_{hyd}/P_{mech}) with head difference using shoe 2 at weir heights of: A) 200 mm, B) 175 mm and C) 150 mm

The results explained are summarized in Table 32, where maximum P_{hyd} is presented for the three weir heights and paddlewheel configuration tested in the experimental work. Head difference, mechanical power and hydraulic efficiency at this maximum hydraulic power are also presented. Values for electric power obtained in the experimental work were very high and

unstable in comparison to mechanical and hydraulic power, as can be seen in Appendix II. This revealed the low energy efficiency of the motor-gearbox set used in these experiments.

Table 32.- Maximum P_{hyd} obtained for weir height 200, 175 and 150 mm with shoe 1, flat and shoe 2 configuration, with head difference, P_{mech} and hydraulic efficiency (P_{hyd}/P_{mech}) at this maximum P_{hyd}

	Shoe 1			Flat			Shoe 2		
z, mm	200	175	150	200	175	150	200	175	150
Maximum P_{hyd}, W	8.9	8.0	3.8	10.2	9.1	7.4	13.1	11.5	9.4
H, mm	72	58	46	96	75	55	100	72	76
P_{mech}	13.3	10.6	8.0	22.1	14.5	10.6	20.0	17.3	13.2
P_{hyd}/P_{mech}	0.67	0.76	0.48	0.46	0.47	0.79	0.66	0.68	0.75

7.2.4 Discussion

The shape of the shoe seems to determine the lifting water efficiency of the system in the range of weir heights tested. As seen in Figure 90, when using shoe 1 the reduction of weir height from 200 to 150 mm reduced the maximum head difference from 113 to 63 mm and maximum hydraulic power from 8.9 to 3.8 W, while with shoe 2 this reduction was from 158 to 128 mm and from 12.1 to 9.4 W. This difference could be explained taking into account that, although none of the shoes were optimized to lift water at the range of depth tested, the performance of shoe 1 (shape with the initial platform described in section 7.2.2.2) was lower than shoe 2 in the range of depth tested. Shoe 1 configuration, however, may be of interest in deeper channels.

The experimental efficiency can be compared with the theoretical efficiency if all the mechanical power in the system were effectively transformed into hydraulic energy. For this, the forces acting on the paddlewheel when one blade is in the vertical position are shown in Figure 92.

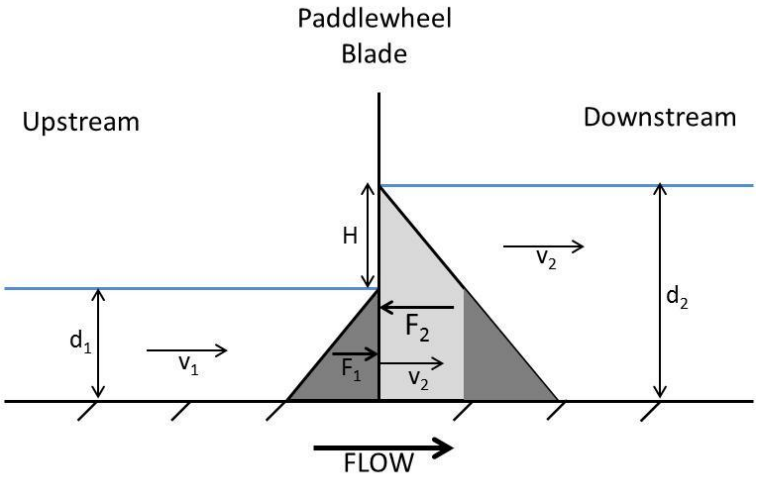

Figure 92.- Schematic of the forces acting in the paddlewheel when it had a blade in vertical position

Hydrostatic pressure is represented in the Figure on both sides of the blade. This pressure increases from zero at the water surface to a maximum at the bed channel. The hydrostatic pressure downstream is higher than upstream ($p_1<p_2$), as the grey area shows, due to the higher depth produced by water lifting downstream. As Eq(51) showed, hydrostatic pressure in both sides of the blade can be calculated as:

$$p_1 = \rho g d_1 \tag{57}$$

$$p_2 = \rho g d_2 \tag{58}$$

The force exerted by the hydrostatic pressure can be calculated as the product of the hydrostatic pressure times the area where this pressure is exerted. In this case, hydrostatic pressure is acting into the submerged blade area, and force in both sides of the blade (F_1 and F_2) can be calculated as Eq(59) and Eq(60), where W_b is the width of the blade (m).

$$F_1 = \rho g \frac{{d_1}^2}{2} W_b \quad (59)$$

$$F_2 = \rho g \frac{{d_2}^2}{2} W_b \quad (60)$$

The effective force that the blade had to overcome to produce movement (*F*) is the resultant of the hydrostatic forces acting in both sides of the blade (Eq(61)).

$$F = F_2 - F_1 = \rho g \frac{{d_2}^2 - {d_1}^2}{2} W_b \quad (61)$$

Assuming the velocity of the blade is v_1, the input power (P_{in}, *W*) necessary to move the wheel, which is the same as the minimum mechanical power to produce movement, is:

$$P_{in} = F v_1 = \rho g \frac{{d_2}^2 - {d_1}^2}{2} W_b v_1 \quad (62)$$

Theoretical efficiency ($\eta_{theoretical}$, %) can be calculated as the ratio between the hydrostatic power obtained from the head difference produced by water lifting in the paddlewheel (Eq(53)) and the power necessary to produce the rotation of the paddlewheel (62).

$$\eta_{theoretical} = \frac{P_{hyd}}{P_{in}} = \frac{2}{1 + \frac{d_2}{d_1}} \quad (63)$$

As Eq(63) shows, assuming no leakage losses theoretical efficiency is a function of the ratio d_2/d_1, and is independent of the blade and liquid velocity. In Figure 93 the experimental efficiency in the three paddlewheel configuration

tested is compared with theoretical efficiency. Experimental efficiencies were closer to theoretical when the shoe was in position, since the water lifting effect produced increased the hydraulic power and, therefore, increased the experimental efficiency. The experimental data for Shoe 1 showed quite high variability. This could be explained by the Shoe 1 shape which produced a very small head difference upstream/downstream at low water depths in the channel. This is confirmed in Figure 93A, where it can be seen that experimental efficiency was lower when the weir was at 150 mm than at higher weir heights. When shoe 2 was used (Figure 93C), however, experimental and theoretical efficiencies were quite similar, indicating that this shoe configuration is effective for water lifting in the range of depths tested. For example, at weir height 200 mm, when d_2/d_1 was 2.0 the efficiency of the system without shoe was 40 % and no significant differences were achieved with shoe 1 configuration. When shoe 2 was in place, however, this efficiency increased to 60 %, highlighting the importance of the design of the combined set paddlewheel + shoe for the specific characteristics of the raceway.

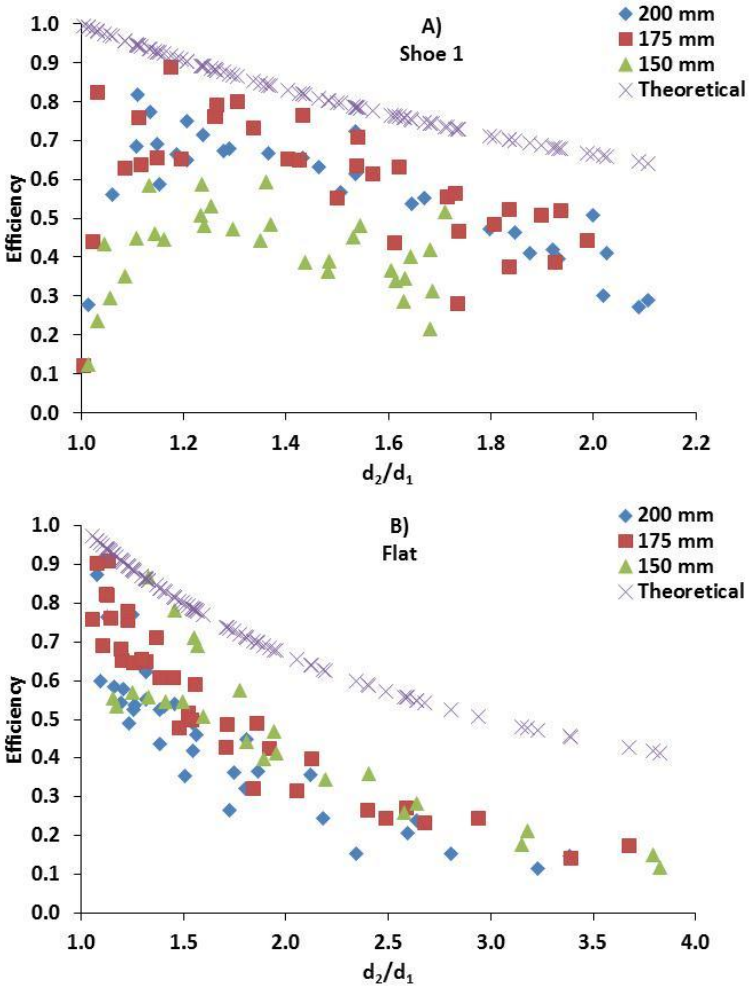

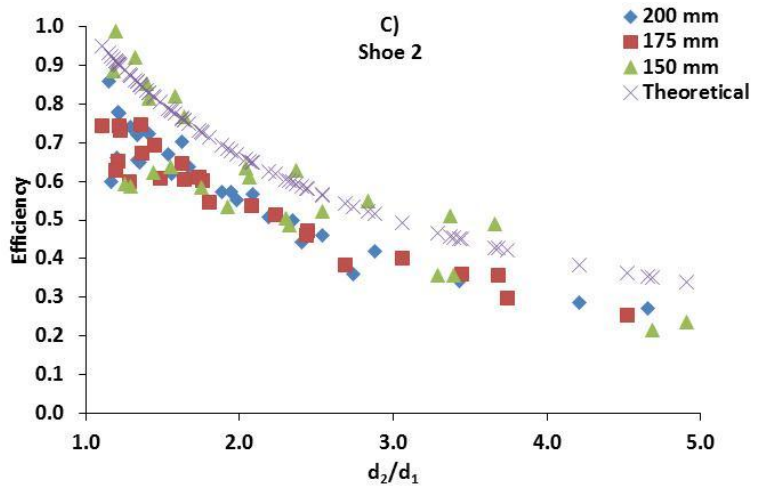

Figure 93.- Comparison between experimental efficiency at three weir height positions and theoretical efficiency with: A) Shoe 1; B) Flat, C) Shoe 2

7.3 Hydrostatic pressure wheel for water lifting in raceways at pilot scale

7.3.1 Objectives

To construct a modified paddlewheel and shoe system based on experience gained in the laboratory study and to install and test this in a pilot-scale raceway. To compare its performance and efficiency with that of an unmodified system without shoe.

7.3.2 Methodology

7.3.2.1 Raceway, paddlewheel and shoe

The HPW for water lifting was tested in the same pilot plant in Almeria (Spain) used in previous experiments. The facilities were as previously described in Chapter III, and the only difference was the construction of a new 12-blade paddlewheel made of marine plywood (Figure 94). The diameter of this new paddlewheel was maintained at 1.2 m and the number of blades was increased from 8 for the previous paddlewheel in order to reduce the distance between them and ensure that at least one blade will always be within the curved area of the shoe. In this way, backflow or leakage was minimized.

Figure 94.- Construction (left) and installation (right) of the new 12-blade paddlewheel

The shoe was designed to maintain the shape previously described for shallow depths in Figure 87B, taking into account that this shoe configuration gave the best performance in the experiments carried out previously in the flume (section 7.2.3). The shoe was made of plastic sheets 1 cm thick (Figure 95) and it was directly bolted to the walls of the raceway under the paddlewheel. Special attention was paid to allow the free paddlewheel rotation, i.e. without any friction with the shoe or walls which may affect the efficiency of the system. The use of the shoe as water lifting device was evaluated and compared to the flat configuration.

Figure 95.- Left: Shoe construction. Right: New 12 blades paddlewheel working with the shoe in position at the bed of the channel

7.3.2.2 Power calculations

The head difference was measured by section in the raceway. For this purpose, 8 damping cylinders were installed along the raceway in the positions shown in Figure 96.

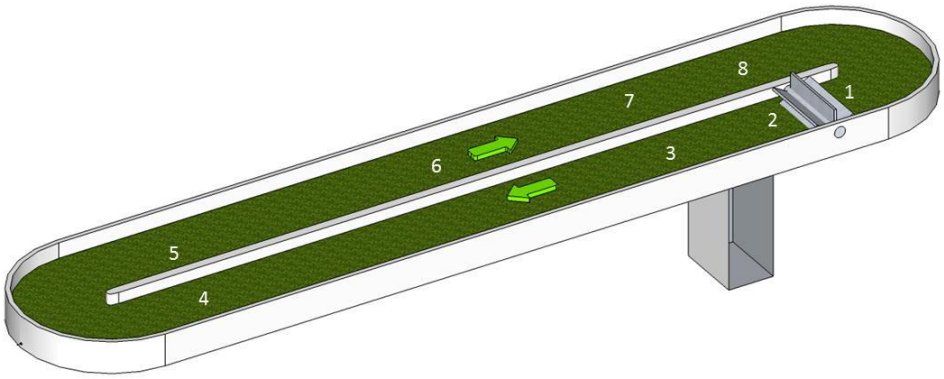

Figure 96.- Location of the damping cylinders in the raceway

In every experiment, the system was set up with the desired conditions and measurements of parameters were taken after the stabilization of the flow. The electrical current in the motor at this point was measured to calculate the electric power as in Eq(44). The paddlewheel rotation speed in rpm was calculated and the head difference in each section was determined by means of a picture of the damping cylinders (Figure 97, Figure 98).

Figure 97.- Use of damping cylinders for measurement of head difference. Left: Zero position with the paddlewheel stopped and water level the same in all the damping cylinders. Right: Head difference in one of the experiments with the

paddlewheel operating. In this case, it is possible to see the head differences between the damping cylinder measurements around the raceway

Figure 98.- Left: Experimental set-up during the experiment. Right: detail of the camera used for image data processing

Although the shoe was specially designed and constructed taking into account the characteristics of the raceway paddlewheel, its size and configuration of the raceway may not be suitable for an efficient circulation of liquid in the reactor. The main difference between the flume and the raceway is that in the flume the inflow and the head difference across the wheel can be adjusted by means of a water pump at the beginning of the flume and a weir at the end; while in the raceway, the flow is determined by the paddlewheel rotation speed and the head loss is produced by the reactor configuration itself. For this reason, a method to modify the head loss in the channel was introduced by means of obstruction blocks. Two different obstructions were used, consisting of concrete or tile blocks placed on the bed of the channel. In this way, it was possible to increase the head difference by different sections and to simulate a different raceway configuration which may be more suited to the paddlewheel and shoe provided; if head loss is increased in the channel, it could be compared with another configuration of the raceway that may fit better with the characteristics of the paddlewheel and the size of the shoe. Obstruction 1 consisted of 12 blocks located in the middle of the second channel, and obstruction 2 consisted of 29 blocks located randomly in the first channel (Figure 99).

Figure 99.- Obstruction blocks used during the experiments to increase the head difference in the raceway. Left: Obstruction 1; Right: Obstruction 2

The hydraulic power was calculated as in Eq(53) and a 126.6 mm high weir (Figure 100) was also installed in the raceway at the end of the first channel to allow calculation of the flow as previously shown in Eq(54) and Eq(55). An alternative method for flow measurement was used when no weir was present in the channel. It consisted in measurement of the time taken by a particle of approximately neutral buoyancy (an orange) travelling in the fluid to traverse a known distance.

Figure 100.- Weir installed in the raceway to calculate the flow

The experimental work in the raceway had an important drawback in comparison to the flume: it was not possible to install a load cell for measurement of the torque produced by the motor as a basis for calculation of the mechanical power. For this reason, an alternative was found in variant of the Prony Brake (Prony, G. 1821). Figure 101 shows the Prony Brake schematically and the final design in position in the raceway. It consists of a

spinning wheel attached to the shaft of the paddlewheel so that both wheels rotate at the same velocity when the motor is connected. There is also a static wheel which remains without rotation despite the friction belt that links it to the spinning wheel due to the action of the force weight (W) produced by a known mass attached to one end of the friction belt.

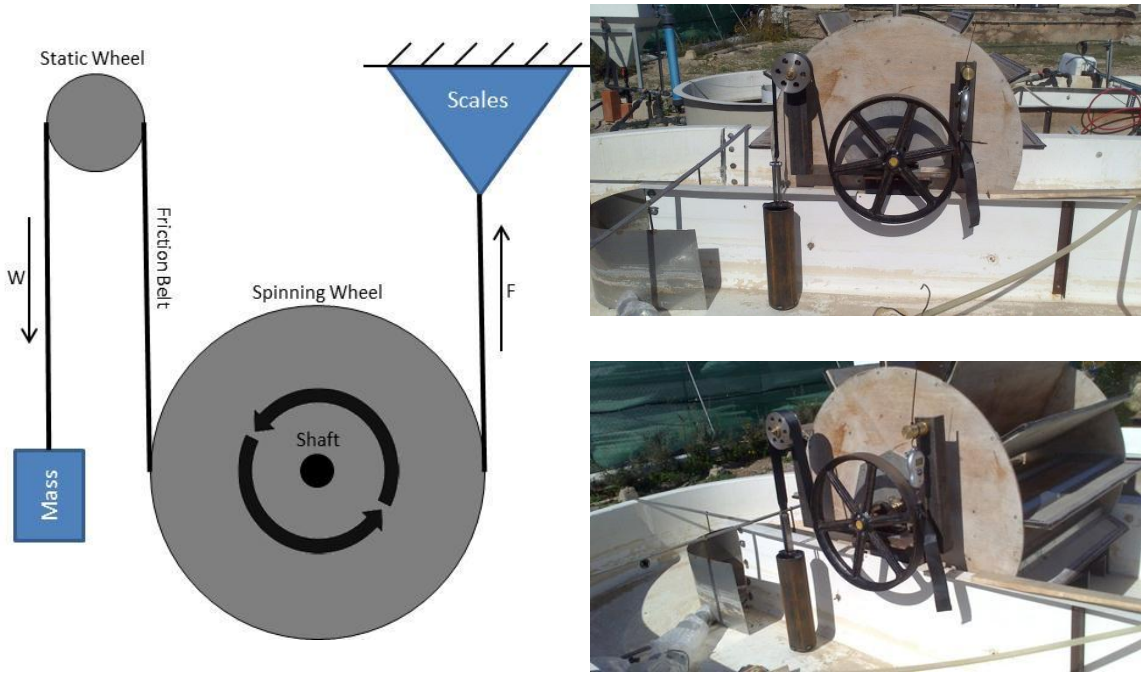

Figure 101.- Left: Schematic of the Prony Brake. Right: Prony Brake installed in the raceway

When the paddlewheel is not connected, the system and the forces involved in the Prony Brake are balanced and the scales in which the other end of the friction belt is attached are set at the zero position. When the paddlewheel is connected, the torque produced a force at the end of the spinning wheel that is transmitted upwards by the friction belt to the scales. Therefore, the reading in the scale will be the negative mass exercised by the rotation of the spinning wheel to compensate the deviation of the equilibrium produced by the rotation of the wheel. The force F (N), then, is calculated as the weight was calculated in Eq(47), indicating the negative value that the force is exerted upwards and the torque can be calculated as Eq(48) showed taking into account that now the force acting in the wheel is F (not weight) and that the radius of the spinning wheel is 0.235 m.

7.3.2.3 Experimental planning

First, the paddlewheel-Prony Brake system was calibrated to find the relation between mechanical and electric power in the system. For this, an increasing series of masses were attached at the end of the friction belt to make the wheel develop different values of torque. Between 7 and 23 kg, 7 different masses were tested and for each mass 7 velocities of paddlewheel rotation speed were evaluated to give a wide range of experimental data and relate them to the electrical power provided to the motor, in each case. In each experiment, the current was measured for calculation of the electric power (Eq(44)), as well as the rotational velocity of the paddlewheel for calculation of the mechanical power (Eq(45)).

Once this calibration was complete, a wide variety of conditions were tested in the raceway with the aim of obtaining a full understanding of the water lifting efficiency of the system. The conditions tested included: air bubbling in the sump to study its effect in the head difference of the system, shoe/flat configuration, changes in head loss due to obstruction configuration and the use of weir to increase the head loss and calculate the flow at two different working depths in the raceway. In each experiment, the velocity of the wheel was modify to give information on different liquid velocities from the lowest that produced water circulation up to the maximum possible in the system.

7.3.3 Results

7.3.3.1 Calibration of Prony Brake

The results of the calibration of the Paddlewheel-Prony Brake system showed a quadratic relation between mechanical and electric power as shown in Figure 102. Equation Eq(64) was therefore used for calibration.

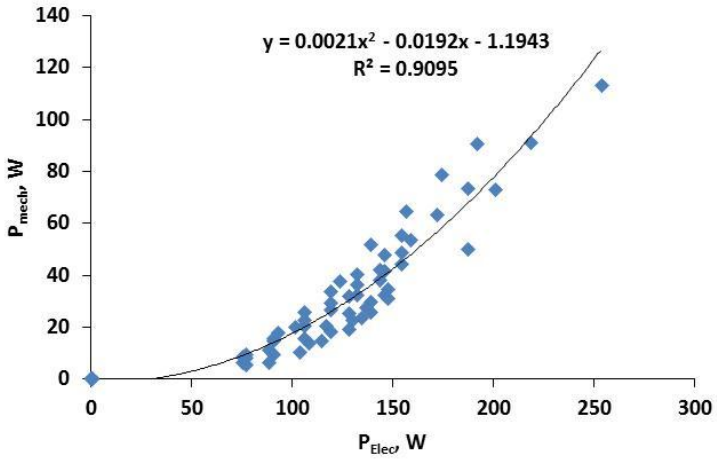

Figure 102.- Calibration of the Prony Brake

$$P_{mech} = 0.0021{P_{elec}}^2 - 0.0192P_{elec} - 1.1943 \quad (64)$$

7.3.3.2 Influence of gas bubbling in head loss

The raceway was operated without a shoe at motor frequencies from 5 to 35 s^{-1} (in 5 s^{-1} increments) without gas injection, and with a constant air flow of 150 L min^{-1}. Figure 103A shows the head difference in the sump section with and without air bubbling. Without air bubbling, the head difference was around 0 mm due to the short length of sump section. When air was bubbled, however, a negative head difference was recorded probably due to disturbances produced by the closeness of the measuring point where the damping cylinder was installed to the sump, where air bubbles caused a high turbulence. If the head difference is studied in the entire raceway before and after the paddlewheel (Figure 103B), the presence of air in the sump increased the head difference in the reactor.

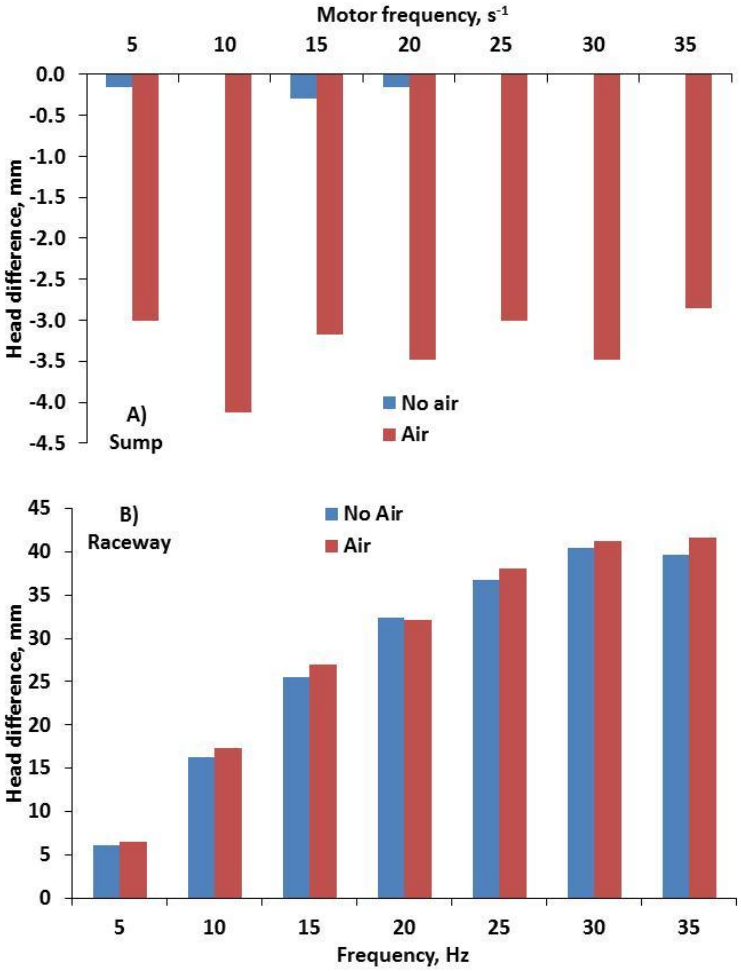

Figure 103.- Head difference with and without air bubbling at different motor frequencies in: A) sump section; B) the entire raceway

7.3.3.3 With/without shoe

The raceway was operated with and without a shoe at different motor frequencies from the minimum producing water motion until the maximum allowed without gas bubbling in the sump. The obstructions previously described in 7.3.2.2 were used to modify head loss in the channel.

Figure 104 shows the results of experiments carried out with and without shoe. Two different block obstructions described in 7.3.2.2 were used to modify the head loss in the channel. In all of the experiments, hydraulic power was slightly higher using obstruction 2 than using obstruction 1. When no shoe was used, the head difference achieved with obstruction 2 was higher than with obstruction 1; when the shoe was used, however, the head difference was higher with obstruction 1. Mechanical power were similar with both obstruction configurations in the range of head difference tested when no shoe

was used, but when the shoe was installed mechanical power increased a lot using obstruction 2 in comparison to obstruction 1.

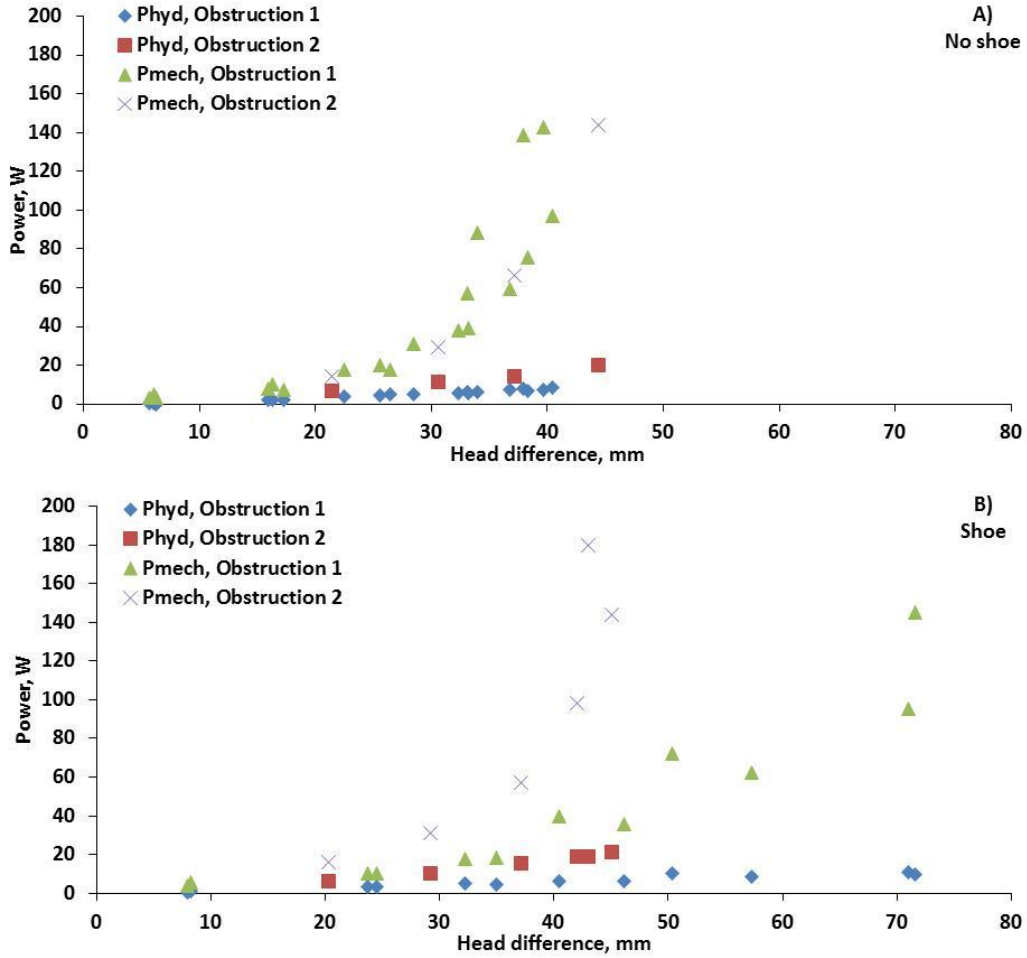

Figure 104.- Hydraulic and mechanical power in the paddlewheel for both obstruction types and: A) without shoe; B) with shoe. The information contained in this graph is presented in Table 37 and Table 38 in the Appendix II

7.3.3.4 Influence of head loss in power

Obstruction 1 was set up in the raceway without the shoe and head loss was decreased progressively while maintaining the paddlewheel rotation speed. Blocks from obstruction 1 were removed to modify the head loss in the channel. As Figure 105 and Table 33 shows, when head loss was reduced by removal of blocks from the obstruction, the head difference across the paddlewheel was also reduced. Mechanical and electric power increased exponentially from 8.48 to 72.93 W and from 72.60 to 192.50 W, respectively, when the head difference increased from 15.14 to 33.65 mm. Variations in

hydraulic power, however, were very small and remained between 4.42 and 6.25 W in the range of head differences tested.

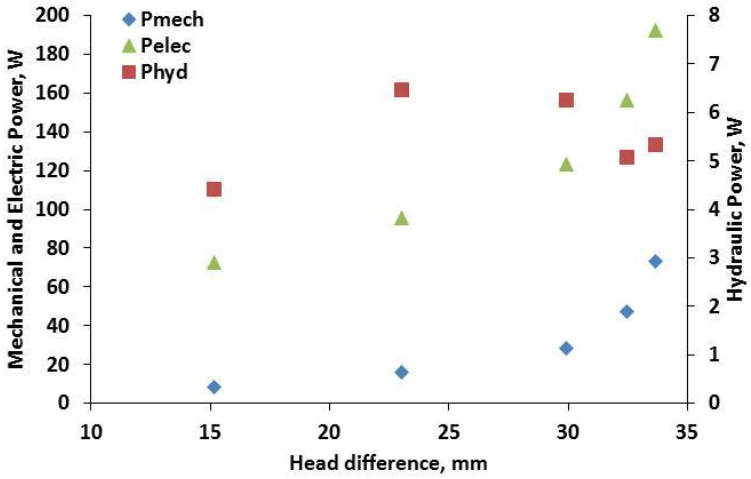

Figure 105.- Mechanical, hydraulic and electric power at different head differences obtained modifying the head loss in the channel

Table 33.- Experimental data (d_1, d_2, H, P_{mech}, P_{hyd}, P_{elec}) obtained during the experiment at variable head loss in the channel

Blocks	d_1, mm	d_2, mm	H, mm	P_{mech}, W	P_{hyd}, W	P_{elec}, W
Full Obstruction 1	127.5	161.1	33.7	72.9	5.3	192.5
2 Blocks less	128.2	160.7	32.5	47.0	5.1	156.2
3 Blocks less	129.8	159.7	29.9	28.3	6.3	123.2
5 Blocks less	135.9	158.9	23.0	16.2	6.5	95.7
No obstruction	142.2	157.3	15.1	8.5	4.4	72.6

7.3.3.5 Experiments with weir: with and without shoe

The weir described in section 7.3.2.2 was installed downstream at the end of the first channel, in which obstruction 2 was located. Experiments were carried out with and without the shoe, and at working depths 12 and 15 cm to ensure that the weir was not submerged.

Figure 106 shows the results at a static water depth of 12 cm without and with the shoe (A and B, respectively). When mechanical power was around 100 W the maximum head difference of around 43 mm was achieved without the shoe. Since mechanical and electric power increased exponentially with head difference, further increases in electric power increased mechanical power but did not produce a higher head difference across the paddlewheel. With the

shoe the situation is different: the maximum head difference achieved was 95 mm (confirming the water lifting produced by shoe) and electric, mechanical and hydraulic power were around 8.5, 55 and 179 W for this head difference.

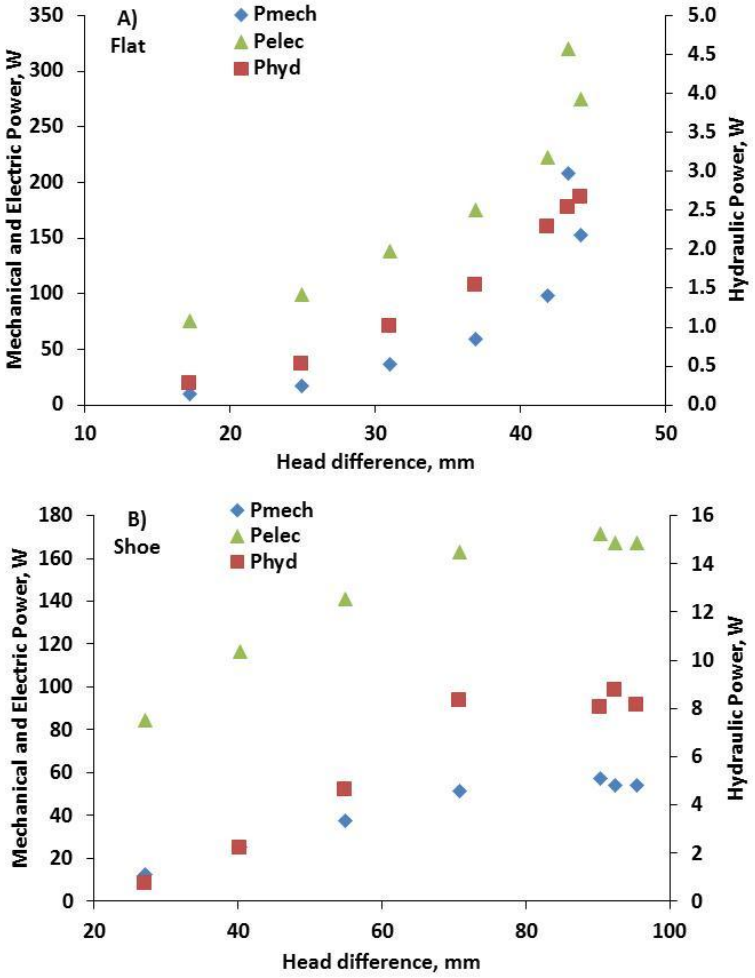

Figure 106.- Mechanical, hydraulic and electric power at different head difference obtained at a working depth of 12 cm: A) without shoe, B) with shoe

Figure 107 shows the results of the experiments carried out at 15 cm. In this case, the maximum head differences achieved were 30 and 54 mm in flat and shoe configurations. These values were lower than at 12 cm depth, and this was the point at which further increases in electric power consumption in the motor increased the mechanical power, but had no influence in head difference and, therefore, in hydraulic power.

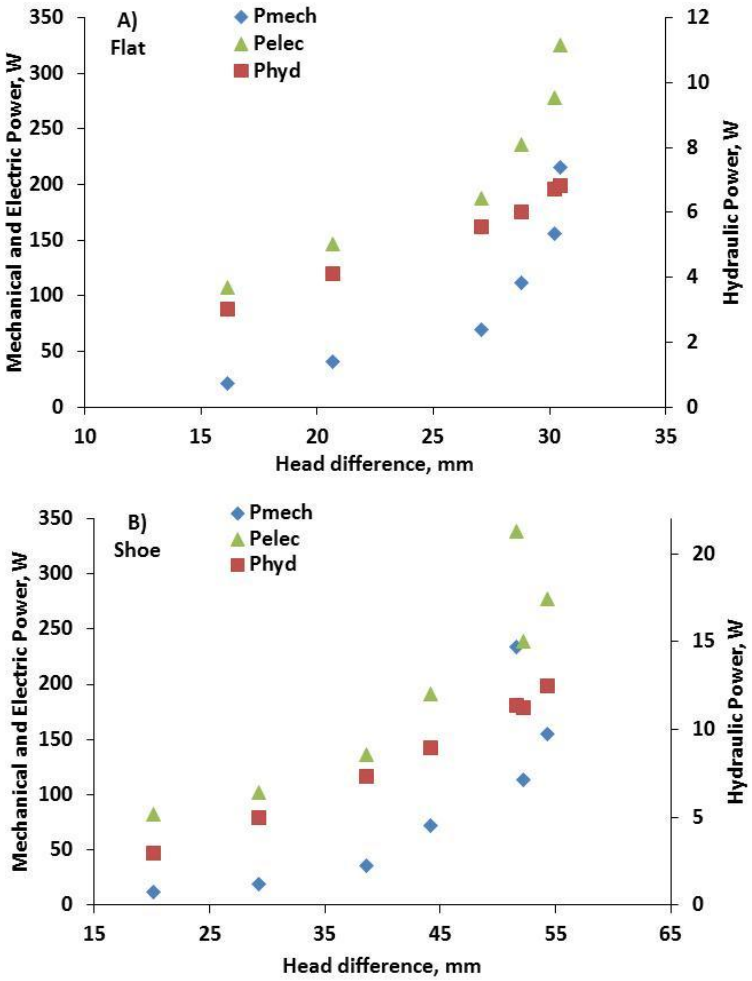

Figure 107.- Variation is mechanical, hydraulic and electric power with head difference at a working depth of 15 cm: a) without shoe, b) with shoe

As can be seen in Figure 107, there is a clear energy benefit from using the shoe. For example, in the flat configuration the electric power requirement for the motor was 250 W (giving a mechanical power of 170 W) to obtain a head difference in the paddlewheel of 30 mm. When the shoe was used, the same head difference was achieved with an electric power of only 100 W (mechanical power of 20 W). This is to say that shoe allowed the same head difference to be achieved with only 40 % of the energy required in the flat configuration. The full results of these experiments can be seen in Table 39 and Table 40 in Appendix II.

7.3.4 Discussion

The bubbling of air in the sump increased the head loss in the raceway overall, although due to the short length of this section in comparison to the

overall reactor, this difference was not significant and it can be concluded that bubbling of gas in the sump at gas flow rates of under 150 L min^{-1} had a limited influence on the hydraulic efficiency of the raceway.

Figure 108A shows the results for efficiency versus the ratio of upstream to downstream depth for a static water depth of 15 cm. A number of conclusions can be drawn. A figure of 10-15 % efficiency for conventional paddlewheels is often quoted in the literature and used as a basis for energy balance calculations, frequently as an engineering 'rule of thumb' without any supporting references. The results for the without-shoe case show that this is not a bad estimate at small head differences; but this value tails off rapidly at larger depth ratios (equivalent to high head differences, and thus to longer raceways).

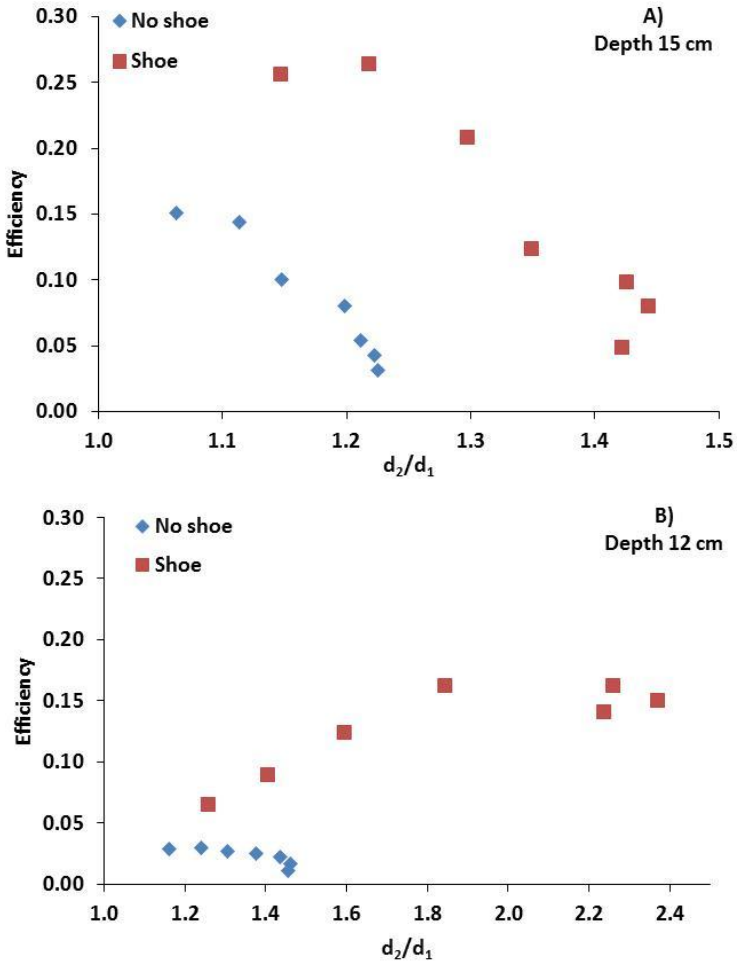

Figure 108.- Experimental hydraulic efficiency obtained with and without shoe at different d_2/d_1 ratio when: A) depth was 15 cm; B) depth was 12 cm

Comparison of the results with and without the shoe shows efficiency is considerably higher with the shoe. Moreover, the ratio between efficiencies with and without the shoe is larger for higher depth ratios (= longer raceways). For example at d_2/d_1 = 1.15 the ratio of efficiencies is approximately 26 %:10 % = 2.5:1, while at d_2/d_1 = 1.22 it is 26 %:4 % = 6:1. This indicates that considerable energy savings may be possible by the addition of a shoe in real-scale commercial installations. Results for static water depth of 12 cm (Figure 108B) also appeared to show an increase in efficiency but the values found were suspect, possibly because the water depth was so low that the HPW could not function correctly in this mode, as demonstrated by the very low upstream depths (Appendix II, Table 39): these low values also made measurement difficult and another technique may needs to be adopted or the work may need to be carried out under laboratory conditions.

Different head losses produced by block obstruction configurations seems to influence the hydraulic efficiency when no shoe was used, meanwhile with the shoe in position the efficiencies were similar in the range of head differences tested (Figure 109). In any case, the use of shoe did not increase the efficiency of the system during these tests. This could be explained due to lack of accuracy in the method used for to measure the flow when no weir was used, based on visual measurement of velocity of floating particles during the experiments.

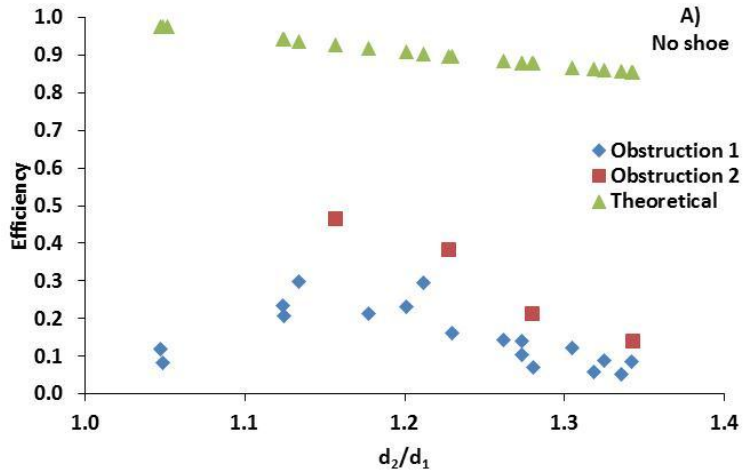

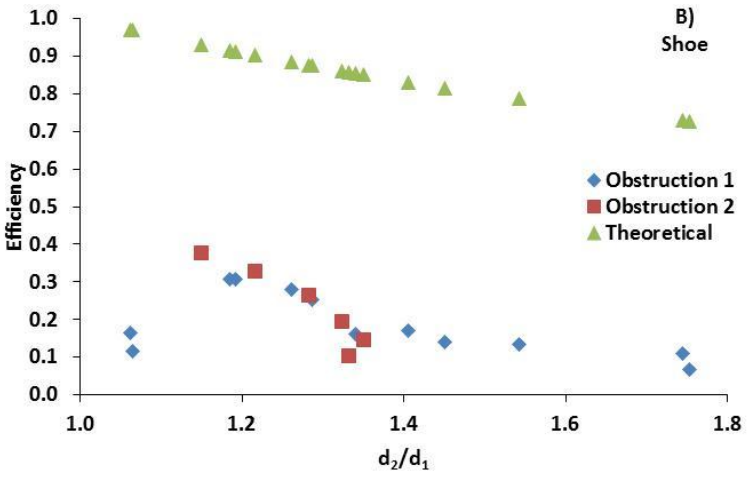

Figure 109.- Experimental hydraulic efficiency obtained using obstruction 1 and obstruction 2 with: A) flat configuration, B) shoe configuration. Theoretical efficiency is also shown

The experimental work carried out had a number of limitations, some of which were related to the operating range of the facilities used and the experimental conditions selected: it must be remembered that the paddlewheel design and shoe size were not optimized for the system before use, but instead the system was operated under a variety of conditions to try and identify effective operating points. There was sometimes insufficient water in the system to 'feed' the wheel, especially when operating at low depths. The use of near-neutral buoyancy objects (oranges) to estimate flow velocities when no weir was in place is a common technique in hydrology and river engineering, but led to quite wide variations in estimated values for velocity in this case and thus to unreliable data points in some cases. The calculation of torque using the Prony Brake added another potential source of inaccuracy due to the fluctuations in the scale reading produced by unbalanced paddlewheels, vibrations, frictions, etc.

The introduction of obstacles in the channel to increase the head loss and decouple it from the raceway length was a successful and useful approach to simulating longer raceways, and could be adopted in future work to test improvements in efficiency of paddlewheels and other devices for raceway circulation. Although the use of the blocks and their empirical distribution along the raceway was an ad hoc decision to obtain experimental data, there may be scope to use similar devices to increase the turbulence in the channels

and, therefore, to enhance productivity by improving mixing. In this case, the design of these obstacles needs to be optimized to improve mixing with the lowest head loss possible, since the success of this technology for algal growth is highly dependent on the final energy balance. Therefore, a balance must be achieved between the loss of energy produced by friction with the obstacles and the potential benefits in productivity that the improvement of mixing may offer. The use of damping cylinders was an adequate solution for depth measuring in the raceway, since they stabilized the variations produced by waves in the raceway. If long-term testing is planned, however, an automated data analysis rather than visual inspection of images could help to improve the accuracy of the obtained results.

The introduction of the shoe clearly improved the paddlewheel efficiency, but the whole system is quite complex and correct sizing of the equipment is likely to depend on a range of factors including raceway size, depth, etc. The current work demonstrated that significant improvements were possible but was only able to test a limited range of factors (e.g. 12-blade wheel, one shoe size etc). It is therefore recommended that further testing across a matrix of conditions should be carried out in a more controlled environment such as a laboratory flume, where a wider range of parameters can be controlled or measured with greater precision. This would allow design guidelines to be developed which would then allow these improvements to be introduced systematically into full-scale plant at the design stage or through retro-fitting.

7.4 Summary conclusions for Chapter VII

In conclusion, the work in this chapter has shown the following:

- The head differences in the flume were not major factors affecting the hydraulic and mechanical power and, therefore, the efficiency of the system HPW + shoe. The instrument used and the methodology must be re-evaluated to obtain more reliable results.
- Shoe 2 was the device which gave better efficiencies in the flume. An increase in experimental efficiency from 0.46-0.47 to 0.66-0.68 could potentially be achieved by using shoe 2 in comparison to flat configuration.

- The power consumption in a raceway equipped with an appropriately-sized shoe could potentially produce the same head difference using only between 40-50 % of energy required in a flat configuration.
- The adequate design of the paddlewheel-shoe set for a particular raceway configuration, taking into account the physical characteristics of the raceway and the desired operating conditions, is essential for the success of this technology.

Chapter VIII

8. Overall conclusions

In the raceway used in the experimental work the specific power consumption was studied in some detail, since the energy balance determines the success of using this technology. Reducing energy inputs and maximizing biomass productivity are the keys to ensure the profitability of the use of raceways for microalgae cultivation.

Several conditions affected the power consumption, with the first studied being the liquid depth in the reactor. It is known that the paddlewheel produces a lifting effect which produces a head difference between upstream and downstream of the wheel. The efficiency of this lifting effect determines, ultimately, the efficiency of the paddlewheel which also depends on the depth of liquid in the raceway. If depth is higher than optimum, the paddlewheel needs more energy to move the blades and the effect of flow back in the gaps between paddlewheel and channel is accentuated. If the depth is lower than a minimum value, the paddlewheel 'overworks', requiring more energy than necessary to lift a small amount of liquid. In both cases, the ratio of energy used for the rotation of the wheel per unit of volume of liquid contained is below the optimal value. In the raceway, the lowest specific power consumption was at a depth of 20 cm, the overall specific power consumption at this depth being between 1.5-8.4 W m^{-3} depending on forward velocity, head loss in bends and, in particular, the presence of the sump baffle. Higher power consumptions at lower depths were probably due to paddlewheel design and could potentially be improved. A water depth of 20 cm is compatible with reported values used to achieve high biomass productivities in raceways, which must also be considered when selecting the depth of the culture, in order to allow adequate light penetration. For this reason, 20 cm was considered as the working depth in the experiments described in the thesis.

The design of the bend is another parameter to be taken into account in the design of raceways. It has been reported that the addition of successive semi-circular baffles in the bends reduces dead zones (which act as energy sinks) and improves energy efficiency. The relative importance of adding baffles, however, has not been studied before experimentally in a pilot scale raceway. For this reason, four bend configurations were used to measure the

benefit produced by addition of baffles: the bend without baffle, bend + 1 baffle, bend + 2 baffles and bend + 3 baffles, dividing the bend into four sections of the same width. The results revealed that selection of the best number of bends is related to the desired liquid velocity. If a liquid velocity of around 0.2 m s^{-1} is set in the raceway, the one bend configuration (the baffle which divided the bend at ¼ of the total radio from the central raceway wall) was the best option in terms of power consumption, with the benefit produced by addition of a further one or two bends being negligible. If one baffle is compared to no baffle in the bend, a significant reduction in power consumption was obtained and the achieved velocity was higher, requiring less energy for water motion. The velocity of 0.20 m s^{-1} was chosen because this is a usual value widely reported for microalgae cultivation in raceways. If it is desired to work at velocities higher than 0.25 m s^{-1}, the use of more bends deflectors can be considered, although this velocity exceeds typical values for raceway cultures, and a higher net energy input is required as velocity increases. In any case, the study of the bend revealed that this section produced major head losses in the raceway, so the number of bends must be minimized in order to improve the energy performance. Therefore, the current design with two bends and one bend-baffle is recommended, rather than other designs with more channels and, consequently, more bends to join the channels.

Light penetration in dense cultures is limited, and in these cases mixing in the raceway is essential. Radial mixing allow cells to interchange their position in the culture from the bottom of the channel where a dark/low productivity zone exists (no light available for photosynthesis) to the surface where there is light available for algae growth. If this interchange is achieved, the productivity of the culture could potentially be optimised. It is important to remark that there is also a thin layer at the surface with low productivity due to photoinhibition, so the width of the productive zone in the raceway is limited, again highlighting the importance of adequate mixing. In the raceway, mixing occurred mainly in the paddlewheel, sump and bends, and was negligible in straight channel sections in comparison with the other parts of the reactor. Because straight sections occupy the largest volume (around 93 % of the total volume), however, the overall flow regime that best describes the behaviour of the reactor was plug flow. This means that the axial and radial interchange of

particles in the raceway is limited, and microalgae cells that are at the bottom remain in this position along the path travelled in the reactor, negatively affecting the biomass productivity.

Calculation of dispersion coefficients indicated that axial mixing was similar to that in closed photobioreactors whereas vertical mixing was very poor. The development of new high-mixing raceway reactors will have to focus on the improvement of channel design, where the highly streamlined flow regime prevents the most efficient use of solar energy by microalgae. For this purpose, special devices could be designed to be inserted in straight stretches in order to improve mixing, but special attention must be paid to the friction produced, the increase in head loss and, therefore, the potential rise in power consumption. In any case, the methodologies applied here were shown to be very useful in determining the fluid dynamics of a raceway photobioreactor.

The insertion of a sump baffle with the aim of enhancing mass transfer in the sump by increasing the contact time between liquid and gas phases gave some relevant information. Firstly its effect on mixing was determined, and it was observed that it created an organization of flow effect in the sump and round the whole reactor. This means that the normal behaviour of the sump which is assimilated to a perfectly mixed bubble column was modified by the baffle, creating an ordinated distribution typical of plug flows in tubes. As consequence, the sump baffle increased the raceway mixing time by 3 hours due to the reduction of the velocity but also by changing the flow pattern in the whole raceway.

The use of sump baffle also greatly increased the power consumption, which was around 2 times higher depending on the liquid velocity. This specific power consumption was higher than the acceptable self-uptake demand of the system, so it is expected that under these conditions the overall energy balance between energy spent in the system and energy obtained from the microalgae biomass would be negative.

The improvement in mass transfer efficiency with sump baffle was limited, with no high improvement in CO_2 absorption efficiency observed. Thus, the hypothetical improvement on mass transfer was insufficient to counteract the adverse effects produced by baffle previously described. For this reason, the use of sump baffle was not recommended unless its

hydrodynamic characteristics can be significantly improved. The results presented were obtained using a specific sump baffle in a raceway reactor with a particular configuration. Therefore, there is scope for optimization of the baffle design, which must improve the mass transfer capacity of the system without increasing the head loss above the feasible limit. The development of new systems to improve mixing and mass transfer is possible, but power consumption is, again, the limiting factor.

Global warming due to GHG emissions is a major issue of our time, and although the potential damage produced by a molecule CO_2 is lower in comparison to other GHG gases, this gas is the most emitted in terms of net amount. Therefore, technologies to promote efficient CO_2 uptake are of potential value. The use of flue gas (~10 % CO_2) as carbon source in microalgae cultures has a double benefit: on one hand it is a free source of CO_2 which is produced in many industries an whose management could potentially become a problem for them and, on the other hand, its use is environmental friendly since every gram of microalgal biomass produced can potentially reduce the demand for fossil fuel sources. In this work it was demonstrated that supply of flue gas could successfully cover the CO_2 requirements of the raceway with only 4% loss via the sump without a baffle. After optimisation, the 100 m^2 raceway required a gas flow rate of 100 L min^{-1} (L/G=27), and this could be effectively provided on demand through controlling the pH at ~8. Algal productivity was 17 g m^{-2} day^{-1} and 66% of the inlet carbon was recovered in the biomass, with most of the lost carbon leaving the raceway as dissolved inorganic carbon in the harvest stream. Only 6% of carbon was lost from the raceway channels by outgassing. The loss of carbon and other nutrients in the harvesting of microalgae when biomass is separated from the medium can be reduced by nutrient recycling, although special attention must be paid to the possibility of the accumulation of salts or recalcitrant substances.

The use of flue gas in microalgae active cultures in comparison to pure CO_2 enhanced productivity by decreasing the concentration of dissolved oxygen peaks at midday in highly productive cultures maintained during months. Moreover, the use of flue gas did not cause any obvious problems in the culture derived from composition of the flue gas itself. For these reasons, flue gas was recommended as the best alternative for carbonation in low cost and highly efficient microalgae cultures.

Oxygen mass transfer occurred primarily in the paddlewheel and sump, which together accounted for ~75% of total transfer. The mass transfer was higher in these zones due to the higher mixing between gas and liquid, which favoured gas/liquid contact and, therefore, increased mass transfer coefficients. Improving mixing could potentially facilitate oxygen desorption in other sections of the raceway as demonstrated in the fact that mass transfer coefficients in all raceway sections increased with liquid velocity. Algal cultivation led to oxygen supersaturation and reduced productivity, especially when using pure CO_2 rather than flue gas. Simulations showed that reducing dissolved oxygen concentrations by improving mass transfer rates should increase the net potential energy yield. Oxygen removal is likely to be a more critical design criterion than carbon supply, and it may be necessary to maintain mass transfer by bubbling even when no carbon is required. The flow of gas in the sump was directly related to mass transfer capacity for removing oxygen from the raceway, although when using gas for dissolved oxygen desorption the risk of CO_2 stripping in cultures with high concentration of bicarbonates must be evaluated.

The improvement of mass transfer, mainly for dissolved oxygen desorption, is an important issue in raceway reactors. It was shown that one sump was enough to provide carbon to the microalgal cultures, due to the high CO_2 mass transfer efficiency achieved. The use of one sump, however, was not enough to reduce dissolved oxygen peaks under the non-inhibition values. This is especially important during spring-summer seasons, when the higher irradiation time and better climate conditions favour photosynthesis. Thus, dissolved oxygen desorption must be necessarily improved if it is desired to maintain an active culture for long periods of time. For this, new efficient-diffusers or sumps may be developed to improve mass transfer.

In the study of the oxygen transfer phenomena, it was shown that the dynamic method successfully determined diffuser efficiency. The selection of the diffuser had a high influence not only on the mass transfer efficiency of the sump, but also on power consumption. Among the studied diffusers, membrane plate was the best option due to the small size of the bubbles generated and the low pressure drop produced when gas is bubbled. As a result of these characteristics, mass transfer is enhanced and power consumption reduced. The identification and development of new diffusers

and their configuration inside the reactor can potentially increase the mass transfer of the sump.

The possibility of oxygen desorption by air bubbling when there is no CO_2 demand in the system was studied but, although maximum peaks were reduced, there was insufficient desorption capacity to reduce oxygen accumulation to acceptable values. The eventual stripping of CO_2 produced when a gas poor in CO_2 is bubbled into a liquid with high bicarbonate concentration was not studied, however,. Under these conditions, not only oxygen is eliminated from the culture broth, but CO_2 can also be removed. In the studied system, most of the carbon losses were through the culture medium in the harvested culture but if gas for oxygen desorption is used the carbon balance may change and CO_2 stripping, which is negligible in the tested conditions, could potentially become a problem.

In any case, the studied sump was identified as a feasible option to enhance mass transfer in raceways due to the high CO_2 absorption rates achieved, although the oxygen desorption capacity was limited. Consideration of dissolved oxygen desorption is, therefore, essential in the planning and design of efficient industrial raceways. This includes new configurations for gas exchange or more than one device, distributed throughout the reactor.

Although experimental efficiencies obtained with the HPW were very low in comparison to theoretical efficiencies, the improvement achieved with the use of the shoe allows some optimism about the future of this technology. In this respect, the final efficiency seems to be influenced by the head losses in the raceway, so the design of a paddlewheel-shoe set for a particular raceway configuration seems to be essential for the success of this technology. Although the shoe used in this work was not optimized for the raceway size and characteristics, it was useful to study its behaviour under real flow conditions. The power consumption in a raceway equipped with a shoe can potentially produce the same head as in a flat configuration using only 40-50 % of energy. Therefore, now it has been shown that the system can operate effectively and that there is scope for improvement, this could be a good starting point for future work based on this technology.

The energy balance of the system could potentially be improved by reducing the velocity of liquid circulation at night, when there is no available

light for photosynthesis and, therefore, mixing is not such an important issue. In this sense, gas bubbling at night is not necessary and special devices can be designed to cover the sump and eliminate the eventual head loss that it may produce (mainly when a sump baffle is used). The use of alternatives such as solar panels or wind turbines, in zones where climate conditions allow taking advantage of renewable energies, may be suitable to reduce external energy dependency and improve the final energy balance. This also highlights the fact that microalgal culture is an interdisciplinary technology that feeds on many branches of knowledge: physics, mechanics, biology, hydraulics, chemistry...

8.1 Further work

The design of the raceway was intended to allow testing of a wide range of operating conditions and parameters, rather than being optimised to reduce head losses and power consumption, to favour mixing or to enhance mass transfer. For this reason, there is scope to improve its design, as identified in the following suggestions for further work:

- To go to larger scale, studying the possibility of modify the aspect ratio (length to width).
- The use of further baffles in the bends may need to be re-evaluated in wider channels, since the presence of dead zones may increase. This could be done by modelling, using the data obtained in the current thesis for model validation.
- To evaluate the possibility of a multiple sump design in order to favour gas exchange, mainly oxygen desorption.
- To improve the hydrodynamic design of the sump baffle to reduce head loss and increase mass transfer. CFD simulations may be useful in this stage.
- To investigate the effects of decreasing liquid velocity at night, when mixing is not important.
- To design special mechanisms to cover the sumps when they are not in use in order to eliminate eventual head losses produced mainly if baffle sumps are used.
- To design and test devices to be inserted along the channels able to increase mixing and whose configuration does not increase

head loss considerably; and to investigate the effects of this on algal biomass productivity and overall energy balance.

- To test at laboratory scale different HPW-Shoe configurations in order to have data enough for the design of this device in raceways at pilot scale.
- To extend the work developed in this thesis by evaluating the downstream alternatives currently available for microalgae culture harvesting and processing.

Appendices

Appendix I

Matlab code for Bodenstein number calculation (Automation, Robotics and Mechatronics Group of the University of Almeria, ARM)

```
clear

%%%%%%%%%%%%%%%%%%%%%%%%%%%%%%%%%%%%%%%%%%%%%%%%%%%%%%%%%%%%%%%%%%%%%%%%%%%%%%%
%%%
%   PRUEBA CON CURVAS REALES                                    %
%   AJUSTE DE MODELO DE DISPERSION                              %
%%%%%%%%%%%%%%%%%%%%%%%%%%%%%%%%%%%%%%%%%%%%%%%%%%%%%%%%%%%%%%%%%%%%%%%%%%%%%%%
%%%


load ensayos.txt
fichero=ensayos;
tiem=fichero(:,1);      % tiempo en segundos
entrada=fichero(:,2);
salida=fichero(:,3);
plot(tiem,entrada,tiem,salida)
pause


N=length(salida);
count=0;
cinf=mean(salida(round(4/5*N):N));
c0=mean(salida(1:20));
cinfe=mean(entrada(round(4/5*N):N));
c0e=mean(entrada(1:20));

% Normalización de valores
salida=(salida-c0)/(cinf-c0);
entrada=(entrada-c0e)/(cinfe-c0e);
plot(tiem,entrada,tiem,salida)
Kest=trapz(salida)/trapz(entrada);
pause

%estimación del tiempo de retardo
maxentrada=0;
for k=1:length(entrada)
    if entrada(k)>maxentrada
        maxentrada=entrada(k);
        tmaxentrada=tiem(k);
    end
end
maxsalida=0;
for k=1:length(salida)
    if salida(k)>maxsalida
        maxsalida=salida(k);
        tmaxsalida=tiem(k);
    end
end
%estimación del tiempo de ciclo
minentrada=maxentrada;
for k=tmaxentrada:2*tmaxentrada
    if entrada(k)<minentrada
```

```
        minentrada=entrada(k);
        tminentrada=tiem(k);
    end
end
maxentrada2=0;
for k=tminentrada:length(entrada)
    if entrada(k)>maxentrada2
        maxentrada2=entrada(k);
        tmaxentrada2=tiem(k);
    end
end
k
N
tmaxentrada
tmaxsalida
tminentrada
tmaxentrada2
tiemporetardo=tmaxsalida-tmaxentrada
tiempociclo=tmaxentrada2-tmaxentrada
tr=tiemporetardo;
pause

% periodo de muestreo
dt=1;

% modelo de dispersión x=1:1:infinito
xfin=1;

% vector de frecuencias (en radianes por segundo) para análisis de
Fourier
count=0;
f=zeros(N,1);
for n=0:1:(N-1)
    count=count+1;
    f(count)=2*pi*n/(N*dt);
end


inp=fft(entrada,N); % Transformada de Fourier de la entrada
inp=fftshift(inp);
H=fft(salida,N);        % Transformada de Fourier de la salida
H=fftshift(H);
Ht=abs(ifft(H));        % Transformada inversa de Fourier de la salida
normalizada

% Comenzamos las iteraciones
Bofeten=40;     % Bodestein calculado
error=1e10;     % error de ajuste

% Inicializaciones para aumentar eficacia en bucles
% N1=length(-f(length(f)):(f(2)-f(1)):f(length(f)));
W=zeros(N,1);
F=W;

Hreal=H./inp;
DeltaBo=4;
Bo=100;
%primer calculo de error
count=0;
for w=-f(length(f))/2:(f(2)-f(1)):f(length(f))/2,
```

```
    count=count+1;
    W(count)=w;
    F(count)=0;
    for x=1:1:xfin
        F(count)=F(count)+Kest*exp(x*0.5*Bo*(1-
sqrt(1+(4*j*tr*w/Bo))));
    end
end
Yp=inp.*F;
Yt1=abs(ifft(Yp));
error=abs(Yt1-Ht)'*abs(Yt1-Ht);
%procedimiento iterativo;
while abs(DeltaBo)>0.1
   count=0;
   Bo=Bo+DeltaBo;
   if Bo<1
      Bo=1;
   end
   for w=-f(length(f))/2:(f(2)-f(1)):f(length(f))/2,
        count=count+1;
        W(count)=w;
        F(count)=0;
        for x=1:1:xfin
            F(count)=F(count)+Kest*exp(x*0.5*Bo*(1-
sqrt(1+(4*j*tr*w/Bo))));
        end
    end
    Yp=inp.*F;
    Yt1=abs(ifft(Yp));
    error1=abs(Yt1-Ht)'*abs(Yt1-Ht);
   [Bo DeltaBo error1 error]
   if(error1>=error)
      DeltaBo=-(0.5*DeltaBo);
   end
   error=error1;
   Yt=Yt1;
    Bofeten=Bo;
    Ffeten=F;
end
Ut=abs(ifft(inp));  % Evolución de la entrada
Bofeten
tiemporetardo
tiempociclo
%save fichero.txt Bofeten tiemporetardo tiempociclo vmaxentrada
vtmaxentrada vminentrada vtminentrada -ascii;
plot([Yt Ht Ut])        % Ojo, las variables son adimensionales
```

Appendix II

Table 34.- Results of the experiments carried out in the flume with shoe 1

CONFIGURATION: SHOE 1							
z, mm	**r.p.m.**	**I, A**	**V', V**	**d_1, mm**	**d_2, mm**	**d_3, mm**	**Torque, N m**
200	1.59	1.51		178	215	223	6.31
200	4.30	2.05	6.73	105	210	222	7.93
200	4.10	2.4	6.73	153	235	241	11.73
200	4.38	1.87	6.73	242	269	263	6.19
200	4.43	1.86	6.73	240	266	262	6.86
200	6.00	2.2	8.75	113	217	226	8.76
200	5.96	2.37	8.75	124	223	232	10.25
200	5.91	2.54	8.75	171	245	253	12.02
200	5.95	2.37	8.75	209	259	266	10.39
200	6.07	2.18	8.75	234	269	274	8.78
200	6.29	1.84	8.75	262	278	283	5.69
200	6.40	1.72	8.75	298	302	292	3.30
200	6.98	2.46	10.57	107	216	225	10.29
200	6.83	2.71	10.57	122	229	236	13.23
200	6.83	2.99	10.57	172	259	259	16.68
200	7.16	2.57	10.57	233	281	282	11.02
200	7.36	2.34	10.57	253	287	291	8.69
200	8.34	2.19	11.78	102	213	223	8.61
200	8.24	2.42	11.78	116	224	235	11.00
200	7.89	2.76	11.78	150	247	254	14.77
200	7.81	2.98	11.78	179	262	268	15.53
200	8.05	2.87	11.78	217	280	283	14.53
200	8.10	2.62	11.78	245	291	293	12.86
200	9.55	2.32	13.20	103	217	226	8.70
200	9.40	2.54	13.20	113	229	235	10.01
200	9.15	3.03	13.20	137	253	250	15.73
200	8.81	3.28	13.20	158	264	263	17.92
200	8.77	3.49	13.20	183	281	275	19.59
200	8.89	3.33	13.20	210	287	287	17.57
200	9.10	3.03	13.20	234	299	297	17.04
200	9.10	2.88	13.20	269	310	305	13.94
175	4.46	1.79	6.7	102	177	189	5.00
175	4.39	1.88	6.66	116	187	198	6.55
175	4.34	1.93	6.65	130	195	205	7.20
175	4.42	1.86	6.67	179	214	222	6.41
175	4.66	1.4	6.74	231	232	238	1.49

Continue

z, mm	r.p.m.	I, A	V', V	d_1, mm	d_2, mm	d_3, mm	Torque, N m
175	6.34	1.75	8.87	98	180	192	3.87
175	6.21	1.89	8.85	110	191	201	5.99
175	6.20	2.12	8.83	133	205	213	6.26
175	6.15	2.18	8.82	170	222	228	6.70
175	6.21	2.06	8.83	199	234	241	5.66
175	6.42	1.71	8.93	243	251	255	1.82
175	7.47	1.81	10.29	93	180	191	2.29
175	7.42	1.89	10.23	104	188	199	4.42
175	7.25	2.1	10.18	124	201	213	6.41
175	7.08	2.3	10.13	155	222	229	8.10
175	7.22	2.3	10.17	187	236	242	8.12
175	7.30	2.05	10.23	229	255	258	5.99
175	7.53	1.75	10.32	263	269	269	2.80
175	9.19	1.82	12.22	93	179	191	2.48
175	8.98	1.9	12.19	99	188	200	3.94
175	8.81	2.12	12.1	119	204	213	6.64
175	8.81	2.45	12.04	145	223	231	9.65
175	8.89	2.55	11.98	168	236	242	10.72
175	8.57	2.51	11.98	203	256	258	10.33
175	8.81	2.42	12.04	234	269	268	9.22
175	8.70	2.2	11.99	256	278	277	7.09
175	10.26	1.73	13.37	90	179	190	1.82
175	9.95	1.95	13.27	104	191	203	4.00
175	9.80	2.22	13.15	119	206	216	6.76
175	9.46	2.44	13.06	142	223	231	9.66
175	9.46	2.63	12.96	169	241	245	11.42
175	9.36	2.67	12.94	190	254	257	11.66
175	9.32	2.65	12.96	212	268	267	11.36
175	9.55	2.48	13.04	255	285	283	9.49
150	4.66	1.49	6.8	92	150	161	2.50
150	4.57	1.61	6.76	108	160	169	4.15
150	4.52	1.76	6.77	145	179	187	5.42
150	4.80	1.61	6.8	192	198	204	3.43
150	6.04	1.58	8.65	95	155	165	2.66
150	6.09	1.68	8.66	99	159	169	3.55
150	5.98	1.88	8.63	130	178	187	6.04
150	6.00	1.89	8.61	153	192	197	6.45
150	6.19	1.88	8.64	184	204	210	5.56
150	6.15	1.66	8.66	211	214	210	2.95

Continue

z, mm	r.p.m.	I, A	V', V	d_1, mm	d_2, mm	d_3, mm	Torque, N m
150	7.65	1.65	10.6	92	155	166	2.68
150	7.94	1.75	10.59	98	161	172	3.26
150	7.71	1.86	10.58	113	173	183	5.28
150	7.68	2.06	10.53	141	192	199	6.32
150	7.65	2.08	10.5	166	205	211	6.86
150	7.97	2.05	10.55	196	222	225	6.11
150	7.74	1.85	10.63	220	230	234	3.88
150	9.27	1.64	11.91	90	154	166	1.36
150	9.27	1.78	11.88	94	158	170	2.36
150	9.05	1.96	11.74	114	176	186	5.00
150	8.94	2.12	11.73	135	194	200	9.87
150	8.45	2.19	11.73	159	206	213	9.79
150	8.53	2.16	11.72	192	223	228	9.46
150	8.72	1.98	11.76	228	241	243	7.70
150	10.43	1.69	13.48	94	158	169	3.72
150	9.95	1.86	13.4	106	171	182	5.63
150	10.05	2.1	13.3	128	190	198	8.63
150	9.69	2.27	13.23	154	208	214	10.73
150	9.69	2.36	13.23	183	227	230	11.39
150	9.95	2.29	13.28	214	245	245	10.71
150	10.00	2.27	13.31	230	250	250	9.74

Table 35.- Results of the experiments carried out in the flume with shoe 2

CONFIGURATION: SHOE 2							
z, mm	**r.p.m.**	**I, A**	**V', V**	**d_1, mm**	**d_2, mm**	**d_3, mm**	**Torque, N m**
200	3.53	3.45	6.40	91	219	231	22.82
200	3.56	3.24	6.41	121	228	240	21.59
200	3.88	2.66	6.48	192	248	259	14.50
200	4.08	2.25	6.55	226	259	269	8.94
200	4.95	3.57	8.06	63	216	228	21.56
200	4.75	3.84	8	84	230	236	29.78
200	4.71	3.67	7.99	155	259	259	25.85
200	5.07	3.17	8.14	186	262	269	19.67
200	5.38	2.67	8.24	227	276	280	14.02
200	6.15	3.68	9.57	52	219	229	23.95
200	5.78	4.14	9.44	82	236	242	28.05
200	5.76	4.14	9.46	119	248	256	27.23
200	5.98	4.05	9.54	164	267	272	24.90
200	6.42	3.32	9.71	208	277	286	21.92
200	6.57	2.95	9.78	236	286	294	14.97
200	7.30	3.78	10.93	47	219	230	22.88
200	6.80	4.5	10.68	96	244	254	30.71
200	6.86	4.48	10.69	133	259	268	29.73
200	7.03	4.08	10.81	180	277	284	26.47
200	7.42	3.56	10.96	217	289	296	21.37
200	7.68	3.22	11.1	245	294	305	17.61
200	7.56	5.02	11.76	110	258	265	34.00
200	7.54	5.09	11.79	120	263	268	34.63
200	7.59	4.85	11.88	133	264	274	33.05
200	8.06	4.48	11.98	181	282	291	29.50
200	8.24	4.01	12.14	218	295	303	25.51
200	8.72	3.31	12.40	264	307	318	18.01
175	3.69	2.89	6.35	71	191	201	18.04
175	3.83	2.92	6.34	120	211	218	18.21
175	3.93	2.38	6.39	195	237	236	11.33
175	4.08	2.01	6.4	222	246	243	7.39
175	5.22	3.05	8.14	51	191	200	18.16
175	4.96	3.33	8.07	86	210	215	21.86
175	5.20	3.34	8.06	134	233	232	22.15
175	5.16	3.05	8.11	172	249	242	19.64
175	5.41	2.63	8.19	219	268	255	14.85

Continue

z, mm	r.p.m.	I, A	V', V	d_1, mm	d_2, mm	d_3, mm	Torque, N m
175	6.83	2.95	9.98	42	190	200	17.28
175	6.57	3.53	9.81	69	211	216	23.01
175	6.27	3.9	9.77	113	235	233	26.38
175	6.36	3.65	9.8	156	253	248	24.60
175	6.51	3.36	9.86	202	274	266	21.81
175	6.93	2.99	10.01	239	288	272	17.61
175	7.77	3.58	11.31	61	210	216	22.77
175	7.33	4.25	11.08	108	241	238	29.39
175	7.33	4.25	11.12	164	269	257	29.53
175	7.53	3.71	11.24	209	286	271	24.26
175	7.83	3.26	11.41	250	299	283	19.13
175	8.53	3.62	12.42	57	210	218	23.10
175	7.97	4.51	12.19	99	241	238	32.05
175	7.94	4.79	12.08	150	270	257	34.56
175	8.14	4.36	12.11	193	286	271	30.11
175	8.42	3.89	12.26	234	300	283	25.15
150	4.25	2.61	6.82	69	175	181	13.40
150	4.17	2.73	6.8	90	186	187	13.85
150	4.25	2.58	6.83	158	220	207	12.24
150	4.38	2.3	6.89	208	245	218	8.99
150	5.48	2.82	8.36	51	172	179	10.97
150	5.29	2.92	8.27	81	192	191	14.36
150	5.22	3.06	8.19	138	226	209	16.62
150	5.26	3.05	8.24	175	247	218	15.79
150	5.80	2.12	8.47	217	239	235	3.17
150	7.25	2.72	10.32	47	172	182	10.35
150	7.03	3.01	10.26	66	187	192	14.02
150	6.76	3.26	10.16	103	210	208	18.36
150	6.90	2.98	10.21	136	215	222	14.35
150	7.12	2.68	10.31	176	232	235	11.41
150	7.27	2.52	10.38	203	242	243	8.35
150	8.16	2.7	11.62	35	164	174	13.84
150	7.97	3	11.51	56	184	190	18.66
150	7.59	3.44	11.36	90	209	208	23.67
150	7.53	3.63	11.29	118	227	219	26.16
150	7.77	3.28	11.39	150	233	233	21.52
150	7.97	3.02	11.45	194	251	245	19.43
150	9.15	2.56	12.79	33	162	176	12.74
150	9.10	2.77	12.66	53	180	191	16.85
150	8.77	3.4	12.57	89	205	212	21.35
150	8.72	3.53	12.49	131	229	231	23.82
150	8.65	3.45	12.54	173	249	245	22.42
150	9.05	3.16	12.64	211	264	256	18.67

Table 36.- Results of the experiments carried out in the flume without shoe

CONFIGURATION: FLAT							
z, mm	**r.p.m.**	**I, A**	**V', V**	**d_1, mm**	**d_2, mm**	**d_3, mm**	**Torque, N m**
200	3.41	3.99	6.50	127	219	227	23.05
200	3.56	3.79	6.52	153	231	237	22.61
200	3.89	3.08	6.58	206	259	255	17.36
200	4.09	2.55	6.65	234	272	264	13.40
200	4.34	2.16	6.78	258	282	273	9.53
200	4.29	4.71	4.71	90	211	220	26.19
200	4.36	4.58	4.58	128	231	236	25.65
200	4.69	4.12	4.12	175	255	255	21.16
200	4.87	3.68	8.03	205	270	265	18.56
200	5.04	3.41	8.08	221	276	275	15.31
200	5.42	2.58	8.14	247	279	282	9.58
200	5.60	2.16	8.18	266	287	291	6.27
200	5.48	5.17	9.52	77	216	225	33.31
200	5.50	5.21	9.55	106	231	238	35.29
200	5.63	4.99	9.55	144	252	252	32.32
200	5.75	4.76	9.62	172	266	261	30.61
200	5.82	4.73	9.66	196	272	270	28.92
200	6.34	3.69	9.89	213	279	283	20.91
200	6.62	3.33	9.97	232	280	290	17.93
200	6.58	5.26	10.62	65	210	223	33.50
200	6.36	5.42	10.54	86	223	235	34.94
200	6.49	5.14	10.42	132	246	256	33.10
200	6.73	4.74	10.69	169	264	271	30.33
200	7.06	4.42	10.85	202	280	284	27.14
200	7.33	3.95	10.97	231	292	294	23.74
200	7.35	3.67	11.53	252	301	301	21.10
200	7.27	5.49	11.80	65	220	230	37.95
200	7.27	5.67	11.79	88	232	243	38.03
200	7.19	5.88	11.77	118	250	258	37.35
200	7.42	5.4	11.88	147	266	271	35.36
200	7.87	5.01	12.00	179	277	283	32.03
200	7.87	4.64	12.12	204	287	292	29.34
200	8.13	4.29	12.25	220	290	299	26.01
200	8.85	3.88	12.41	241	298	302	22.95
175	3.72	3.29	6.4	103	190	204	18.28
175	3.84	2.99	6.45	137	203	215	14.82
175	4.20	2.45	6.54	180	221	232	9.16
175	4.59	2.14	6.6	203	230	241	5.77
175	4.45	1.91	6.64	221	238	248	4.41

Continue

z, mm	r.p.m.	I, A	V', V	d_1, mm	d_2, mm	d_3, mm	Torque, N m
175	4.86	3.82	8.09	76	189	203	22.84
175	4.86	3.83	8.12	97	199	210	22.37
175	5.03	3.35	8.18	145	221	229	19.15
175	5.29	2.98	8.26	176	232	241	14.55
175	5.55	2.69	8.34	203	244	251	12.55
175	5.70	2.36	8.4	227	256	259	8.04
175	5.93	2.02	8.48	256	270	269	4.81
175	6.02	4.12	9.67	72	193	207	25.42
175	5.98	4.25	9.66	83	199	211	25.50
175	6.13	4.01	9.71	131	224	231	24.53
175	6.24	3.84	9.76	153	236	241	23.82
175	6.47	3.48	9.85	175	242	251	18.94
175	6.67	3.1	9.94	201	253	260	15.92
175	6.98	2.67	10.07	236	270	273	10.59
175	7.08	4.17	10.83	56	190	200	26.75
175	6.88	4.33	10.85	78	202	215	27.35
175	6.91	4.37	10.85	115	221	232	25.72
175	7.06	4.18	10.81	135	231	241	24.83
175	7.27	3.78	11	171	248	256	21.39
175	7.47	3.4	11.09	200	259	267	18.01
175	7.81	3.02	11.24	223	266	275	13.75
175	7.94	2.52	11.36	251	277	285	9.38
175	7.91	4.33	12.12	52	191	205	26.64
175	7.68	5.02	12.01	69	203	214	28.29
175	7.84	4.57	12.05	105	223	234	28.37
175	7.83	4.53	12.08	127	236	245	27.70
175	8.31	4.21	12.32	162	252	261	24.65
175	8.39	3.82	12.4	194	265	272	19.36
175	8.93	3.35	12.62	223	274	283	14.13
175	9.19	2.95	12.76	255	287	295	9.63
150	4.05	2.79	6.69	84	164	176	10.29
150	4.15	2.68	6.71	116	180	190	8.99
150	4.38	2.16	6.77	160	197	207	4.54
150	4.50	2.08	6.82	178	204	214	2.36
150	5.18	3.13	8.2	61	161	175	13.80
150	5.13	3.12	8.19	91	177	187	13.16
150	5.33	2.78	8.25	138	201	207	10.81
150	5.41	2.67	8.25	160	211	215	8.55
150	5.80	2.12	8.4	192	219	228	2.84

Continue

z, mm	r.p.m.	I, A	V', V	d_1, mm	d_2, mm	d_3, mm	Torque, N m
150	6.54	3.28	10.15	40	153	166	15.18
150	6.57	3.52	10.07	74	178	189	17.49
150	6.56	3.33	10.09	112	199	207	16.54
150	6.71	3.23	10.13	134	210	216	14.72
150	6.93	2.96	10.24	167	222	230	11.11
150	7.27	2.53	10.35	195	233	240	6.79
150	7.35	2.4	10.4	212	240	246	5.84
150	7.50	3.55	11.24	53	167	180	22.94
150	7.57	3.57	11.22	69	178	191	24.00
150	7.50	3.57	11.2	104	197	209	23.52
150	7.57	3.37	11.26	133	212	222	21.23
150	7.83	3.09	11.35	158	223	232	19.15
150	7.91	2.81	11.44	189	236	243	16.05
150	8.20	2.55	11.53	212	245	251	12.75
150	8.61	3.52	12.54	43	163	178	22.37
150	8.46	3.76	12.45	55	175	187	24.46
150	8.42	3.87	12.44	89	195	207	26.18
150	8.50	3.81	12.43	116	210	221	25.19
150	8.57	3.5	12.58	153	229	237	22.50
150	9.01	3.18	12.72	181	241	248	19.92
150	9.19	2.71	12.85	216	253	259	14.88

Table 37.- Head difference achieved in the paddlewheel without shoe with the two obstruction configurations. Mechanical, hydraulic and electric power achieved with this head loss is also presented

Blocks	Head loss, mm	P_{mech}, W	P_{hyd}, W	P_{elec}, W
Obstruction 1	5.71	3.43	0.41	51.70
	6.04	5.07	0.42	59.40
	6.32	3.00	0.00	49.50
	15.90	7.86	1.84	70.40
	16.28	10.12	2.10	78.10
	17.27	7.56	2.24	69.30
	22.49	17.93	3.80	100.10
	25.55	20.20	4.64	105.60
	26.44	17.49	5.15	99.00
	28.50	31.12	5.06	128.70
	32.33	37.73	5.41	140.80
	33.11	57.35	5.93	171.60
	33.20	39.00	5.50	143.00
	34.00	88.42	6.20	211.20
	36.74	59.69	7.24	174.90
	37.96	138.90	7.92	262.90
	38.29	75.56	6.64	195.80
	39.65	142.51	7.28	266.20
	40.44	97.22	8.32	221.10
Obstruction 2	21.40	14.16	6.57	90.20
	30.62	29.42	11.29	125.40
	37.14	66.14	14.02	183.70
	44.39	143.72	20.19	267.30

Table 38.- Head difference achieved in the paddlewheel with shoe in position and with the two obstruction configurations. Mechanical, hydraulic and electric power achieved with this head loss is also presented

Blocks	Head loss, mm	P_{mech}, W	P_{hyd}, W	P_{elec}, W
Obstruction 1	8.01	3.65	0.60	52.80
	8.29	5.86	0.68	62.70
	23.70	10.46	3.21	79.20
	24.48	10.12	3.11	78.10
	32.23	17.49	4.87	99.00
	34.95	18.37	4.66	101.20
	40.43	39.65	6.44	144.10
	46.13	35.87	6.06	137.50
	50.34	72.06	10.13	191.40
	57.35	62.07	8.27	178.20
	70.98	95.23	10.55	218.90
	71.58	144.93	9.72	268.40
Obstruction 2	20.27	16.20	6.09	95.70
	29.22	31.12	10.18	128.70
	37.13	57.35	15.20	171.60
	42.07	98.22	19.09	222.20
	43.00	179.70	18.82	298.10
	45.07	143.72	21.17	267.30

Table 39.- Mechanical, hydraulic and electric power obtained at different head differences in the experiments carried out with the weir at a working depth of 12 cm

	d_1, mm	d_2, mm	H, mm	P_{mech}, W	P_{hyd}, W	P_{elec}, W
No shoe	108.67	125.81	17.14	9.45	0.28	75.90
	104.74	129.62	24.88	17.49	0.54	99.00
	101.76	132.71	30.95	36.49	1.02	138.60
	98.79	135.64	36.85	59.69	1.55	174.90
	96.36	138.18	41.82	98.22	2.29	222.20
	96.05	140.10	44.05	152.34	2.68	275.00
	95.69	138.90	43.21	207.83	2.55	320.10
Shoe	104.84	131.73	26.89	12.25	0.80	84.70
	98.70	138.76	40.06	25.12	2.24	116.60
	91.91	146.64	54.73	37.73	4.69	140.80
	83.79	154.39	70.61	51.34	8.36	162.80
	69.52	164.76	95.24	54.30	8.17	167.20
	72.97	163.21	90.24	57.35	8.08	171.60
	73.24	165.55	92.31	54.30	8.81	167.20

Table 40.- Mechanical, hydraulic and electric power obtained at different head differences in the experiments carried out with the weir at a working depth of 15 cm

	d_1, mm	d_2, mm	H, mm	P_{mech}, W	P_{hyd}, W	P_{elec}, W
No shoe	144.82	153.91	9.10	11.16	1.68	81.40
	141.85	158.00	16.15	21.14	3.03	107.80
	139.75	160.45	20.69	40.94	4.11	146.30
	136.66	163.75	27.09	69.50	5.55	188.10
	135.86	164.63	28.77	111.72	6.01	236.50
	135.66	165.86	30.20	156.11	6.72	278.30
	135.28	165.76	30.48	215.19	6.83	325.60
Shoe	137.48	157.62	20.14	11.51	2.95	82.50
	134.45	163.73	29.27	18.82	4.97	102.30
	129.93	168.54	38.61	35.26	7.34	136.40
	126.52	170.71	44.19	72.06	8.95	191.40
	122.75	175.00	52.25	113.88	11.27	238.70
	122.42	176.69	54.27	154.85	12.46	277.20
	122.15	173.71	51.57	233.35	11.40	338.80

Appendix III

Related publications 2011 to 2016

Peer review journals

- Mendoza, J.L., Granados, M.R., de Godos, I., Acién, F.G., Molina, E., Banks, C., Heaven, S. 2013a. Fluid-dynamic characterization of real-scale raceway reactors for microalgae production. Biomass and Bioenergy, 54, 267-275.

- Mendoza, J.L., Granados, M.R., de Godos, I., Acien, F.G., Molina, E., Heaven, S., Banks, C.J. 2013b. Oxygen transfer and evolution in microalgal culture in open raceways. Bioresource Technology, 137, 188-95.

- Mendoza Martín, J.L., Heaven, S., Acién Fernández, F.G., Banks, C.J., Molina Grima, E. Cultivation of *Scenedesmus* spp. in a raceway reactor. 21st European Biomass Conference and Exhibition, 3-7 June 2013, Copenhagen, Denmark. Conference proceedings.

- de Godos, I., Mendoza, J.L., Acien, F.G., Molina, E., Banks, C.J., Heaven, S., Rogalla, F. 2014. Evaluation of carbon dioxide mass transfer in raceway reactors for microalgae culture using flue gases. Bioresource Technology, 153, 307-14.

- Tran, K.C., Mendoza Martin, J.L., Heaven, S., Banks, C.J., Acien Fernandez, F.G., Molina Grima, E. 2014. Cultivation and anaerobic digestion of Scenedesmus spp. grown in a pilot-scale open raceway. Algal Research, 5, 95-102.

- Pawlowski, A., Mendoza, J.L., Guzmán, J.L., Berenguel, M., Acién, F.G., Dormido, S. 2014. Effective utilization of flue gases in raceway reactor with event-based pH control for microalgae culture. Bioresource Technology, 170, 1-9.

- Pawlowski, A., Mendoza, J.L., Guzmán, J.L., Berenguel, M., Acién, F.G., Dormido, S. 2015. Selective pH dissolved oxygen control strategy for a raceway reactor within an event-based approach. Control Engineering Practice, 44, 209-218.

- Fernandez, I., Acién, F.G., Guzman, J.L, Berenguel, M., Mendoza, J.L. Dynamic model of an industrial raceway reactor for microalgae production. Under revision.

- Duarte Santos, T., Mendoza Martin, J.L., Acién Fernandez, F.G., Molina, E., Vieira Costa, J.A., Heaven, S., Optimization of CO_2 supply in raceway reactors: influence of CO_2 molar fraction and gas flow rate. Under revision.

Conference presentations and posters

As first author:

- 1st Meeting for interdepartmental research divulgation (Almería, Spain, 2011). Captación de CO_2 mediante cultivo de microalgas a gran escala en reactores raceway.

- 1st International Symposium about Microalgae Biotechnology for Young Researchers (Almeria, Spain, 2012). Fluid-dynamic characterization of real-scale raceway reactors for microalgae production.

- 21st European Biomass Conference and Exhibition (Copenhagen, Denmark, 2013). Cultivation of *Scenedesmus* spp. in a raceway reactor.

- Symposium research divulgation (Almeria, Spain, 2013). Oxygen transfer in raceway reactors.

- Euro-Mediterranean Microalgal Biotechnology Seminar & Workshop (Almeria, Spain, 2014). Raceway system requirements for low-cost energy-efficient algal biomass cultivation.

- EU-China Workshop on Resource Recovery from Biomass and Green Technology in Waste/Wastewater Treatment (Shanghai, China, 2014). Characterization of O_2 mass transfer in raceway reactors for algae growth.

- 5th UK Algae Conference (Glasgow, United Kingdom, 2015). Characterization of raceway requirements for efficient algal biomass cultivation

- 11th IWA Specialist Group Conference on Wastewater Pond Technology, (Leeds, United Kingdom, 2016). Raceway operation for efficient algal biomass cultivation.

As co-author:

- 9th European Workshop "Biotechnology of Microalgae" (Potsdam, Germany, 2012). Assessment of open raceway ponds for the production of microalgae.
- III Latin American Congress of Solabia. (Chiriquí, Panama, 2013). Key factors in the design of open raceways for the production of microalgae at large scale.
- 5th International Congress of the International Society for Applied Phycology (ISAP) 2014 (Sydney, Australia, 2014). Characterization of raceway reactors for CO_2 capture and microalgae production.

List of References

Bibliography

International Energy Outlook 2008. What will it take to stabilize carbon dioxide concentrations? http://www.eia.doe.gov/oiaf/ieo/scdc.html.

Acién Fernández, F.G., Fernández Sevilla, J.M., Sánchez Pérez, J.A., Molina Grima, E., Chisti, Y. 2001. Airlift-driven external-loop tubular photobioreactors for outdoor production of microalgae: assessment of design and performance. *Chemical Engineering Science*, **56**, 2721-2732.

Acien Fernandez, F.G., Gonzalez-Lopez, C.V., Fernandez Sevilla, J.M., Molina Grima, E. 2012. Conversion of CO_2 into biomass by microalgae: how realistic a contribution may it be to significant CO_2 removal? *Applied Microbiology and Biotechnology*, **96**, 577-586.

Acien, F.G., Fernandez, J.M., Magan, J.J., Molina, E. 2012. Production cost of a real microalgae production plant and strategies to reduce it. *Biotechnology Advances*, **30**, 1344-1353.

AEMET. Agencia Estatal de Meteorología, Ministerio de Agricultura, Alimentación y Medio Ambiente. http://www.aemet.es/es/serviciosclimaticos/datosclimatologicos/valoresclimatologicos?l=6325O&k=and.

Alabi, A.O., Tampier, M., Bibeau, E. 2009. Microalgae technologies and processes for biofuels/bioeneergy production in Columbia: current technology, suitability and barrier to implementation. *See Science Ltd.Report. The British Clumbia Innovation Council*.

Ali, H., Cheema, T.A., Yoon, H.S., Do, Y., Park, C.W. 2014. Numerical prediction of algae cell mixing feature in raceway ponds using particle tracing methods. *Biotechnology and Bioengineering*, **9999**, 1-11.

All-gas. 2010. All-gas Project: ENERGY.2010.3.4-1: Bio-fuels from algae. Seventh Framework Programme (FP7).

Andersen, R.A. 2005. Algal culturing techniques. *Elsevier Academic Press, Phycological Society of America*.

APHA. 2005. Standard Methods for the Examination of Water and Wastewater. *21st Ed. Washington DC, USA: American Public Health Association/American Water Works Association/Water Environment Federation, 2005.*

ARM. Grupo de investigación: Automática, robótica y mecatrónica. Universidad de Almería. *http://cvirtual.ual.es/webual/jsp/investigacion/nuevo/pInicio.jsp?id_grupo=TEP197&idioma=es*.

Azar, C., Lindgren, K., Andersson, B.A. 2003. Global energy scenarios meeting stringent CO_2 constrainst. Cost-effective fuel choices in the transportation sector. *Energy Policy*, **31**, 961-976.

Azov, Y., Shelef, G. 1982. Operation of high-rate oxidation ponds. Theory and experiments. *Water Resources*, **16**, 1153-1160.

Babcock, R.W., Malda, J., Radway, J.C. 2002. Hydrodynamics and mass transfer in a tubular airlift photobioreactor. *Journal of Applied Phycology*, **14**, 169-184.

Badger, M.R., Andrews, T.J., Whitney, S.M., Ludwig, M., Yellowlees, D.C., Leggat, W., Price, G.D. 1998. The diversity and coevolution of Rubisco, plastids pyrenoids, and chloroplast-based CO_2 concentrating mechanisms in algae. *Canadian Journal of Botany*, **76**, 1052-1071.

Bahadar, A., Bilal Khan, M. 2013. Progress in energy from microalgae: A review. *Renewable and Sustainable Energy Reviews*, **27**, 128-148.

Bao, Y., Liu, M., Wu, X., Cong, W., Ning, Z. 2012. *In situ* carbon supplementation in large-scale cultivations of *Spirulina platensis* in open raceway pond. *Biotechnology and Bioprocess Engineering*, **17**(1), 93-99.

Beardall, J., Raven, J.A. 2013. Limits to phototrophic growth in dense culture: CO_2 suply and light. In Algae for Biofuels and Energy. *Developments in Applied Phycology*, **5**, 91-97.

Becker, E.W. 1994. Large scale cultivation. *In: Microalgae: Biotechnology and Microbiology. Cambridge University Press, Cambridge.*

Becker, E.W. 2007. Micro-algae as a source of protein. *Biotechnology Advances*, **25**, 207-210.

Becker, W. 2004. Microalgae in Human and Animal Nutrition in: *Handbook of Microalgal Culture: Biotechnology and Applied Phycology*, (Ed.) A. Richmond, Blackwell Publishing.

Belay, A., Kato, T., Ota, Y. 1996. *Spirulina* (*Arthrospira*). Potential application as an animal feed supplement. *Journal of Applied Phycology*, **8**, 303-311.

Benemann, J. 2013. Microalgae for Biofuels and Animal Feeds. *Energies*, **6**, 5869-5886.

Benemann, J., Oswald, W.J. 1996. Systems and economic analysis of microalgae ponds for conversion of CO_2 to biomass. Final technical report. *Assistant Secretary for Fossil Energy, Washington, DC (United States)*.

Benemann, J.R. 2000. Hydrogen production by microalgae. *Journal of Applied Phycology*, **12**, 291-300.

Benemann, J.R., Tillett, D.M., Weissman, J.C. 1987. Microalgae biotechnology. *Trends in Biotechnology*, **5**, 47-53.

Berenguel, M., Rodríguez, F., Acién, F.G., García, J.L. 2004. Model predictive control of pH in tubular photobioreactors. *Journal of Process Control*, **14**, 377-387.

Bilanovic, D., Andargatchew, A., Kroeger, T., Shelef, G. 2009. Freshwater and marine microalgae sequestering of CO_2 at different C and N concentrations – Response surface methodology analysis. *Energy Conversion and Management*, **50**, 262-267.

Borowitzka, M.A. 2010. Algae oils for biofuels: chemistry, physiology, and production. . *In: Cohen Z., Ratledge, C. (eds) Single cell oils. Microbial and algal oils. AOCS Press, Urbana.*, 271-289.

Borowitzka, M.A. 2005. Culturing microalgae in outdoor ponds. *In: Algal Culturing Techniques. Ed. Elsevier, New York*.

Borowitzka, M.A. 1998. Limits to growth. *In : Wong YS, Yam NFY (eds) Wastewater treatment with algae. Springer, Berlin*, 203-226.

Borowitzka, M.A. 2013. Species and Strain Selection. *In Developments in Applied Phycology. Algae for Biofuels and Energy. (eds) Springer Dordrecht Heidelberg New York London*, **4**.

Borowitzka, M.A., Moheimani, N.R. 2013. Developments in Applied Phycology. *In: Algae for Biofuels and Energy. (eds) Springer Dordrecht Heidelberg New York London*, **5**.

Boussiba, S., Sandbank, E., Shelef, G., Cohen, Z., Vonshak, A., Ben-Amotz, A., Arad, S., Richmond, A. 1988. Outdoor cultivation of the marine microalga *Isochrysis galbana* in open reactors. *Aquaculture*, **72**, 247-253.

Brechtelsbauer, C., Ricard, F. 2001. Reaction engineering evaluation and utilization of static mixer technology for the synthesis of pharmacauticals. *Organic Process Research & Development*, **5**, 646-651.

Brennan, L., Owende, P. 2010. Biofuels from microalgae - A review of technologies for production, processing, and extractions of biofuels and co-products. *Renewable and Sustainable Energy Reviews*, **14**, 557-577.

Brown, M.R., Jeffrey, S.W., Volkman, J.K., Dunstan, G.A. 1997. Nutritional properties of microalgae for mariculture. *Aquaculture*, **151**, 315-331.

Brune, D.E., Lundquist, T.J., Benemann, J.R. 2009. Microalgal Biomass for Greenhouse Gas Reductions: Potential for Replacement of Fossil Fuels and Animal Feeds. *Journal of Environmental Engineering*, **135**, 1136-1144.

BS-ISO-1438:2008. Hydrometry. Open channel flow measurement using thin-plate weirs.

Burlew, J.S. 1976. Algal culture. From laboratory to pilot plant. *(eds) Carnegie institution of Washington publication 600. Washington, D.C.*

Cajamar. http://www.fundacioncajamar.es/es/comun/estacion-experimental-palmerillas/.

Camacho Rubio, F., Acién Fernández, F.G., Sánchez Pérez, J.A., García Camacho, F., Molina Grima, E. 1999. Prediction of dissolved oxygen and carbon dioxide concentration profiles in tubular photobioreactors for microalgal culture. *Biotechnology and Bioengineering*, **62**, 71-86.

Carvalho, A.P., Meireles, L.A., Malcata, F.X. 2006. Microalgal Reactors: A Review of Enclosed System Designs and Performances. *Biotechnology Progress*, **22**, 1490-1506.

Certik, M., Shimizu, S. 1999. Biosynthesis and regulation of microbial polyunsaturated fatty acid production. *Journal of Bioscience and Bioengineering*, **1**, 1-14.

Collet, P., Helias, A., Lardon, L., Ras, M., Goy, R.A., Steyer, J.P. 2011. Life-cycle assessment of microalgae culture coupled to biogas production. *Bioresource Technology*, **102**, 207-214.

COP. 2012. Conference of the Parties. UN Climate Change Conference COP18. *www.cop18.qa*.

Craggs, R., Sutherland, D., Campbell, H. 2012. Hectare-scale demonstration of high rate algal ponds for enhanced wastewater treatment and biofuel production. *Journal of Applied Phycology*, **24**, 329-337.

Chacón-Lee, T.L., González-Mariño, G.E. 2010. Microalgae for "Healthy" Foods-Possibilities and Challenges. *Comprehensive Reviews in Food Science and Food Safety*, **9**, 655-675.

Chaumat, H., Billet-Duquenne, A.M., Augier, F., Mathieu, C., Delmas, H. 2005. Mass transfer in bubble column for industrial conditions-effects of organic medium, gas and liquid flow rates and column design. *Chemical Engineering Science*, **60**, 5930-5936.

Cheng, L., Zhang, L., Chen, H., Gao, C. 2006. Carbon dioxide removal from air by microalgae cultured in a membrane-photobioreactor. *Separation and Purification Technology*, **50**, 324-329.

Chiaramonti, D., Prussi, M., Casini, D., Tredici, M.R., Rodolfi, L., Bassi, N., Zittelli, G.C., Bondioli, P. 2013. Review of energy balance in raceway ponds for microalgae cultivation: Re-thinking a traditional system is possible. *Applied Energy*, **102**, 101-111.

Chisti, Y. 2007. Biodiesel from microalgae. *Biotechnology Advances*, **25**, 294-306.

Chisti, Y. 2008. Biodiesel from microalgae beats bioethanol. *Trends in Biotechnology*, **26**, 126-131.
Chisti, Y. 2012. Raceways-based production of algal crude oil. in: *Microalgal Biotechnology: Potential and Production*, (Eds.) P. Clemens, W. Christian. Degruyter, Göttingen, pp. 113-146.
Chisti, Y. 1980. An unusual hydrocarbon. *Journal of the Ramsay Society*, **27-28**, 24-26.
Chisti, Y., Fujimoto, K., Moo-Young, M. 1987. Hydrodynamic and oxygen mass transfer sutdies in bubble columns and airlift bioreactors. *In : Biotechnolgoy processes scale-up and mixing.*, 72-81.
Chisti, Y., Yan, J. 2011. Energy from algae: Current status and future trends algal biofuels - A status report. *Applied Energy*, **88**, 3277-3279.
Chiu, S.Y., Kao, C.Y., Chen, C.H., Kuan, T.C., Ong, S.C., Lin, C.S. 2008. Reduction of CO_2 by a high-density culture of *Chlorella* sp. in a semicontinuous photobioreactor. *Bioresource Technology*, **99**, 3389-96.
Christenson, L., Sims, R. 2011. Production and harvesting of microalgae for wastewater treatment, biofuels, and bioproducts. *Biotechnology Advances*, **29**, 686-702.
Davies, J.T. 1972. Turbulence phenomena at free surfaces. *American Institute of Chemical Engineers Journal*, **18**, 169-73.
de Godos, I., Arbib, Z., Feria, M.J., Lara, E., Santiago, J.R., Rogalla, F., Fernández, M., de la Rubia, M.A. 2013. Proyecto All-gas. Cultivo de microalgas con producción de biocombustibles y eliminación de nutrientes. *Revista técnica de medio ambiente (RETEMA). Especial bioenergía 2013.*
de la Noie, J., Lalibert, G., Proulx, D. 1992. Algae and waste water. *Journal of Applied Phycology*, **4**, 247-254.
De Schamphelaire, L., Verstraete, W. 2009. Revival of the biological sunlight-to-biogas energy conversion system. *Biotechnology and Bioengineering*, **103**, 296-304.
Demirbas, A. 2006. Oily products from mosses and algae via pyrolysis. *Energy Source Part A*, **28**, 933-940.
Demirbas, M.F. 2011. Biofuels from algae for sustainable development. *Applied Energy*, **88**, 3473-3480.
Dismukes, G.C., Carrieri, D., Bennette, N., Ananyev, G.M., Posewitz, M.C. 2008. Aquatic phototrophs: efficient alternatives to land-based crops for biofuels. *Current Opinion in Biotechnology*, **19**, 235-40.
Eckardt, N.A. 2005. Photorespiration Revisited. *The Plant Cell*, **17**, 2139-2141.
EEA. 2012. Potent greenhouse gases – fluorinated gases in the European Union. *European Environment Agency*, http://www.eea.europa.eu/highlights/potent-greenhouse-gases.
Eichenberger, W., Gribi, C. 1997. Lipids of Pavlova lutheri: cellular site and metablolic role of DGCC. *Phytochemistry*, **45**, 1561-1567.
EPA. 1985. United States Environment Protection Agency.
Etheridge, D.M., Steele, L.P., Langenfelds, R.L., Francey, R.J. 1996. Natural and anthropogenic changes in atmospheric CO_2 over the las 1000 years from air in Antarctic ice and firn. *Journal of Geophysical Research*, **101**, 4115-4128.
Fabregas, J., Maseda, A., Dominguez, A., Otero, A. 2004. The cell composition of *Nannochloropsis* sp. changes under different irradiances in semicontinuous culture. *World Journal of Microbiology and Biotechnology*, **20**, 31-35.

Fenton, O., hUallacháin, D.O. 2012. Agricultural nutrient surpluses as potential input sources to grow third generation biomass (microalgae): A review. *Algal Research*, **1**, 49-56.

Fenton, O., Ohuallachain, D. 2012. Agricultural nutrient surplus as potential input sources to grow third generation biomass (microalgae): a review. *Algal Research*, **1**, 49-56.

Fukuda, H., Kondo, A., Noda, H. 2001. Biodiesel fuel production by transesterification of oils. *Journal of Bioscience and Bioengineering*, **92**, 405-416.

Fulke, A.B., Mudliar, S.N., Yadav, R., Shekh, A., Srinivasan, N., Ramanan, R., Krishnamurthi, K., Devi, S.S., Chakrabarti, T. 2010. Bio-mitigation of CO_2, calcite formation and simultaneous biodiesel precursors production using *Chlorella* sp. *Bioresource Technology*, **101**, 8473-8476.

Gates, W.E., Borchardt, J.A. 1964. Nitrogen and phosphorus extraction from domestic wastewater treatment plan effluents by controlled algal culture. *Journal of Water Pollution Control Federation*, **36**, 443-462.

Gavrilescu, M., Chisti, Y. 2005. Biotechnology - A sustainable alternative for chemical industry. *Biotechnology Advances*, **23**, 471-99.

Giordano, M., Beardall, J., Raven, J.A. 2005. CO_2 concentrating mechanisms in algae: mechanisms, environmental modulation, and evolution. *Annual Review of Plant Physiology*, **56**, 99-131.

Goldman, J.C. 1977. Temperature effects on phytoplankton growth in continuous culture. *Limnology and Oceanography*, **22**, 932-936.

Gomez, C., Escudero, R., Morales, M.M., Figueroa, F.L., Fernandez-Sevilla, J.M., Acien, F.G. 2013. Use of secondary-treated wastewater for the production of *Muriellopsis* sp. *Applied Microbiology and Biotechnology*, **97**, 2239-49.

González-Fernández, C., Sialve, B., Bernet, N., Steyer, J.-P. 2012. Impact of microalgae characteristics on their conversion to biofuel. Part II: Focus on biomethane production. *Biofuels, Bioproducts and Biorefining*, **6**, 205-218.

González-López, C.V., Acién Fernández, F.G., Fernández-Sevilla, J.M., Sánchez Fernández, J.F., Molina Grima, E. 2012. Development of a process for efficient use of CO_2 from flue gases in the production of photosynthetic microorganisms. *Biotechnology and bioengineering*, **109**, 1637-1650.

GoogleMaps. 2015. https://www.google.es/maps/place/Almer%C3%ADa/@44.383461,-0.1082535,5z/data=!4m2!3m1!1s0xd7a9e00ecccf2c1:0x8d9da01f8ebc485e?hl=es.

Gouleke, C.G., Oswald, W.J., Gotaas, H.B. 1956. Anaerobic digestion of algae. *Sanitary Engineering Research Laboratory, Department of Engineering, University of California, Berkeley, California*, **5**, 47-55.

Granados, M.R., Acien, F.G., Gomez, C., Fernandez-Sevilla, J.M., Molina Grima, E. 2012. Evaluation of flocculants for the recovery of freshwater microalgae. *Bioresource Technology*, **118**, 102-10.

Griffiths, M.J., Harrison, S.T.L. 2009. Lipid productivity as a key characteristic for choosing algal species for biodiesel production. *Journal of Applied Phycology*, **21**, 493-507.

Grobbelaar, J.U. 2004. Algal Nutrition: Mineral Nutrition. in: *Handbook of Microalgal Culture: Biotechnology and Applied Phycology*, (Ed.) A. Richmond. Blackwell Science.

Grobbelaar, J.U. 2012. Microalgae mass culture: the constraints of scaling-up. *Journal of Applied Phycology*, **24**, 315-318.

Guschina, I.A., Harwood, J.L. 2006. Lipids and lipid metabolism in eukaryotic algae. *Progress in Lipid Research*, **45**, 160-186.

Hall, C.A.S., Benemann, J.R. 2011. Oil from algae? *Bioscience*, **61**, 741-742.

Hall, D.O., Fernández, F.G., Guerrero, E.C., Rao, K.K., Grima, E.M. 2003. Outdoor helical tubular photobioreactors for microalgal production: modeling of fluid-dynamics and mass transfer and assessment of biomass productivity. *Biotechnology and bioengineering*, **82**, 62-73.

Hannon, M., Gimpel, J., Tran, M., Rasala, B., Mayfield, S. 2010. Biofuels from algae. Challenges and potential. *Biofuels*, **1**, 763-784.

Harwood, J.L. 1998. Involvement of chloroplast lipids in the reaction of plants submitted to stress. *In: Siegenthaler P-A, Murata N (eds). Lipids in photosynthesis: structure, function and genetics. Fluwer Academic Publishers, Dordrecth*, 287-302.

Hase, R., Oikawa, H., Sasao, C., Morita, M., Watanabe, Y. 2000. Photosynthetic production of microalgal biomass in a raceway system under greenhouse conditions in Sendai City. *Journal of Bioscience and Bioengineering*, **89**, 157-163.

Hodaifa, G., Martinez, E., Sanchez, S. 2008. Use of industrial wastewater from olive-oil extraction for biomass production of *Scenedesmus obliquus*. *Bioresource Technology*, **99**, 1111-1117.

Hsieh, C.H., Wu, W.T. 2009. Cultivation of microalgae for oil production with a cultivation strategy of urea limitation. *Bioresource Technology*, **100**, 3921-3926.

IEA. 2007. International Energy Agency. Technology essentials - biofuelproduction.

IEA. 2006. International Energy Agency. World energy outlook 2006. Paris: International Energy Agency.

Igou, T., Van Ginkel, S.W., Penalver-Argueso, P., Fu, J., Doi, S., Rarode, A., Cherevu, S., Shang, Q., Hassan, F., Woodruff, F., Chen, Y. 2014. Effect of Centrifugation on Water Recycling and Algal Growth to Enable Algae Biodiesel Production. *Water Environment Research*, **86**, 2325-2329.

Illman, A.M., Scragg, A.H., Shales, S.W. 2000. Increase in *Chlorella* strains calorific values when grown in low nitrogen medium. *Enzyme and Microbial Technology*, **27**, 631-635.

IPCC. Intergovernmental Panel on Climate Change. www.ipcc.ch/index.htm.

James, S.C., Boriah, V. 2010. Modeling algae growth in an open-channel raceway. *Journal of Computational Biology*, **17**, 895-906.

Jensen, G.S., Ginsberg, D.I., Drapeau, C. 2001. Blue Green Algae as an inmmuno enhancer and biomodulator. *Ancient Sun Nutrition Inc.*, **3**, 24-30.

Jiménez, C. 2003. Relationship between physicochemical variables and productivity in open ponds for the production of *Spirulina*: a predictive model of algal yield. *Aquaculture*, **221**, 331-345.

Jiménez, C., Cossio, B.R., Labella, D., Niell, F.X. 2003. The feasibility of industrial production of *Spirulina* (*Arthrospira*) in Southern Spain. *Aquaculture*, **217**, 179-190.

Jonker, J.G.G., Faaij, A.P.C. 2013. Techno-economic assessment of micro-algae as feedstock for renewable bio-energy production. *Applied Energy*, **102**, 461-475.

Jorquera, O., Kiperstok, A., Sales, E.A., Embirucu, M., Ghirardi, M.L. 2010. Comparative energy life-cycle analyses of microalgal biomass production in open ponds and photobioreactors. *Bioresource Technology*, **101**, 1406-1413.

Ketheesan, B., Nirmalakhandan, N. 2011. Development of a new airlift-driven raceway reactor for algal cultivation. *Applied Energy*, **88**, 3370-3376.

Ketheesan, B., Nirmalakhandan, N. 2012. Feasibility of microalgal cultivation in a pilot-scale airlift-driven raceway reactor. *Bioresource Technology*, **108**, 196-202.

Kheshgi, H.S., Prince, R.C., Marland, G. 2000. The potential of biomass fuels in the context of global climate change: Focus on transportation fuels. *Annual Review of Energy and the Environment*, **25**, 199-244.

Kliphuis, A.M.J., Martens, D.E., Janssen, M., Wijffels, R.H. 2011. Effect of O_2:CO_2 ratio on the primary metabolism of *Chlamydomonas reinhardtii*. *Biotechnology and Bioengineering*, **208**, 2390-2402.

Korb, R.E., Saville, P.J., Johnston, A.M., Raven, J.A. 1997. Sources of inorganic carbon for photosynthesis by three species of marine diatom. *Journal of Phycology*, **33**, 433-440.

Kromkamp, J.C., Beardall, J., Sukenik, A., Kopecky, J., Masojidek, J., Van Bergeijk, S., Gabai, S., Shaham, E., Yamshon, A. 2009. Short-term variations in photosynthetic parameters of *Nannochloropsis* cultures grown in two types of outdoor mass cultivation systems. *Aquatic Microbial Ecology*, **56**, 309-322.

Labatut, R.A., Ebeling, J.M., Bhaskaran, R., Timmons, M.B. 2007. Hydrodynamics of a Large-scale Mixed-Cell Raceway (MCR): Experimental studies. *Aquacultural Engineering*, **37**, 132-143.

Lashof, D.A., Ahuja, D.R. 1999. Relative contributions of greenhouse gas emission to global warming. *Nature*, **344**, 529-531.

Lee, J.W. 2008. Designer organisms for photosynthetic production of ethanol from carbon dioxide. *PCT Patent Application WO2008/039450*.

Li, S., Luo, S., Guo, R. 2013. Efficiency of CO_2 fixation by microalgae in a closed raceway pond. *Bioresource Technology*, **136**, 267-272.

Liang, Y., Sarkany, N., Cui, Y., Ysuf, J., Trushenski, J., Blackbrun, J.W. 2010. Use of sweet sorghum juice for lipid production by *Schizochytrium limacinum* SR21. *Bioresource Technolgy*, **101**, 3623-3627.

Lu, C., Vonshak, A. 1999. Photoinhibition in outdoor *Spirulina platensis* cultures assessed by polyphasic chlorophyll fluorescence transients. *Journal of Applied Phycology*, **11**, 355-359.

Lucas, R. 2011. Optimal shoe design for hydrostatic pressure wheel. *Dissertation, University of Southampton*.

Lundquist, T., Benemann, J. 2007. Using CO_2 and algae to treat wastewater and produce biofuel feedstock. *First Western Forum on Water & Energy Sustainability. Bren School, UCSB*.

Lundquist, T.J., Woertz, I., Benemann, J.R. 2010. Microalgae for wastewater treatment and biofuels production. *American Chemical Society. National Meeting Book of Abstracts*.

Márquez, F.J., Sasaki, K., Nishio, N., Nagai, S. 1995. Inhibitory effect of oxygen accumulation on the growth of *Spirulina Platensis*. *Biotechnology Letters*, **17**, 225-228.

Masojidek, J., Koblizek, M., Torzillo, G. 2004. Photosynthesis in Microalgae. in: *Handbook of Microalgal Culture: Biotechnology and Applied Phycology*, (Ed.) A. Richmond, Blackwell Publishing Ltd.

Mata, T.M., Martins, A.A., Caetano, N.S. 2010. Microalgae for biodiesel production and other applications: A review. *Renewable and Sustainable Energy Reviews*, **14**, 217-232.

Mathez, E.A. 2009. Climate Change: The Science of Global Warming and Our Energy Future. *http://www.amnh.org/learn/climate/Resource13*.

Meher, L., Vidyasagar, D., Naik, S. 2006. Technical aspects of biodiesel production by transesterification - A review. *Renewable and Sustainable Energy Reviews*, **10**, 248-268.
Mendoza, J.L., Granados, M.R., de Godos, I., Acién, F.G., Molina, E., Banks, C., Heaven, S. 2013. Fluid-dynamic characterization of real-scale raceway reactors for microalgae production. *Biomass and Bioenergy*, **54**, 267-275.
Metzger, P., Largeau, C. 2005. *Botryococcus braunii*: a rich source for hydrocarbons and related ether lipids. *Applied Microbiology and Biotechnology*, **66**, 486-96.
Moheimani, N.R., Borowitzka, M.A. 2007. Limits to productivity of the alga *Pleurochrysis carterae* (Haptophyta) grown in outdoor raceway ponds. *Biotechnology and Bioengineering*, **96**, 27-36.
Molina Grima, E., Garcia Camacho, F., Sanchez Perez, J.A., Acien Fernandez, F.G., Fermindez Sevilla, J.M. 1997. Evaluation of photosynthetic efficiency in microalgal cultures using averaged irradiance. *Enzyme and Microbial Technology*, **21**, 375-381.
Moo-Young, M., Chisti, Y. 1994. Bioreactor application in waste treatment. *Resources, Conservation and Recycling,*, **11**, 13-24.
Moody, J.W., McGinty, C.M., Quinn, J.C. 2014. Global evaluation of biofuel potential from microalgae. *Proceedings of the National Academy of Sciences, USA*, **111**, 8691-6.
Moomaw, W., Yamba, F., Kamimoto, M., Maurice, L., Nyboer, J., Urama, K., Weir, T. 2011. Renewable Energy and Climate Change. In IPCC Special Report on Renewable Energy Sources and Climate Change Mitigation. *Cambridge University Press, Cambridge, United Kingdom and New York, NY, USA.*
Moreno, J. 2003. Outdoor cultivation of a nitrogen-fixing marine cyanobacterium, *Anabaena* sp. ATCC 33047. *Biomolecular Engineering*, **20**, 191-197.
Muñoz, R., Kollner, C., Guieysse, B. 2009. Biofilm photobioreactors for the treatment of industrial wastewaters. *Journal of Hazardous Materials*, **161**, 29-34.
Musgrove, E., Heaven, S. 2015. Investigating the hydrodynamic performance of carbonation sumps in High Rate Algal Pond (HRAP)raceways using computational fluid dynamics (CFD). *Biofuels*, **5**, 723-739.
Narasimhan, A.M. 2010. Microalgal bioremediation of nutrients in wastewater and carbon dioxide in flue gas. Thesis. *Missouri University*.
Nock, W. 2015. An investigation into gas transfer from bubbles into water. *Thesis for the degree of Doctor of Philosophy. School of Civil Engineering and the Environment. Unviersity of Southampton.*
Ogawa, T., Fujii, T., Aiba, S. 1980. Effect of oxygen on the growth (yield) of *Clorella vulgaris*. *Archives of Microbiology*, **127**, 25-31.
Oilgae. 2015. http://www.oilgae.com/algae/cult/cos/cem/cem.html.
Oswald, W.J., Borowitzka, M.A. 1988. *Large scale algal culture systems.*, London, Cambridge.
Oswald, W.J., Gouleke, C.G. 1960. Biological transformation of solar energy. *Advances in Applied Microbiology*, **2**, 223-262.
Oswald, W.J., Gouleke, C.G. 1968. *Large scale production of microalgae.* MIT Press Cambridge, MA.
Park, J.B., Craggs, R.J. 2010. Wastewater treatment and algal production in high rate algal ponds with carbon dioxide addition. *Water Science and Technology*, **61**, 633-9.

Park, J.B., Craggs, R.J., Shilton, A.N. 2011. Wastewater treatment high rate algal ponds for biofuel production. *Bioresource Technology*, **102**, 35-42.
Pawlowski, A., Mendoza, J.L., Guzman, J.L., Berenguel, M., Acien, F.G., Dormido, S. 2014. Effective utilization of flue gases in raceway reactor with event-based pH control for microalgae culture. *Bioresource Technology*, **170**, 1-9.
Pearson, P.N., Palmer, M.R. 2000. Atmospheric carbon dioxide concentrations over the past 60 million years. *Nature*, **406**, 695-699.
Persoone, G., Morales, J., Verlet, H., De Paw, N. 1980. Air-lift pumps and the effect of mixing on algal growth. *Algae Biomass*, 505-522.
Pienkos, P.T., Darzins, A. 2009. The promise and challenges of microalgal-derived biofuels. *Biofuels, Bioproducts and Biorefining*, **3**, 431-440.
Pittman, J.K., Dean, A.P., Osundeko, O. 2011. The potential of sustainable algal biofuel production using wastewater resources. *Bioresource Technology*, **102**, 17-25.
Posten, C. 2009. Design principles of photo-bioreactors for cultivation of microalgae. *Engineering in Life Sciences*, **9**, 165-177.
Prussi, M., Buffi, M., Casini, D., Chiaramonti, D., Martelli, F., Carnevale, M., Tredici, M.R., Rodolfi, L. 2014. Experimental and numerical investigations of mixing in raceway ponds for algae cultivation. *Biomass and Bioenergy*, **67**, 390-400.
Pulz, O., Gross, W. 2004. Valuable products from biotechnology of microalgae. *Applied Microbiology and Biotechnology*, **65**, 635-48.
Putt, R., Singh, M., Chinnasamy, S., Das, K.C. 2011. An efficient system for carbonation of high-rate algae pond water to enhance CO_2 mass transfer. *Bioresource Technology*, **102**, 3240-5.
Radmann, E.M., Reinehr, C.O., Costa, J.A.V. 2007. Optimization of the repeated batch cultivation of microalga *Spirulina platensis* in open raceway ponds. *Aquaculture*, **265**, 118-126.
Ramanan, R., Kannan, K., Deshkar, A., Yadav, R., Chakrabarti, T. 2010. Enhanced algal CO_2 sequestration through calcite deposition by *Chlorella* sp. and *Spirulina platensis* in a mini-raceway pond. *Bioresource Technology*, **101**, 2616-22.
Raven, J.A. 1997. Putting the C in phycology. *European Journal of Phycology*, **32**, 319-333.
Richmond, A. 2004a. Biological principles of mass cultivation. *In: Richmond A (ed) Handbook of microalgal culture: biotechnology and applied phycology. Blackwell Science, Oxford*(125-177).
Richmond, A. 2004b. Principles for attaining maximal microalgal productivity in photobioreactors. An overview. *Hydrobiologia*, **512**, 33-37.
Richmond, A., Cheng-Wu, Z. 2001. Optimization of a flat plate glass reactor for mass production of *Nannocholorpsis* sp. outdoors. *Journal of Biotechnology*, **85**, 259-269.
Richmond, A., Lichtenberg, E., Stahl, B., Vonshak, A. 1990. Quantitative assessment of the major limitations on productivity of *Spirulina platensis* in open raceways. *Journal of Applied Phycology*, **2**, 195-206.
Rodríguez-Maroto, J.M., Jiménez, C., Aguilera, J., Niell, F.X. 2005. Air bubbling results in carbon loss during microalgal cultivation in bicarbonate-enriched media: experimental data and process modeling. *Aquacultural Engineering*, **32**, 493-508.
Rogers, J.N., Rosenberg, J.N., Guzman, B.J., Oh, V.H., Mimbela, L.E., Ghassemi, A., Betenbaugh, M.J., Oyler, G.A., Donohue, M.D. 2014. A critical

analysis of paddlewheel-driven raceway ponds for algal biofuel production at commercial scales. *Algal Research*, **4**, 76-88.
San Pedro, A., Gonzalez-Lopez, C.V., Acien, F.G., Molina-Grima, E. 2013. Marine microalgae selection and culture conditions optimization for biodiesel production. *Bioresource Technology*, **134**, 353-361.
Schenk, P.M., Thomas-Hall, S.R., Stephens, E., Marx, U.C., Mussgnug, J.H., Posten, C., Kruse, O., Hankamer, B. 2008. Second Generation Biofuels: High-Efficiency Microalgae for Biodiesel Production. *BioEnergy Research*, **1**, 20-43.
Senior, J. 2009. Hydrostatic pressure converters for the exploitation of very low head hydropower potential. *Thesis for the degree of Doctor of Philosophy. School of Civil Engineering and the Environment. Unviersity of Southampton.*
Senior, J., Saenger, N., Müller, G. 2010. New hydropower converters for very low-head differences. *Journal of Hydraulic Research*, **48**, 703–714.
Setlik, I., Sust, M., Malek, I. 1970. Dual purpose open circulation units for large scale culture of algae in temperate zones. Basic design consideration and scheme of pilot plant. *Algological Studies*, **1**, 111-164.
Sharma, R., Chisti, Y., Banerjee, U.C. 2001. Production, purification, characterization, and applications of lipases. *Biotechnology Advances*, **19**, 627-662.
Sheeman, J., Dunahay, T., Benemann, J., Roessier, P. 1998. A look back at the U.S. Department of Energy's Azuatic Species Program-Biodiesel from Algae. *Golde (CO): National Renewable Energy Laboratory Report No.:NREL/TP-580-24190. Contract. No: DE-AC36-83CH10093. Sponsored by the U.S. Department of Energy.*
Sialve, B., Bernet, N., Bernard, O. 2009. Anaerobic digestion of microalgae as a necessary step to make microalgal biodiesel sustainable. *Biotechnology Advances*, **27**, 409-416.
Sierra, E., Acién, F.G., Fernández, J.M., García, J.L., González, C., Molina, E. 2008. Characterization of a flat plate photobioreactor for the production of microalgae. *Chemical Engineering Journal*, **138**, 136-147.
Singh, D.P., Singh, N., Verma, K. 1995. Photooxidative damage to the Cyanobacterium *Spirulina platensis* mediated by single oxygen. *Current Microbiology*, **31**, 44-48.
Singh, M.K., Majumder, S.K. 2011. Co- and counter-current mass transfer in bubble column. *International Journal of Heat and Mass Transfer*, **54**(11-12), 2283-2293.
SMC. http://www.smcpneumatics.com/PF3W740-F06-F-M.html.
Soeder, C.J., Stengel, F. 1974. Physico-Chemical Factors affecting Metabolism and Growth Rate. *W. D. P. Stewart (ed.) Algal Physiology and Biochemistry, Blackwell Publ., London*, 714-740.
Sompech, K., Chisti, Y., Srinophakun, T. 2012. Design of raceway ponds for producing microalgae. *Future-Science*, **3**, 387-397.
Spolaore, P., Joannis-Cassan, C., Duran, E., Isambert, A. 2006. Commercial applications of microalgae. *Journal of Bioscience and Bioengineering*, **101**, 87-96.
Stephens, E., Ross, I.L., Mussgnug, J.H., Wagner, L.D., Borowitzka, M.A., Posten, C., Kruse, O., Hankamer, B. 2010. Future prospects of microalgal biofuel production systems. *Trends in Plant Science*, **15**, 554-564.
Stephenson, P.G., Moore, C.M., Terry, M.J., Zubkov, M.V., Bibby, T.S. 2011. Improving photosynthesis for algal biofuels: toward a green revolution. *Trends in Biotechnology*, **29**, 615-623.

Suali, E., Sarbatly, R. 2012. Conversion of microalgae to biofuel. *Renewable and Sustainable Energy Reviews*, **16**, 4316-4342.

Sun, A., Davis, R., Starbuck, M., Ben-Amortz, A., Pate, R., Pienkos, P.T. 2011. Comparative cost analysis of algal oil production for biofuels. *Energy*, **36**, 5169-5179.

Sutherland, D.L., Turnbull, M.H., Craggs, R.J. 2013. Increased pond depth improves algal productivity and nutrient removal in wastewater treatment high rate algal ponds. *Water Research*, **53**, 271-281.

Thompson, G.A.J. 1996. Lipids and membrane function in green algae. *Biochimica et Biophysica Acta*, **1302**, 17-45.

Tomaselli, L. 2004. The Microalgal Cell. in: *Handbook of Microalgal Culture: Biotechnology and Applied Phycology*, (Ed.) A. Richmond. Blackwell Science.

Torzillo, G., Scoma, A., Faraloni, C., Ena, A., Johanningmeier, U. 2009. Increased hydrogen photoproduction by means of a sulfur-deprived *Clamydomonas reinhardtii* D1 protein mutant. *International Journal of Hydrogen Energy*, **34**, 4529-4536.

Tran, K.C., Mendoza Martin, J.L., Heaven, S., Banks, C.J., Acien Fernandez, F.G., Molina Grima, E. 2014. Cultivation and anaerobic digestion of Scenedesmus spp. grown in a pilot-scale open raceway. *Algal Research*, **5**, 95-102.

UCC. 2010. Universidad Católica de Chile. Desarrollo de la energía nuclear en el mundo. Masgister Ingeniería de la energía.

Uduman, N., Qi, Y., Danquah, M.K., Forde, G.M., Hoadley, A. 2010. Dewatering of microalgal cultures: A major bottleneck to algae-based fuels. *Journal of Renewable and Sustainable Energy*, **2**.

Ugwu, C.U., Aoyagi, H., Uchiyama, H. 2007. Influence of irradiance, dissolved oxygen concentration, and temperature on the growth of *Chlorella sorokiniana. Photosynthetica*, **45**, 309-311.

UI. University of Iowa. http://wiki.uiowa.edu/display/greenergy/Production.

UN. 1995. The Science of Climate Change: Summary for Policymakers and Technical Summary of the Working Group I. *United Nations. Framewok Convention of Climate Change*, 22.

UN. United Nations. Framework Convention on Climate Change. Kyoto Protocol.

UN. United Nations. Our Common Future, Chapter2: Towards Sustainable Develpment. *UN Documents: Gathering a Body of Global Agreements*.

UN. 2012. Unitetd Nations. Framework Convention on Climate Change. *http://unfccc.int/meetings/doha_nov_2012/session/7049.php*.

Van den Hoek, C., Mann, D.G., Jahns, H.M. 1995. Algae. An introduction to Phycology. *Cambridge University Press*.

Verlaan, P., Van Eijs, A.M.M., Tramper, J., Vant Riet, K. 1989. Estimation of axial dispersion in individual sections of an airlift-loop reactor. *Chemical Engineering Science*, **44**, 1139-1146.

Vlaski, A., van Breemen, A.N., Alaerts, G.J. 1997. The role of particle size and density in dissolved air flotation and sedimentation. *Water Science Technology*, **36**, 177-189.

Vonshak, A. 1997. *Spirulina*: growth, physiology and biochemistry. *In: Vonshask, A. (Ed.), Spirulina platensis (Arthrospira): Physiology, Cell-Biology and Biotechnology.*

Vonshak, A., Guy, R. 1992. Photoadaptation, photoinhibition and productivity in the blue-green alga *Spirulina platensis* grown outdoors. *Plant Cell and Environment Journal*, **13**, 613-616.

Vonshak, A., Torzillo, G., Tomaselli, L. 1994. Use of chlorophyll fluorescence to estimate the effect of photoinhibition in outdoor cultures of *Spirulina platensis*. *Journal of Applied Phycology*, **6**, 31-34.

Wang, Y.-H., Turton, R., Semmens, K., Borisova, T. 2008. Raceway design and simulation system (RDSS): An event-based program to simulate the day-to-day operations of multiple-tank raceways. *Aquacultural Engineering*, **39**, 59-71.

Ward, A.J., Lewis, D.M., Green, F.B. 2014. Anaerobic digestion of algae biomass: A review. *Algal Research*, **5**, 204-214.

Weissman, J.C., Goebel, R.P. 1987. Design and analysis of microalgal open pond systems for the purpose of producing fuels. A subcontract report. *United States: SERI/STR-231-2840*.

Weissman, J.C., Goebel, R.P., Benemann, J.R. 1988. Photobioreactor design: mixing, carbon utilization and oxygen accumulation. *Biotechnology and Bioengineering*, **31**, 336-344.

Weissman, J.C., Radway, J.C., Wilde, E.W., Benemann, J.R. 1998. Growth and production of thermophilic cyanobacteria in a simulated thermal mitigation process. *Bioresource Technology*, **65**, 87-95.

Weissman, J.C., Tillet, D.M., Goebel, R.P. 1989. Design and operation of an outdoor microalgae test facility. *Solar Energy Research Institute. U.S. Department of Energy*.

White, D.A., Pagarette, A., Rooks, P., Ali, S.T. 2012. The effect of sodium bicarbonate supplementation on growth and biochemical composition of marine microalgae cultures. *Journal of Applied Phycology*, **25**, 153-165.

Widjaja, A., Chien, C.C., Ju, Y.H. 2009. Study of increasing lipid production from fresh water microalgae *Chlorella vulgaris*. *Journal Taiwan Instute Chemical Engineering*, **40**, 13-20.

Wilde, E.W., Benemann, J. 1993. Bioremoval of heavy metals by the use of microalgae. *Biotechnology Advances*, **11**, 781-812.

Williams, P.J.l.B., Laurens, L.M.L. 2010. Microalgae as biodiesel & biomass feedstocks: Review & analysis of the biochemistry, energetics & economics. *Energy & Environmental Science*, **3**, 554-590.

Yamaguchi, K. 1997. Recent advances in microalgal bioscience in Japan, with special reference to utilization of biomass and metabolites: A review. *Journal of Applied Phycology*, **8**, 487-502.

Yeh, K.-L., Chang, J.-S., chen, W.-m. 2010. Effect of light supply and carbon source on cell growth and cellular composition of a newly isolated microalga Chlorella vulgaris ESP-31. *Engineering in Life Sciences*, **10**, 201-208.

Zah, R., Böni, H., Gauch, M., Hischier, R., Lehmann, M., Wäger, P. 2007. Life cycle assessment of energy products: environmental assessment of biofuels. *Swiss federal laboratories for material science and technology (EMPA)*.